MICROBIAL COMMUNITY COMPOSITION AND THE TRANSFORMATION OF DISSOLVED ORGANIC MATTER IN SUPRAGLACIAL ENVIRONMENTS

by

Heidi Jean Smith

A dissertation submitted in partial fulfillment
of the requirements for the degree

of

Doctor of Philosophy

in

Ecology and Environmental Sciences

MONTANA STATE UNIVERSITY
Bozeman, Montana

April 2016

DEDICATION

To Mom and Dad for your constant love, inspiration, and support for my love of science.

ACKNOWLEDGEMENTS

First and foremost, I would like to thank my major advisor Dr. Christine Foreman, for her continued support, encouragement, and inspiration. Her love for polar science and interdisciplinary research is inspiring. I am profoundly thankful for the the many opportunities that she has given me, and for her commitment to my professional and personal development. I am additionally grateful for the valuable guidance from my committee members Dr. Diane McKnight, Dr. Matthew Fields, and Dr. Tracy Sterling. I would like to thank my current and past lab group for all of the help, friendship, and laughter.

To my parents, who have always supported me throughout every undertaking I have embarked on. You taught me to reach for the stars, and I am forever grateful for your unwavering support. Dylan, thank you for coming into my life when I needed you most, for continually offering encouragement and strength, thank you for being by my side. To my brothers Eric and Jeffery, thank you for being my two best friends through everything. To my family and friends thank you for your support, optimism, and laughter through all of the years.

This research was funded by the NSF Office of Polar Programs, NSF Division of Graduate Education, and by the NASA Earth and Science Space Fellowship program.

TABLE OF CONTENTS

1. AN OVERVIEW OF AQUATIC DISSOLVED ORGANIC MATTER AND MICROBIAL BIODIVERSITY 1

Dissolved Organic Matter in Aquatic Ecosystems 1
Significance of Glaciers to the Global Carbon Cycle 5
Antarctic Supraglacial Hydrologic Features a Refuge for Life 7
The Glacial Microbial Loop 8
Microbial Biodiversity 11
Thesis Hypotheses and Goals 14
References 16

2. ORGANIC MATTER SHAPES COMMUNITY COMPOSITION IN GLACIAL ENVIRONMENTS 24

Contribution of Authors 24
Manuscript Information 25
Abstract 26
Introduction 27
Methods 30
Study Sites and Sample Collection 30
Water Chemistry 33
Fluorescence Spectroscopy 33
DNA Extraction and PCR Amplification 35
Sequencing and Sequence Analysis 36
Statistical Analysis of Sequencing Samples 37
Results 38
Microbial Assemblages 38
Microbial Biodiversity 39
Predicted Metabolic Function 44
Stream Water Geochemistry 47
Relationship of Environmental Variables to Microbial Biodiversity 52
Discussion 54
Conclusion 61
Acknowledgements 62
References 63

TABLE OF CONTENTS - CONTINUED

3. MICROBIAL FORMATION OF LABILE GLACIAL ORGANIC CARBON....69

Contribution of Authors....69
Manuscript Information....70
Abstract....71
Introduction....72
Results and Discussion....73
Methods....86
Bulk Biological Analyses....86
Stable Isotope Labeling and Incubation Experiments....88
Hybridization and Microscopic Evaluation....89
NanoSIMS Analysis....90
Optical Analysis....92
Viral Abundances....93
Acknowledgements....93
References....95

4. SUPRAGLACIAL DISSOLVED ORGANIC MATTER A LABILE BUT UNSUSTAINABLE CARBON SOURCE....99

Contribution of Authors....99
Manuscript Information....100
Abstract....101
Introduction....102
Materials and Methods....105
Experimental Setup....105
Fluorescence Spectroscopy....106
FT-ICR MS....107
Cellular Respiration....109
External Metabolite Extraction and DOM Source Material Characterization....109
UPLC-Q-TOF MS Based Molecular Constituent Analysis....110
Results....112
DOM Source Material Characterization....112
DOM Source Lability Classification....115
Cellular Respiration....118
Fluorescent Characterization of DOM Transformations....119
Analysis of DOM Molecular Constituent Transformations....120
Discussion....124
Acknowledgements....130

TABLE OF CONTENTS - CONTINUED

References....131

5. BIOFILMS ON GLACIAL SURFACES: HOTSPOTS FOR BIOLOGICAL ACTIVITY....136

Contribution of Authors....136
Manuscript Information....137
Abstract....138
Introduction....139
Methods....140
Study Site Sample Collection and Preparation....140
Bacterial Community Composition....141
NanoSIMS Sample Preparation....142
Preparation, Hybridization, and Microscopic Evaluation....143
NanoSIMS Analysis....145
Confocal Laser Scanning Microscopy (CLSM) Imaging and Data Processing....149
Fluorescence Spectroscopy....151
Sediment Analysis....151
Chemical Analysis....153
Results and Discussion....153
Acknowledgements....163
References....165

6. EPILOGUE....169

References....178

REFERENCES CITED....181

APPENDICES....200

APPENDIX A: Genome Sequence of *Janthinobacterium* sp. CG23_2, a Violacein Producing Isolate from an Antarctic Supraglacial Stream....201
APPENDIX B: Draft Genome Sequence of a Metabolically Diverse Antarctic Supraglacial Stream Organism: *Polaromonas* sp. Strain CG9_12 Determine Using Pacific Biosciences Single-Molecule Real Time (SMRT) Sequencing Technology....209

APPENDICIES– CONTINUED

APPENDIX C: Draft Genome Sequence and Description of *Janthinobacterium* sp. Strain CG3, A Psychrotolerant Antarctic Supraglacial Stream Bacterium 217
APPENDIX D: Supplemental Information to Chapter 4 225

LIST OF TABLES

Table Page

2.1 SIMPER analysis of the top 200 most abundant OTUs that make up ~50% of the sequence dissimilarity between environmental groups....43

2.2 Pairwise permanova comparisons of microbial community composition....45

2.3 Summary of previously identified fluorophore designations....50

2.4 Stream water chemistry and physical measurements for the Cotton Glacier stream and Canada Stream. 51

3.1 Summary of previously identified fluorophore designations....75

3.2 Summary of 16S rRNA targeted oligonucleotide probes, target organisms, competitor sequences and formamide (FA) concentrations, and probe references....79

3.3 Average incorporation rates of ^{13}C-labeled exudates and ^{13}C-labeled amino acids 83

5.1 Comparison of the relative abundances of 454 Pyrosequencing sequences for cryoconite sediment organisms at the phylum taxonomic classification level and Cyanobacterial sequences at the genus classification. 154

5.2 Summary of 16S rRNA targeted oligonucleotide probes, target organisms, competitor sequences and formamide (FA) concentrations, and probe references....154

5.3 Thermo-gravimetric analysis of organic matter as percentage of dry weight from cryoconite sediments....160

AD.1 DOM molecular species percent composition and more- and less-labile nature (richness) for the three carbon sources: Cotton Glacier, Pony Lake, and Suwannee River 229

AD.2 Pairwise permanova comparisons of microbial community composition....230

LIST OF FIGURES

Figure Page

2.1 Relative abundance of MiSeq 16S rRNA amplicon sequences with individual samples grouped together based on location 40

2.2 Microbial α diversity indices 41

2.3 Multidimensional scaling plot of Bray–Curtis indices on the relative abundance of OTUs 46

2.4 PICRUSt analysis showing the relative abundance of KEGG orthologs 48

2.5 Canonical correspondence analysis of the influence of environmental variables and stream water EEMs 49

2.6 Canonical correspondence analysis of the influence of fluorescent OM variables on the relative abundance of OTUs 54

3.1 EEMs from Cotton Glacier stream water and exuded DOM feedback 75

3.2 PICRUST generated predicted genetic function profile of the Cotton Glacier stream bacterial community 78

3.3 NanoSIMS analysis of ^{13}C-exudate uptake by Cotton Glacier stream community 80

3.4 NanoSIMS analysis of ^{13}C-algal amino acid uptake by Cotton Glacier stream community 82

3.5 Schematic of glacial carbon cycling 84

4.1 Lability classification of DOM source materials 114

4.2 Van Krevelen diagrams and percent composition of DOM source materials 115

4.3 Cellular respiration of DOM source materials and molecular constituent changes 119

LIST OF FIGURES – CONTINUED

Figure Page

4.4 Change in fluorescent intensity of DOM source materials over time 121

4.5 Heatmap of changes in molecular constituents....123

5.1 Confocal laser scanning microscopy images of cryoconite sediment with associated microbial communities and biofilm Figure Name 156

5.2 Concentration of exuded organic matter in the boundary layer of a filamentous cell....158

5.3 NanoSIMS analysis of ^{13}C-sodium bicarbonate and $^{15}NH_4$ uptake by cryoconite microorganisms 159

5.4 Powder XRD spectral profile of cryoconite sediments....161

5.5 EEMs from cryoconite sediment and water....161

6.1 A multi-scale approach for environmental analysis....170

AD.1 EEMs for DOM source material from day 1 and day 98 228

AD.2 Changes in molecular constituent abundances....229

ABSTRACT

Relating microbial community composition to ecosystem function is a fundamental goal in ecological analyses, with physico-chemical parameters largely controlling this relationship. This investigation aimed to elucidate the impact of physico-chemical factors on biodiversity in glacial habitats, with an emphasis on dissolved organic matter (DOM). DOM is a complex mixture of organic compounds and the primary substrate for microbial activity. Considering the variety of DOM sources in aquatic systems, little is still known about the biological release and bio-transformation of microbially-derived, autochthonous DOM. Continental Antarctica, typically lacking terrestrial carbon inputs, is largely governed by autochthonous DOM, making it an ideal site to investigate microbial biodiversity and the microbial formation of DOM. Different glacial ecosystems were selected, with a strong focus on the supraglacial Cotton Glacier stream, to investigate: i) the microbial diversity and underlying environmental factors governing biogeographical trends, ii) the contribution of exuded carbon to the DOM pool and subsequent heterotrophic uptake/transformation, and iii) how biofilm influences nutrient cycling in supraglacial environments.

Findings from this study highlight distinct microbial assemblages in meltwater streams/sediments, ice, snow, and cryoconite across local and regional geographic scales. Specifically, nutrient availability and DOM quality influenced trends in microbial diversity. *In situ* DOM exudation was sufficiently high to support bacterial carbon demands, while the spatial organization of microorganisms in biofilms was advantageous in transferring nutrients between community members. Furthermore, compared to other more recalcitrant and chemically heterogeneous DOM sources, the highly labile supraglacial DOM was unable to sustain the same magnitude of microbial metabolism. The present study revealed dynamic carbon cycling in supraglacial environments, mediated by the tight coupling between *in situ* carbon fixation, DOM exudation, and rapid consumption. Statistical analyses failed to show the impact of any physical parameters on community composition. However, data from the Greenland Ice Sheet imply that interactions between community composition and meltwater dynamics are susceptible to environmental changes, shifting ecosystem function and microbial communities, with unforeseen consequences to downstream environments. A multi-scale approach contributed to a better understanding of microbial biogeography, carbon cycling, and cellular spatial organization in glacial surface environments.

CHAPTER 1

AN OVERVIEW OF AQUATIC DISSOLVED ORGANIC MATTER AND MICROBIAL BIODIVERSITY

Dissolved Organic Matter in Aquatic Ecosystems

Dissolved organic matter (DOM) is a complex and heterogeneous pool of organic compounds that is present in all aquatic ecosystems. Additionally, DOM is a significant carbon reservoir in the global carbon cycle and participates in a variety of environmentally relevant processes including: UV shielding for aquatic organisms, metal chelation/speciation, and organic contaminant binding (Findlay and Sinsabaugh, 2003). DOM also plays an integral role in aquatic food webs and nutrient cycling dynamics, with the molecular composition of DOM largely affecting its availability as a substrate for microbial metabolism (Fellman *et al.*, 2010). With advances in DOM characterization and the increase in interdisciplinary research, it is now widely accepted that the reactivity of aquatic DOM has implications for all aspects of aquatic ecosystem ecology and that aquatic DOM is not only dominated by highly processed and refractory material (Fellman *et al.*, 2010).

Biodegradation is recognized as a major mechanism responsible for the bulk of DOM remineralization, whereas photodegradation is primarily involved in the loss of chromophoric and lignin derived DOM components (Benner and Kaiser, 2011). DOM is arguably one of the largest sources of biologically available organic carbon (OC), and the mineralization of DOM represents a major sink of OC in the biosphere. Thus, much

interest is focused on discerning the factors that control biological DOM consumption (Cole *et al.*, 2007; Battin *et al.*, 2008; Guillemette and del Giorgio, 2011). While extrinsic environmental factors (e.g., temperature, ultraviolet radiation, nutrient availability) will doubtlessly impact DOM consumption rates (Kirchman *et al.*, 2005; Amon and Benner, 1996; Anesio *et al.*, 2005; Reitner *et al.*, 1997; Zweifel, 1999), the *in situ* bioavailability of DOM is essentially determined by the distribution of labile and recalcitrant DOM constituents, the DOM molecular weight distribution, and DOM nutrient content (Mopper *et al.*, 2007). Operationally, DOM can be divided into three categories that are dependent upon its biological availability: labile DOM, semi-labile DOM, and recalcitrant DOM (Jiao *et al.*, 2010). Labile DOM is defined as a bioavailable fraction of carbon that promotes net heterotrophic activity over a short period of time (hours to days), semi-labile DOM can persist for months to years, and recalcitrant DOM can be stored for millennia (Jiao *et al.*, 2010). The ultimate fate of DOM from aquatic environments is intrinsically linked to biological lability, and is proposed to follow two major pathways. DOM will either be completely oxidized to CO_2, or partially oxidized and transported to downstream aquatic environments (Battin *et al.*, 2009). It is the less-labile and recalcitrant fractions of DOM that are expected to persist in aquatic environments. These fractions are typically characterized as humic-like substances (HLS) (Cory and Kaplan, 2012). The majority of DOM in most freshwater habitats is comprised of HLS (50-80%) which are typically derived from the degradation of plant material, leaching of soil, and biogeochemical processes (Farjalla *et al.*, 2009). Less than 30% of DOM is composed of biologically labile components which include proteins, carbohydrates, and lipids

(Williams *et al.*, 1986). The biological transformation of DOM alters DOM reactivity, including its bioavailability, and thus influences microbial assemblage composition (e.g. Judd *et al.*, 2006; Logue *et al.*, 2015).

The ability for microorganisms to use various DOM constituents is dependent on the type of organism and the metabolic capability of functionally distinct bacterial groups (Osterholz *et al.*, 2016; Judd *et al.*, 2006; Carlson *et al.*, 2004; Kirchman, 2002). Much of our current knowledge regarding the biological utilization and processing of labile carbon comes from the addition of radiolabeled simple carbon substrates (glucose and amino acids) (Hobbie *et al.*, 1972; Brophy and Carlson, 1989; Gruber *et al.*, 2006; Hartley *et al.*, 2010; Rousk *et al.*, 2014) as these monomers largely support bacterial growth and are the constituents of biopolymers and macromolecules found in the natural environment. For bacterial communities amended with glucose and leucine, these compounds were transformed into higher molecular weight (HMW) materials that persisted throughout the six-month of incubation (Brophy and Carlson, 1989). When successively fed back to the microbial community, only 1-17% of these HMW materials were respired, compared to 40-75% of added monomers in the initial incubation experiment (Brophy and Carlson, 1989). Studies typically focus on glucose, and ignore other environmentally relevant monosaccharides, which, depending on aquatic habitat type could significantly underestimate carbon fluxes (Findlay and Sinsabaugh, 2003). It has been shown that allochthonous materials could contain higher glucose concentrations compared to autochthonous DOM (Biddanda and Benner, 1997) which is typically dominated by low molecular weight (LMW) compounds. Thus, based on the molecular composition of

DOM, a more rigorous consideration of the origin and environmental relevance of selected carbon sources would advance understanding of DOM processing in the environment.

More recent studies have moved away from amending microbial consortia with simple carbon substrates and have focused on incubations (from weeks to months) monitoring non-carbon amended DOM transformations (Osterholz *et al.*, 2016; Logue *et al.*, 2015). In these studies, close relationships between DOM structure and community composition have been observed as well as inconsistent trends (Crump *et al.*, 2003; Judd *et al.*, 2006). Logue *et al.* 2016 discovered in non-carbon amended incubations that the ability for *in situ* microbial communities to degrade LMW materials is a common function present in all sampled bacterial communities. Conversely, the capability of organisms to utilize HMW compounds is restricted to particular phylogenetic clades. However, even with these recent advances, it remains to be determined which specific metabolic traits and community members (rare or abundant) are ecologically important for regulation of DOM processing. It is not known if a single phylogeny is responsible for the majority of DOM processing, or if DOM transformations are dependent on sequences of transformations carried out by functionally distinct microbial community members. Overall, this lack of information on DOM composition related to bacterial community structure limits what is known about DOM bioavailability and exchange across ecosystems globally. Therefore, to understand how different carbon reservoirs interact and are biologically transformed more studies evaluating DOM composition from a variety of locations are necessary.

Significance of Glaciers to the Global Carbon Cycle

Globally, glaciers and polar ice sheets cover approximately 11% of the Earth's land surface and contain ~75% of the freshwater on Earth. Due to climatic warming and seasonal variations in temperature there is the potential for significant losses in the volume of the cryosphere, and the long term implications of climate mediated changes on ecosystem function are not fully understood (Hodson *et al.*, 2015). OC concentrations in glacial meltwater are low (~0.12 mg L^{-1} – 0.72 mg L^{-1}), but considering the sheer volume of glacial runoff from e.g. the Greenland Ice Sheet, fluxes of bioavailable OC to downstream environments could be significant (Hood *et al.*, 2009; Singer *et al*., 2012; Lawson and Wadham, 2013; Bhatia *et al.*, 2013). Glaciers are a large reservoir of OC and an estimated six petagrams of OC are stored within glacial ice, ~ 93% of which is stored within the Antarctic Ice Sheet (AIS) (Hood *et al.*, 2015). None the less, such estimates for the AIS are based on a relatively small number of samples (n = 19). The majority of data used in this analysis were from the McMurdo Dry Valleys (n = 11), which are 2.5X higher than the other measurements (Hood *et al.*, 2015). Considering the size of the AIS, this minimal dataset may not sufficiently account for the variability of OC concentrations throughout the AIS. Increased sample resolution is of particular importance when elucidating the link between glacially stored OC and the proposed effect on downstream aquatic ecosystems.

The origin of DOM in glacier ecosystems has been attributed to a variety of sources, including: the deposition of aerosols, byproducts of fossil fuel combustion, aoelian deposition, overridden vegetation in subglacial settings, and supra-, en-, and sub-

glacial biological process (Bhatia *et al.*, 2010; Hodson *et al.*, 2008; Singer *et al.*, 2012; Anesio *et al.*, 2010; Antony *et al.*, 2014; Stubbins *et al.*, 2012). Recently, DOM from coastal temperate glaciers has been shown to be old in age (Hood *et al.*, 2009; Stubbins *et al.*, 2012; Spencer *et al.*, 2014), and it is inferred based on incubation studies that the ancient fraction of glacial DOM is highly labile and capable of supporting bacterial productivity (Hood *et al.*, 2009). Compositionally, DOM in glacier ecosystems has a strong protein-like fluorescence signature (Barker *et al.*, 2006; Hood *et al.*, 2009), which further supports the high presumed bioavailability of glacial DOM.

Large proportions of DOM in englacial and supraglacial settings are composed of microbially derived products (Singer *et al*., 2012; Antony *et al.*, 2014; Bhatia *et al.*, 2010). Photosynthetic microbes in supraglacial environments have the potential to fix as much as 64 Gg C yr^{-1}, generating up to 10 Gg C yr^{-1} of OC (Anesio *et al.*, 2009), rates that are efficiently high enough to accumulate OC in supraglacial environments over time (Anesio *et al.*, 2010; Bagshaw *et al.*, 2016). Conversely, Cook *et al.* 2012 showed that supraglacial habitats could also be net heterotrophic, rendering generalizations about the global supraglacial carbon reservoir to still be determined. In addition to contrasting data, *in vitro* experiments performed to explore the microbial production/transformation of OC in supraglacial environments have not accounted for the specific OC factions (i.e., labile vs. recalcitrant), age, or organisms involved in carbon processing. More specifically, direct transfer of OC between autotrophs and heterotrophs has not been demonstrated in these icy ecosystems leaving a gap in our understanding about the fate and metabolic suitability of glacial DOM (Stibal *et al.*, 2012).

Antarctic Supraglacial Hydrologic Features a Refuge for Life

Life in polar regions can be highly constrained due to the dominance of ice and snow in glacial ecosystems. Since liquid water is a requirement for cellular life, meltwater is a major determinant of the biological functioning on ice sheet surfaces (Laybourn-Parry *et al.*, 2012). Meltwater dynamics on glacial surfaces are primarily governed by shortwave radiation (accounting for 60-80% of melt), and latent and sensible heat (Rothlisberger and Lang, 1987), with biological energy having a minimal impact on the glacial heat budget (McIntyre, 2011). The albedo of snow and ice is typically high, reflecting 70-90% of incoming solar radiation (Paterson, 1996). Furthermore, it is now recognized that surface darkening by aeolian and biological materials can cause a reduction in surface albedo (Takeuchi *et al.*, 2001; Lutz *et al.*, 2014).

Supraglacial freshwater habitats include cyroconite, cryolakes, and streams. Cryoconite holes are vertical, cylindrical depressions composed of a layer of sediments that is overlain by either liquid water or an ice lid depending of the time of year (Nordenskjöld, 1875; Fountain *et al.*, 2004). Unlike cryoconite holes, cryolakes form as meltwater accumulates in glacial surface depressions. Supraglacial streams are defined by the rapid rate of channel incision and the degree of change that occurs throughout the ablation season (Knighton, 1981). Of these, cryoconite holes are the most extensively studied supraglacial hydrologic features (e.g. Foreman *et al.*, 2007; Christner *et al.*, 2003; Porazinska *et al.*, 2004; Fountain *et al.*, 2004; Wharton *et al.*, 1981; Bagshaw *et al.*, 2007; Telling *et al.*, 2014) while information on supraglacial streams and lakes in Antarctica is scarce (Keskitalo, Leppäranta and Arvola, 2013a; Foreman *et al.*, 2013). The information

available regarding the distribution of Antarctic cryoconite indicates that the percent coverage ranges between 3-15% across four Antarctic glaciers (Fountain *et al.*, 2004).

Supraglacial environments play an important role by acting as a place of refuge for organisms in the otherwise hostile and extreme Antarctic environment (Wharton *et al.*, 1981). Additionally, supraglacial features have the ability to influence surface melt, large scale nutrient fluxes, and the transport of materials across polar landscapes, all impacting downstream biological processes (Cook *et al.*, 2015).

The Glacial Microbial Loop

Polar habitats typically lack higher trophic levels and thus have truncated food webs, dominated by the microbial loop (Stibal and Tranter, 2007). Even in the absence of higher trophic levels, these ecosystems harbor relatively complex food webs and biogeochemical cycles (Priscu *et al*., 1999; Wolf, *et al.*, 1999) that lend themselves to targeted studies focusing on the release and successive uptake of microbially derived autochthonous DOM. In glacial ecosystems photoautotrophy is the basis for complex food webs, and the organisms responsible for carrying out photosynthesis are a taxonomically diverse assemblage that includes: algae especially diatoms, protozoa, and cyanobacteria (Boetius *et al.*, 2015). Typically composed of simple organic acids, sugars, carbohydrates, pigments, and enzymes (Wetzel, 2001), DOM exuded by these phototrophic community members is believed to be a high quality metabolic substrate that is rapidly utilized by bacteria (Cole *et al.*, 1982). Extracellular release of DOM occurs via passive leakage across cell membranes or through the active excretion by autotrophic organisms. However, the amount of photoautotrophically released DOM

depends largely on external environmental conditions (Kujawinski, 2011; Findlay and Sinsabaugh, 2003). A wide range of percent extracellular release (PER) has been reported for diverse environments (2-68%) (Van den Meersche and Middelburg, 2004; Teira *et al.*, 2001), bracketing Antarctic ecosystems (25%) (Takacs *et al.*, 2001). In Antarctic systems, exuded, autochthonous DOM may account for up to 56% of the annual carbon pool in Dry Valley lakes (Takacs *et al.*, 2001), and contributes significantly to the carbon demands of heterotrophic bacteria (Priscu, Wolf, *et al.*, 1999; Takacs *et al.*, 2001). In Arctic cryoconite the extra cellular release of DOM has been estimated to contribute approximately 10% to the total DOC pool and was found to be in excess of bacterial respiration, suggesting the potential for exudate flushing to neighboring habitats (Anesio *et al.*, 2009). Beyond the quantification of PER, little is known about how these exuded carbon substrates are utilized and processed by heterotrophic glacial microorganisms. Not only is exuded carbon potentially the link between primary production and the microbial loop, but also it is a highly labile fraction of DOM that has the potential to influence activities of adjacent ecosystems.

More recently the important role of viruses and their contribution to the DOM pool in aquatic ecosystems has been recognized. Viruses infect bacteria, protozoa, and algae in aquatic environments causing cell lysis, which essentially short circuits the microbial loop and returns carbon to the pool before it is consumed by heterotrophic organisms (Laybourn-Parry *et al.*, 2012). In polar inland waters viral to bacterial ratios (VBR) ranging from 1.15- 57 have been reported (Säwström *et al.*, 2008). The strong impact of viral lysis in polar environments becomes obvious for examples from

cryoconite (Anesio and Bellas, 2011), where rates of phage infection were greater than in temperate oceans and freshwater habitats (Boetius *et al.*, 2015). Similarly, for ultra-oligotrophic Antarctic lakes the amount of carbon released by viral lysis may contribute up to 69% to the OC pool (Säwström *et al.*, 2007). In contrast, lower VBR have been reported from Antarctic supraglacial streams (0.021) (Foreman *et al.*, 2013), suggesting minor viral effects. To date, the extent of viral mediated carbon production is still poorly understood in glacial ecosystems. Säwström *et al.* (2008) proposed that the autochthonous nature of carbon substrates in Antarctic environments would support low VBR, rendering viral lysis as a potentially minor contribution to the organic carbon pool.

Heterotrophic organisms are responsible for the uptake and processing of DOM, tying the flow of energy and DOM directly to the microbial loop (Findlay and Sinsabaugh, 2003). This link, however, is poorly understood in glacial environments, and current attempts have only investigated and quantified bulk microbial processes (Telling *et al.*, 2014; Anesio *et al.*, 2010; Foreman *et al.*, 2007; Hodson *et al.*, 2007). Specifically, Foreman *et al.* 2007 found that bacterial production in Antarctic cryoconite ranged between 59.6 and 1580 ng C l^{-1} d^{-1} in the overlying ice and sediment layers, respectively. Anesio *et al.* (2010) found similar bacterial production rates, and concluded that Antarctic glaciers have the ability to utilize between 1.2-7% of the carbon stored within the sediments of cryoconite holes. These findings demonstrate that carbon originating from bacterial production is sufficiently high enough to fuel bacterial activity on glacial surfaces (Anesio *et al.* 2010). Despite the importance of newly fixed carbon in glacial settings (Anesio *et al.*, 2009; Cook *et al.*, 2012), the direct link between heterotrophic

microbial metabolism and the source of DOM remains poorly resolved.

When studying DOM dynamics in aquatic ecosystems it is a challenge to distinguish between allochthonous and autochthonous DOM. Autochthonous DOM can be produced at all levels of the microbial food web, and in some environments is produced in high enough concentrations to support a significant proportion of bacterial growth demands (Kawasaki and Benner, 2006). Since there are no higher order vascular plants in continental Antarctica, DOM in Antarctic aquatic environments is predominantly of microbial origin (McKnight *et al.*, 2001). Antarctic environments offer a unique opportunity to discern linkages between microbes and the microbial loop due to the simplified microbial assemblages, truncated food webs, and the autochthonous origin of DOM. Greater insight regarding the initial synthesis and transformation of DOM in glacial ecosystems would allow for more accurate estimates of global carbon budgets, and a better understanding of the implications of glacial OC on downstream aquatic ecosystems.

Microbial Biodiversity

Microbial biodiversity is of global significance as microorganisms are at the base of aquatic food webs and are capable of inhabiting all environments on planet Earth. According to the *Global Biodiversity Assessment* 1,000,000 bacterial species are present on Earth, with less than 4,500 being described and cultivated. Biodiversity, or the variety of biological organisms found within a particular ecosystem, can have an overall effect on ecosystem function (Hooper *et al.*, 2008). The study of biodiversity across different environments has enabled the discovery of novel physiologies, biogeochemical pathways,

survival strategies, and stress response mechanisms (Margesin *et al.*, 2007). Microorganisms have the ability to inhabit distinct niches that span across moderate to extreme environmental regimes (Wilkins *et al.*, 2012). For instance, a total of 10^{25}-10^{28} microbial cells are estimated for the AIS alone (Boetius *et al.*, 2015). Despite such large numbers, questions remain about the environmental factors influencing microbial community structure, the metabolic capabilities of cold temperature organisms, and which mechanisms have evolved for growth in cold temperatures.

It has recently been argued that collectively icy habitats represent a distinct biome (Anesio and Laybourn-Parry, 2012). For many years, icy habitats were overlooked as environments capable of supporting life due to the scarcity of water, cold temperatures, and nutrient limitation. However, in addition to the preservation and burial of microbial biomass (Priscu *et al.*, 2008), it is now recognized that viable, metabolically active, and diverse organisms thrive in icy Antarctic ecosystems (Foreman *et al.*, 2007; Telling *et al.*, 2014; Anesio *et al.*, 2010; Carpenter *et al.*, 2000; Priscu *et al*, 1999; Wolf, *et al.*, 1999). Studies on microbial diversity across the AIS have been conducted in cryoconite (e.g., Foreman *et al.*, 2007; Christner *et al.*, 2003), supraglacial lakes (Keskitalo, Leppäranta and Arvola, 2013), supraglacial streams (Foreman *et al.*, 2013), snow (Carpenter *et al.*, 2000), subglacial outflow (Mikucki *et al.*, 2009), glacier ice (Lanoil *et al.*, 2009), and in accretion ice of subglacial lakes (e.g., Priscu, Adams, *et al.*, 1999; Christner *et al.*, 2014). All of these studies indicate that the AIS is a hospitable environment for microbial communities. Based on cultured organisms and 16S rRNA gene amplification the dominant organisms inhabiting icy environments can be grouped into six main genera.

Identified phylotypes belong to the *Alphaproteobacteria*, *Betaproteobacteria*, *Gammaproteobacteria*, *Actinobacteria*, *Firmicutes*, and *Bacteroidetes* lineages (Priscu *et al.*, 2008), with *Proteobacteria* being the most abundant and phylogenetically diverse lineage (Irvine-Fynn *et al.*, 2012). Archaea have been detected, but are a minor component of glacial communities (Cameron *et al.*, 2012; Christner *et al.*, 2014).

To accurately assess trends in glacial biodiversity, several methodological considerations must be taken into account. Since the application of molecular techniques to explore the phylogenetic composition of frozen environments is still in its infancy, it is probable that there are many unknown taxa of microbial life awaiting discovery. The application of molecular techniques will greatly enhance our understanding of glacial biodiversity and the factors governing these trends. However, these studies must be approached with care in order to produce credible results. This is not a trivial issue because cell concentrations are low in icy ecosystems (Priscu *et al*., 1999; Adams, *et al.*, 1999) and contaminants could falsely inflate the taxonomic biodiversity. While not a standard routine in next generation sequencing protocols, several studies have noted the importance of sequencing procedural samples as a potential source for contaminants and that the subsequent subtraction of these "blank samples" is essential for accurate next generation sequencing (Salter *et al.*, 2014; Nguyen *et al.*, 2015). Additionally, it is difficult to acquire samples from icy habitats over significant spatial and temporal scales. Therefore caution must be used when interpreting results from "snap shot" sample collections, as these samples are likely not representative of the temporal variation in these habitats. With the drastic decrease in sequencing costs and ease of acquiring

sequencing data in comparison to earlier techniques, sample design needs to address issues of pseudo-replication and reproducibility (Prosser, 2010). Moving forward, appropriate blank subtraction, and experimental design must be considered when studying the microbial ecology of such pristine environments.

Thesis Hypotheses and Goals

Overarching Hypothesis

In environmentally similar habitats fed by glacial melt, substrate quality (i.e., DOM composition) rather than physico-chemical parameters, dictates microbial communities in diverse supraglacial habitats across local and regional landscapes. In light of this hypothesis, *in situ* synthesis, extracellular release, uptake, and transformation of DOM are part of a tight, close-range network between autotrophic producers and heterotrophic consumers in otherwise inhospitable environments.

The goal of this research was to characterize the microbial community present within supraglacial meltwater driven ecosystems. This was done in order to answer questions regarding microbial assemblages across geographical scales in respect to key environmental factors. Additionally, I sought to identify environmentally relevant organisms for carbon bio-transformations. While bulk measurements of photoautotrophic and bacterial productivity answer questions about larger ecosystem wide processes, I was primarily interested in focusing on specific phylogenetic taxa and determining cell specific rates of DOM assimilation. Throughout this research both field and environmentally relevant laboratory based studies were conducted to answer the following null hypotheses:

H0 1: *Microbial assemblages in glacial meltwater fed ecosystems are indistinguishable across local and regional scales. Further, microbes found in stream water are a subset of local microbial assemblages found in other supraglacial habitats such as ice, snow, cryoconite, and stream sediments.* (Rationale and objectives are detailed in Chapter 2).

H0 2: *Different physico-chemical parameters (in particular DOM) present across polar landscapes do not govern the microbial composition within distinct glacial meltwater fed habitat types.* (Rationale and objectives are detailed in Chapter 2).

H0 3: *Extracellular release of DOM does not meet in situ bacterial carbon demands, and the release of ancient carbon stored within the ice is the dominant source of labile carbon in a supraglacial stream.* (Rationale and objectives are detailed in Chapter 3).

H0 4: *DOM bioavailability, as a substrate for heterotrophic metabolism, does not change with respect to source (i.e., autochthonous vs. allochthonous) or chemical composition (i.e., labile vs. recalcitrant). As such, microbially derived DOM from the Cotton Glacier stream is of equal substrate availability as more recalcitrant DOM from the coastal Antarctic Pony Lake or terrestrially dominated DOM from Suwannee River.* (Rationale and objectives are detailed in Chapter 4).

H0 5: *The spatial organization in the form of biofilm adherent to mineral particles does not promote a preferential transfer of nutrients from primary producers to consumers.* (Rationale and objectives are detailed in Chapter 5).

References

Amon RMW, Benner R. (1996). Photochemical and microbial consumption of dissolved organic carbon and dissolved oxygen in the Amazon River system. *Geochimica et Cosmochimica Acta* **60**: 1783–1792.

Anesio AM, Bellas CM. (2011). Are low temperature habitats hot spots of microbial evolution driven by viruses? *Trends Microbiol* **19**: 52–57.

Anesio AM, Granéli W, Aiken GR, Kieber DJ, Mopper K. (2005). Effect of Humic Substance Photodegradation on Bacterial Growth and Respiration in Lake Water. *Appl Environ Microbiol* **71**: 6267–6275.

Anesio AM, Hodson AJ, Fritz A. (2009). High microbial activity on glaciers: importance to the global carbon cycle. *Glob Change Biol* **15**: 955–960.

Anesio AM, Laybourn-Parry J. (2012). Glaciers and ice sheets as a biome. *Trends Ecol Evol (Amst)* **27**: 219–225.

Anesio AM, Sattler B, Foreman C, Telling J. (2010). Carbon fluxes through bacterial communities on glacier surfaces. *Annals of Glaciology*, ***51*(56)**: 32-40.

Antony R, Grannas AM, Willoughby AS, Sleighter RL, Thamban M, Hatcher PG. (2014). Origin and sources of dissolved organic matter in snow on the East Antarctic ice sheet. *Environ Sci Technol* **48**: 6151–6159.

Bagshaw EA, Tranter M, Fountain AG, Welch KA, Basagic H, Lyons WB. (2007). Biogeochemical evolution of cryoconite holes on Canada Glacier, Taylor Valley, Antarctica. *J Geophys Res* **112**: G(4).

Bagshaw EA, Tranter M, Wadham JL, Fountain AG, Dubnick A, Fitzsimons S. (2016). Processes controlling carbon cycling in Antarctic glacier surface ecosystems. *Geochem Persp Let* **2**: 44–54.

Barker JD, Sharp MJ, Fitzsimons SJ, Turner RJ. (2006). Abundance and Dynamics of Dissolved Organic Carbon in Glacier Systems. *Arctic, Antarctic, and Alpine Research* **38**: 163–172.

Battin TJ, Kaplan LA, Findlay S, Hopkinson CS, Marti E, Packman AI, *et al.* (2008). Biophysical controls on organic carbon fluxes in fluvial networks. *Nature Geoscience* **1**: 95–100.

Battin TJ, Luyssaert S, Kaplan LA, Aufdenkampe AK, Richter A, Tranvik LJ. (2009). The boundless carbon cycle. *Nature Geoscience* **2**: 598–600.

Benner R, Kaiser K. (2011). Biological and photochemical transformations of amino acids and lignin phenols in riverine dissolved organic matter. *Biogeochemistry* **102**: 209–222.

Bhatia MP, Das SB, Longnecker K, Charette MA, Kujawinski EB. (2010). Molecular characterization of dissolved organic matter associated with the Greenland ice sheet. *Geochimica et Cosmochimica Acta* **74**: 3768–3784.

Bhatia MP, Das SB, Xu L, Charette MA, Wadham JL, Kujawinski EB. (2013). Organic carbon export from the Greenland ice sheet. *Geochimica et Cosmochimica Acta* **109**: 329–344.

Biddanda B, Benner R. (1997). Carbon, nitrogen, and carbohydrate fluxes during the production of particulate and dissolved organic matter by marine phytoplankton. *Limnol Oceanogr* **42**: 506–518.

Boetius A, Anesio AM, Deming JW, Mikucki JA, Rapp JZ. (2015). Microbial ecology of the cryosphere: sea ice and glacial habitats. *Nat Rev Microbiol*.

Brophy JE, Carlson DJ. (1989). Production of biologically refractory dissolved organic carbon by natural seawater microbial populations. *Deep Sea Research Part A Oceanographic Research Papers* **36**: 497–507.

Cameron KA, Hodson AJ, Osborn AM. (2012). Structure and diversity of bacterial, eukaryotic and archaeal communities in glacial cryoconite holes from the Arctic and the Antarctic. *FEMS Microbiol Ecol* **82**: 254–267.

Carlson CA, Giovannoni SJ, Hansell DA, Goldberg SJ, Parsons R, Vergin K. (2004). Interactions among dissolved organic carbon, microbial processes, and community structure in the mesopelagic zone of the northwestern Sargasso Sea. *Limnol Oceanogr* **49**: 1073–1083.

Carpenter EJ, Lin S, Capone DG. (2000). Bacterial Activity in South Pole Snow. *Applied and Environmental Microbiology* **66**: 4514-4517.

Christner BC, Kvitko BH II, Reeve JN. (2003). Molecular identification of Bacteria and Eukarya inhabiting an Antarctic cryoconite hole. *Extremophiles* **7**: 177–183.

Christner BC, Priscu JC, Achberger AM, Barbante C, Carter SP, Christianson K, *et al.* (2014). A microbial ecosystem beneath the West Antarctic ice sheet. *Nature* **512**: 310–313.

Cole JJ, Likens GE, Strayer DL. (1982). Photosynthetically produced dissolved organic carbon: An important carbon source for planktonic bacteria. *Limnol Oceanogr* **27**: 1080–1090.

Cole JJ, Prairie YT, Caraco NF, McDowell WH, Tranvik LJ, Striegl RG, *et al.* (2007). Plumbing the Global Carbon Cycle: Integrating Inland Waters into the Terrestrial Carbon Budget. *Ecosystems* **10**: 172–185.

Cook J, Edwards A, Takeuchi N, Irvine-Fynn T. (2015). Cryoconite The dark biological secret of the cryosphere. *Progress in Physical Geography* 1–46.

Cook JM, Hodson AJ, Anesio AM. (2012). An improved estimate of microbially mediated carbon fluxes from the Greenland ice sheet. *Journal of Glaciology* **58**: 1098-1108.

Cory RM, Kaplan LA. (2012). Biological lability of streamwater fluorescent dissolved organic matter. *Limnol Oceanogr* **57**: 1347–1360.

Crump BC, Kling GW, Bahr M, Hobbie JE. (2003). Bacterioplankton community shifts in an arctic lake correlate with seasonal changes in organic matter source. *Appl Environ Microbiol* **69**: 2253–2268.

Farjalla VF, Amado AM, Suhett AL, Meirelles-Pereira F. (2009). DOC removal paradigms in highly humic aquatic ecosystems. *Environ Sci Pollut Res Int* **16**: 531–538.

Fellman JB, Hood E, Spencer RGM. (2010). Fluorescence spectroscopy opens new windows into dissolved organic matter dynamics in freshwater ecosystems: A review. *Limnol Oceanogr* **55**: 2452–2462.

Findlay S, Sinsabaugh RL. (2003). Aquatic Ecosystems. Elsevier Science: San Diego.

Foreman CM, Cory RM, Morris CE, SanClements MD, Smith HJ, Lisle JT, *et al.* (2013). Microbial growth under humic-free conditions in a supraglacial stream system on the Cotton Glacier, Antarctica. *Environ Res Lett* **8**: 035022.

Foreman CM, Sattler B, Mikucki JA, Porazinska DL, Priscu JC. (2007). Metabolic activity and diversity of cryoconites in the Taylor Valley, Antarctica. *J Geophys Res* **112**: G04S32.

Fountain AG, Tranter M, Nylen TH, Lewis KJ, Mueller DR. (2004). Evolution of cryoconite holes and their contribution to meltwater runoff from glaciers in the McMurdo Dry Valleys, Antarctica. *Journal of Glaciology* **50**: 35–45.

Gruber DF, Simjouw J-P, Seitzinger SP, Taghon GL. (2006). Dynamics and characterization of refractory dissolved organic matter produced by a pure bacterial culture in an experimental predator-prey system. *Appl Environ Microbiol* **72**: 4184–4191.

Guillemette F, del Giorgio PA. (2011). Reconstructing the various facets of dissolved organic carbon bioavailability in freshwater ecosystems. *Limnol Oceanogr*. **56**: 734-748.

Hartley, Hopkins, Sommerkorn, Wookey. (2010). The response of organic matter mineralisation to nutrient and substrate additions in sub-arctic soils. *Soil Biology and Biochemistry* **42**: 9–9.

Hobbie JE, Holm Hansen O, Packard TT, Pomeroy LR, Sheldon RW, Thomas JP, *et al.* (1972). A Study of the Distribution and Activity of Microorganisms in Ocean Water. *Limnol Oceanogr* **17**: 544–555.

Hodson A, Anesio AM, Ng F, Watson R, Quirk J, Irvine-Fynn T, *et al.* (2007). A glacier respires: Quantifying the distribution and respiration CO 2flux of cryoconite across an entire Arctic supraglacial ecosystem. *J Geophys Res* **112**: G04S36.

Hodson A, Anesio AM, Tranter M, Fountain A, Osborn M, Priscu J, *et al.* (2008). GLACIAL ECOSYSTEMS. *Ecological Monographs* **78**: 41–67.

Hodson A, Ben Brock, Pearce D, Laybourn-Parry J, Tranter M. (2015). Cryospheric ecosystems: a synthesis of snowpack and glacial research. *Environ Res Lett* **10**: 110201.

Hood E, Battin TJ, Fellman J, O'Neel S, Spencer RGM. (2015). Storage and release of organic carbon from glaciers and ice sheets. *Nature Geoscience* **8**: 91–96.

Hood E, Fellman J, Spencer RGM, Hernes PJ, Edwards R, D'Amore D, *et al.* (2009). Glaciers as a source of ancient and labile organic matter to the marine environment. *Nature* **462**: 1044–1047.

Hooper DU, Chapin FS III, Ewel JJ, Hector A, Inchausti P, Lavorel S, *et al.* (2008). Effects of Biodiversity on Ecosystem Functioning: A Consensus of Current Knowledge. *Ecological monographs* **75**: 3-35.

Irvine-Fynn TDL, Edwards A, Newton S, Langford H, Rassner SM, Telling J, *et al.* (2012). Microbial cell budgets of an Arctic glacier surface quantified using flow cytometry. *Environ Microbiol* **14**: 2998–3012.

Jiao N, Herndl GJ, Hansell DA, Benner R, Kattner G, Wilhelm SW, *et al.* (2010). Microbial production of recalcitrant dissolved organic matter: long-term carbon storage in the global ocean. *Nat Rev Microbiol* **8**: 593–599.

Judd KE, Crump BC, Kling GW. (2006). Variation in dissolved organic matter controls bacterial production and community composition. *Ecology* **87**: 2068–2079.

Kawasaki N, Benner R. (2006). Bacterial release of dissolved organic matter during cell growth and decline: Molecular origin and composition. *Limnol Oceanogr* **51**: 2170–2180.

Keskitalo J, Leppäranta M, Arvola L. (2013). First records of primary producers of epiglacial and supraglacial lakes in western Dronning Maud Land, Antarctica. *Polar Biol* **36**: 1441–1450.

Kirchman DL. (2002). The ecology of Cytophaga–Flavobacteria in aquatic environments. *FEMS Microbiology Ecology* **39**: 91-100.

Kirchman DL, Malmstrom RR, Cottrell MT. (2005). Control of bacterial growth by temperature and organic matter in the Western Arctic. *Deep Sea Research Part II: Topical Studies in Oceanography* **52**: 3386–3395.

Knighton AD. (1981). Channel Form and Flow Characteristics of Supraglacial Streams, Austre Okstindbreen, Norway. *Arctic and Alpine Research* **13**: 295.

Kujawinski EB. (2011). The Impact of Microbial Metabolism on Marine Dissolved Organic Matter. *Ann Rev Mar Sci* **3**: 567–599.

Lanoil B, Skidmore M, Priscu JC, Han S, Foo W, Vogel SW, *et al.* (2009). Bacteria beneath the West Antarctic ice sheet. *Environ Microbiol* **11**: 609–615.

Lawson EC, Wadham JL. (2013). Greenland Ice Sheet exports labile organic carbon to the Arctic oceans. *Biogeosciences* **10**: 19311–19345.

Laybourn-Parry J, Tranter M, Hodson A (eds). (2012). The Ecology of Snow and Ice Environments.

Logue JB, Stedmon CA, Kellerman AM, Nielsen NJ, Andersson AF, Laudon H, *et al.* (2015). Experimental insights into the importance of aquatic bacterial community composition to the degradation of dissolved organic matter. *ISME J*.

Lutz S, Anesio AM, Villar SEJ, Benning LG. (2014). Variations of algal communities cause darkening of a Greenland glacier. *FEMS Microbiol Ecol* **89**: 402–414.

Margesin R, Miteva V. (2011). Diversity and ecology of psychrophilic microorganisms. *Research in Microbiology* **162**: 346–361.

Margesin R, Schinner F, Marx JC, Gerday C. (2007). Psychrophiles: From Biodiversity to Biotechnology. Springer Science and Business Media.

McIntyre NF. (2011). Cryoconite hole thermodynamics. *Canadian Journal of Earth Sciences* **21**: 152-156.

McKnight DM, Boyer EW, Westerhoff PK. (2001). Spectrofluorometric characterization of dissolved organic matter for indication of precursor organic material and aromaticity. *Limnol and Oceanography*. **46:** 38-48.

Mikucki JA, Pearson A, Johnston DT, Turchyn AV, Farquhar J, Schrag DP, *et al.* (2009). A contemporary microbially maintained subglacial ferrous "ocean". *Science* **324**: 397–400.

Mopper K, Stubbins A, Ritchie JD, Bialk HM, Hatcher PG. (2007). Advanced instrumental approaches for characterization of marine dissolved organic matter: extraction techniques, mass spectrometry, and nuclear magnetic resonance spectroscopy. *Chem Rev* **107**: 419–442.

Nguyen NH, Smith D, Peay K, Kennedy P. (2015). Parsing ecological signal from noise in next generation amplicon sequencing. *New Phytol* **205**: 1389–1393.

Nordenskjöld NE. (1875). Cryoconite found 1870, July 19th-25th, on the inland ice, east of Auleitsivik Fjord, Disco Bay, Greenland. *Geological Magazine* **2**: 157–162.

Osterholz H, Singer G, Wemheuer B, Daniel R, Simon M, Niggemann J, *et al.* (2016). Deciphering associations between dissolved organic molecules and bacterial communities in a pelagic marine system. *ISME J*.

Paterson W. (1996). The Physics of Glaciers 3rd edition. Butterworth-Heinemann.

Porazinska DL, Fountain AG, Nylen TH, Tranter M, Virginia RA, Wall DH. (2004). The Biodiversity and Biogeochemistry of Cryoconite Holes from McMurdo Dry Valley Glaciers, Antarctica. *Arctic, Antarctic, and Alpine Research* **36**: 84–91.

Priscu JC, Adams EE, Lyons WB, Voytek MA, Mogk DW, Brown RL, *et al.* (1999). Geomicrobiology of subglacial ice above Lake Vostok, Antarctica. *Science* **286**: 2141–2144.

Priscu JC, Tulaczyk S, Studinger M, Christner BC, Foreman CM. (2008). Antarctic subglacial water: origin, evolution and ecology. *Polar lakes and rivers*, 119-136.

Priscu JC, Wolf CF, Takacs CD, Fritsen CH, Laybourn-Parry J, Roberts EC, *et al.* (1999). Carbon Transformations in a Perennially Ice-Covered Antarctic Lake. *BioScience* **49**: 997–1008.

Prosser JI. (2010). Replicate or lie. *Environ Microbiol* **12**: 1806–1810.

Reitner B, Herndl GJ, Herzig A. (1997). Role of ultraviolet-B radiation on photochemical and microbial oxygen consumption in a humic-rich shallow lake. *Limnol Oceanogr*. **42**: 950-960.

Rothlisberger H, Lang H. (1987). Glacio-Fluvial Sediment Transfer: An Alpine Perspective. *John Wiley and Sons*, 207-284.

Rousk J, Hill PW, Jones DL. (2014). Using the concentration-dependence of respiration arising from glucose addition to estimate in situ concentrations of labile carbon in grassland soil. *Soil Biology and Biochemistry* **77**: 81–88.

Salter SJ, Cox MJ, Turek EM, Calus ST, Cookson WO, Moffatt MF, *et al.* (2014). Reagent and laboratory contamination can critically impact sequence-based microbiome analyses. *BMC Biology* **12**: 87.

Säwström C, Anesio MA, Granéli W, Laybourn-Parry J. (2007). Seasonal viral loop dynamics in two large ultraoligotrophic Antarctic freshwater lakes. *Microb Ecol* **53**: 1–11.

Säwström C, Lisle J, Anesio AM, Priscu JC, Laybourn-Parry J. (2008). Bacteriophage in polar inland waters. *Extremophiles* **12**: 167–175.

Singer GA, Fasching C, Wilhelm L, Niggemann J, Steier P, Dittmar T, Battin TJ. (2012b). Biogeochemically diverse organic matter in Alpine glaciers and its downstream fate. *Nature Geoscience* **5**: 710–714.

Spencer RGM, Vermilyea A, Fellman J, Raymond P, Stubbins A, Scott D, *et al.* (2014). Seasonal variability of organic matter composition in an Alaskan glacier outflow: insights into glacier carbon sources. *Environ Res Lett* **9**: 055005.

Stibal M, Sabacka M, Zarsky J. (2012). Biological processes on glacier and ice sheet surfaces. *Nature Geoscience* **5**: 771–774.

Stibal M, Tranter M. (2007). Laboratory investigation of inorganic carbon uptake by cryoconite debris from Werenskioldbreen, Svalbard. *Journal of Geophysical Research: Biogeosciences (2005–2012)* **112**.

Stubbins A, Hood E, Raymond PA, Aiken GR, Sleighter RL, Hernes PJ, *et al.* (2012). Anthropogenic aerosols as a source of ancient dissolved organic matter in glaciers. *Nature Geoscience* **5**: 198–201.

Takacs CD, Priscu JC, McKnight DM. (2001). Bacterial dissolved organic carbon demand in McMurdo Dry Valley lakes, Antarctica. *Limnol Oceanogr* **46**: 1189–1194.

Takeuchi N, Kohshima S, Seko K. (2001). JSTOR: Arctic, Antarctic, and Alpine Research, Vol. 33, No. 2 (May, 2001), pp. 115-122. *Arctic*.

Teira E, Pazó MJ, Serret P. (2001). Dissolved organic carbon production by microbial populations in the Atlantic Ocean - Teira - 2001 - Limnology and Oceanography - Wiley Online Library. *Limnology and Oceanogr* **46**: 1370–1377.

Telling J, Anesio AM, Tranter M, Fountain AG, Nylen T, Hawkings J, *et al.* (2014). Spring thaw ionic pulses boost nutrient availability and microbial growth in entombed Antarctic Dry Valley cryoconite holes. *Front Microbiol* **5**: 694–694.

Van den Meersche K, Middelburg JJ. (2004). Carbon-nitrogen coupling and algal-bacterial interactions during an experimental bloom: Modeling a 13C tracer experiment - Van den Meersche - 2004 - Limnology and Oceanography - Wiley Online Library. *Limnology and …* **49**: 862–878.

Wetzel R. (2001). Limnology. Third Eiditon. Elsevier: San Diego.

Wharton RA Jr., Vinyard WC, Parker BC, Simmons GM Jr., Seaburg KG. (1981). Algae in cryoconite holes on Canada Glacier in Southern Victorialand, Antarctica. *Phycologia* **20**: 208–211.

Wilkins D, Yau S, Williams TJ, Allen MA, Brown MV, DeMaere MZ, *et al.* (2012). Key microbial drivers in Antarctic aquatic environments. *FEMS Microbiol Rev* **37**: 303–335.

Williams PM, Carlucci AF, Henrichs SM, Van Vleet ES, Horrigan SG, Reid FMH, *et al.* (1986). Chemical and microbiological studies of sea-surface films in the Southern Gulf of California and off the West Coast of Baja California. **19**: 17–98.

Zweifel UL. (1999). Factors Controlling Accumulation of Labile Dissolved Organic Carbon in the Gulf of Riga. *Estuarine, Coastal and Shelf Science* **48**: 357–370.

CHAPTER 2

ORGANIC MATTER SHAPES COMMUNITY COMPOSITON IN GLACIAL ENVIRONMENTS

Contribution of Authors and Co-Authors

Author: Heidi J Smith

Contributions: Designed the experiment, collected samples, analyzed data, wrote the manuscript.

Co-Author: Markus Dieser

Contributions: Assisted with sequence analysis and manuscript preparation.

Co-Author: Christine Foreman.

Contributions: Principal investigator of field sample collection, data analysis, manuscript preparation and editing

Manuscript Information Page

Heidi Smith, Markus Dieser, Christine Foreman
International Society for Microbial Ecology (ISME)
Status of Manuscript:
__X_ Prepared for submission to a peer-reviewed journal
____ Officially submitted to a peer-review journal
____ Accepted by a peer-reviewed journal
____ Published in a peer-reviewed journal

Abstract

Vast expanses of Earth's surface are covered by glacial ecosystems, which provide refuge for active microorganisms. Little is known regarding the biogeographical distribution of microorganisms in these icy habitats and the environmental factors influencing microbial community composition. We examined the microbial community composition from Antarctic and Greenlandic habitats fed by glacial meltwater and evaluated the physico-chemical factors influencing trends in biogeography. While Antarctic environments were hydrologically isolated, high surface runoff and flushing of cryoconite holes on the Greenland Ice sheet (GrIS) interconnected habit types. Antarctic environments were dominated by *Sphingobacteria*, *Flavobacteria*, and *Betaproteobacteria*. Supraglacial habitats from the GrIS were dominated by *Gammaproteobacteria* and *Sphinobacteria*. A core community was not identified, with only 3.1% of the identified operational taxonomic units present across all glacial settings. Microbial assemblages differed across Antarctic glaciers and the GrIS but, clustered within the same geographical locations separated by habitat type (i.e., ice, cryoconite, sediment, and stream water). The predicted metabolic functionality of microbial assemblages was similar for all of the sampled Antarctic habitats; however, significant differences were detected between all Antarctic and GrIS habitats. While the physical environment was unable to explain microbial communities, dissolved organic matter (DOM) quality contributed heavily toward community dissimilarities. Our results demonstrate the establishment of distinct microbial communities poised within diverse ephemeral glacial meltwater driven habitats, with DOM playing an integral role in shaping these communities on local and large spatial scales.

Introduction

Glaciers and ice sheets cover an estimated 11% of the Earth's surface, have both regional and global impacts, and have been proposed to represent a distinct biome (Anesio and Laybourn-Parry, 2012). It is well documented that icy ecosystems are dominated by diverse and biologically active microorganisms that are directly involved in biogeochemical cycling (Boetius *et al.*, 2015; Simon *et al.*, 2009; Anesio and Laybourn-Parry, 2012). Icy environments play a pivotal role in global biogeochemistry cycles, and the sensitivity of these environments to changes in climate will not only affect these cycles but will also impact *in situ* microbial biodiversity (Chown *et al.*, 2015; Cavicchioli, 2015).

On a global scale microbial communities vary along environmental gradients, but little is known about the factors that control the distribution of microorganisms. Even in the advent of non culture-based approaches the assessment of microbial community composition remains one of the most challenging aspects of microbiology due to the enormous microbial diversity (Staley and Gosink, 1999) and the lack of comparable datasets (Ghiglione *et al.*, 2012). The study of biodiversity and diversity across different environments (biogeography) has enabled the discovery of novel physiologies, biogeochemical pathways, survival strategies, and stress response mechanisms (Margesin *et al.*, 2007). However, questions that remain unanswered involve the geographic distribution of prokaryotes (Nemergut *et al.*, 2011), or the scale at which endemic species or cosmopolitans vary across regions (Staley and Gosink, 1999).

To date, fewer studies have focused on regional and global microbial comparisons in cold and icy environments. Conducted studies have explored the biodiversity in marine sea ice (Staley and Gosink, 1999), deep and surface marine waters (Ghiglione *et al.*, 2012), cryoconite environments (Edwards *et al.*, 2014; Cameron *et al.*, 2012; Cameron *et al.*, 2015) snow (Cameron *et al.*, 2015), soils (Van Horn *et al.*, 2013), and across latitudinal gradients (Hodgson *et al.*, 2010; Namsaraev *et al.*, 2010). However, the number of microbial diversity studies is still relatively small to fully understand patterns of microbial diversity in icy environments. For instance, neither Peat *et al.* 2007 nor Neufeld and Mohn 2005 found clear trends in the microbial diversity related to latitudinal gradients in continental Antarctica and the Arctic tundra respectively, while other reports showed a decline in species richness with latitude along the Antarctic Peninsula (Peat *et al.*, 2007). Such conflicting results are further supported by Howard-Williams *et al.* 2010 who found that species diversity varied greatly on a local micro-scale, and that significant latitude-scale effects only emerged when transects were extended into maritime and sub-Antarctic regions. Despite their geographical separation (Arctic vs. Antarctic vs. alpine, lower vs. higher latitude), icy environments are subjected to relatively similar environmental conditions, including extremely low minimum temperatures, frequent freeze-thaw cycles, low water availability, desiccation, and nutrient limitation. As such, the presence of distinct microbial communities in geographically separated ice masses under comparable environmental regimes (e.g., Cameron et al. 2012, 2015) offers intriguing research questions about the factors influencing trends in biogeography, the

metabolic function of individual communities, and the implications of microorganisms on biological processes.

Of the biogeochemical processes occurring within supraglacial environments, the carbon cycle has received particular attention (e.g., Anesio *et al.*, 2009; Cook *et al.*, 2012; Hodson *et al.*, 2010; Stibal *et al.*, 2012). Typically, organic carbon (OC) concentrations are low in glacial environments (~1 mg C L^{-1} on a global average Hood *et al.*, 2015); however, glaciers on a global scale may contain an estimated six petagrams of OC (Hood *et al.*, 2015). Generally, the dominant sources of OC in glacial environments are from aeolian deposition (Stubbins *et al.*, 2012; Antony *et al.*, 2014) and *in situ* microbial production (Anesio *et al.*, 2009). Unlike mountain glaciers and the Greenland Ice Sheet (GrIS) (Telling *et al.*, 2012; Stibal *et al.*, 2008; Edwards *et al.*, 2013; 2014), continental Antarctic supraglacial environments are impoverished in terrestrial OC from aeolian deposition and a sustainable microbial community would therefore be hypothesized to strongly rely on *in situ* production. As microbial communities are influential in the production and processing of labile OC (Anesio *et al.*, 2009; Cook *et al.*, 2012; Hood *et al.*, 2009), we further assume that the quality of glacial OC (labile vs. recalcitrant) as a substrate for heterotrophic metabolism will shape the microbial community composition of a given glacial environment.

In this study, samples were collected from both Antarctic (stream water, stream sediments, glacial ice, snow, and cryoconite holes) and Greenlandic (cryolakes and cryoconite water) glacial meltwater environments that are likely to be exposed to climatic changes. Antarctic samples were collected from hydrologically connected ecosystem

components of both a supraglacial and terrestrial stream ecosystem. While Greenlandic samples were collected from melt-water habitats not directly connected by hydrology. Illumina MiSeq 16S rRNA gene amplicons were analyzed to assess differences in community structures and infer potential metabolic functions. Geochemical parameters were measured to determine effects on community composition. The primary objective was to evaluate potential trends in biogeography and biodiversity across regional and global polar ecosystems fed by glacial melt water. Specifically, emphasis was placed on two Antarctic streams to evaluate the underlying environmental factors governing trends in biogeography. Since glacial habitats are highly susceptible to climate change, a better insight into the environmental factors that shape the community composition and biogeochemical processes will aid our understanding of the spatial variability of diverse supraglacial habitats. Comprehending the impact of local and regional conditions that drive microbial life in glacial ecosystems will be of particular importance when addressing or extrapolating the biogeochemical potential within the biologically active area of ice masses.

Methods

Study Sites and Sample Collection

To assess the biodiversity, biogeography, and environmental parameters that shape the microbial diversity of habitats fed by glacial melt water, multiple glacial ecosystems in Antarctica and Greenland were sampled. The habitats sampled in Antarctica included a supraglacial and terrestrial stream, stream sediments, cryoconite

holes, and glacial ice. Supraglacial features from Greenland included cryoconite holes and cryolakes.

The two glacially fed Antarctic stream ecosystems are located in the McMurdo Dry Valleys. The Cotton Glacier (CG) stream (77°07'S 161°40'E) is a supraglacial stream consisting of a network of braided channels and mostly lacks a sediment-water interface. Sediments are primarily located on lateral margins of the stream and herein referred to as parafluvial sediments. The CG stream is approximately 20 km long and ultimately terminates into the McMurdo Sound. CG stream water (n=10), parafluvial stream sediments (n=11), snow (n=1), and surrounding ice (n=5) were sampled repeatedly during three consecutive summer field seasons between 2009-2012. Canada Stream (77°61'S, 162°59' E) was selected due to its geographical proximity to the CG stream and represents a proglacial stream that flows over a constant layer of coarse sediment. Canada stream ecosystem samples were collected during the 2009/2010 and 2010/2011 field seasons and included: stream water (n=5), stream sediment (n=3), surrounding ice (n=4), snow (n=1), and croyoconite (n=4).

Temperature, pH, conductivity, dissolved oxygen, and total dissolved solids (TDS) measurements were measured on site using a Manta Sub2 probe. Aqueous samples were collected in acid-washed, deionized water (DIW) rinsed (6×) fluorinated carboys. Samples for DOM analysis were collected in acid-washed, DIW rinsed (6×) combusted (450°C for 5 hrs) amber bottles. Sediment samples were aseptically collected with sterile spatulas and placed into cyovials. Snow samples were collected with sterile spatulas and placed into Whirl-Pack high-density polyethylene bags. Ice core and frozen cryoconite

samples were cored with a manual ice corer (Kovacs or SIPRE). Cores were placed into sterile Whirl-Pack high-density polyethylene bags. Samples were transported via helicopter to either the Lake Fryxell field camp or McMurdo Station within 24 hrs for analysis or sample preparation. Cored samples were cleaned to remove any potential contaminants by removing the outer ice (~2 mm) using ethanol cleaned razor blades. Snow samples were slowly melted at 4°. Samples (0.5 - 1L) for microbial community analysis from Antarctic aqueous environments were filtered onto 47 mm Supor®-200 0.2 μm pore size sterile membranes (PALL) under low pressure (<7 psi). Filters were transferred to cryovials containing 4 mL TES buffer (100 mM Tris, 100 mM EDTA, and 2% SDS). Filters and sediments were flash frozen in liquid nitrogen, and stored at −80°C until DNA extraction.

Supraglacial features from the GrIS, positioned within the Paakitsoq region of West Greenland, were sampled during the 2011 summer. Cryoconite water samples (n=9) (69.576N-49.812W) were collected at an elevation of 880 m and hole diameters ranged between 10-18 cm. Cryolake samples (n=5) were collected from Half Moon Lake (69.573N -49:805E) and Lake Ponting (69. 589 N-49.783 E). Throughout the 2011 sampling season the maximum recorded depth, surface area and volume for Half Moon Lake was 1.6 m, 60 000 m^2 and 200,000 m^3, and for Lake Pointing 5.2 m, 480,000m^2 and 1,500,000m^3 (Tedesco *et al.*, 2013). For all GrIS supraglacial habitats aqueous meltwater samples were collected for microbial community analysis on 0.2 μm Sterivex filters (Millipore) with a hand pump. Between 0.5 - 1L of sample water was passed through the filters. Sterivex filter were sealed and filled with RNA*later*® (Ambion) and stored on ice

during transport to the laboratory. Subsequently, samples were kept frozen at -20°C. Upon arrival at Montana State University samples were stored at -80°C until further processing.

Water Chemistry

Water samples were analyzed following the protocols of the McMurdo Dry Valleys LTER Group (Priscu and Wolf, 2000). Samples for non-purgeable dissolved organic carbon (DOC) were filtered in the dark through 25 mm pre-combusted GF/F filters and analyzed on a Shimadzu TOC-V. Water was filtered through 25 mm pre-combusted GF/F filters for macronutrient analysis and frozen prior to analysis on a Lachatt autoanalyzer. Samples for anion and cation analysis were filtered through 0.4 μm 47 mm Nucleopore filters and the filtrate was analyzed on a Dionex DX-ion chromatography system. Samples for particulate organic carbon (POC) and particulate organic nitrogen (PON) were filtered through 25 mm pre-combusted GF/F filters, allowed to air dry at room temperature for 12 hrs and frozen prior to analysis. POC/PON samples were analyzed using a Flash EA 112 ThermoQuest elemental analyzer. Infrared gas analysis was used to measure dissolved inorganic carbon. Geochemical data were statistically analyzed using a general linear model (GLM) of analysis of variance (ANOVA) in Minitab 17.

Fluorescence Spectroscopy

Samples were filtered through pre-combusted GF/F filters into acid washed pre combusted amber bottles prior to optical analysis. Samples were then analyzed for UV-absorbance using an Agilent 8453 UV-spectrophotometer in a 1 cm quartz cuvette and

were scanned from 190 nm to 1100 nm. Absorbance measurements greater than 0.3 at 254 nm were diluted with Milli-Q water to prevent inner-filter effects during collection of emission excitation matrices (EEMs) (Miller and McKnight, 2010). EEMs for the 2009-2010 field season were collected with a Horiba Jobin Yvon Fluoromax-3, while EEMs for the 2010-2011 and 2011-2012 field seasons were collected with a Fluoromax-4 Spectrofluorometer. Both instruments were equipped with a Xenon lamp light source and a 1 cm path length quartz cuvette. Excitation (Ex) wavelengths were scanned from 240-450 nm in 10 nm intervals and emission (Em) was recorded between 300-550 nm for the Fluoromax-3 and 300-560 for the Fluoromax-4, in 2 nm increments, with a 5 nm slit width and 0.25 s data integration time for both instruments. Post processing was completed in MATLAB to generate EEMs corrected for inner filter effects, Raman scattering, and blank water subtraction (McKnight *et al.*, 2001; Lawaetz and Stedmon, 2009).

Fluorescence intensity (F.I.) values were normalized across different sample locations (F.I.-minimum F.I/ maximum F.I - minimum F.I.). F.I. values were then summed based on DOM classifications (Coble, 1996) and peak maxima in these specific fluorescent regions. For this study protein-like fluorescence was divided into the following individual fluorescing components: B1: Ex/Em 240-260/300-326, B2: Ex/Em 270-290/300-326, T1: Ex/Em 240-260, and T2: Ex/Em 270-290/328-350. More recalcitrant humic-like fluorescence regions were split into the A: Ex/Em 240-260/400-425 and C: Ex/Em 300-360/400-450 fluorophores.

DNA Extraction and PCR Amplification

The PowerSoil DNA extraction kit (MoBio, Carlsbad, CA, USA) was used to extract genomic DNA from filters and sediment samples following manufacture's recommendations. For samples collected on Sterivex filters genomic DNA was extracted using the PowerWater Sterivex extraction kit (MoBio, Carlsbad, CA, USA) following manufacture's recommendations. Extracted genomic DNA was quantified using Qubit DNA Assay Kit (Molecular Probes, Eugene, OR, USA) with either the high sensitivity or broad range quantification standards. The V3/V4 regions of the 16S rRNA gene were amplified in 50 µl PCR reactions. PCR reactions contained 100-200 pg of extracted genomic DNA, 0.1 µM of each primer (UW Biotechnology Center, Madison, WI, USA), a 1X final concentration of Bulls Eye PREMIUM Taq 2X Mix (Midwest Scientific, St Louis, MO, USA), and adjusted volumes of nuclease free water. The primer design used for amplification of the 16S rRNA gene consisted of the Illumina adaptor sequences followed by either the universal 341F 5'acactctttccctacacgacgctcttccgatctCCTACGGGNGGCWGCAG -3' or 805R 5'gtgactggagttcagacgtgtgctcttccgatctGACTACHVGGGTATCTAATCC -3'. PCR was performed in an Eppendorf Mastercycler pro S. The amplification protocol consisted of an initial denaturation at 95°C for 3 min, followed by 30 cycles of denaturation at 95°C for 30 s, annealing at 55°C for 30 s, extension at 72°C for 30 s, and a final extension step at 72°C for 5 min. A negative PCR control without DNA template added was included in the PCR protocol. Additionally, DNA extractions from filter- and extraction blanks were PCR amplified (Nguyen *et al.*, 2015; Salter *et al.*, 2014). The presence of PCR products

of the correct size were confirmed by band visualization in a 1.0% agarose 1X TAE buffered gel stained with GelRed™.

Sequencing and Sequencing Analysis

Amplified DNA was submitted to the University of Wisconsin-Madison Biotechnology Center. Paired end, 250 bp sequencing was performed using the Illumina MiSeq Sequencer and a MiSeq 500 bp (v2) sequencing cartridge. Images were analyzed using the standard Illumina Pipeline, version 1.8.2. Forward and reverse sequence were joined with the Quantative Insights Into Microbial Ecology (QIIME) toolkit version 1.9.0 (Caporaso *et al.*, 2010). Subsequently, contigs were analyzed with the Mothur platform v.1.34.4 (Schloss *et al.*, 2009). For sequence quality refinement sequences containing ambiguous bases, homopolymers longer than eight bases, or an average quality score below 30 over a 50 bp window were excluded from further analysis (Schloss *et al.*, 2011). The maximum sequence length from a bidirectional MiSeq run was 467, and sequences shorter than 450 bp were removed. Processed sequences were aligned against the SILVA Gold database in Mothur followed by the identification and removal of chimeric sequences with UCHIME (Edgar *et al.*, 2011) in combination with the SILVA Gold database followed by a second chimera check using the sequence collection from the present study as a database. Sequences were classified with a Bayesian method (Wang *et al.*, 2007) using the Mothur formatted version of the RDP classifier. An operational taxonomic unit (OTU) was defined at ≥97% 16S rRNA sequence identity. All OTUs found in the sequenced blank samples (extraction kit blank, filter blank, PCR

blank) were removed from each corresponding sample to remove any potential source of contamination.

Statistical Analysis of Sequencing Samples

The Antarctic McMurdo Dry Valleys are a polar desert and precipitation events are rare, only a single snow sample from both the CG stream and Canada Stream were available and thus excluded from subsequent statistical analysis. For individual samples OTU richness (Chao1; Chao, 1984); and inverse Simpson, (Simpson, 1949)) were calculated within the Mothur platform v.1.34.4. Comparisons of OTUs grouped together by environmental location were made using a non-parametric multivariate analysis of OTU similarities (ANOSIM; Clarke and Warwick, 2001) approach within the Mothur platform v.1.34.4. ANOSIM produces the test statistic R. As such, large R values (close to 1) are indicative of complete separation of two groups, while small R values (close to zero) imply little or no segregation implying that the null hypothesis is true (Clarke and Warwick 2001). The first 200 OTUs which accounted for 89% of the entire sequence library, were subjected to similarity percentage (SIMPER) analysis using PAST version 3.10 to identify the taxa that were mainly responsible for the differences observed between groups. A canonical correspondence analysis (CCA) was performed with Canoco v4.5 (Microcomputer Power Inc., Ithaca, NY, USA), to determine relationships between geochemical measurements, including DOM quality, and OTU matrices from the individual environments. OTU profiles were square root transformed and environmental variables were standardized to unit variance prior to CCA analysis. Within Canoco, detrended canonical correspondence analysis (DCCA) was used to obtain the

length of the gradient in the species data. This allowed for the selection of the appropriate method (unimodal or linear) of CCA analysis where a gradient length ≥4 supports the use of a unimodal method of analysis (gradient length = 5.74 and 4.03 for the comparison between all ecosystem components, respectively). Bray Curtis dissimilarity matrices were created from OTU tables using non-metric multidimensional scaling (MDS) refined by the Kruskal's stress. The Phylogenetic Investigation of Communities by Reconstruction of Unobserved States (PICRUSt) bioinformatics tool (Langille *et al.*, 2013) was used to predict gene family abundances from OTUs classified with Greengenes within Mothur v.1.34.4. Functional gene profiles were generated with the Statistical Analysis of Metagenomic Profiles (STAMP; version 2.1.3) software.

Results

Microbial Assemblages

Samples of CG stream water (n=10), CG stream parafluvial sediments (n=11), CG ice (n=4), Canada Stream water (n=5), Canada Stream sediments (n=4), Canada Glacier ice (n=4), Canada Glacier cryoconite (n=4), Greenland cryoconite (n=9), and Greenland cryolakes (n=5) were collected for molecular analysis and DNA was successfully extracted from all of the above samples. The raw Illumina MiSeq data set consisted of 76026 ± 15449 (average ±S.D.) reads per sample. Quality refined sequence libraries contained on average 8913 ± 5640 reads, which clustered into a total of 2156 OTUs across all samples. Of these OTUs, 25.7, 37.0, and 3.8% were unique to the different geographic locations Cotton Glacier, Canada Glacier, and Greenland, respectively. Only

3.1% of the OTUs were present in all three glacial settings. Cotton and Canada Glacier microbial assemblages shared 29.3% of the OTUs, while assemblage similarities between Antarctic and Greenlandic glacial environments were <1.0%. Taxonomic analysis at the class level showed that the relative abundance of sequences from glacial Antarctic environments were dominated by *Sphingobacteria* (48% ± 6%), *Flavobacteria* (20% ± 11%), *Betaproteobacteria* (8% ± 3%), and *Gammaproteobacteria* (4% ± 2%) while supraglacial aquatic habitats from Greenland were primarily dominated by *Gammaproteobacteria* (66% ± 11%), *Sphingobacteria* (24% ± 8%), and *Betaproteobacteria* (3% ± 2%) (Figure 2.1). We acknowledge that the primer pair used in this study did not amplify cyanobacteria and therefore our results may not represent the true structure of microbial assemblages.

Microbial Biodiversity

The observed number of OTUs across all sampled habitats showed similar patterns when compared to the predicted alpha diversity indices (Chao and Inv Simpson) indicating that microbial assemblages were sequenced to a sufficient depth (Figure 2.2) The greatest diversity based in Chao richness estimates was on average found in the Canada Stream water (524.0 – 535.6; 95% CI), followed by the CG stream water (395.3 – 411.4; 95% CI). Species richness for stream sediments, ice, and cryoconite from Cotton and Canada Glacier ranged on average between 116.4 and 258.6 (95% CI). The lowest numbers of species richness were calculated for supraglacial lake (54.8 – 64.0; 95% CI) and cryoconite (52.9 – 62.2, 95% CI) microbial assemblages from the GrIS.

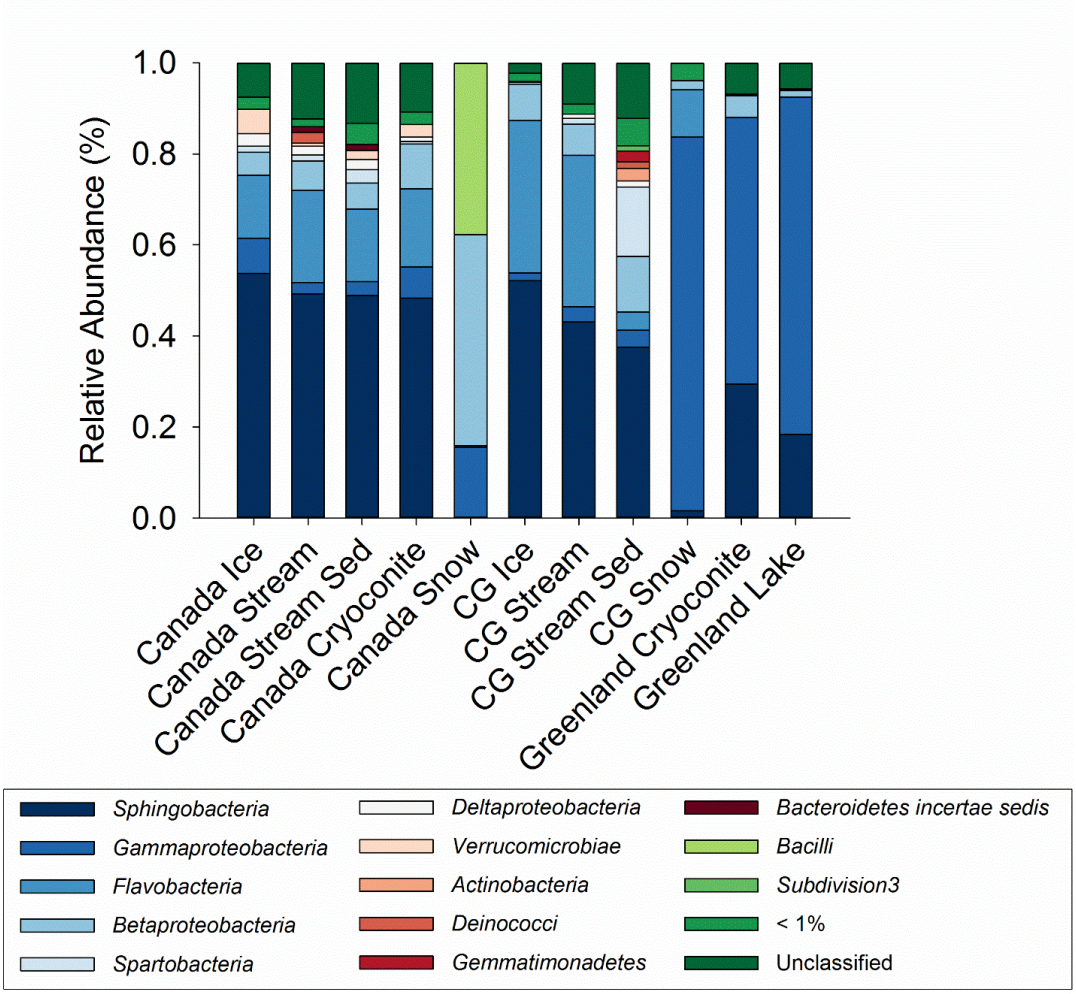

Figure 2.1. Relative abundance of MiSeq 16S rRNA amplicon sequences representing the distribution of microbial assemblages with individual samples grouped together based on sampling location. Percentages are reported at the class taxonomy level.

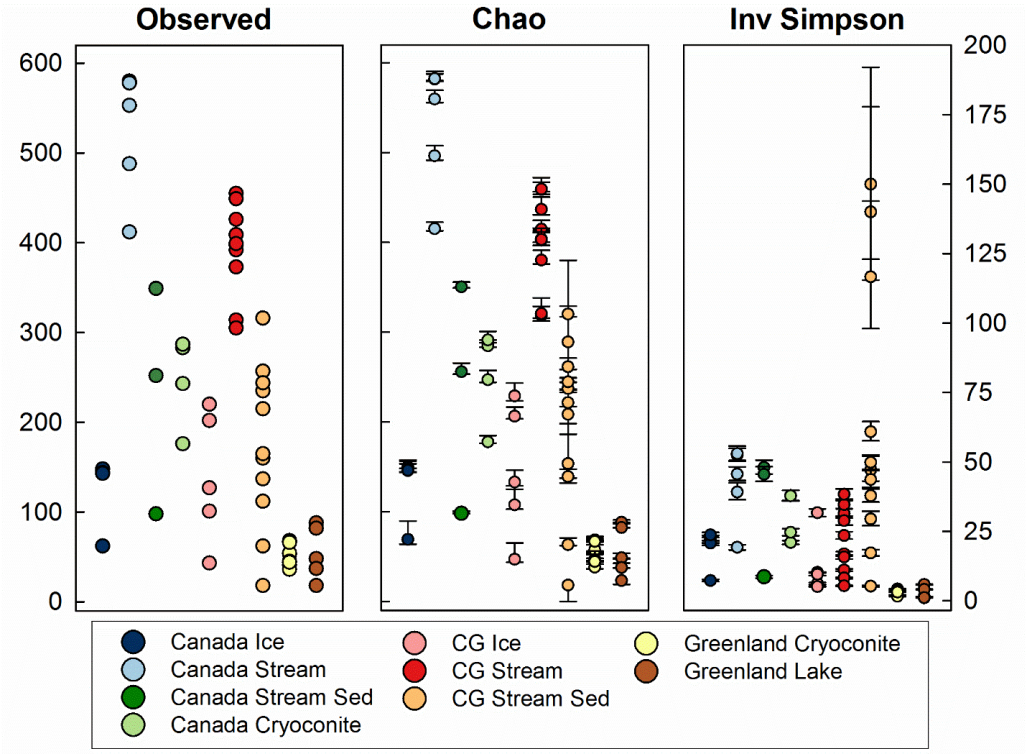

Figure 2.2. Microbial α diversity indices (from left to right), of the number of observed OTUs for each sample color coded based on sample location. Middle panel is the Chao1 estimated species richness, and far right is the inverse Simpson's species richness estimation. Both diversity indices yielded species richness patterns similar to the observed richness, suggesting that all environmental locations were sequenced at sufficient depth.

Inverse Simpson which accounts for richness and evenness estimated the largest biodiversity on average for CG stream sediments (55.4 – 75.1; 95% CI; Figure 2.2), similar to Chao, species biodiversity was lowest for supraglacial samples from Greenland (2.7 – 3.2; 95% CI).

To show which phenotypes contributed the most to the dissimilarity between environments, the 200 most abundant OTUs were tested with SIMPER analysis, using a Bray–Curtis dissimilarity matrix (Table 2.1). The overall dissimilarities between Antarctic vs. Greenland, and CG vs. Canada Glacier microbial assemblages were 96.6%

and 86.3% respectively. In general, only a small number of OTUs accounted for ~50% of the differences observed between Antarctic vs. Greenland (8 OTUs) and CG vs. Canada Glacier (24 OTUs). OTUs closely related to *Pseudomonadaceae* (21.3%) and *Sphingobacteriaceae* (11.6%) were the strongest indicators in distinguishing Antarctic vs. Greenland microbial assemblages, while *Cytophagaceae* (15.9%), *Flavobacteriaceae* (15.0%), and *Chitinophagaceae* (13.7%) were mainly responsible for the differences between the CG vs. Canada Glacier environment. The overall dissimilarity between pairwise comparisons of different Antarctic locations ranged from 60.1% to 82.9% (Table 2.1). Similarly, the number of OTUs explaining ~50% of the dissimilarities was small, ranging between 7-16 OTUs. Pairwise differences between locations from CG were driven by *Cytophagaceae* (22.9-34.7%) and *Flavobacteriaceae* (18.6-23.85%), while, in addition to these two families, *Sphingobacteriaceae* (13.3%) and *Chitinophagaceae* (13.7%) contributed to dissimilarities between Canada Stream sediment vs. Canada Stream and Canada cryoconite vs. Canada ice respectively. Differences between Greenland cryolake and cryoconite were mainly described by two *Pseudomonas* phenotypes (48.8%).

Table 2.1. SIMPER analysis of the top 200 most dominant OTUs (that make up ~50% of the dissimilarity between samples) of samples grouped together by environmental location. Amplicons related to the family taxonomic classification with the corresponding percent dissimilarity (Bray-Curtis) between environments and the number or OTUs.

	Percent dissimilarity between environments and number of OTUs ()							
Taxonomy at the Family Level	**CG Ice vs. CG Stream**	**CG Stream vs. Canada Stream**	**CG Stream Sed vs. CG Stream**	**Canada Stream Sed vs. Canada Stream**	**Canada Cryoconite vs. Canada Ice**	**Greenland Cryolake vs. Greenland Cryoconite**	**All CG vs. All Canada**	**All Antarctic vs. All Greenland**
Cytophagaceae	34.7 (4)	22.9 (5)	18.1 (4)	12.0 (2)	11.9 (4)		15.9 (5)	3.2 (1)
Flavobacteriaceae	18.6 (3)	23.8 (6)	16.5 (3)	19.2 (5)	7.1 (2)		15.0 (8)	3.7 (1)
Sphingobacteriaceae		3.7 (1)		13.3 (2)	8.6 (2)		7.0 (2)	11.6 (1)
Chitinophagaceae			8.8 (3)		13.7 (6)		10.1 (7)	5.3 (1)
Spartobacteria_family_incertae_sedis			2.9 (1)	3.1 (1)			1.4 (1)	
Moraxellaceae			2.1 (1)					
Oxalobacteraceae			1.7 (1)					
Verrucomicrobiaceae				2.9 (1)				
Pseudomonadaceae						48.8 (2)		21.3 (2)
Enterobacteriaceae								3.3 (1)
Xanthomonadaceae					2.9 (1)		1.3 (1)	2.8 (1)
Cryomorphaceae					3.5 (1)			
Total number of OTUs explaining 50% dissimilarity	7	12	13	11	16	2	24	8
Cummulative overall mean realtive abundance of OTUs per location (%) that contributed ~50% of dissimilarity	46/53	32/48	50/27	28/26	39/50	26/55	34/45	13/75
Overall average dissimilarity	60.1	63.9	82.9	82.3	67.9	86.3	96.6	74.7

Global multivariate data from the ANOSIM comparison (Table 2.2) established a statistically significant difference between all sites ($R=0.728$, $P<0.001$). A subsequent pairwise comparison revealed that only CG ice microbial assemblages showed a strong overlap with the CG stream ($R=0.410$, $P=0.011$) and Canada stream ($R=0.400$, $P=0.005$) microbial assemblages. R-values <0.25 for Canada cryoconite vs. Canada ice ($R=0.198$, $P=0.081$) and Greenland cryoconite vs. Greenland cryolake ($R=0.112$, $P=0.156$) indicated that the microbial assemblages were undistinguishable. All other pairwise comparisons produced R values varying from mid-range ($R=0.559$) to unity ($R=1$) and were inferred to be statistically different at P-values between <0.001 - 0.035. These R-values indicated groups were overlapping, but clearly different ($R>0.5$) or distinct ($R>0.75$). Lastly, MDS of Bray-Curtis indices of OTU profiles clustered the three glacial location into distinct clades (Figure 2.3). Within each clade sample types clustered into their own separate group with the exception of one CG sediment sample that grouped more closely with Canada Glacier samples. Overlap was found between CG ice and CG stream samples.

Predicted Metabolic Function

Out of the eight generally assigned functional classes more than 50% of the predicted genes were assigned to metabolism (Figure 2.4). Relatively little variability in the percentage of genes associated with general metabolic features were found for Antarctic environments (53.7-57.2%) and only CG stream sediments were statistically different from any other Antarctic environment ($P<0.01$). Conversely, both Greenland

Table 2.2. Pairwise permanova comparisons of microbial community composition (RDP aligned OTU (97% sequence similarity) profiles) from different environmental locations.

Sample ID	R-value	P-value
All Samples	0.7279	<0.001*
CG_Ice-CG_Sed	0.7483	<0.001*
CG_Ice-CG_Stream	0.4102	0.011
CG_Ice-Canada_Cryoconite	0.7625	0.006
CG_Ice-Canada_Ice	0.8188	0.012
CG_Ice-Canada_Stream	0.4000	0.005
CG_Ice-Canada_Stream_Sed	0.7436	0.020
CG_Ice-Greenland_Cryoconite	0.9377	<0.001*
CG_Ice-Greenland_Lake	0.8960	0.008
CG_Sed-CG_Stream	0.7349	<0.001*
CG_Sed-Canada_Cryoconite	0.8487	0.001*
CG_Sed-Canada_Ice	0.9553	<0.001*
CG_Sed-Canada_Stream	0.8059	<0.001*
CG_Sed-Canada_Stream_Sed	0.8913	0.002
CG_Sed-Greenland_Cryoconite	0.9987	<0.001*
CG_Sed-Greenland_Lake	0.9681	<0.001*
CG_Stream-Canada_Cryoconite	0.8441	0.002
CG_Stream-Canada_Ice	1.0000	<0.001*
CG_Stream-Canada_Stream	0.5585	0.002
CG_Stream-Canada_Stream_Sed	0.9444	0.006
CG_Stream-Greenland_Cryoconite	0.9956	<0.001*
CG_Stream-Greenland_Lake	0.9556	<0.001*
Canada_Cryoconite-Canada_Ice	0.1979	0.081
Canada_Cryoconite-Canada_Stream	0.8313	0.009
Canada_Cryoconite-Canada_Stream_Sed	0.5741	0.035
Canada_Cryoconite-Greenland_Cryoconite	0.9987	0.002
Canada_Cryoconite-Greenland_Lake	0.9000	0.005
Canada_Ice-Canada_Stream	0.9688	0.008
Canada_Ice-Canada_Stream_Sed	0.5926	0.028
Canada_Ice-Greenland_Cryoconite	0.9987	0.001*
Canada_Ice-Greenland_Lake	0.9438	0.005
Canada_Stream-Canada_Stream_Sed	0.6923	0.020
Canada_Stream-Greenland_Cryoconite	0.9990	<0.001*
Canada_Stream-Greenland_Lake	0.8578	0.011
Canada_Stream_Sed-Greenland_Cryoconite	0.9677	0.003
Canada_Stream_Sed-Greenland_Lake	0.8769	0.013
Greenland_Cryoconite-Greenland_Lake	0.1121	0.156

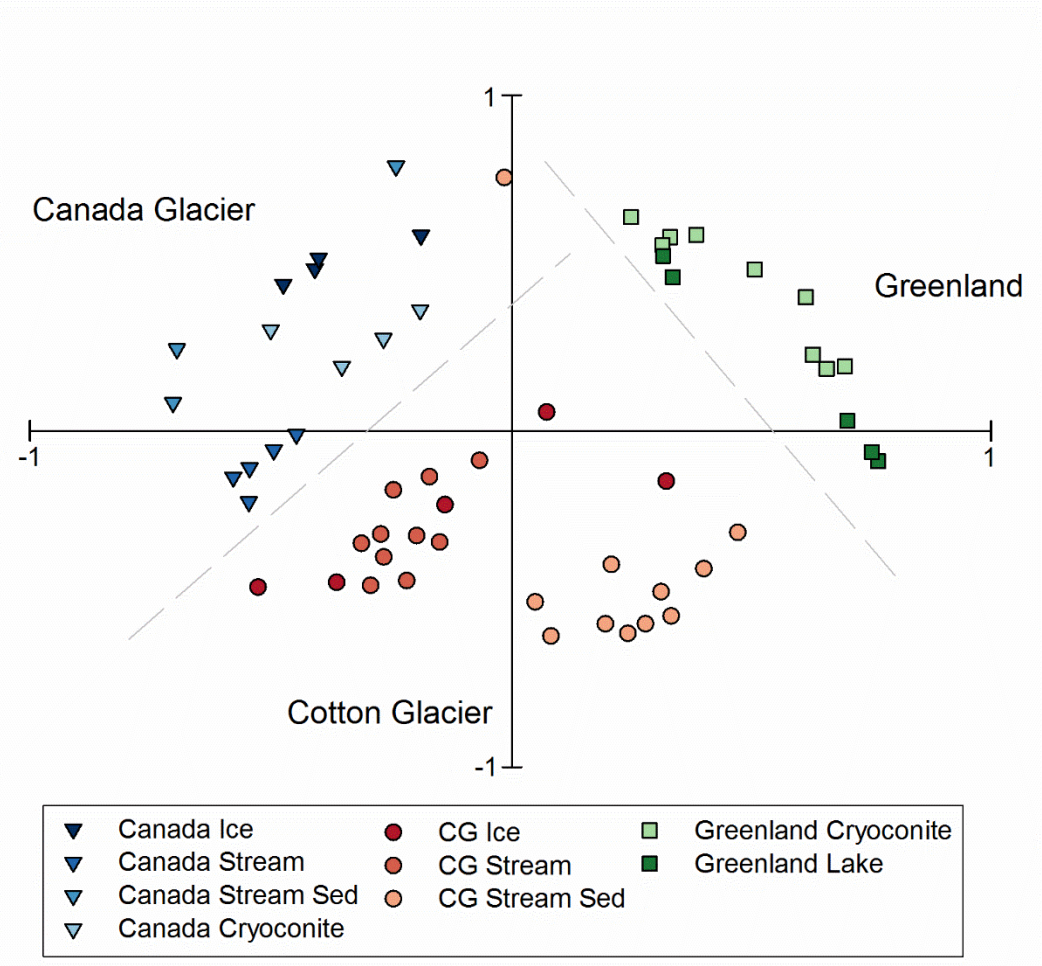

Figure 2.3. Multidimensional scaling plot of Bray–Curtis indices on the relative abundance of OTU (97% sequence similarity) profiles for different environmental locations. Dashed lines delineate the different sampled environmental locations (CG stream, Canada Stream, and Greenland)

supraglacial environments showed a wider range of proportion of sequences related to metabolic features (47.0-56.8% of the total predicted genes). Additionally, the predicted metabolic function of Greenland supraglacial environments was significantly different from Canada Stream, Canada stream sediments, CG stream, and CG ice ($P<0.05$). Specifically, of the 64 lower level functional annotations, 33.5-39.0% of the sequence predicted functions in all environments were represented by membrane transport,

carbohydrate, amino acid, and energy metabolism. No significant differences ($P<0.1$ to $P>0.1$) were found for these predominate four lower level functional classifications between the different Antarctic environments. In contrast, membrane transport, carbohydrate, amino acid, and energy metabolism were more represented in some of the CG and Canada Glacier microbial assemblages (mainly CG Steam, CG ice, and Canada Stream) when compared to the DNA pool within cryolakes and cryoconite microbial assemblages from Greenland ($P<0.05$; Figure 2.4).

Stream Water Geochemistry

Distinct DOM signatures were present between the CG stream and Canada Stream water (Figure 2.5B-C). Most notably was the absence of both the humic-like A and C peaks in the CG stream water samples compared to the Canada Stream OM. The OM signatures for both the CG stream and the Canada Stream remained relatively consistent throughout the field seasons. The identified regions of fluorescence maxima did not drastically shift across sample environments (Table 2.3), while the relative proportions of fluorophores measured in F.I. were significantly different across environments. The F.I. for B1, B2, and T1 for the Canada Stream were significantly different from the other locations ($P<0.04$). For the humic-like A fluorophore significant differences based on location were observed specifically for the Canada Stream, Canada Cryoconite and CG ice locations, while humic-like C followed a similar trend and the Canada Stream and CG ice F.I. were significantly different from the other locations ($P<0.01$).

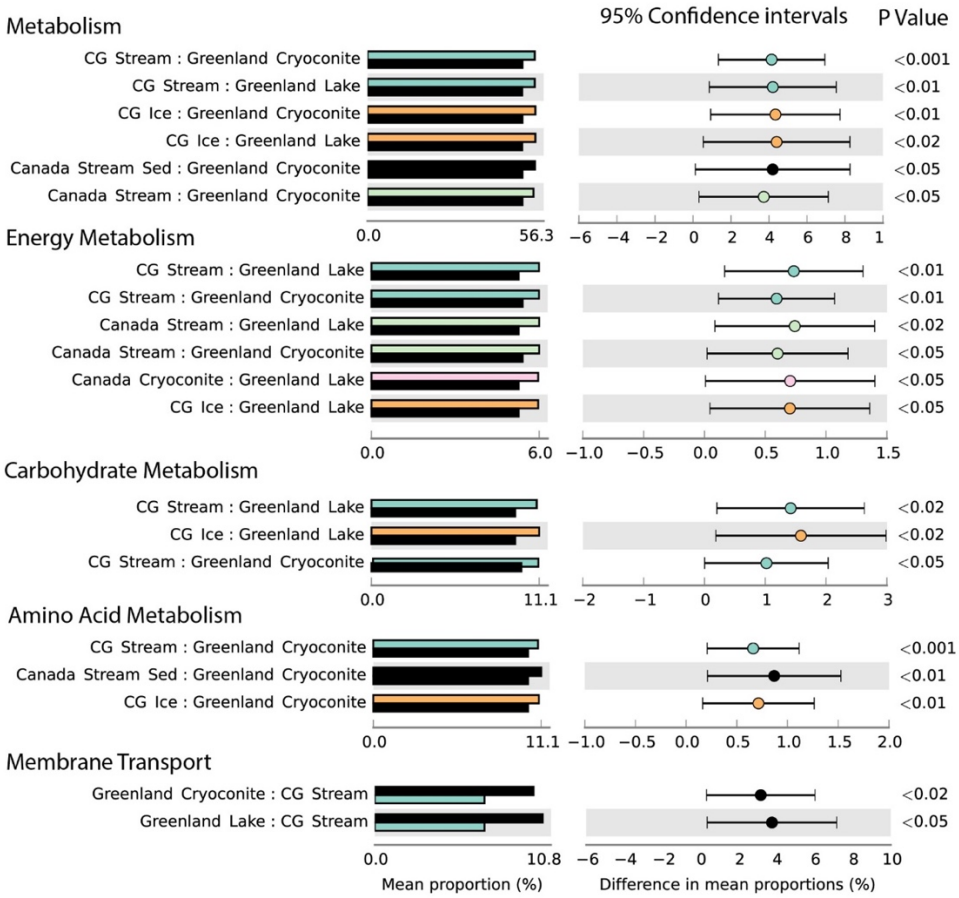

Figure 2.4. Results of PICRUSt analysis showing the relative abundance of Kyoto Encyclopedia of Genes and Genomes (KEGG) ortholog groups for sampled polar environments. Only comparisons that were significantly different in the proportions of predicted genes for a specific function ($P<0.05$) between sample locations for different metabolic and genetic functions are displayed.

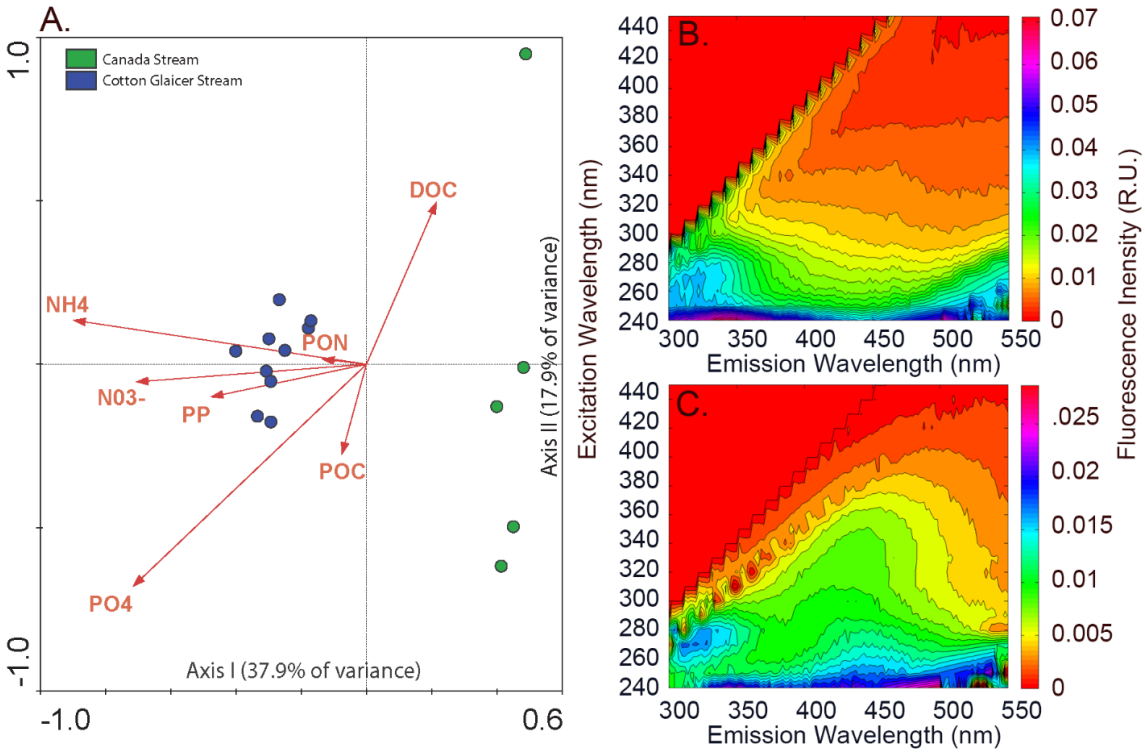

Figure 2.5. Canonical correspondence analysis of the influence of environmental variables on the relative abundance of square root transformed OTU (97% sequence similarity) profiles for the CG and Canada streams. Excitation emission matrices (EEMs) of DOM from: B.) the CG stream and the C.) Canada Stream. Colored contours are representative of emission fluorescence intensities (F.I.). Note the absence of a peak maxima and low F.I. of humic-like A and C peaks in the CG stream compared to the Canada Stream.

Table 2.3. Summary of previously identified fluorophore designations (Coble 1996, Marhaba et al. 2000), and the range of the Ex/Em maxima for fluorescing regions present fluorescence intensity maxima in for each environmental location.

			Environmental Location						
Fluorophore Designation	Ex/Em Max (nm)	Compositional Description	Canada Stream Ex/Em Max (nm)	CG stream Ex/Em Max (nm)	CG Ice Ex/Em Max (nm)	CG Sediment Ex/Em Max (nm)	Canada Glacier Cryoconite Ex/Em Max (nm)	Canada Glacier Ice Ex/Em Max (nm)	Canada Stream Sediment Ex/Em Max (nm)
	225-237/309-321	Protein-like	240/316-326	240-260/300-326	240-260/308-324	240-260/300-322	240-260/300-324	240/324-326	240-260/326
B	275/310	(Tryrosine)	270-290/300-326	260-270/300-322	270/300-324	270-290/300-302	270-290/300-302	270-290/304-326	270/300-326
		B1/B2 F-Max	0.067/0.083	0.234/0.228	0.238/0.282	0.158/0.177	0.087/0.116	0.119/0.109	0.573/0.742
	225-237/340-381	Protein-like	240/328-348	240/338-350	240/328-332	250/340-350	240/338-346	240/340-348	240/328-348
T	275/340	(Tryptophan)	270-280/328-350	270/328-350	270/328-334	270/328	270/328	290/328-348	270/328
		T1/T2 F-Max	0.058/0.037	0.571/0.345	0.235/0.266	0.196/0.098	0.066/0.068	0.239/0.271	0.679/0.786
A	237-260/400-500	Humic-like	240/420-444	240/420-450	240/420-430	240/420	240/422-424	240/420-422	240/420-436
		A F-Max	0.071	0.0352	0.013	0.123	0.068	0.064	0.749
C	300-370 / 400-500	Humic-like	330/428-438	300/400-420	330-360/400-408	330/400-414	330/420-446	330/400-408	300/400-450
		C F-Max	0.020	0.009	0.003	0.024	0.006	0.014	0.014

Table 2.4. Stream water chemistry and physical measurements for the Cotton Glacier stream and Canada Stream. Cotton Glacier stream data (DOC, pH, Chl-*a*, DIC, NH_4^+, NO_3^-, $PO4^{-2}$, Cl^-, SO_4^{-2}, Na^+, K^+, Mg^{+2}, and Ca^{+2}) for the 2009/2010 and 2010/2011 sampling dates is from SanClements et al. In Review (2016). Samples were averaged across the two locations, the mean values in bold indicate a statistically significant differences between the two stream locations ($P<0.05$, ANOVA, GLM)

	Sampling Date	DOC (mg/L)	DIC (mg C/L)	µg N as NH_4^+/L	µg N as $N0_3^-$/L	µg P as PO_4^{-2}/L	Chl-*a* (µg/L)	F^- (mg/L)	Cl^- (mg/L)	SO_4^{-2} (mg/L)	Na^+ (mg/L)	K^+ (mg/L)	Mg^{+2} (mg/L)	Ca^{+2} (mg/L)	PON (µg/L)	POC (µg/L)	PP (µg/L)	pH	Conductivity (µS/cm²)	DO (mg/L)	Stream Temp (°C)
Cotton Glacier Stream	12/09/2009	0.68	0.78	5.28	95.89	1.73	0.01	0.04	1.65	1.07	1.07	0.24	0.28	0.90	24.35	309.45	23.39	6.01	NA	14.50	0.77
	12/15/2009	0.44	0.74	5.49	57.87	1.46	0.45	0.03	1.36	1.22	1.00	0.23	0.23	0.87	12.63	216.29	11.51	6.40	15.40	13.70	1.90
	12/23/2009	0.95	0.97	6.19	62.35	1.85	0.40	0.05	1.75	1.93	1.23	0.22	0.27	1.09	8.07	199.14	14.42	6.56	12.60	14.50	1.20
	12/30/2009	0.71	0.82	4.37	46.35	1.65	0.21	0.05	1.37	1.38	0.93	0.21	0.20	0.67	8.30	165.53	24.54	6.70	10.10	14.60	1.30
	11/24/2010	1.68	0.44	4.22	50.25	1.65	0.27	0.02	1.52	1.08	0.93	0.12	0.43	0.94	37.91	318.50	3.24	7.45	12.90	NA	1.95
	12/7/2010	1.33	0.85	5.43	75.27	1.17	0.08	0.03	2.49	1.69	1.42	0.13	0.52	1.38	34.33	540.06	5.53	6.34	18.10	14.16	1.68
	12/13/2010	1.21	0.76	5.75	47.88	1.63	0.09	0.04	2.33	1.68	1.38	0.13	0.47	1.20	21.89	380.80	5.24	6.82	17.10	14.36	2.56
	12/29/2010	0.32	0.75	4.24	23.50	1.81	0.09	0.02	1.46	0.99	0.94	0.11	0.41	0.85	30.47	592.31	6.82	8.01	8.30	14.39	0.40
	01/12/2011	0.44	NA	4.21	21.33	1.53	0.17	0.02	2.33	0.92	0.93	0.10	0.32	0.87	29.18	587.63	6.23	NA	NA	NA	NA
	01/10/2012	0.31	0.76	5.36	24.55	1.68	0.33	0.02	2.12	1.08	0.97	0.12	0.23	1.03	7.22	160.89	5.35	6.46	14.20	8.96	1.64
Mean		0.81	**0.76**	**5.05**	**50.53**	**1.62**	0.21	0.03	1.84	**1.30**	**1.08**	**0.16**	0.34	**0.98**	21.43	347.06	**10.63**	6.75	**13.59**	**13.65**	**1.49**
Canada Stream	12/07/2009	0.04	1.13	2.09	29.76	1.36	0.08	ND	2.99	2.08	1.54	0.49	0.30	2.36	19.72	410.23	7.49	7.46	16.95	10.74	6.85
	12/14/2009	0.36	1.24	2.61	16.40	1.58	0.10	0.04	2.28	1.83	1.58	0.56	0.26	2.54	11.32	305.13	6.98	6.96	15.96	12.50	4.04
	12/09/2010	1.8	1.44	2.88	7.22	ND	0.09	0.03	1.82	2.04	1.18	0.46	0.47	2.25	17.25	232.67	2.06	6.38	47.50	9.52	5.82
	12/17/2010	2.46	2.34	2.81	12.27	0.88	0.22	0.04	5.34	6.00	2.12	0.84	0.77	5.33	23.40	308.01	2.10	6.52	25.50	10.82	3.48
	12/22/2010	0.20	1.01	2.02	13.45	1.12	0.13	0.02	1.60	2.04	1.07	0.40	0.43	1.84	18.92	353.83	5.22	6.70	19.86	10.03	7.49
Mean		0.97	**1.43**	**2.48**	**15.82**	**1.23**	0.12	0.03	2.81	**2.80**	**1.50**	**0.55**	0.45	**2.86**	18.12	321.98	**4.77**	6.80	**25.15**	**10.72**	**5.54**

Both the CG stream and Canada Stream had low ionic strength and near neutral pH (mean pH 6.77 ± 0.50). Of notable importance is the significantly higher concentrations of NH_4^+, NO^{3-}, PO_4^{-2}, and particulate phosphorous ($P<0.01$) within the CG stream.

Relationship of Environmental Variables to Microbial Biodiversity

The CCA of CG steam and Canada stream water OTU profiles and associated geochemistry was used to infer whether any of the environmental variables had an effect on the microbial assemblages between the two stream locations. Initially, all collected stream geochemistry measurements were included in the analysis, but in order to develop a statistically significant and robust model, several variables were removed (Table 2.4). In particular, temperature, pH, dissolved oxygen, and conductivity were statistically insignificant parameters for explaining microbial assemblages. The established model (Figure 2.5A) explained 76.5% ($P=0.024$) of the total variation within the 16S rRNA community profiles while avoiding collinearity and variance inflation. The first three axes explained 66.5% of the total variance (all model eigenvalues >0.10) with the first axis explaining 37.9% of the variance ($P=0.004$). The patterns identified by the CCA indicated separate clustering of the samples from the two streams; each stream location clustered together on opposites sides of the second axis in the model. The CCA model emphasized the influence of nitrogen and phosphorus on the microbial assemblages in the CG stream. Neither of the two streams clustered closely around the DOC variable, suggesting that the overall OC concentrations were not responsible for influencing the microbial assemblages. Specific fractions of nitrogen (NH_4^+ and NO_3^-) as well as PO_4^-

had longer vectors and appeared to be responsible for explaining the CG microbial assemblages in comparison to the Canada Stream.

To determine the effect of DOM quality on microbial assemblages in glacial environments, a CCA model was generated including the F.I. for different DOM fluorophores and OTU profiles (Figure 2.6). The established model explained 86.9% (P=0.004) of the total variation across all OTU profiles; thereby, 77.9% of the total model variance being described by the first three axes (all model eigenvalues >0.16). The first axis explaining 51.2% of the variance (P=0.002). Microbial assemblages from the GrIS clustered closely together and were best explained by the protein-like component B1. Canada Stream microbial assemblages were clearly described by the presence of humic-like fractions of DOM. Phylotype composition from Canada Stream sediment, Canada Cryoconite, and CG sediment samples were partially influenced by humic- and protein-like DOM constituents. Based on the model, OTUs found in the CG stream, CG ice, and Canada ice were best described by protein-like B2 and T2 fluorophores of DOM.

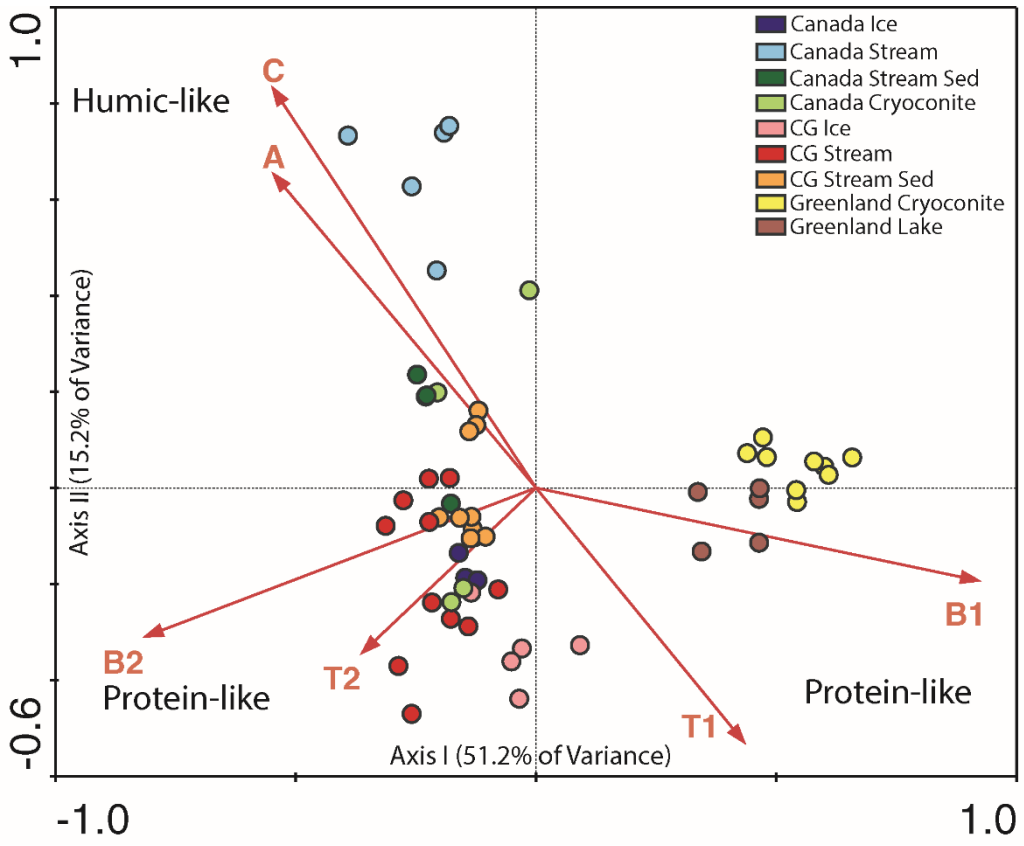

Figure 2.6. Canonical correspondence analysis of the influence of fluorescent OM variables on the relative abundance square root transformed OTU (97% sequence similarity) profiles for sampled glacial environments represented by different colored circles. Fluorescing OM variables are fluorescence intensities (F.I.) of fluorophores commonly observed in natural waters (Coble 1996) from each sample. F.I. from the protein-like fluorescent OM components are represented as B1 and B2 (tyrosine-like) and T1 and T2 (tryptophan-like). F.I. from humic-like fluorescent OM components are represented by A and C.

Discussion

Greenland and Antarctica are two geographically isolated polar locations that have similar environmental conditions (e.g. temperature, UV exposure, nutrient limitation, carbon concentrations), but vary considerably in the amount of surface melt. While studies on the comparison of the microbial community composition across polar

regions are scarce (Cameron *et al.*, 2012; Boetius *et al.*, 2015), local and regional similarities/dissimilarities between same type ecosystems on glaciers and ice sheets are evident (Cameron, Hagedorn, *et al.*, 2015; Edwards *et al.*, 2014; Stibal *et al.*, 2015). However, whether diversity is dependent on environmental type, location, physico-chemical parameters, or a combination of these factors remains poorly understood.

Glacial runoff is pivotal to glacial hydrology as it is responsible for the connectivity between individual supraglacial ecosystem components and for the transport of nutrients, DOM, and microorganisms across landscapes (Fountain *et al.*, 2004; Stibal *et al.*, 2010). The extensive supraglacial stream network on the GrIS (Rennermalm *et al.*, 2013; Smith *et al.*, 2015) is expected to more evenly distribute microbes across the ice surface, compared to colder Antarctic supraglacial ecosystems that can remain isolated over decadal time scales prior to flushing events (Fountain *et al.*, 2004). *A priori*, it was reasonable to assume that the bulk composition of microbial assemblages occupying different habitats within the biologically active margin of the GrIS were more similar to each other than local microbial assemblages in more isolated supraglacial Antarctic environments.

Phyla identified across all samples for this study were typical for glacial ecosystems (Boetius *et al.*, 2015). With the exception of *Gammaproteobacteria* present in snow, all Antarctic environments were dominated by phylotypes related to *Sphingobacteria* and individual ecosystems clustered together based on phylotypes present in each geographical location (Figure 2.3). Nonetheless, statistical evidence of similarity and dissimilarity was found, supporting local and regional variations in the

microbial assemblages across the environments investigated (Table 2.2). Notably, the observed differences in microbial assemblages between environments were explained by the most abundant bacterial taxa, which on average accounted for 39.9 ± 10.8% of the total diversity in these environments. Specifically, the overall average dissimilarity between stream and other supraglacial environments ranged between 60.1-82.9%, supporting a minor impact of other surface communities on meltwater stream assemblages.

Meltwater streams evolve seasonally, fed by surface and snow melt, runoff from saturated slush, or surface lake drainage. Subcommunities from reservoirs such as ice, snow, and cryoconite are a proposed pathway for the biological seeding of meltwater streams (Cameron *et al.*, 2015). Nonetheless, distinct microbial assemblages were present in glacial ice and cryoconite compared to the stream community from Canada Glacier (ANOSIM: $R>0.831$; $P<0.009$). Snow microbial assemblages were vastly different from stream samples, dominated by OTUs related to *Gammaprotepbacteria* that were unique to the snow community (Figure 2.1). Hydrologic contributions of snow to meltwater volume in the McMurdo Dry Valleys is also low (Fountain *et al.*, 2010) likely diminishing seeding effects on other meltwater communities. Unlike Wilhelm *et al*. 2013 who reported a high degree of community overlap between stream water and sediment associated biofilm communities in glacially fed alpine streams, heterogeneity was found between sediment and planktonic microbial assemblages in both CG and Canada Stream. Considering the low turbidity of Canada Stream during sampling dates (7-13 NTU) it is safe to assume that sediments were insufficiently reworked to homogenize benthic and

planktonic microbial assemblages, suggesting that none of these environments were a direct source of microorganisms to the glacial meltwater streams in Antarctica. The only microbial assemblages that showed a strong overlap were from CG stream and CG ice. Primary seeding of glacial environments by microbes is likely a result of aeolian deposition (snow, dust) (Šabacká *et al.*, 2012; Musilova *et al.*, 2015), however, the dominant bacterial phylotypes in the aeolian samples (*Gammaproteobacteria*) neither establish themselves in ice nor meltwater communities. Following this trajectory, microbial assemblages were further altered along the hydrological flow path from ice to stream water. Both ANOSIM (R=0.410, P=0.011) and Bray-Curtis dissimilarities (SIMPER: 60.1%) provide rationale that microbes preserved within the ice matrix served as a source of biota to the CG stream water during ice melt and channel erosion as well as for the development of a distinct stream water assemblage subsequent analyses.

Similar to our findings of biogeographical variations in Antarctic supraglacial environments, local and regional differences in supraglacial communities on the GrIS have been evident (Cameron, Hagedorn, *et al.*, 2015). Environmental regimes can sustain stable surface communities, unaffected by deposition of airborne microbes (Musilova *et al.*, 2015). While Antarctic supraglacial streams form single meltwater conduits, the ablation zone of the GrIS contains a vast hydrologic system, littered with supraglacial ponds and a dense network of supraglacial streams. Overall, samples collected from the GrIS were highly dissimilar from all Antarctic environments (ANISOM: $R>0.858$, $P<0.013$), and were dominated by *Gammaproteobacteria*, more specifically by *Pseudomonadales*. The dominance of this class has previously been reported for

Greenland snow microbial assemblages (Cameron *et al.*, 2015) but not for other supraglacial habitats in the biologically active margin of the GrIS (Cameron *et al.*, 2015, Stibal, *et al.*, 2015). Sample collection coincided with the third largest mean melt extent for the period June through August since 1979, with liquid water present on 41% of the ice sheet surface (Mernild and Liston, 2012). Notably, supraglacial habitats were continuously flushed during sampling. Since microorganisms from aeolian deposition typically would not establish themselves in other supraglacial communities (Musilova *et al.*, 2015), we speculate that elevated surface runoff during the summer months in 2011 led to a fast community turnover affected by snow and surface melt while hindering the establishment of stable surface communities.

Despite the overall dissimilarity in the microbial community structures across local and distant geographic locations, predicted metabolic capabilities of microbial assemblages between Antarctic environments were not significantly different ($P>0.05$), while significant differences did exist between Antarctic and Greenlandic communities ($P<0.05$). In particular, no significant differences were found in energy, carbohydrate, and amino acid metabolisms between Antarctic microbial assemblages. Recent studies highlight the metabolic versatility of Antarctic organisms (Smith *et al.*, 2014; Gunnigle *et al.*, 2015), which may allow for opportunistic advantages in competition with other heterotrophic organisms in oligotrophic environments. Since our data suggest a certain degree of redundancy in metabolic functionality, we hypothesized that the local geochemical environment may in large part shape the microbial diversity in Antarctic habitats.

Substrate quality is a major factor influencing the utilization of OM. Given the variation in OM composition between the glacial environments we expected these differences to be reflected in the microbial community composition. To date a significant fraction of research focusing on microbial interactions with OM has focused on terrestrial (Logue *et al.*, 2015; Fasching *et al.*, 2014; Judd *et al.*, 2006) and marine environments (Ogawa *et al.*, 2001; McCarren *et al.*, 2010; Jiao *et al.*, 2010; Osterholz *et al.*, 2016), containing both autochthonous and allochthonous sources of OM. In contrast, much less is known about the influence of microbially derived labile autochthonous OM on microbial community structure. To avoid shifts in community composition as a result of laboratory based incubations (Christian and Capone, 2002), we directly studied the interplay of geochemical parameters and OM composition with microbial assemblages from different glacial environments. The initial CCA analysis, evaluating the effect of geochemistry on microbial community composition of the CG and Canada Stream water, showed that physical parameters such as temperature, pH, or conductivity did not significantly describe the differences in assemblage composition. Primarily nutrient (i.e., nitrogen, phosphorus) were attributed to clustering effects, while DOC concentrations did not contribute to the observed differences in microbial assemblages (Figure 2.5). To further elucidate the effect of DOM as the preferential substrate for heterotrophs we probed DOM quality as a potential driver for differences in community structure. Only the sediment laden Canada Stream microbial assemblages were consistently influenced by humic-like fractions of DOM. Ice and ice meltwater driven supraglacial habitats were best explained by protein-like DOM fluorescence with assemblages from the GrIS clearly

separating from Antarctic environments. These are intriguing results as previous research in mesophilic stream and lake environments has documented shifts in bacterial communities in response to compositionally different sources of DOM (Judd *et al.*, 2006). Similarly, Logue *et al*. 2015 showed that certain taxa are responsible for the uptake of high versus low molecular weight compounds.

Although supraglacial streams share similar morphological features to alluvial and bedrock rivers (e.g., meandering; Karlstrom *et al.*, 2013) they are hydrologically unique in that they are devoid of significant quantities of suspended and benthic substrates (Scott *et al.*, 2010). CG stream lacks benthic microbial mats and DOM is primarily derived from the active exudation of labile DOM produced by in stream phototrophic microorganisms (Smith *et al*. In Prep see Chapter 3). CG DOM lacks stable humic signatures (Foreman *et al.*, 2013), likely due to the short residence time of nutrients in supraglacial streams (Scott *et al.*, 2010), and does not persist inter-seasonally (SanClements *et al*. In Review). While DOM from Antarctic environments is predominantly autochthonous and of microbial origin (McKnight *et al.*, 2001; Pautler *et al.*, 2013; 2012; 2011), DOM from the Canada Stream was compositionally differed and contained distinct humic-like fluorescence signatures. The presence of humic-like fluorescence in the Canada Stream is driven by accumulation of DOM from perennial cyanobacterial mats (McKnight and Tate, 1997). Similarly, our data suggest partial accumulation of DOM in stream sediment and cryoconite habitats. The presence of substrate supports biological “hotspots” in supraglacial environments and the accumulation of DOM ((Cook *et al.*, 2015) and references within). These findings

support our working hypothesis that compositional DOM differences could influence the distribution of organisms across environmental scales.

Conclusion

While it is acknowledged that icy ecosystems possess diverse and metabolically active organisms (Boetius *et al.*, 2015), glacial biodiversity and the physico-chemical parameters that shape these microbial assemblages are poorly understood. Results from this study highlight that spatially isolated local and distant environments harbor distinct microbial communities, driven by varying nutrient and DOM composition. While physical parameters had a negligible effect on microbial assemblages in glaciated Antarctic environments, the supraglacial microbial community in the ablation zone of the GrIS were shaped by high levels of melt water, counteracting the development of stable communities as previously reported (Musilova *et al.*, 2015). Further, the existing microbial consortia in supraglacial environments deviated largely from bacteria found in snow, indicating the development of sovereign, habitat specific microbial assemblages.

Icy environments are vulnerable ecosystems that need to be understood within the context of climate change. Results from this study present a compelling case for developing a better understanding for how increases in meltwater and discharge from the GrIS may create a more transient surface environment, which may inhibit the establishment of stable and productive microbial communities; ultimately decreasing the high levels of predicted carbon discharge from the GrIS (Anesio *et al.*, 2009; Cook *et al.*, 2012; Hodson *et al.*, 2015). With respect to Antarctica there is evidence on the effect of

climate change in the McMurdo Dry Valley lakes (Foreman *et al.*, 2004), however the effect of climate induced alterations on continental, glacial environments and their resident microbial communities remains an open question. Our data indicate that ecosystem stability could easily shift based on a combination of physico-chemical parameters.

Acknowledgements

This work was supported by the National Science Foundation Division of Antarctic Sciences through ANT-0838970 and ANT-1141978, by the NSF Division of Graduate Education through DGE-0654336, and through a NASA Earth and Science Space Fellowship to HJS. We acknowledge and thank the Cotton Glacier field team, in particular D.M. McKnight, M. SanClements, and Y-P. Chin. Any opinions, findings, or conclusions expressed in this material are those of the authors and do not necessarily reflect the views of the National Science Foundation.

References

Anesio AM, Hodson AJ, Fritz A. (2009). High microbial activity on glaciers: importance to the global carbon cycle. *Glob Change Biol* **15**: 955–960.

Anesio AM, Laybourn-Parry J. (2012). Glaciers and ice sheets as a biome. *Trends Ecol Evol (Amst)* **27**: 219–225.

Antony R, Grannas AM, Willoughby AS, Sleighter RL, Thamban M, Hatcher PG. (2014). Origin and sources of dissolved organic matter in snow on the East Antarctic ice sheet. *Environ Sci Technol* **48**: 6151–6159.

Boetius A, Anesio AM, Deming JW, Mikucki JA, Rapp JZ. (2015). Microbial ecology of the cryosphere: sea ice and glacial habitats. *Nat Rev Microbiol*. doi:10.1038/nrmicro3522.

Cameron KA, Hagedorn B, Dieser M, Christner BC, Choquette K, Sletten R, *et al.* (2015). Diversity and potential sources of microbiota associated with snow on western portions of the Greenland Ice Sheet. *Environ Microbiol* **17**: 594–609.

Cameron KA, Hodson AJ, Osborn AM. (2012). Structure and diversity of bacterial, eukaryotic and archaeal communities in glacial cryoconite holes from the Arctic and the Antarctic. *FEMS Microbiol Ecol* **82**: 254–267.

Cameron KA, Stibal M, Zarsky JD, Gözdereliler E, Schostag M, Jacobsen CS. (2015). Supraglacial bacterial community structures vary across the Greenland ice sheet. *FEMS Microbiol Ecol*.

Caporaso JG, Kuczynski J, Stombaugh J, Bittinger K, Bushman FD, Costello EK, *et al.* (2010). QIIME allows analysis of high-throughput community sequencing data. *Nat Meth* **7**: 335–336.

Cavicchioli R. (2015). Microbial ecology of Antarctic aquatic systems. *Nat Rev Microbiol* **13**: 691–706.

Chao A. (1984). Nonparametric Estimation of the Number of Classes in a Population on JSTOR. *Scandinavian Journal of statistics*.

Chown SL, Clarke A, Fraser CI, Cary SC, Moon KL, McGeoch MA. (2015). The changing form of Antarctic biodiversity. *Nature* **522**: 431–438.

Christian RR, Capone DG. (2002). Overview of issues in aquatic microbial ecology. 2nd ed. Manual of Environmental Microbiology: Washington.

Clarke KR, Warwick RM. (2001). Change in Marine Communities: An approach to statistical analysis and interpretation, 2nd edition. *Primer-E Ltd, Plymouth UK*.

Coble PG. (1996). Characterization of marine and terrestrial DOM in seawater using excitation-emission matrix spectroscopy. **51**: 325–346.

Cook J, Edwards A, Takeuchi N, Irvine-Fynn T. (2015). Cryoconite The dark biological secret of the cryosphere. *Progress in Physical Geography* 1–46.

Cook JM, Hodson AJ, Anesio AM. (2012). An improved estimate of microbially mediated carbon fluxes from the Greenland ice sheet. *Journal of Glaciology* **58**: 1098–1108.

Edgar RC, Haas BJ, Clemente JC, Quince C, Knight R. (2011). UCHIME improves sensitivity and speed of chimera detection. *J Gerontol* **27**: 2194–2200.

Edwards A, Mur LAJ, Girdwood SE, Anesio AM, Stibal M, Rassner SME, *et al.* (2014). Coupled cryoconite ecosystem structure-function relationships are revealed by comparing bacterial communities in alpine and Arctic glaciers. *FEMS Microbiol Ecol* **89**: 222–237.

Edwards A, Pachebat JA, Swain M, Hegarty M, Hodson AJ, Irvine-Fynn TDL, *et al.* (2013). A metagenomic snapshot of taxonomic and functional diversity in an alpine glacier cryoconite ecosystem. *Environ Res Lett* **8**: 035003.

Fasching C, Behounek B, Singer GA, Battin TJ. (2014). Microbial degradation of terrigenous dissolved organic matter and potential consequences for carbon cycling in brown-water streams. *Sci Rep* **4**: 4981.

Foreman CM, Cory RM, Morris CE, SanClements MD, Smith HJ, Lisle JT, *et al.* (2013). Microbial growth under humic-free conditions in a supraglacial stream system on the Cotton Glacier, Antarctica. *Environ Res Lett* **8**: 035022.

Foreman CM, Wolf CF, Priscu JC. (2004). Impact of Episodic Warming Events. *Aquat Geochem* **10**: 239–268.

Fountain AG, Nylen TH, Monaghan A, Basagic HJ, Bromwich D. (2010). Snow in the McMurdo Dry Valleys, Antarctica. *International Journal of Climatology* **30**: 633–642.

Fountain AG, Tranter M, Nylen TH, Lewis KJ, Mueller DR. (2004). Evolution of cryoconite holes and their contribution to meltwater runoff from glaciers in the McMurdo Dry Valleys, Antarctica. *Journal of Glaciology* **50**: 35–45.

Ghiglione J-F, Galand PE, Pommier T, Pedrós-Alió C, Maas EW, Bakker K, *et al.* (2012). Pole-to-pole biogeography of surface and deep marine bacterial communities. *Proc Natl Acad Sci USA* **109**: 17633–17638.

Gunnigle E, Ramond J-B, Guerrero LD, Makhalanyane TP, Cowan DA, Lund DP. (2015). Draft genomic DNA sequence of the multi-resistant Sphingomonas sp. strain

AntH11 isolated from an Antarctic hypolith Lund, DP (ed). *FEMS Microbiology Letters* **362**.

Hodgson DA, Convey P, Verleyen E, Vyverman W, McInnes SJ, Sands CJ, *et al.* (2010). The limnology and biology of the Dufek Massif, Transantarctic Mountains 82° South. *Polar Science* **4**: 197–214.

Hodson A, Ben Brock, Pearce D, Laybourn-Parry J, Tranter M. (2015). Cryospheric ecosystems: a synthesis of snowpack and glacial research. *Environ Res Lett* **10**: 110201.

Hodson A, Bøggild C, Hanna E, Huybrechts P, Langford H, Cameron K, *et al.* (2010). The cryoconite ecosystem on the Greenland ice sheet. *Annals of Glaciology* **51**: 123–129.

Hood E, Battin TJ, Fellman J, O'Neel S, Spencer RGM. (2015). Storage and release of organic carbon from glaciers and ice sheets. *Nature Geoscience* **8**: 91–96.

Hood E, Fellman J, Spencer RGM, Hernes PJ, Edwards R, D'Amore D, *et al.* (2009). Glaciers as a source of ancient and labile organic matter to the marine environment. *Nature* **462**: 1044–1047.

Howard-Williams C, Hawes I, Gordon S. (2010). The environmental basis of ecosystem variability in Antarctica: research in the Latitudinal Gradient Project. *Antarctic Science* **22**: 591–602.

Jiao N, Herndl GJ, Hansell DA, Benner R, Kattner G, Wilhelm SW, *et al.* (2010). Microbial production of recalcitrant dissolved organic matter: long-term carbon storage in the global ocean. *Nat Rev Microbiol* **8**: 593–599.

Judd KE, Crump BC, Kling GW. (2006). Variation in dissolved organic matter controls bacterial production and community composition. *Ecology* **87**: 2068–2079.

Karlstrom L, Gajjar P, Manga M. (2013). Meander formation in supraglacial streams. *Journal of Geophysical Research: Earth Surface* **118**: 1897–1907.

Langille MGI, Zaneveld J, Caporaso JG, McDonald D, Knights D, Reyes JA, *et al.* (2013). Predictive functional profiling of microbial communities using 16S rRNA marker gene sequences. *Nat Biotechnol* **31**: 814–821.

Lawaetz AJ, Stedmon CA. (2009). Fluorescence intensity calibration using the Raman scatter peak of water. *Appl Spectrosc* **63**: 936–940.

Logue JB, Stedmon CA, Kellerman AM, Nielsen NJ, Andersson AF, Laudon H, *et al.* (2015). Experimental insights into the importance of aquatic bacterial community composition to the degradation of dissolved organic matter. *ISME J*.

Margesin R, Schinner F, Marx JC, Gerday C. (2007). Psychrophiles: From Biodiversity

to Biotechnology.

McCarren J, Becker JW, Repeta DJ, Shi Y, Young CR, Malmstrom RR, *et al.* (2010). Microbial community transcriptomes reveal microbes and metabolic pathways associated with dissolved organic matter turnover in the sea. *Proc Natl Acad Sci USA* **107**: 16420–16427.

McKnight DM, Boyer EW, Westerhoff PK. (2001). Spectrofluorometric characterization of dissolved organic matter for indication of precursor organic material and aromaticity. *Limnol and Oceanogr* **46**: 38–48.

McKnight DM, Tate CM. (1997). Canada Stream: A Glacial Meltwater Stream in Taylor Valley, South Victoria Land, Antarctica. *Journal of the North American Benthological Society* **16**: 14.

Mernild SH, Liston GE. (2012). Surface melt extent for the Greenland Ice Sheet, 2011. *Geografisk Tidsskrift-Danish Journal of Geography* **112**: 84–88.

Miller MP, McKnight DM. (2010). Comparison of seasonal changes in fluorescent dissolved organic matter among aquatic lake and stream sites in the Green Lakes Valley. *Journal of Geophysical Research: Biogeosciences (2005–2012)* **115**: G00F12.

Musilova M, Tranter M, Bennett SA, Wadham J, Anesio AM. (2015). Stable microbial community composition on the Greenland Ice Sheet. *Front Microbiol* **6**: 193.

Namsaraev Z, Mano MJ, Fernandez R, Wilmotte A. (2010). Biogeography of terrestrial cyanobacteria from Antarctic ice-free areas. *Annals of ...* **51**: 171–177.

Nemergut DR, Costello EK, Hamady M, Lozupone C, Jiang L, Schmidt SK, *et al.* (2011). Global patterns in the biogeography of bacterial taxa. *Environ Microbiol* **13**: 135–144.

Nguyen NH, Smith D, Peay K, Kennedy P. (2015). Parsing ecological signal from noise in next generation amplicon sequencing. *New Phytol* **205**: 1389–1393.

Ogawa H, Amagai Y, Koike I, Kaiser K, Benner R. (2001). Production of refractory dissolved organic matter by bacteria. *Science* **292**: 917–920.

Osterholz H, Singer G, Wemheuer B, Daniel R, Simon M, Niggemann J, *et al.* (2016). Deciphering associations between dissolved organic molecules and bacterial communities in a pelagic marine system. *ISME J*.

Pautler BG, Dubnick A, Sharp MJ, Simpson AJ. (2013). Comparison of cryoconite organic matter composition from Arctic and Antarctic glaciers at the molecular-level. ... *et Cosmochimica Acta* **104**: 1-18.

Pautler BG, Simpson AJ, Simpson MJ, Tseng L-H, Spraul M, Dubnick A, *et al.* (2011).

Detection and structural identification of dissolved organic matter in Antarctic glacial ice at natural abundance by SPR-W5-WATERGATE 1H NMR spectroscopy. *Environ Sci Technol* **45**: 4710–4717.

Pautler BG, Woods GC, Dubnick A, Simpson AJ, Sharp MJ, Fitzsimons SJ, *et al.* (2012). Molecular characterization of dissolved organic matter in glacial ice: coupling natural abundance 1H NMR and fluorescence spectroscopy. *Environ Sci Technol* **46**: 3753–3761.

Peat HJ, Clarke A, Convey P. (2007). ORIGINAL ARTICLE: Diversity and biogeography of the Antarctic flora. *Journal of Biogeography* **34**: 132–146.

Priscu JC, Wolf CF. (2000). Priscu: Limnological methods for the McMurdo Dry Valleys Long Term Ecological Research Program. (www.mcmlter.org/data/lakes/MCM Limno Methods.pdf).

Rennermalm AK, Moustafa SE, Mioduszewski J, Chu VW, Forster RR, Hagedorn B, *et al.* (2013). Understanding Greenland ice sheet hydrology using an integrated multi-scale approach. *Environ Res Lett* **8**: 015017.

Salter SJ, Cox MJ, Turek EM, Calus ST, Cookson WO, Moffatt MF, *et al.* (2014). Reagent and laboratory contamination can critically impact sequence-based microbiome analyses. *BMC Biology* **12**: 87.

Schloss PD, Gevers D, Westcott SL. (2011). Reducing the effects of PCR amplification and sequencing artifacts on 16S rRNA-based studies. *PLoS ONE* **6**: e27310.

Schloss PD, Westcott SL, Ryabin T, Hall JR, Hartmann M, Hollister EB, *et al.* (2009). Introducing mothur: open-source, platform-independent, community-supported software for describing and comparing microbial communities. *Appl Environ Microbiol* **75**: 7537–7541.

Scott D, Hood E, Nassry M. (2010). In-stream uptake and retention of C, N and P in a supraglacial stream. *Annals of Glaciology* **51**: 80–86.

Simon C, Wiezer A, Strittmatter AW, Daniel R. (2009). Phylogenetic diversity and metabolic potential revealed in a glacier ice metagenome. *Appl Environ Microbiol* **75**: 7519–7526.

Simpson EH. (1949). Measurement of diversity. *Nature* **163**: 688–688.

Smith HJ, Foreman CM, Ramaraj T. (2014). Draft Genome Sequence of a Metabolically Diverse Antarctic Supraglacial Stream Organism, Polaromonas sp. Strain CG9_12, Determined Using Pacific Biosciences Single-Molecule Real-Time Sequencing Technology. *Genome Announc* **2**.

Smith LC, Chu VW, Yang K, Gleason CJ, Pitcher LH, Rennermalm AK, *et al.* (2015).

Efficient meltwater drainage through supraglacial streams and rivers on the southwest Greenland ice sheet. *Proc Natl Acad Sci USA* **112**: 1001–1006.

Staley JT, Gosink JJ. (1999). Poles Apart: Biodiversity and Biogeography of Sea Ice Bacteria. *Annual Reviews in Microbiology* **53**: 189-215.

Stibal M, Lawson EC, Lis GP, Mak KM, Wadham JL, Anesio AM. (2010). Organic matter content and quality in supraglacial debris across the ablation zone of the Greenland ice sheet. *Annals of Glaciology* **51**: 1–8.

Stibal M, Sabacka M, Zarsky J. (2012). Biological processes on glacier and ice sheet surfaces. *Nature Geoscience* **5**: 771–774.

Stibal M, Schostag M, Cameron KA, Hansen LH, Chandler DM, Wadham JL, *et al.* (2015). Different bulk and active bacterial communities in cryoconite from the margin and interior of the Greenland ice sheet. *Environ Microbiol Rep* **7**: 293–300.

Stibal M, Tranter M, Benning LG. (2008). Microbial primary production on an Arctic glacier is insignificant in comparison with allochthonous organic carbon input. *Environmental Microbiology* **10**: 2172–2178.

Stubbins A, Hood E, Raymond PA, Aiken GR, Sleighter RL, Hernes PJ, *et al.* (2012). Anthropogenic aerosols as a source of ancient dissolved organic matter in glaciers. *Nature Geoscience* **5**: 198–201.

Šabacká M, Priscu JC, Basagic HJ, Fountain AG. (2012). Aeolian flux of biotic and abiotic material in Taylor Valley, Antarctica. *Geomorphology*.

Tedesco M, Willis IC, Hoffman MJ, Banwell AF, Alexander P, Arnold NS. (2013). Ice dynamic response to two modes of surface lake drainage on the Greenland ice sheet. *Environ Res Lett* **8**: 034007.

Telling J, Anesio AM, Tranter M, Stibal M, Hawkings J, Irvine-Fynn T, *et al.* (2012). Controls on the autochthonous production and respiration of organic matter in cryoconite holes on high Arctic glaciers. *J Geophys Res* **117**: G01017.

Van Horn DJ, Van Horn ML, Barrett JE, Gooseff MN, Altrichter AE, Geyer KM, *et al.* (2013). Factors Controlling Soil Microbial Biomass and Bacterial Diversity and Community Composition in a Cold Desert Ecosystem: Role of Geographic Scale. *PLoS ONE* **8**: e66103.

Wang Q, Garrity GM, Tiedje JM, Cole JR. (2007). Naive Bayesian classifier for rapid assignment of rRNA sequences into the new bacterial taxonomy. *Appl Environ Microbiol* **73**: 5261–5267.

CHAPTER 3

MICROBIAL FORMATION OF LABILE GLACIAL ORGANIC CARBON

Contribution of Authors and Co-Authors

Author: Heidi J Smith

Contributions: Designed the experiment, conducted experiments, analyzed data, wrote the manuscript.

Co-Author: Rachel Foster

Contributions: Assisted with nanoSIMS experimental design and data collection, edited manuscript.

Co-Author: Diane McKnight

Contributions: Assisted experimental design and edited manuscript.

Co-Author: John Lisle

Contributions: Enumerated and analyzed viral and bacterial abundances and edited manuscript.

Co-Author: Daniela Tienken

Contributions: Collected nanoSIMS measurements

Co-Author: Marcel Kuypers

Contributions: Provided support for nanoSIMS analysis and edited manuscript

Co-Author: Christine Foreman.

Contributions: Principal investigator of field and laboratory experiments data analysis, manuscript preparation and editing

Manuscript Information Page

Heidi Smith, Rachel Foster, Diane McKnight, John Lisle, Daniela Tienken, Marcel Kuypers, Christine Foreman
Nature Geosciences
Status of Manuscript:
__X_ Prepared for submission to a peer-reviewed journal
____ Officially submitted to a peer-review journal
____ Accepted by a peer-reviewed journal
____ Published in a peer-reviewed journal

Abstract

Recent investigations suggest that up to six petagrams of organic carbon (OC) are stored within glaciers and ice sheets of the world. Chemical characterization determined that one component of this OC is of an old age (Hood *et al.*, 2009) and incubation experiments showed that a portion of this OC is highly bioavailable (Hood *et al.*, 2009; Lawson *et al.*, 2013; Singer *et al.*, 2012). In addition to the storage of ancient OC (Stubbins *et al.*, 2012) and new atmospheric deposition (Antony *et al.*, 2014), microbial activity in glacial ecosystems may contribute substantially to the flux of OC from glaciers (Anesio *et al.*, 2010; Cook *et al.*, 2012). Current estimates of microbial carbon cycling on glaciers range from net respiration (Hodson *et al.*, 2010) to net carbon fixation (Anesio *et al.*, 2009; Cook *et al.*, 2012) however, these modeling efforts have not considered the Antarctic Ice Sheet and supraglacial streams. The continuous sunlight and warmer temperatures that promote melting on glaciers in polar regions would also promote growth of microbial phototrophs and production of organic matter (OM) in supra-glacial streams. We investigated the biogeochemical sequence of OM production by microbial phototrophs and OM uptake by heterotrophic microbes in an Antarctic supraglacial stream. We used complementary methods including high-resolution nanometer scale secondary ion mass spectrometry, fluorescence spectroscopy, stable isotope analysis, and incubation experiments to track organic carbon through a supraglacial microbial food web. Rather than relying on legacy organic carbon released from the melting ice, our findings demonstrate the importance of highly labile, organic carbon derived from microbial phototrophs in supraglacial environments (Singer *et al.*, 2012). Microbial exudates were directly utilized by heterotrophs within 24 hrs, and were sufficient to support bacterial growth demands. The tight coupling of this microbially released OC and rapid uptake by heterotrophs points towards a dynamic local carbon cycle; as temperatures continue to increase so will the positive feedback between glacial melt and microbial transformations of organic carbon.

Introduction

Recent studies have focused on the fate and downstream implications of ancient OC from coastal temperate and alpine glaciers (Hood *et al.*, 2009; Stubbins *et al.*, 2012; Singer *et al.*, 2012), this residual OC originates from terrestrial or anthropogenic sources. Concomitant with this focus on the deposition and storage of allochthonous carbon, numerous studies have suggested that a large proportion of OM in supra- and englacial settings may be composed of microbially generated products (Singer *et al.*, 2012; Antony *et al.*, 2014; Bhatia *et al.*, 2010; Pautler *et al.*, 2011), with *in situ* primary production being sufficiently high to accumulate OC in glacial environments (Anesio *et al.*, 2010). Studies on the biological activity in cryoconite, in all glacial environments excluding Antarctica, showed that the phototrophic microbial community within these supraglacial environments has the potential to fix as much as 64 Gg C yr^{-1}, generating up to 10 Gg C yr^{-1} dissolved organic carbon (DOC) (Anesio *et al.*, 2009). The relative importance of authochthonous dissolved organic matter (DOM) production may be greater for the continent of Antarctica, which lacks vascular plants, and receives low annual inputs of aeolian material compared to other geographic locations (Li *et al.*, 2008). In particular, black carbon deposition is roughly 10 times less in Antarctica than in Greenland (Bauer *et al.*, 2013). Further, recent work on Antarctic snow found that autochthonous OC was the dominant source in supraglacial environments (Antony *et al.*, 2014). Therefore, we hypothesize that biological contributions are an important component of polar OC pools, particularly in supraglacial Antarctic environments. The metabolic suitability of OC produced by microbial phototrophs in glacial environments, however, is largely

unexplored and a recent review highlights this gap in our understanding (Stibal *et al.*, 2012).

Ecosystems in the polar deserts of Antarctica have truncated microbial food webs, making them an ideal environment to study this gap in understanding. The goal of this study was to determine the composition and uptake rate of photosynthetically fixed OC within a large Antarctic supraglacial stream, in order to advance our understanding of glacial carbon dynamics and global carbon cycles. The supraglacial Cotton Glacier (CG) stream located in the McMurdo Dry Valleys of Antarctica is currently the largest Antarctic supraglacial stream to be studied. The stream is approximately 16 km long and forms braided stream networks that flow over ice and sediments, eventually discharging into the Ross Sea (SanClements *et al.* In Review). DOC concentrations throughout the summer in the CG stream ranged from 0.4-1.68 mg C L^{-1} (SanClements *et al*. In Review), similar to reported DOC concentrations of other glacial meltwaters (Barker *et al.*, 2006; Bhatia *et al.*, 2013; Hood *et al.*, 2009). Here we examine the autochthonous contribution to glacial OC by utilizing microbiological and geochemical techniques that allowed us to trace microbial OM inception, uptake, and transformation.

Results and Discussion

We found that the DOM fluorescence signature of the freshly collected CG stream water was dominated by protein-like fluorophores (designations B and T; 93%) (Figure 3.1A), which are associated with biogeochemically labile DOM and have been observed with other glacial meltwaters (Barker *et al.*, 2013) (Table 3.1). The fluorescent fraction of freshly synthesized microbial exudates from incubation experiments consisted of 97%

protein-like fluorescence signatures, with a greater tyrosine-like fluorescence compared to the CG stream water sample (Figure 3.1B). After microbial processing, exudates were comprised of 53% and 47% protein- and humic-like fluorescence signatures, respectively (Figure 3.1C), indicative of the biological formation of more refractory materials (Ogawa *et al.*, 2001). The $\delta^{13}C$ values for the CG stream water OC were enriched ranging from -19.0 to -19.9 ‰ when compared to the range of $\delta^{13}C$ values for the surrounding glacial ice derived OC (-29.5 to -30.1 ‰) ($p<0.001$, two tailed, *t* test). As the glacial ice serves as the stream water source, such differences in $\delta^{13}C$ values would be characteristic of in stream OC production and transformation (Musilova *et al.*, 2015), providing strong support that the OC was derived from *in situ* production by microbial phototrophs.

The percent of extracellularly released OC in the CG stream at the height of the summer was found to be 50.7%. Variations in extracellular released carbon (reported values range between <2% and 70% (Teira *et al.*, 2001; Van den Meersche and Middelburg, 2004)) are governed by environmental factors such that temperature, nutrients, and light availability have significant effects on the amount of carbon released and processed. To assess the importance of excreted OC to the overall bacterial productivity of the CG stream, we determined that the bacterial OC demand was 0.62 ug C $L^{-1}d^{-1}$, while the supply of excreted carbon was 2.32 ug C L^{-1} d^{-1}. From this comparison, we conclude that the *in situ* bacterial carbon demand was not only met by the amount of carbon excreted by in-stream microbial phototrophs, but also approximately four times in excess, corroborating past studies in other microbially

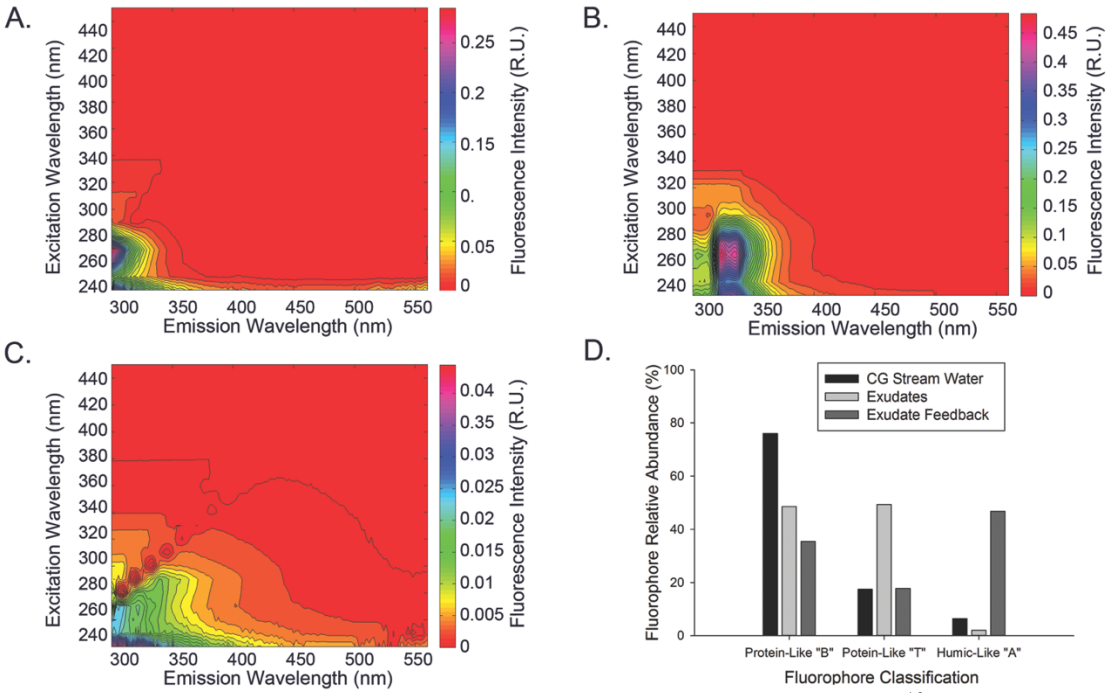

Figure 3.1. EEMs from: (A.) Cotton Glacier stream water, (B.) exuded ^{13}C-labeled DOM after 72 hrs incubation and removal of unincorporated ^{13}C-DIC, (C.) DOM after a 24 hr feedback of exuded DOM to the *in situ* Cotton Glacier stream microbial community. (D.) Change in the abundance of specific fluorophores B (protein-like), T (protein-like), and A (humic-like) relative to the total fluorescence within a sample. Fluorescence was normalized to maximum and minimum fluorescence values across the three samples.

Table 3.1. Summary of previously identified fluorophore designations (Coble 1996, Marhaba et al. 2000) adapted from D'Andrilli et al. 2013, of the Ex/Em maxima for fluorescing regions present in this study.

Fluorophore Designation	Ex/Em Max (nm)	Compositional Description	CG Stream Water Ex/Em Max (nm)	Exudate Ex/Em Max (nm)	Exudate Feedback Ex/Em Max (nm)
	225-237/309-321				
B	275/310	Protein-like (Tyrosine)	270/300	280/304	240/326
	225-237/340-381				
T	275/340	Protein-like (Tryptophan)	240/326	280/326	240/328
A	237-260/400-500	Humic-like	240/400	240/452	240/400

dominated, limnetic Antarctic environments (Takacs *et al.*, 2001). Thus, our findings support the idea that microbially produced OC is in high enough quantities to accumulate and impact the activity of downstream ecosystems and is therefore an important constituent of glacial carbon cycling (Anesio *et al.*, 2010).

Previous studies have also recognized viral lysis of bacterial cells as a major source of microbially derived DOM. As such, viruses may cause 10-30% of microbial cell lysis, directly impacting aquatic biogeochemical cycles (Suttle, 2007). In glaciated systems allochthonous carbon inputs are believed to foster higher the viral to bacterial ratio (VBR); low VBR have been explained in part by the autochthonous nature of carbon substrates in Antarctic environments (Säwström *et al.*, 2008). Additionally, VBR significantly less than 10 have been shown to be more prevalent in waters where the bacterial concentrations are low, like those found in the glacier streams (Wigington *et al.*, 2016). Our study determined that the virus-like particle (VLP) abundance in the CG stream ranged from $7.84 \times 10^2 – 1.56\ 10^3$ VLP mL^{-1}, and VBR ranged from 0.12 - 0.44. VBRs in the CG stream were considerably lower than average VBR in both marine (ranging from 10-40 and in places exceeding 100), and polar inland waters (ranging from 1.15- 57) (Wilhelm and Suttle, 1999; Säwström *et al.*, 2008). In two Vestfold Hills Antarctic Lakes the VBR at the peak of the summer was about 5.4 and 8.1, respectively, with viral cell lysis estimated to contribute <20% to the OC pool (Säwström *et al.*, 2007). Although our study did not account for virus induced OC release, the low VBR ratios and low viral abundances detected in the CG stream strongly suggest minor viral effects,

supporting our hypothesis that OC was predominantly derived from the active exudation of photosynthetically synthesized OC.

The CG stream bacterial assemblage, as determined by catalyzed reported deposition fluorescent *in situ* hybridization (CARD-FISH), consisted of 4.93×10^4 cells mL^{-1}, 85% of which was comprised of the following lineages: *Bacteroidetes* sp. (40%), *Betaproteobacteria* sp. (30%), and *Alphaproteobacteria* sp. (15%). Within the class *Betaproteobacteria*, the genus *Polaromonas* accounted for 56%. Importantly, based on the constructed metabolic profile of the CG stream community, the phylotypes present have the metabolic capability to degrade low molecular weight, carbohydrate-like compounds (Figure 3.2).

High-resolution nanometer scale secondary ion mass spectrometry (nanoSIMS) was used to quantify the single cell uptake of microbially synthesized and excreted ^{13}C-labeled exudates (Fig. 3.3 B). ^{13}C-labeled exudates were significantly enriched and taken up by the *Bacteroidetes* and *Betaproteobacteria* lineages, while no uptake was detected by *Alphaproteobacteria* ^{13}C enrichment (Figure 3.3 D). Using a linear mixed model to fit an ANOVA with random effects, no statistically significant difference was found in the rate of uptake between the *Bacteroidetes* (ranging from 8.31×10^{-5} to 5.41×10^{-4} pmol C $cell^{-1}$ d^{-1}) and *Betaproteobacteria* (ranging from 2.56×10^{-5} to 6.69×10^{-4} pmol C $cell^{-1}$ d^{-1}) lineages ($P>0.05$). Photosynthetically derived exudates from the CG stream primary producers were capable of supporting bacterial growth demands; and rapidly utilized (within 24 hrs) by heterotrophic bacteria.

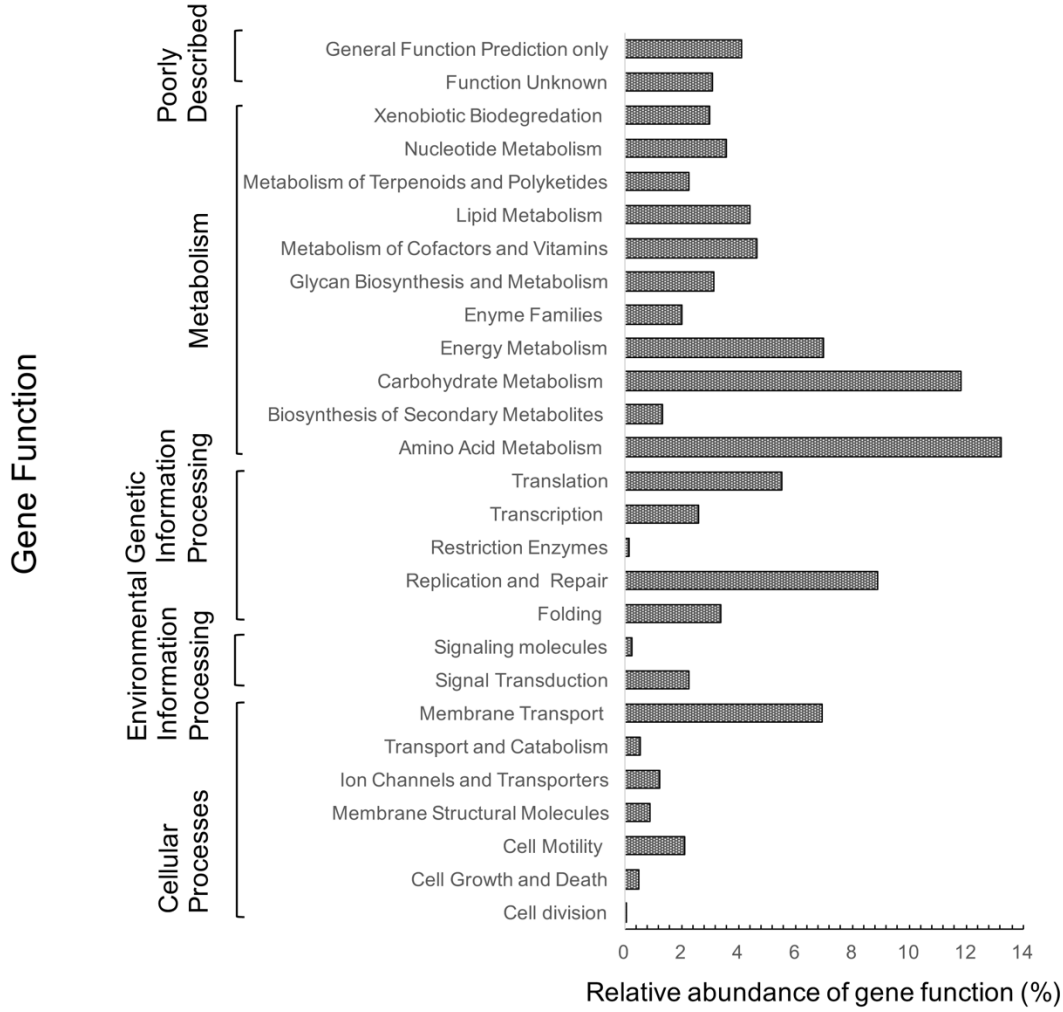

Figure 3.2. PICRUST generated predicted genetic function profile of the Cotton Glacier Stream bacterial community, providing functional evidence for the degradation of *in situ* OM dominated by amino acid-like fluorescence.

Table 3.2. Summary of 16S rRNA targeted oligonucleotide probes, target organisms, competitor sequences and formamide (FA) concentrations, and references for the probes selected in this study. All FA concentrations used were the optimal concentrations recommended by each respective publication.

Probe and Target Organism	Probe Sequence (5'-3')	Target Position	Target	% FA	Reference
For Bacteria (used in equal amounts)					
EUB338-I	GCT GCC TCC CGT AGG AGT	338-355	16S	35	Amann *et al.* (1990)
EUB338-II	GCA GCC ACC CGT AGG TGT	338-355	16S	35	Damis *et al.* (1999)
EUB338-III	GCT GCC ACC CGT AGG AGT	338-355	16S	35	Damis *et al.* (1999)
Antisense of EUB338					
NON338	ACT CCT ACG GGA GGC AGC	338-355	16S	35	Wallner *et al.* (1993)
Most Flavobacteria, some Bacteroidetes and some Sphingobacteria					
CF319a	TGG TCC GTG TCT CAG TAC	319-336	16S	35	Manz *et al.* (1996)
CF319b	TGG TCC GTA TCT CAG TAC	319-336	16S	35	Manz *et al.* (1996)
Alphaproteobacteria, some Deltaproteobacteria, Spirochaetes (used in equal amounts)					
ALF1B	CGT TCG YTC TGA GCC AG	19-35	16S	20	Manz *et al.* (1992)
ALF968	GGT AAG GTT CTG CGC GTT	968-985	16S	20	Neef (1997)
Gammaproteobacteria					
GAM42A	GCC TTC CCA CAT CGT TT	1027-1043	23S	35	Manz *et al.* (1992)
Competitor	GCC TTC CCA CTT CGT TT		23S		
Betaproteobacteria					
BET42a	GCC TTC CCA CTT CGT TT	1027-1043	23S	35	Manz *et al.* (1992)
Competitor	GCC TTC CCA CTT CGT TT		23S		

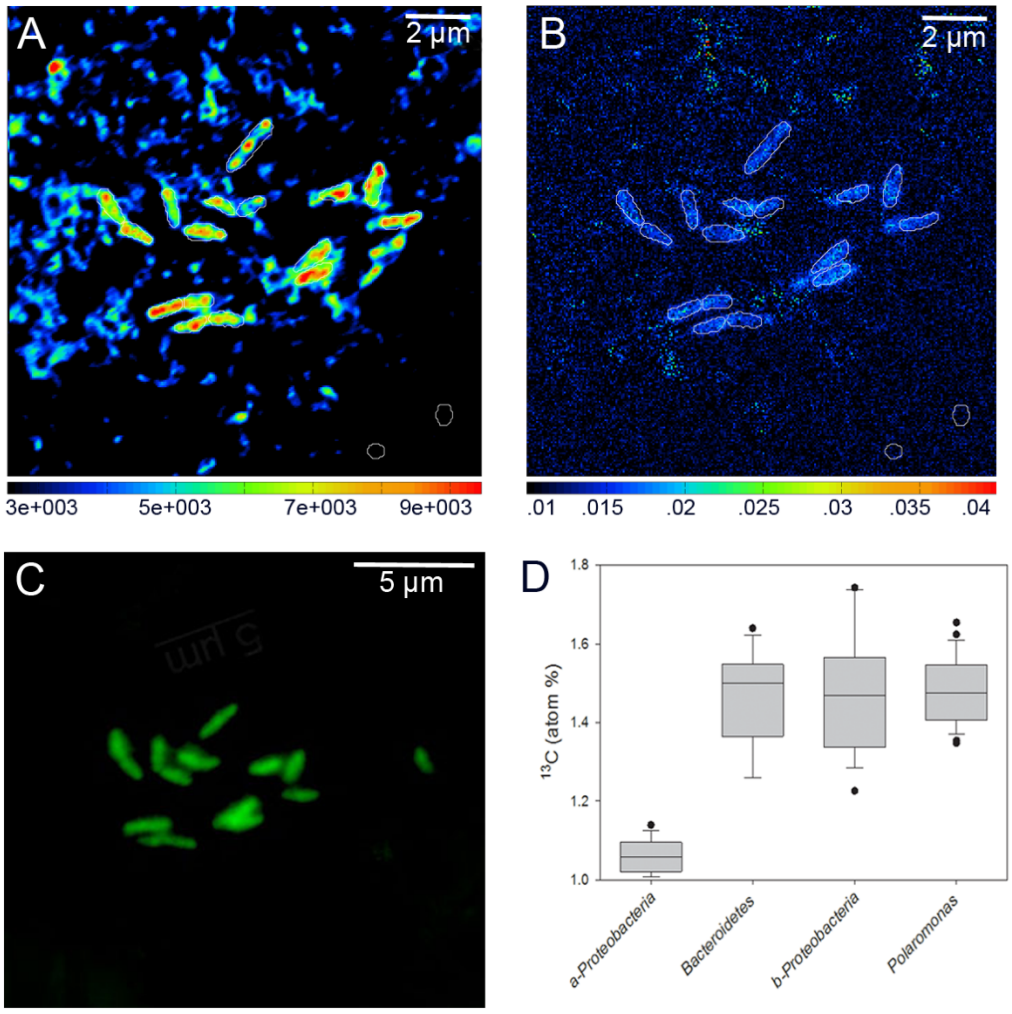

Figure 3.3. Example of analyzed *Polaromonas* sp. cells enriched in ^{13}C-labeled exudates (A.) nanoSIMS image of nitrogen content as $^{12}C^{14}N$ that were used to define ROIs (B.) nanoSIMS isotope ratio image for the $^{13}C/^{12}C$ ratio for cells enriched in ^{13}C labeled exudates, white lines indicate ROIs used for enrichment calculations of analyzed bacterial cells. (C.) Epifluorescence overlay used to confirm cell identification of *Polaromonas* sp. cells hybridized with HRP-labeled Pomo828 oligonucleotide probe where the probe emits a green signal. (D.) Summary boxplot of nanoSIMS analyses of ^{13}C-exudate enriched cells, reported in atom % (AT%) for *Alphaproteobacteria* sp., *Bacteroidetes* sp., *Betaproteobacteria* sp., and *Polaromonas* sp. The whiskers represent the 25th and 75th percentile (lower and upper quartiles, respectively) the mean is shown as a solid line, and outliers are represented by (•).

To confirm that *Alphaproteobacteria* sp. were metabolically active, but not involved in the initial transformation of exuded carbon, samples were amended with a commercially available ^{13}C-labeled algal amino acid mixture (^{13}C-AA; Cambridge Isotopes). All investigated phylogenetic lineages in the CG stream were enriched in ^{13}C (Figure 3.4 B) with incorporation rates of ^{13}C-AA ranging from 5.80×10^{-4} to 1.28×10^{-3} pmol C cell^{-1} d^{-1} (Table 3.3). Using a linear mixed effects model, the rate of ^{13}C-AA assimilation was significantly lower for *Bacteroidetes* cells ($P<0.0001$) compared to the other lineages, while there was no significant difference in the rate of assimilation between *Alphaproteobacteria* sp., *Betaproteobacteria* sp., and *Polaramononas* sp. ($P>0.093$). It is important to note that the measured rates of uptake are an underestimation, given the recent findings that ^{13}C (and ^{15}N) fractions are subject to dilution after treatment with chemical fixations and CARD-FISH assay (Musat *et al.*, 2014). However, our ability to visualize and quantify by nanoSIMS the direct transfer of photosynthetically produced exudates to heterotrophic organisms reaffirms the critical role of microbially mediated carbon cycling on glacial surfaces.

Any exuded carbon that is not rapidly assimilated will be a fraction of glacial organic carbon that may contribute to the metabolic functioning of downstream supraglacial ecosystems or may be exported to the ocean (Figure 3.5). Isotopic analysis was used to quantify the amount of exuded carbon from the CG stream.

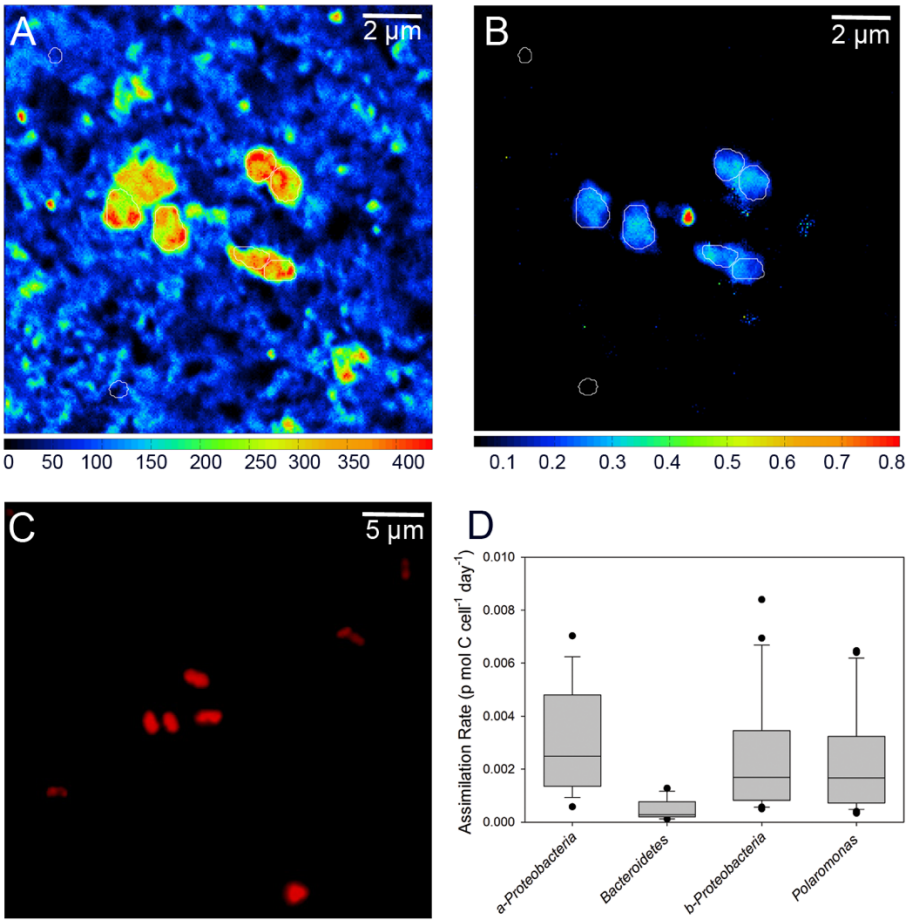

Figure 3.4. Example of analyzed *Alphaproteobacteria* sp. cells enriched in a ^{13}C-labeled algal amino acid (^{13}C-AA) mixture (A.) nanoSIMS image of ^{32}S that was used to define regions of interest (B.) nanoSIMS isotope ratio image for the ^{13}C/^{12}C ratio for cells enriched in ^{13}C labeled AA mixture, white lines indicate ROIs used for enrichment calculations of analyzed bacterial cells. (C.) Epifluorescence overlay used to confirm cell identification of *Alphaproteobacteria* sp. cells hybridized with ALF1B and ALF968 oligonucleotide probes (used in equal amounts) (D.) Summary of nanoSIMS analyses of ^{13}C-exudate enriched cells, reported in pmol C cell^{-1} d^{-1} for *Alphaproteobacteria* sp., *Bacteroidetes* sp., *Betaproteobacteria* sp., and *Polaromonas* sp.

Table 3.3. Average incorporation rates of ^{13}C-labeled exudates and ^{13}C-labeled amino acids ±1 standard deviation. Enrichment that was not above natural abundances is considered not enriched and below detection (ND).

Phylogenetic Identity	^{13}C-Exudate Incorporation Rate (pmol C cell^{-1} d^{-1})	^{13}C Algal Amino Acid Incorporation Rate (pmol C cell^{-1} d^{-1})
Betaproteobacteria sp.	2.39 x 10^{-4} (1.83 x 10^{-4})	2.48 x 10^{-3} (2.20 x 10^{-3})
Alphaproteobacteria sp.	ND	2.88 x 10^{-3} (2.02 x 10^{-3})
Bacteroidetes sp.	2.98 x 10^{-4} (1.18 x 10^{-4})	4.68 x 10^{-4} (3.70 x 10^{-4})
Polaromonas sp.	2.45 x 10^{-4} (1.11 x 10^{-4})	2.20 x 10^{-3} (1.94 x 10^{-3})

Combining the average excess of exuded OC (2.17 ug C L^{-1} d^{-1}), the number of days of stream flow representative of Antarctic streams (60 days; Kohler *et al.*, 2015), and the discharge for the CG stream (0.119 m^3/s; SanClements *et al*. In Review) we conservatively estimate for low flow seasons that a total of 8.03 x 10^4 g C can be exported from the CG stream to downstream aquatic environments. A modest upper estimate of the amount of excess exuded carbon from high flow seasons is derived by coupling discharge measurements from the nearby Onyx River to the CG stream. Discharge measurements from the Onyx River (http://www.mcmlter.org) during the 2010/11 high flow season were 10-fold higher than low flows for the CG stream measured in 2009/10. Therefore, during high flow seasons a total of 8.03 x 10^5 g C could be transported from the CG stream. Using a mean continent-wide meltwater volume, excluding floating ice shelves, of 32 x 10^{12} L/yr (Kuipers Munneke *et al.*, 2012) we estimate that 0.69 Gg C could be discharged yearly

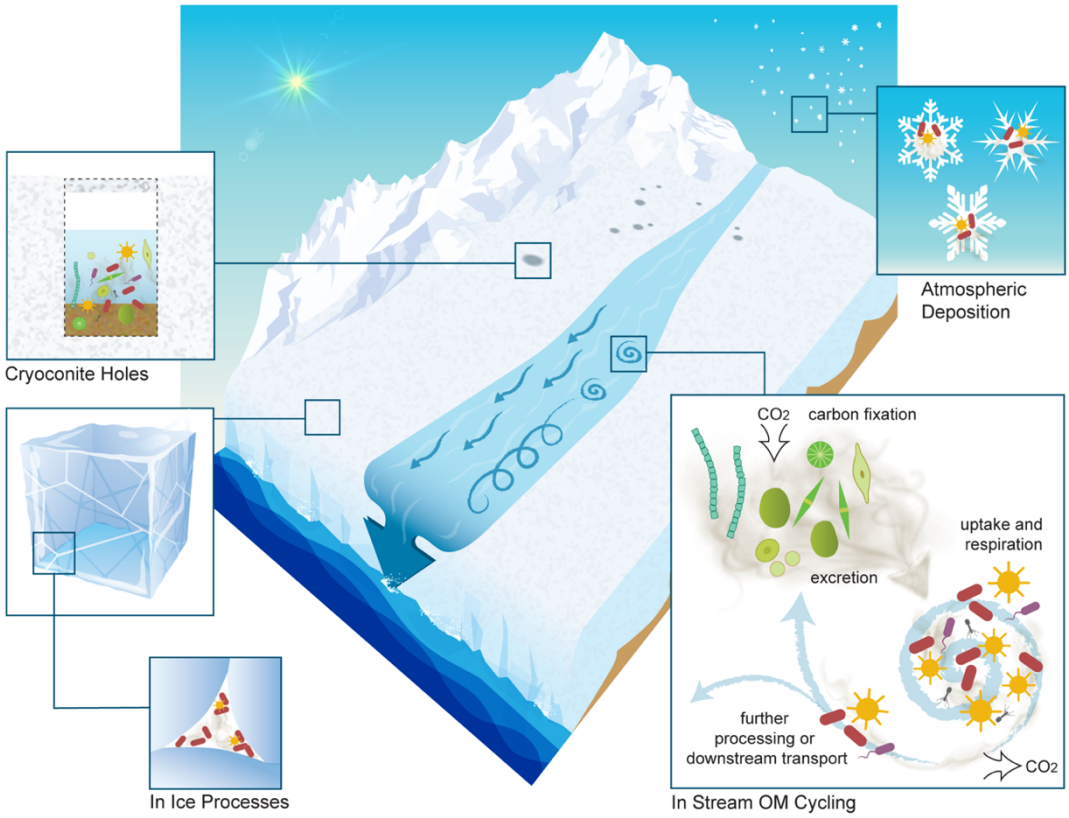

Figure 3.5. A schematic of the different sources and sinks of organic matter (OM) present on the glacier surfaces. Globally, glaciers represent a significant reservoir of organic carbon, and supraglacial biogeochemical cycles contribute microbially produced bioavaible OM to the overall glacial carbon pool. The major sources of glacial OM include aeolian deposition and *in situ* microbial production. Four major compartments of supraglacial OM cycling are depicted, including: cryoconites, aeolian deposition, in ice processes, and in stream OM cycling. The sun represents the role of photo-oxidation processes in altering OM composition. The diverse microorganisms that are present within all of these surficial locations are capable of processing and transforming OM. The truncated microbial loop within streams is a major source of biolabile microbially produced OM and is represented by spirals. The first step in the supraglacial microbial loop is the fixation of atmospheric CO_2 by photoautotrophic microorganisms, recently fixed organic carbon is then released (brown cloud) and is successively taken up by heterotrophic organisms. OM that is utilized by microorganisms is either partially or completely biologically oxidized to CO_2 transforming OM to be potentially more recalcitrant and less bioavaible. In stream arrows represent OM that is not immediately taken up by microorganisms and can be transported or further processed downstream. Ultimately the fate of glacial OM is transport to downstream aquatic ecosystems that eventually will be exported to the ocean.

from the Antarctic Ice Sheet (AIS). In the absence of direct runoff measurements, our estimation solely refers to excess biologically labile OM, and therefore may underestimate total carbon transport from the AIS. This estimated OC flux is one to two orders of magnitude lower than OC flux estimates from the Greenland Ice Sheet (Bhatia *et al.*, 2013; Hodson *et al.*, 2010).

Although glacial environments harbor relatively low amounts of OC, because of their sheer mass they are believed to represent an important component in the global carbon cycle (Priscu and Christner, 2004; Anesio *et al.*, 2009; Hood *et al.*, 2009). Approximately 11% of the Earth's surface is covered by polar ice sheets and glaciers, yet limited information regarding the compositional quality, quantity, and origin of glacial OC is available. Variability exists in estimates of the concentration of OC stored within ice masses, varying from 0.11 to 0.40 mg C L^{-1} for the AIS alone (Priscu and Christner, 2004; Hood *et al.*, 2015). Thus, based on the number, type, and location of samples included in these calculations estimates of total OC contained within the AIS range from ~3.3 to 8.4 petagrams, exceeding the conservative global estimate of six petagrams (Priscu and Christner, 2004; Hood *et al.*, 2015). In addition to differences in geographic location, potential sources of glacial OC range from deposition of aerosols (Stubbins *et al.*, 2012; Antony *et al.*, 2014) and terrestrially derived materials to autochthonous microbial synthesis (Singer *et al.*, 2012) (Edwards *et al.*, 2013), which could affect ecosystem function and biogeochemical cycles in different ways. Therefore, it is useful to consider that glacial OC is not uniform in nature across glacial environments, to refine estimates of role of glacial OC on a local and global scale as more data become available.

The bioavailability assays using bulk glacial OC conducted previously (Hood *et al.*, 2009; Singer *et al.*, 2012; Lawson *et al.*, 2013), provided information on only a portion of the OC utilized by the heterotrophic microorganisms. Based on these findings it was inferred that the highly labile fraction OC is old in age and representative of the entire labile OC pool liberated from ice. This study presents the first direct evidence that OC produced by microbial phototrophs is an important substrate for supra-glacial stream communities. This result adds another source to the initial scenario that aeolian deposited carbon locked in ice is the primary contributor to glacial carbon cycling (Stubbins *et al.*, 2012). The present results demonstrate that microbially released OC is highly bioavailable, and that the interplay between phototrophs and heterotrophs forms a highly dynamic carbon cycle in glacial ecosystems.

Methods

Bulk Biological Analyses

Samples were collected in December 2010 and December 2011 and in January 2012 from the Cotton Glacier supraglacial stream (77°07'S 161°40'E). Stream water was collected in milli-Q rinsed fluorinated carboys, and transported to either the Lake Fryxell field camp or McMurdo Station within 2 hrs for subsequent analyses.

Heterotrophic bacterial productivity was measured with ^{3}H-Leucine incorporation (final concentration 20 nM) following the protocol described in (Kirchman *et al.*, 1985). Leucine incorporation assays were performed in triplicate with two corresponding formalin killed controls (5% formalin added 30 min prior to ^{3}H-Leucine addition), samples were incubated at 4°C for 24 hrs. Primary productivity (PPR) was measured

using ^{14}C-carbonate/bicarbonate incorporation (8.4 mCi mmol^{-1}, pH 9.5, MP Biomedicals) following the protocol of Lizotte et al. (1996). Five light assays were run per sample in combination with three dark controls. All samples were incubated in a light incubator closely mimicking environmental conditions (50.6 photons m^{-2}) at 4°C for 24 hrs. After incubation, samples were gently filtered (<7 psi) through pre-combusted GF/F filters in the dark. Filters were then placed into 20 mL scintillation vials, acidified with 500 µL 3M HCl and allowed to dry at 60°C for 8 hrs. Samples for extracellular release measurements were performed in triplicate with ^{14}C-bicarbonate amendments (8.4 mCi mmol^{-1}, pH 9.5, MP Biomedicals), following a 24 hr incubation under environmentally relevant conditions (same as above). The samples were gravity filtered to minimize any artificial enhancement of extracellularly released carbon due to autotrophic cellular damage. The filtrate was collected in clean borosilicate bottles, acidified to a ~pH 2.0 with 6N HCl, sparged with N_2 gas to remove any unincorporated dissolved inorganic carbon (DIC) and was dried on a warming plate at 60°C. For both PPR and extracellular release (ECR) samples, 10 mL of Ecolume scintillation cocktail were added to each scintillation vial and samples were analyzed using a liquid scintillation counter (Beckman LS 6000). Percent extracellular release (PER) was calculated as follows: PER=ECR/total primary production x 100 (Coveney, 1982). ^{13}C-DOC samples were analyzed at the University of California, Davis stable isotope facility using an O.I. Analytical Model 1010 TOC analyzer interfaced to a PDZ Europa 20–20 isotope ratio mass spectrometer (Sercon Ltd).

Determination of the biological carbon demand followed the calculations described in (Vick and Priscu, 2012), where bacterial rates of heterotrophic bacterial productivity were converted to bacterial carbon production and considered the biological carbon demand (D). The supply of OC from excreted products was calculated as a percentage from the total primary productivity (S). Finally, the comparison of the D:S ratio was used to determine that the bacterial carbon demand was met by the supply of exuded carbon. To calculate the amount of OC in excess of the bacterial carbon demand the average uptake of released as determined by nanoSIMS was subtracted from the total amount of exuded.

Stable Isotope Labeling and Incubation Experiments

Catalyzed reported deposition fluorescent *in situ* hybridization secondary ion mass spectrometry (CARD-SIMS) was used to determine the rate and identify the organisms responsible for the uptake of exuded photosynthate products (Musat *et al.*, 2008). Whole water samples from the Cotton Glacier stream were initially incubated with ^{13}C-labeled bicarbonate (~99% ^{13}C, Cambridge Isotopes Laboratories Inc., Andover, MA, USA, 1 mM final concentration) in 1 L bottles in a light incubator to simulate *in-situ* light (50.6 photons m^{-2}) and temperature (4°C) conditions for 72 hrs. After the 72 hr incubation cellular biomass and incorporated ^{13}C-labeled bicarbonate were removed with filtration (<7 psi), while the filtrate containing the newly ^{13}C-labeled exudates was collected. The filtrate was acidified to ~pH 3.5 and sparged with N_2 gas for 1 hr to remove any unincorporated ^{13}C-labeled bicarbonate. After sparging, the pH of the exudates was brought back to ~pH 7.0, which is the pH of the Cotton Glacier stream.

Samples were collected for ^{13}C TOC analysis to determine the starting concentration of exudates, which was necessary for uptake calculations. Cotton Glacier stream water containing the active microbial assemblage was then added to the newly synthesized ^{13}C-exudates and incubated under the same conditions as above for 24 hrs. After incubation the samples were fixed with paraformaldehyde (final concentration 2%) for 1.5 hrs at room temperature. Subsamples were then filtered onto gold-palladium pre-coated 0.2 μm GTTP polycarbonate filters (Millipore) under low vacuum pressure (<7 psi) and washed three times with 1X phosphate buffered saline (PBS). Filters were dried and stored in cryovials at -20°C until further processing

Hybridization and Microscopic Evaluation

Sections (5 mm diameter) of filters were excised and hybridized with fluorescent *in situ* hybridization (FISH) horseradish peroxidase (HRP)-labeled oligonucleotide probes following the CARD-FISH protocol described by (Pernthaler *et al.*, 2004). To avoid detachment of cells throughout sample preparation, filters were initially embedded in 0.1% low melting point agarose. Gram negative bacterial cells were permeabilized with a lysozyme (10 mg mL^{-1} in 0.05M EDTA, pH 8.0) and 0.1M Tris-HCl treatment at 37°C for 1 hr. After permeabilization filters were washed three times with ultrapure water (MQ, Millipore) and endogenous peroxidases were bleached with 3% H_2O_2 at 20°C for 10 min. Prior to hybridization filters were washed three times for 1 min with ultrapure water, submerged in 96% ethanol for 1 min, and allowed to air dry completely. Filters were subjected to a 1 hr pre-hybridization step without the probe, then probes were added (1:150 v/v) and hybridized at 46°C for 6 hrs using a previously described protocol (Musat

et al., 2008). The oligonucleotide probes and corresponding formamide concentrations used for this study are provided in Table SI1. For FISH with horseradish peroxidase (HRP) labeled oligonucleotide probes a tyramide signal amplification step was done following the protocol described in (Pernthaler *et al.*, 2002), where hybridized cells were counterstained with 4',6'-diamindino-2-phenylindole (DAPI) at a final concentration of 1 $\mu g\ mL^{-1}$ in the dark for 10 min. Filter sections were covered in mounting solution containing 4 parts Citifluor (Citifluor, Ltd., London, United Kingdom) and 1 part VectaShield (Vector Laboratoires, Burlingame, CA). Ten randomly chosen fields (grid size of 15,625 μm^2) corresponding to 1,000-1,200 DAPI stained cells were counted using a Zeiss Axioskop II fluorescence microscope (Zeiss, Berlin, Germany) with a final magnification of 1,000X. Counts are reported as mean averages from triplicate cell counts that have been converted based on phylogenetic classification to percentages of the total number of cells counted. Areas of interest for nanoSIMS were marked with arrows and numbers using a Laser Micro Dissection (LMD) microscope 6500 (Leica, Berlin, Germany). Microscopic pictures were taken and used for orientation purposes during the subsequent nanoSIMS analysis and post processing using look@nanoSIMS software (see below).

NanoSIMS Analysis

NanoSIMS analysis was performed using a Cameca NanoSIMS 50L instrument (Cameca, Gennevilliers, France). After re-identifying the laser marked regions of interest (ROIs) with the CCD camera, samples were pre-sputtered for 1-2 min and rastered with 16 keV Cesium (Cs^+) primary ions with a current between 1 and 3 pA beam size <100

nm. Mass resolving power in the majority of the measurements was >8000. The primary ion beam was used to raster the analyzed area with an image area of 256 x 256 pixels over the chosen raster size with a dwelling time of 1 or 2 ms per pixel. Negative secondary ions (^{12}C, ^{13}C, ^{19}F, $^{12}C^{14}N$, $^{12}C^{15}N$, and ^{32}S) were collected simultaneously in electron multiplier detectors. All scans (40-50 planes) were corrected for drift of the beam and sample stage after acquisition using the look@nanoSIMS software package (Polercky et al. 2012). Isotope ratio images were created as the ratio of a sum of counts for each pixel over all recoded planes of the investigated main isotope. Individual regions of interest (ROIs) were defined using the $^{12}C^{14}N$ (^{13}C-labeled exudates) and ^{32}S (^{13}C-labeled algal amino acids) ratio images and were compared to fluorescent images for DAPI stained and CARD-FISH hybridized cells.

The equations used for C assimilation were as previously described in (Foster *et al.*, 2011). Estimations of biovolume were calculated following (Sun, 2003). For biovolume estimations of individual cells the equation of a sphere was used ($V = (\pi/6) \times d^3$). Since analyzed populations were not in culture, cellular carbon content was estimated based on the relationship described in (Verity *et al.*, 1992), $Log[C] = -0.363 + (0.863 \times (Log(V))$. The estimated carbon content per cell was then converted to N content per cell assuming the Redfield ratio of 6.6. The isotopic ratios based on ROI selection and measured by nanoSIMS were used in order to calculate atom percent enrichment (AT%) for both isotopic ratios of $^{13}C/^{12}C$, where AT% of $^{13}C = (^{13}C/^{12}C)/(^{13}C/^{12}C + 1)$. AT% enrichment was then converted to cell specific C assimilation where A_C is cells specific assimilation ^{13}C. $A_C = (^{13}C\text{-excess} \times C\text{-content})/(^{13}C\text{-initial})$. Using an EA-IRMS ^{13}C content was

measured for non-enriched samples, these measurements were used as the natural isotopic abundance values for ^{13}C-initial. The natural abundance values were incorporated in the calculation to determine the labeling percentage and used to normalize the atom % enrichment of ^{13}C. All nanoSIMS enrichment and rate assimilation data was log transformed prior to statistical analysis with the *stats* package in R (Team, 2014) where a liner mixed effects model was used to analyze ^{13}C enrichment for both of the tracers used in this study (^{13}C-labeled exudate, and ^{13}C-labeled algal amino acids).

Optical Analysis

Dissolved organic matter (DOM) from the Cotton Glacier stream and subsequent experimental incubations were analyzed using excitation emission matrices (EEMs), which were collected over an excitation range of 240–450 nm in 10 nm increments while emission was monitored from 300–560 nm in 2 nm increments on a Fluoromax-4 spectrofluorometer (HORIBA Jobin-Yvon). Samples were analyzed for UV absorbance with a Thermo Scientific Genesys 10 scanning UV spectrophotometer; from 190-1100 nm on optically dilutes samples (absorbance values < 0.3 at 254 nm). EEMs data were post-processed to correct for instrument-specific bias using manufacturer-generated correction files for excitation, emission, and blank subtraction. Fluorescence intensities were normalized across the three different samples (where $F_{min}/(F_{max}-F_{min})$) and then specific regions of fluorescence were defined for each carbon source corresponding to previously identified natural organic matter fluorophores (Coble, 1996). Fluorescence intensity values in the proteinaceous regions (B and T fluorophores) were summed and classified as more-labile, while humic-like fluorescence (A fluorophore) were combined

and classified as less-labile and more recalcitrant. The fluorescence for defined regions was individually summed for each respective sample and presented as a percentage of the total fluorescence found in each sample. amino acids).

Viral Abundances

Water samples collected for bacterial and bacteriophage enumeration were collected in sterile flasks, immediately flash froze in liquid nitrogen and kept at -80°C until analyzed. Samples were stained using SYBR® Green I (Thermo Fisher Scientific, Inc.) and counted using a Becton Dickinson FACSCalibur™ flow cytometer (BD Bioscience) following the protocol of Brussaard 2004(Brussaard, 2004). Bacterial and viral counts were derived from the number of events retained within pre-determined regions for bacteria and viruses after approximately 10 min sampling intervals. The constraints for the bacteria and virus regions were based on distributions of known suspensions of SYBR® Green I stained bacteria and viruses.

Acknowledgements

This work was supported by the National Science Foundation Division of Antarctic Sciences through ANT-0838970 and ANT-1141978, by the NSF Division of Graduate Education through DGE-0654336, and through a NASA Earth and Science Space Fellowship to HJS. The Max Plank Society supported the nanoSIMS and EA-IRMS analyses. Sten Litmann, Gabriele Klockgether, and Guate Lavik from MPI Bremen are acknowledged for assistance in the nanoSIMS and EA-IRMS analyses. RAF is funded by the Knut and Alice Wallenberg Foundation and ^{13}C-DOC measurements were

supported by NSF grant to RAF (BIO-OCE0929015). Flow cytometry was performed by Drs. David Dunigan and Ahmed Esmael, University of Nebraska-Lincoln. Any opinions, findings, or conclusions expressed in this material are those of the authors and do not necessarily reflect the views of the National Science Foundation.

References

Anesio AM, Hodson AJ, Fritz A. (2009). High microbial activity on glaciers: importance to the global carbon cycle. *Glob Change Biol* **15**: 955–960.

Anesio AM, Sattler B, Foreman C, Telling J. (2010). Carbon fluxes through bacterial communities on glacier surfaces. *Annals of Glaciology* **51**: 32–40.

Antony R, Grannas AM, Willoughby AS, Sleighter RL, Thamban M, Hatcher PG. (2014). Origin and sources of dissolved organic matter in snow on the East Antarctic ice sheet. *Environ Sci Technol* **48**: 6151–6159.

Barker JD, Dubnick A, Lyons WB, Chin YP. (2013). Changes in Dissolved Organic Matter (DOM) Fluorescence in Proglacial Antarctic Streams. *Arctic, Antarctic, and Alpine Research* **45**: 305–317.

Barker JD, Sharp MJ, Fitzsimons SJ, Turner RJ. (2006). Abundance and Dynamics of Dissolved Organic Carbon in Glacier Systems. *Arctic, Antarctic, and Alpine Research* **38**: 163–172.

Bauer SE, Bausch A, Nazarenko L, Tsigaridis K, Xu B, Edwards R, *et al.* (2013). Historical and future black carbon deposition on the three ice caps: Ice core measurements and model simulations from 1850 to 2100. *Journal of Geophysical Research: Atmospheres* **118**: 7948–7961.

Bhatia MP, Das SB, Longnecker K, Charette MA, Kujawinski EB. (2010). Molecular characterization of dissolved organic matter associated with the Greenland ice sheet. *Geochimica et Cosmochimica Acta* **74**: 3768–3784.

Bhatia MP, Das SB, Xu L, Charette MA, Wadham JL, Kujawinski EB. (2013). Organic carbon export from the Greenland ice sheet. *Geochimica et Cosmochimica Acta* **109**: 329–344.

Brussaard CPD. (2004). Optimization of procedures for counting viruses by flow cytometry. *Appl Environ Microbiol* **70**: 1506–1513.

Coble PG. (1996). Characterization of marine and terrestrial DOM in seawater using excitation-emission matrix spectroscopy. **51**: 325–346.

Cook JM, Hodson AJ, Anesio AM. (2012). An improved estimate of microbially mediated carbon fluxes from the Greenland ice sheet. *Journal of …* **58**: 1098–1108.

Coveney MF. (1982). Bacterial Uptake of Photosynthetic Carbon from Freshwater Phytoplankton. *Oikos* **38**: 8.

Edwards A, Pachebat JA, Swain M, Hegarty M, Hodson AJ, Irvine-Fynn TDL, *et al.* (2013). A metagenomic snapshot of taxonomic and functional diversity in an alpine glacier cryoconite ecosystem. *Environ Res Lett* **8**: 035003.

Foster RA, Kuypers MMM, Vagner T, Paerl RW, Musat N, Zehr JP. (2011). Nitrogen fixation and transfer in open ocean diatom–cyanobacterial symbioses. *ISME J* **5**: 1484–1493.

Hodson A, Bøggild C, Hanna E, Huybrechts P, Langford H, Cameron K, *et al.* (2010). The cryoconite ecosystem on the Greenland ice sheet. *Annals of Glaciology* **51**: 123–129.

Hood E, Battin TJ, Fellman J, O'Neel S, Spencer RGM. (2015). Storage and release of organic carbon from glaciers and ice sheets. *Nature Geoscience* **8**: 91–96.

Hood E, Fellman J, Spencer RGM, Hernes PJ, Edwards R, D'Amore D, *et al.* (2009). Glaciers as a source of ancient and labile organic matter to the marine environment. *Nature* **462**: 1044–1047.

Kirchman D, K'nees E, Hodson R. (1985). Leucine incorporation and its potential as a measure of protein synthesis by bacteria in natural aquatic systems. *Appl Environ Microbiol* **49**: 599–607.

Kohler TJ, Stanish LF, Crisp SW, Koch JC, Liptzin D, Baeseman JL, *et al.* (2015). Life in the Main Channel: Long-Term Hydrologic Control of Microbial Mat Abundance in McMurdo Dry Valley Streams, Antarctica. *Ecosystems* **18**: 310–327.

Kuipers Munneke P, Picard G, Broeke den MR, Lenaerts JTM, Meijgaard E. (2012). Insignificant change in Antarctic snowmelt volume since 1979. *Scientific Investigations Report* **39**(1).

Lawson EC, Wadham JL. (2013). Greenland Ice Sheet exports labile organic carbon to the Arctic oceans. *Biogeosciences* **10**: 19311–19345.

Li F, Ginoux P, Ramaswamy V. (2008). Distribution, transport, and deposition of mineral dust in the Southern Ocean and Antarctica: Contribution of major sources. *Journal of Geophysical Research: Atmospheres* **113** D(10).

Musat N, Halm H, Winterholler B, Hoppe P, Peduzzi S, Hillion F, *et al.* (2008). A single-cell view on the ecophysiology of anaerobic phototrophic bacteria. *Proc Natl Acad Sci USA* **105**: 17861–17866.

Musat N, Stryhanyuk H, Bombach P, Adrian L, Audinot J-N, Richnow HH. (2014). The effect of FISH and CARD-FISH on the isotopic composition of ^{13}C- and ^{15}N-labeled Pseudomonas putida cells measured by nanoSIMS. *Systematic and Applied Microbiology* 1–10.

Musilova M, Tranter M, Bennett SA, Wadham J, Anesio AM. (2015). Stable microbial community composition on the Greenland Ice Sheet. *Front Microbiol* **6**: 193.

Ogawa H, Amagai Y, Koike I, Kaiser K, Benner R. (2001). Production of refractory dissolved organic matter by bacteria. *Science* **292**: 917–920.

Pautler BG, Simpson AJ, Simpson MJ, Tseng L-H, Spraul M, Dubnick A, *et al.* (2011). Detection and structural identification of dissolved organic matter in Antarctic glacial ice at natural abundance by SPR-W5-WATERGATE 1H NMR spectroscopy. *Environ Sci Technol* **45**: 4710–4717.

Pernthaler A, Pernthaler J, Amann R. (2002). Fluorescence in situ hybridization and catalyzed reporter deposition for the identification of marine bacteria. *Appl Environ Microbiol* **68**: 3094–3101.

Pernthaler A, Pernthaler J, Amann R, Kowalchuk GA, Bruijn FJ de, Head IM, *et al.* (2004). Sensitive multi-color fluorescence in situ hybridization for the identification of environmental microorganisms. Kluwer Academic Publishers Volumes 1 and 2: 711-725.

Priscu JC, Christner BC. (2004). Earth's icy biosphere. *Microbial Diversity and Prospecting*.

M. D. SanClements, H. J. Smith, D. M. McKnight, C. M. Foreman, and M. Tedesco. Characterizing the functioning of a supraglacial ecosystem: The Cotton Glacier Stream. Submitted: Arctic Antarctic and Alpine research

Säwström C, Anesio MA, Granéli W, Laybourn-Parry J. (2007). Seasonal viral loop dynamics in two large ultraoligotrophic Antarctic freshwater lakes. *Microb Ecol* **53**: 1–11.

Säwström C, Lisle J, Anesio AM, Priscu JC, Laybourn-Parry J. (2008). Bacteriophage in polar inland waters. *Extremophiles* **12**: 167–175.

Singer GA, Fasching C, Wilhelm L, Niggemann J, Steier P, Dittmar T, *et al.* (2012). Biogeochemically diverse organic matter in Alpine glaciers and its downstream fate. *Nature Geoscience* **5**: 710–714.

Smith, H., Foster, R., J. Lisle, M.M. Kuypers, and C.M. Foreman. Microbial formation of labile glacial organic carbon. In Prep: Nature Geosciences Letters.

Stibal M, Sabacka M, Zarsky J. (2012). Biological processes on glacier and ice sheet surfaces. *Nature Geoscience* **5**: 771–774.

Stubbins A, Hood E, Raymond PA, Aiken GR, Sleighter RL, Hernes PJ, *et al.* (2012). Anthropogenic aerosols as a source of ancient dissolved organic matter in glaciers. *Nature Geoscience* **5**: 198–201.

Sun J. (2003). Geometric models for calculating cell biovolume and surface area for phytoplankton. *Journal of Plankton Research* **25**: 1331–1346.

Suttle CA. (2007). Marine viruses - major players in the global ecosystem. *Nat Rev Microbiol* **5**: 801–812.

Takacs CD, Priscu JC, McKnight DM. (2001). Bacterial dissolved organic carbon demand in McMurdo Dry Valley lakes, Antarctica. *Limnol Oceanogr* **46**: 1189–1194.

Team, R. C. (2014). R: A language and environment for statistical computing. Vienna, Austria: R Foundation for Statistical Computing; 2013.

Teira E, Pazó MJ, Serret P. (2001). Dissolved organic carbon production by microbial populations in the Atlantic Ocean - Teira - 2001 - Limnology and Oceanography - Wiley Online Library. *Limnology and Oceanogr* **46**: 1370–1377.

Van den Meersche K, Middelburg JJ. (2004). Carbon-nitrogen coupling and algal-bacterial interactions during an experimental bloom: Modeling a 13C tracer experiment - Van den Meersche - 2004 - Limnology and Oceanography - Wiley Online Library. *Limnology and Oceanogr* **49**: 862–878.

Verity PG, Robertson CY, Tronzo CR, Andrews MG, Nelson JR, Sieracki ME. (1992). Relationships between cell volume and the carbon and nitrogen content of marine photosynthetic nanoplankton. *Limnol Oceanogr* **37**: 1434–1446.

Vick TJ, Priscu JC. (2012). Bacterioplankton productivity in lakes of the Taylor Valley, Antarctica, during the polar night transition. *Aquat Microb Ecol* **68**: 77-90.

Wigington CH, Sonderegger D, Brussaard CPD, Buchan A, Finke J, Fuhrman J, *et al.* (2016). Re-examination of the relationship between marine virus and microbial cell abundances. *Nature*.

Wilhelm SW, Suttle CA. (1999). Viruses and Nutrient Cycles in the Sea Viruses play critical roles in the structure and function of aquatic food webs. *BioScience* **49**: 781–788.

CHAPTER 4

SUPRAGLACIAL DISSOLVED ORGANIC MATTER: A LABILE BUT UNSUSTAINABLE CARBON SOURCE

Contribution of Authors and Co-Authors

Author: Heidi J Smith*

Contributions: Designed the experiment, conducted experiments, analyzed data, wrote the manuscript.

Co-Author: Michelle Tigges*

Contributions: Designed the experiment, conducted experiments, analyzed data, wrote the manuscript.

Co-Author: Juliana D'Andrilli

Contributions: Data analysis, manuscript preparation

Co-Author: Albert Parker

Contributions: Data analysis, manuscript editing

Co-Author: Brian Bothner

Contributions: Co-principal investigator of laboratory experiments data analysis, manuscript preparation and editing

Co-Author: Christine Foreman

Contributions: Co-principal investigator of laboratory experiments data analysis, manuscript preparation and editing

*Authors contributed equally

Manuscript Information Page

Heidi J. Smith, Michelle Tigges, Juliana D'Andrilli, Albert Parker, Brian Bothner, Christine Foreman
Limnology and Oceanography
Status of Manuscript:
__X__ Prepared for submission to a peer-reviewed journal
____ Officially submitted to a peer-review journal
____ Accepted by a peer-reviewed journal
____ Published in a peer-reviewed journal

Abstract

Large quantities of organic carbon are stored in glacial ice, with the Antarctic Ice Sheet being the largest repository. Presumably labile in nature, released dissolved organic matter (DOM) is predicted to stimulate downstream environments, making glacial DOM of increased importance in global carbon cycling with future climatic warming. Coupling the release of DOM to microbial metabolic responses, however, is challenging due to the complexity of DOM and microbial communities. By combining exometabolomics with microbiological and biogeochemical techniques, we established proxies to predict DOM lability from various end-member environments associated with microbial DOM processing. Our study showed that a single organism is capable of processing compositionally diverse sources of DOM, but, while labile, glacially derived DOM was unable to support sustained cellular respiration. In view of projected changes in glacier DOM export these findings imply that biogeochemical impacts on downstream environments will largely depend on the chemical composition of liberated DOM.

Introduction

Dissolved organic matter (DOM) in freshwater environments is an important source of organic carbon, supporting heterotrophic bacterial respiration over local and regional scales. Rivers and estuaries are the connection between freshwater and marine ecosystems, globally transporting 0.9 petragrams or carbon per year to the oceans (Cole *et al.*, 2007). DOM is comprised of a heterogeneous mixture of labile and recalcitrant chemical compounds, which affects its overall bioavailability to microorganisms and directly influences biological processing and turnover rates (Mopper *et al.*, 2007; Vahatalo *et al.*, 2010). Labile DOM is a bioavailable fraction of carbon that promotes net heterotrophic activity and ultimately becomes a source of CO_2 released from aquatic environments (Battin *et al.*, 2008). Freshwater DOM transported to downstream ecosystems was previously thought to be highly degraded, however recent reports indicate that exported DOM may also be labile (Bianchi, 2011).

DOM lability has previously been operationally defined as a function of biological availability and time (Jiao *et al.*, 2010). However, lability is best interpreted in the context of both chemical composition and microbial metabolism (Nelson and Wear, 2014). Representative labile carbon sources used in laboratory experiments to examine the transformation of DOM are generally simple substrates, such as glucose or combinations of amino acids (Nelson and Carlson, 2012; Nikrad *et al.*, 2012; Jørgensen *et al.*, 2014; Lechtenfeld *et al.*, 2015). Unfortunately, these substrates lack environmental relevance and do not address the chemical complexity of naturally occurring DOM. Investigations from diverse glacial environments show that glacially derived DOM can

be highly bioavailable to microorganisms (Hood *et al.*, 2009; Bhatia *et al.*, 2013; Lawson and Wadham, 2013), suggesting that these environments are a reservoir of labile freshwater DOM. Therefore, we used carbon sources isolated from Antarctica, as Antarctica represents an optimal environment to study the processing of bioavailable microbially derived freshwater DOM. To deepen the understanding of microbially mediated transformations of DOM, three carbon sources representing different environmental end-members and a continuum of labilities were selected: microbially derived DOM from the oligotrophic supraglacial Cotton Glacier stream, Antarctica (CG), microbially derived DOM from the eutrophic coastal pond, Pony Lake, Antarctica (International Humic Substances Society [IHSS] Pony Lake Fulvic Acid; PL), and as a counterpoint terrestrially derived DOM from the Suwannee River, USA (IHSS Natural Organic Matter; SR).

Heterotrophic organisms are involved in all aspects of DOM cycling, including synthesis, transformation, and degradation. Biodegradation is a major mechanism mediating the processing, cycling, and decomposition of DOM globally. The transfer of carbon from DOM to bacteria has been proposed to follow four major pathways; direct, photolytic, sorption, and via extracellular enzymes (Findlay and Sinsabaugh, 1999). Currently, our understanding of biological DOM processing is dominated by oceanographic studies (Hansell and Carlson, 2014; Jiao *et al.*, 2013; Mou *et al.*, 2008; Kujawinski, 2011; Jiao *et al.*, 2010; Nelson and Carlson, 2012), with far less known about the process in freshwater environments. Thus, there is a significant gap in knowledge regarding how individual organisms interact with complex DOM from

different freshwater sources.

Coupling changes in DOM composition to *in situ* microbial community processing is inherently difficult because of methodological challenges associated with analyzing DOM due to its molecular complexity. This is further complicated by the phylogenetic diversity of natural microbial assemblages. Recent evidence indicates that individual species of marine organisms can affect ecosystem-wide processes, and may be responsible for significant DOM fluxes and nutrient mineralization (Pedler *et al.*, 2014). Single organism studies therefore provide a definitive way to resolve the contributions of individual microorganisms to bulk processing. To investigate the biological transformation of freshwater DOM of varying lability, we conducted extended incubations under environmentally relevant conditions with a single metabolically diverse and globally relevant organism, *Janthinobacterium* sp. strain CG3 (CG3) (Smith *et al.*, 2013). CG3 was isolated from a supraglacial stream on the Cotton Glacier, Antarctica, and specifically chosen because of its predicted ability to process diverse sources of DOM. The CG3 genome is 6.12 Mbp and possesses genomic evidence for complete central carbon metabolism and fermentative pathways. The metabolic flexibility of CG3 makes it an exemplary organism for an in depth study of the biodegradation of environmentally relevant carbon sources.

To characterize the complex interactions that occur between heterotrophic bacteria and heterogeneous DOM, a combination of metabolomic, microbiological, and biogeochemical techniques were employed. Excitation Emission Matrix spectroscopy (EEMs), Fourier Transform Ion Cyclotron Resonance Mass Spectrometry (FT-ICR MS),

and Ultra Performance Liquid Chromatography coupled Quadrupole-Time of Flight Mass Spectrometry (UPLC-Q-TOF MS) based analyses generated a complementary description of the composition and lability for the three DOM sources. UPLC-Q-TOF MS and EEMs provide information on exometabolite transformations (biologically mediated changes in DOM over time). When combined with respirometry and microbial growth analysis, the role of metabolic plasticity in microbial DOM degradation can be described with a new level of detail. This study provides a straight-forward approach for predicting DOM lability without the need for challenging and costly long-term microbial experiments.

Materials and Methods

Experimental Setup

CG3 was grown from freezer stock for two generations to mid-exponential phase in a low nutrient media, R2A (Difco). Second generation mid-exponential cells were concentrated by centrifugation at 6,000 rpm for 10 min and cells were washed twice with a 1X saline buffer. Washed cells were inoculated to a final concentration of 10^5 cells/mL into a carbon free minimal M9 media (Difco). Three carbon source amendments (CG, PL, SR) were added to 125mL combusted amber bottles, to a mass balanced final concentration of 5 mg/L C. CG DOM was isolated from its supraglacial stream whole water by reverse osmosis, and SR natural organic matter and PL fulvic acid were obtained from the IHSS isolated by reverse osmosis (SR) and XAD-8 (PL). Five biological replicates of these innocula were set up for destructive sampling at four time points over the 98 day experiment for UPLC-Q-TOF MS analysis. Aliquots in biological triplicate were also divided for daily respirometry measurements of each carbon source.

All samples were incubated under environmentally relevant conditions at 15 °C, in the dark, and shaken at 30 rpm. All glassware used in the experiments were acid washed and combusted at 450°C for 5h to remove organic material prior to use.

Fluorescence Spectroscopy

Prior to analysis, samples were filtered through 0.2 μm low carbon syringe tip filters into combusted amber glass vials. Samples were collected 1-2 times per week for optical analysis. EEMs were collected over an excitation range of 240–450 nm in 10 nm increments and emission was monitored from 300–560 nm in 2 nm increments on a Fluoromax-4 spectrofluorometer (HORIBA Jobin-Yvon). Samples were analyzed for UV absorbance with a Thermo Scientific Genesys 10 scanning UV spectrophotometer; from 190-1100 nm on optically dilutes samples (absorbance values < 0.3 at 254 nm). A total of 14 samples per carbon source treatment were collected. EEMs data were post-processed to correct for instrument-specific bias using manufacturer-generated correction files for excitation, emission, and media blank subtraction (carbon free M9 minimal media). For temporal samples, EEMs were normalized according to the fluorescent intensity normalization calculation in the DOMFluor Toolbox (Stedmon and Bro, 2008). Specific regions of fluorescence were defined for each carbon source corresponding to previously identified natural organic matter fluorophores (Coble, 1996). For the duration of the experiment, CG amended samples showed one region of maximum fluorescence (Ex: 240-280 nm, Em: 300-350 nm) corresponding to the more-labile, proteinaceous fluorophores B and T, (Coble, 1996; Stedmon *et al.*, 2003). Over time, CG DOM fluorescence developed at longer emission wavelengths (Ex: 240-280nm, Em: 400-450

nm), representing a humic-like fluorophore from region A. Four fluorophores (B, T, C and A) were identified in both the PL and SR DOM throughout the course of the experiment. Fluorescence intensity values in the proteinaceous regions (B and T fluorophores) were summed and classified as more-labile, while humic-like fluorescence regions (A and C fluorophores) were combined and classified as less-labile and more recalcitrant. The fluorescence for both defined regions was summed and converted to the percentage change relative to the previous sampling point.

FT-ICR MS

FT-ICR MS provides a method for unambiguous molecular formulae assignment of environmental samples while routinely producing ultrahigh mass resolving power ($m/\Delta m_{50\%}$ >750,000 at *m/z* 500) and ultrahigh mass accuracy (error < 1ppm). Therefore, the data generated here are more extensive in molecular composition coverage of complex natural OM samples than any other single analytical technique. Mass spectra were obtained with a custom-built superconducting 9.4 Tesla FT-ICR MS at the National High Magnetic Field Laboratory located in Tallahassee, Florida. Electrospray Ionization (ESI) and FT-ICR MS instrumental parameters are described in detail in (D'Andrilli *et al.*, 2013), therefore only a brief description will be provided.

Prior to mass spectral analysis, negatively charged gaseous ions were produced with a custom-built ESI source (Emmett *et al.*, 1998) and transferred into the mass spectrometer. Experimental parameters were selected based on previous natural DOM FT-ICR MS analysis and restructured for optimal DOM chemical composition characterization (D'Andrilli *et al.*, 2013). Moreover, these settings reduce the potential

for ion suppression, ion collisions, and irreproducible ion contamination between spectra scans. Samples were pumped through the ESI source at a flow rate of 0.5 µL/min, 200 time domain acquisitions were co-added, Hanning apodized, and zero-filled once before rapid Fourier transformation and magnitude calculation to produce the FT-ICR mass spectrum. CG and SR DOM MS were internally calibrated with two $-CH_2$ homologous series commonly found in natural organic matter. A calibrated peak list was then generated for MS peaks with 6x the rms noise.

The composition of each carbon source was determined by analyzing assigned $C_cH_hN_nO_oS_s$ molecular formulae for variations in heterogeneity (N and/or S) as well as hydrogen, carbon, and oxygen saturation. Molecular formulae were divided into chemical categories from the classifications commonly used on the van Krevelen diagram and quantified to compare the character between each carbon source (Fig. 2D). This analysis method was modeled after (Santl-Temkiv *et al.*, 2013), including the modified aromaticity index calculation from (Koch and Dittmar, 2006), and a minor adjustment to describe the following molecular categories: (1) peptides, having molecular formulae at $1.5 \leq H/C \leq 2.0$ and $O/C \leq 0.8$, (2) sugars, with molecular formulae $1.5 \leq H/C \leq 2.0$ and $O/C > 0.8$, (3) saturated fatty acids have molecular formulae at $H/C > 2.0$ over all O/C ratios, (4) highly unsaturated constituents at $H/C < 1.5$, over all O/C ratios, and a modified aromaticity index (AI_{mod}) < 0.5, (5) phenols with the same boundary conditions of the previous category, highly unsaturated constituents, at $AI_{mod} \geq 0.5$ with less than 12 C atoms, and (6) polyphenols, with the same boundary conditions as phenols, but extending the category to include molecular formulae ≥ 12 C atoms.

Cellular Respiration

A Micro-Oxymax closed-circuit respirometer (Columbus Instruments) was used to measure O_2 concentrations. Each carbon source plus bacterial cells was run in triplicate, and a blank without cells was included. After the completion of the experiment, blank values for each carbon source were subtracted from the O_2 consumption values at each time point. Respirometry data was analyzed for average consumption and broken line relationships. Using R (R Development Core Team, 2014), mean cellular respiration among carbon treatments were compared for each time point separately by ANOVA and Tukey-HSD, and a Bonferroni correction across the 98 time points was applied. For carbon source treatments with broken line relationships, break-points were estimated by the R's *segmented* package for R (Muggeo, 2008). Before and after each breakpoint, the linear rates were compared among carbon sources by a linear mixed effects model (Pinheiro and Bates, 2000), fit by R's *nlme* package (Pinheiro *et al.*, 2015). The model included a random intercept and a random slope over time for each treatment vial, a fixed effect for carbon source, a covariate for time, and an interaction effect added between carbon and time. High resolution respirometry data in combination with EEMs was monitored for shifts to determine sampling intervals and frequency for external metabolite sampling.

External Metabolite Extraction DOM
Source Material Characterization

CG3 cells were removed from the microbiological media with 0.2µm, low-carbon binding syringe tip filters. Filtered external metabolites from samples and source material samples were passed through Solid Phase Extraction (SPE) PPL cartridges (Agilent Bond

Elut) to concentrate small molecules and remove inorganic salts (Dittmar *et al.*, 2008). Retained small molecules were eluted into combusted glass vials with HPLC grade methanol, dried down under nitrogen, and stored in the dark at -20°C prior to analysis.

UPLC-Q-TOF MS Based
Molecular Constituent Analysis

Mass spectra of external metabolites were obtained by a 1290 Ultra Performance Liquid Chromatography system coupled to a 6538 Ultra High Definition Accurate-Mass Quadrupole-Time of Flight mass spectrometer operated in positive mode with an electrospray ionization source (Agilent Technologies). External metabolites were re-suspended in 50% (v/v) acetonitrile, and were separated using a reverse-phase Kinetix 1.7 µm C18, 100A, 150 mm × 2.1 mm column. The mobile solvent system consisted of A = 0.1% formic acid in water and B = 0.1% formic acid in acetonitrile. The C18 linear gradient was 2% B -95% B with an injection volume of 8 µL and a flow rate of 600µL/min. ESI conditions were as follows: gas temperature 350°C, drying gas of 8 L/min, nebulizer 60 psig, fragmentor 100 V, and skimmer 45 V. Mass spectral acquisitions included *m/z* range 50–1000 at 2 spectra /s. Data was visualized with the MassHunter software package (Agilent Technologies). All UPLC-Q-TOF MS data was processed by XCMS and XCMS online suite of software (Colin A Smith *et al.*, 2006; Tautenhahn *et al.*, 2012; Gowda *et al.*, 2014). Abundance (sum of intensity over time) reports were created for ions present in all biological replicates of at least one of the sample groups.

Pairwise abundance comparisons were carried out between consecutive time points within individual carbon sources. Welch *t-tests* were performed by XCMS,

followed by a Benjamini Hochberg correction for multiple testing to maintain a false discovery rate (FDR) of 5% (Benjamini and Hochberg, 1995). Log transformed abundance values for each constituent were evaluated across time within individual carbon sources by ANOVA. The presence or absence of significantly changed features was compared across carbon sources to assess the compositional differences in bacterial transformation of DOM components. A two-factor ANOVA (carbon source, time point) was performed on the log transformed abundances of each constituent to test for differences in the degree of a constituent's change in abundance over time among the three carbon sources. All ANOVA based analyses were followed by a Benjamini Hochberg correction to maintain a FDR of 1%. For molecular features with an adjusted p-value < 0.01, fold change values for a given molecular constituent were calculated based on the ratio of abundance change between consecutive time points, $\log_2$ transformed, and visualized using R's *gplots* package (Warnes *et al.*, 2015). Hierarchical clustering with bootstrapping was performed using Euclidean distance and the complete agglomeration method in R's *pvclust* package (Suzuki and Shimodaira, 2011). All feature comparisons were carried out using the metaXCMS software (Tautenhahn *et al.*, 2011; Patti *et al.*, 2012). The influence of the lability classification on the magnitude of fold change for the significantly changed constituents was determined using a linear model with fixed effects for lability (levels of more and less), carbon source (CG, PL, SR), and time (early, mid, late). Interactions were investigated with interaction plots and significance tests.

Results

DOM Source Material Characterization

Total fluorescence analysis by EEMs is a well established method for characterizing DOM at the bulk level (Coble *et al.*, 1990; McKnight *et al.*, 2001). CG DOM has maximum fluorescence at low excitation and emission wavelengths in a protein-like region (Figure 4.1A, fluorophore peak B, Ex:Em 240:314 nm). In addition to protein-like fluorescence, PL and SR DOM have humic-like fluorescence (Figure 4.1A): fluorophore peak A (Ex:Em 240:424 nm) and peak C (Ex:Em 300-320:400-450 nm).

Molecular level DOM source composition was determined by FT-ICR MS, a method routinely utilized to unambiguously determine DOM elemental contributions ($C_cH_hN_nO_oS_s$) and chemical character (Brown and Rice, 2000; Kim *et al.*, 2003). FT-ICR MS data for CG, PL, and SR DOM contain molecular formulae in each chemical species group (CHO, $CHOS_1$, $CHON_1$, $CHON_1S_1$, $CHON_2$, $CHON_2S_1$, see Table AD1). CG, PL, and SR DOM were primarily made up of CHO containing molecular components, with PL having the lowest percentage of CHO molecular species (25.9%) as compared to CG (49.8%) and SR (56.6%), indicating a higher degree of heterogeneity for PL DOM (Table S1).

The chemical classifications of CG and SR DOM based on H/C and O/C ratios are provided as van Krevelen diagrams in Fig. 2A-B with PL described in (D'Andrilli *et al.*, 2013). On the diagrams, each dot represents one assigned molecular formula from one resolved mass spectral peak generated by FT-ICR MS. Molecular data appear in all chemical class regions of the van Krevelen diagrams (classifications provided on Figure

4.2C). Different heteroatom species (molecular formulae containing $C_cH_hO_o$ and varying amounts of N_n and S_s, where n=0, 1, or 2 and s=0 or 1) are displayed with different symbols and colors, over broad H/C and O/C ratios. Molecular formulae common to all carbon sources, containing CHO, $CHOS_1$, $CHON_1$, and $CHON_2$ are present in the peptide-, sugar-, highly unsaturated-, phenolic-, and polyphenolic-like regions of the van Krevelen diagram (Figure 4.2C). CG DOM contained the greatest protein-like character discerned from the percentage of peptide-like molecular constituents (41.0%; Figure 4.2D) determined by FT-ICR MS compared to PL and SR DOM (20.3% and 5.85%), which was expected due to the microbial influence in each carbon source. Conversely, the highly unsaturated chemical species were the smallest for CG DOM followed by PL and SR. These species, having more recalcitrant nature, were also expected to follow this trend as SR represents a terrestrial carbon source end member with more lignin-like contributors in the environment.

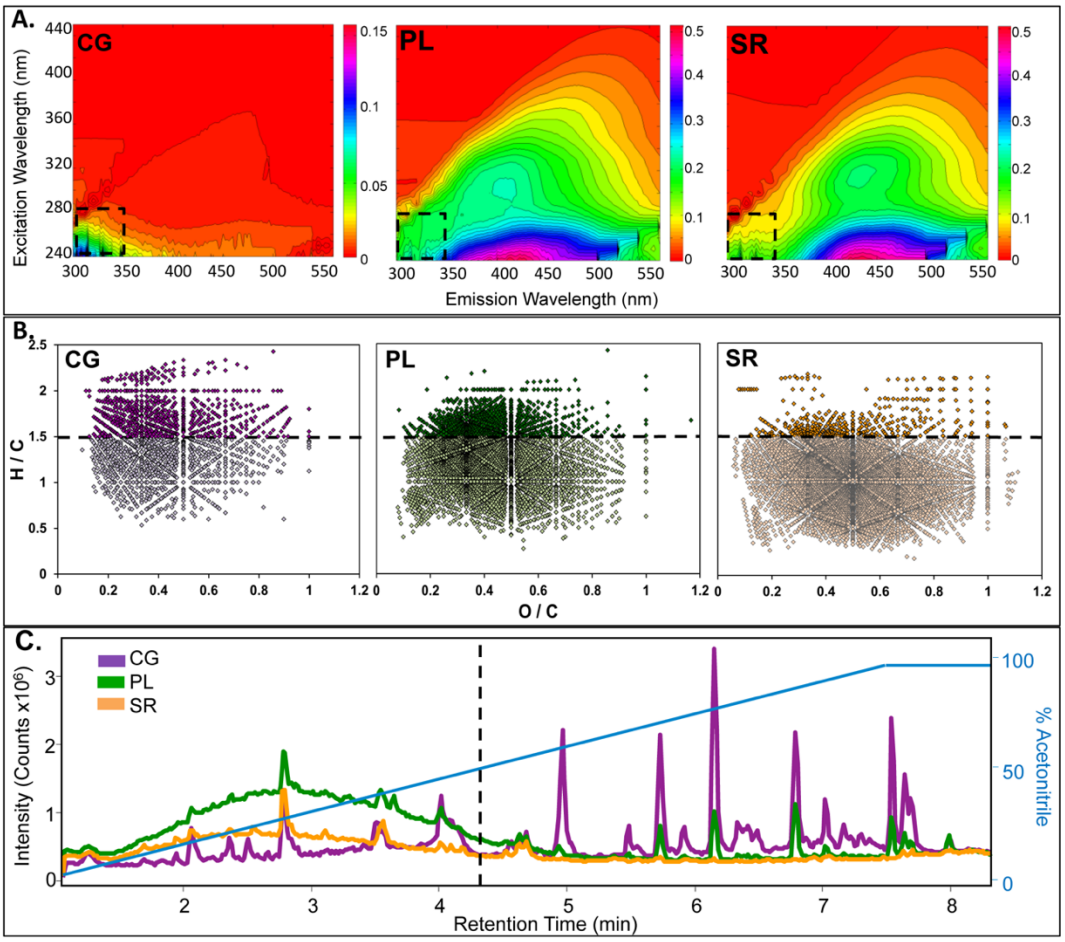

Figure 4.1. Cotton Glacier (CG), Pony Lake (PL), and Suwannee River (SR) DOM source material characterization and lability proxies detected by A) EEMs, where dashed lines represent the boundary of the more-labile fluorescence region, B) FT-ICR MS where the molecular lability boundary is highlighted as a dashed line, with more-labile constituents having H/C $\geq$ 1.5, and C) reverse-phase UPLC-Q-TOF MS total ion chromatograms overlaid with the solvent elution profile where the dashed line represents the cutoff utilized for more-(right) and less-(left) labile classification.

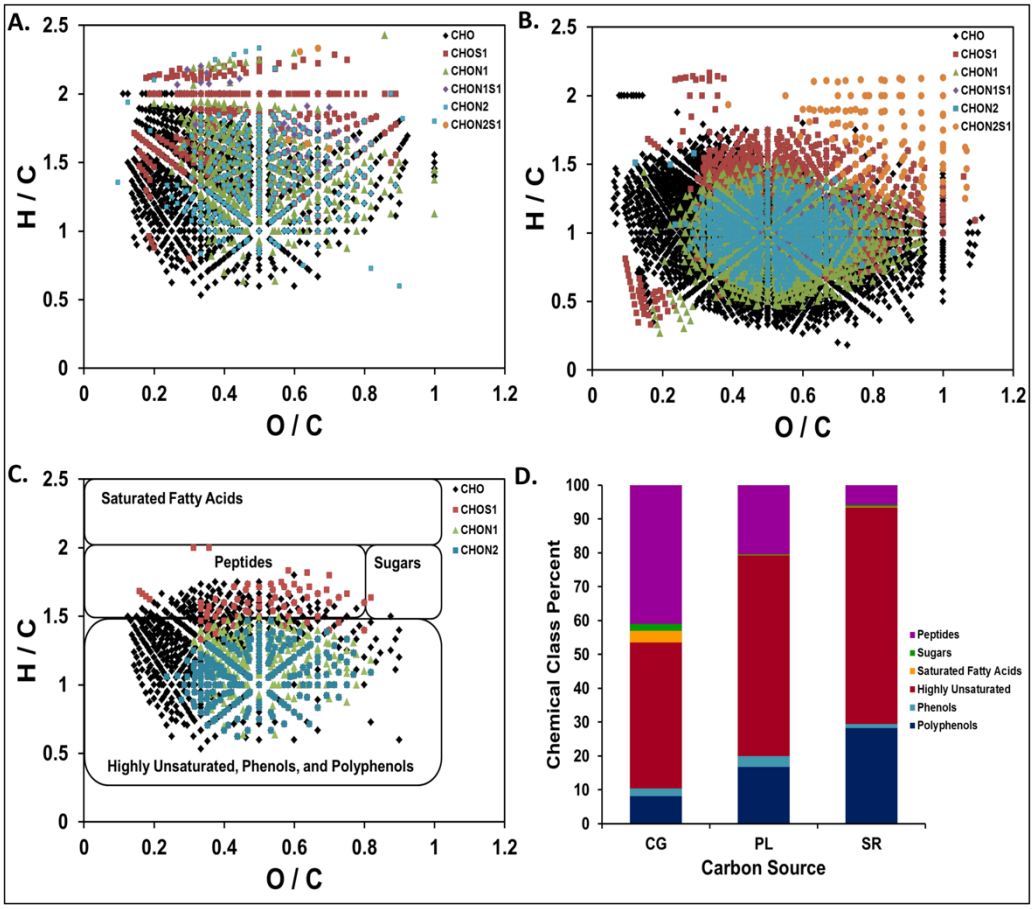

Figure 4.2. Van Krevelen diagrams for organic matter isolated from A) Cotton Glacier and B) IHSS Suwannee River NOM. Molecular formulae detected in all carbon sources (CG, Pony Lake, and SR) are shown in (C) with labeled chemical class regions corresponding to the boundary conditions presented in (D), which shows the chemical class percentages contributing to each carbon source calculated from the molecular formulae.

DOM Source Material and Lability Classification

Defining and categorizing the DOM carbon sources by their labile nature was an essential aspect of understanding carbon bioavailability in this study. With no single method capable of capturing the entire DOM pool of constituents, lability approximations were made for EEMs, FT-ICR MS, and UPLC-Q-TOF MS data by dividing each dataset

into two chemical classes consisting of more- or less-labile molecular components. Each method captures a different portion of the DOM pool, giving a more comprehensive global analysis of bioavailability and labile character in the environment.

Fluorescent investigations of naturally occurring DOM have used EEMs to probe ecosystem lability (Cory and Kaplan, 2012); in this study, we apply similar boundaries to identify the fluorescent source material DOM lability. More-labile DOM components were defined within and around the protein-like region, defined by the ranges Ex: 240-270 nm and Em: 300-350 nm. Humic-like, and therefore less-labile, more recalcitrant DOM fluoresces at higher emission wavelengths. The less-labile region for this study was defined by combining the humic-like regions of peaks A and C (Ex: 240-440 nm and Em: 400-560 nm). EEMs based DOM carbon source lability fell into a continuum such that CG>PL>SR with CG fluorescent DOM containing the most labile character at 34.3%, followed by 17.7% for PL, and 4.9% for SR (Figure 4.1A).

We applied a molecular lability boundary (MLB) for FT-ICR MS data, determined from molecular constituents with higher hydrogen saturation (H/C) values linked to protein-, amino sugar-, and lipid-like chemical class regions corresponding to less lignin-like or less recalcitrant DOM character on van Krevelen diagrams (Kim *et al.*, 2003; D'Andrilli *et al.*, 2013). The MLB was set at H/C = 1.5, with DOM constituents above it being more-labile and those below less-labile, more recalcitrant in nature (Figure 4.1B). While the boundary for biological classification is somewhat ambiguous, this approach allowed for a relatively unbiased comparison of DOM lability richness by FT-ICR MS. CG DOM contained more-labile molecular constituents with 46.5% above the

MLB, whereas PL and SR had more-labile nature at 20.8% and 6.72% (Table AD.1). This assigned a lability continuum of CG>PL>SR, consistent with the EEMs data. Expanding beyond chemical species lability richness, diversity within the more- and less-labile regions was calculated by incorporating the relative abundance values of each mass spectral peak from the FT-ICR MS data. This calculation weights the effect of ionized elemental compositions to the overall distribution within each group. The diversity calculation produced the same overall results as reported for richness with CG>PL>SR at 68.6, 17.4, and 2.82 percentages, respectively.

Previous studies have shown a trend of decreasing polarity and increasing hydrogen saturation of DOM components based on their elution position in reverse-phase liquid chromatography (RPLC) (Koch *et al.*, 2008; Stenson, 2008). Additionally, RPLC coupled to fluorescence analysis has indicated that humic-like fluorescent peaks elute in more polar solvents, while proteinaceous-like fluorescent peaks elute in less polar solvent conditions (Wu *et al.*, 2003; Li *et al.*, 2013). These trends indicate that elution position in RPLC can be used to separate DOM based on characteristics associated with lability. Since we can relate DOM hydrogen saturation to lability via FT-ICR MS analysis, we reasoned that assessing the degree of polarity and thus hydrogen saturation by reverse-phase UPLC-Q-TOF MS could provide complementary information on DOM lability. To test this, reverse-phase UPLC-Q-TOF MS chromatograms of the carbon source materials were divided into two groups, less polar (more-labile) and more polar (less-labile) based on elution in solvent containing greater than or less than 50% acetonitrile, respectively. Comparisons of the abundances of more- and less-labile components indicate that CG

DOM contains the most labile nature, 73.4%, followed by PL at 65.0%, and SR at 59.5% (Figure 4.1C). While this method provides a much less definitive lability boundary than EEMs and FT-ICR MS the results were consistent with the overall lability continuum reported with these methods.

Cellular Respiration

Cellular respiration is a direct measure of metabolism, linking bacterial growth to the rate of carbon source utilization. To investigate specific metabolic rates, CG3 was grown with each of the three DOM carbon sources (CG, PL, and SR), and also in a control sample in the absence of a carbon source. All samples were incubated for 98 days. Cellular respiration was measured every 24 hours in the control and carbon treatments (Figure 4.3). All treatments with DOM amendments were shown to support microbial respiration over the course of 98 days. No significant difference in mean O_2 consumption for each carbon treatment was observed during the first 17 days of the experiment ($P>0.156$). After 17 days of incubation, conversion of the three carbon source materials to CO_2 by CG3 diverged between PL and both CG and SR ($P<0.001$). The first statistically significant difference in O_2 consumption between CG and SR occurred at day 59 ($P=0.0352$), with O_2 consumption remaining significantly different ($P<0.001$) for the duration of the experiment. Broken line regression analysis of all carbon sources identified significant break-points in respiration data, indicating a difference in the rate of DOM O_2 consumption by CG3. Break-points were identified for CG at day 64 ($P<0.001$) and for SR at day 56 ($P<0.001$). No significant break-point was identified for PL ($P>0.076$). Overall, PL DOM supported the greatest rate of respiration for CG3 at 32.76

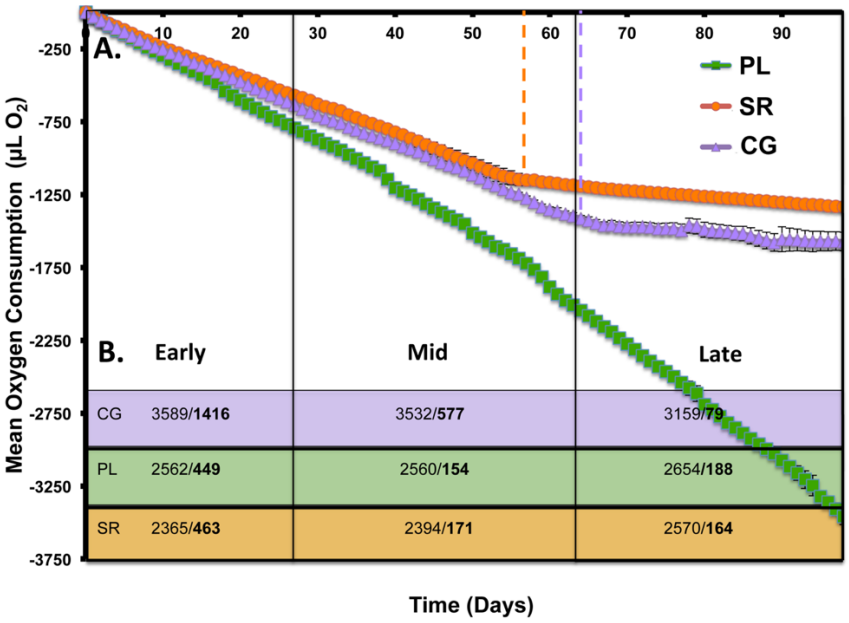

Figure 4.3. Measures of biological transformation of DOM over time. A) Mean oxygen consumption (µL O_2) by CG3 for Cotton Glacier (CG), Pony Lake (PL), and Suwannee River (SR) under constant incubation conditions, error bars ± 1 SD. O_2 measurements were taken every 24 hours for 98 days (N=3). Dashed lines indicate a significant break-point in linearity for CG (day 64) and SR (day 56). B) Number of molecular constituents measured/ constituents with significantly changed abundance in bold (adjusted P<0.05) between time points (Early=days 0-27, Mid=d27-62, and Late=d62-98) for CG3 incubations with CG, PL and SR DOM sources.

µL O_2 consumed/day, followed by CG at 21.78 and SR at 20.17. After each break-point, CG3 respired the CG and SR DOM at reduced rates (18.82 and 16.02 µL O_2 consumed/day, respectively). These break-points in linearity were used to inform sampling time points for UPLC-Q-TOF MS molecular constituent characterization.

Fluorescent Characterization of DOM Transformations

Throughout the 98 day incubations, fluctuations in both the more- and less-labile fluorescent regions were detected by EEMs showing the generation or loss of specific fluorophores. Each set of carbon source specific EEMs were normalized to directly

compare changes in fluorescence by CG3 over time. During the experiment, a pattern of increasing protein-like fluorescence, followed by decreasing fluorescence emerged for all carbon sources (Figure 4.4). Although the fluctuations in DOM fluorescence were less pronounced for the humic-like, less-labile region over time, changes were observed throughout the course of the experiment for all carbon sources.

Analysis of DOM Molecular Constituent Transformations

Liquid chromatography coupled mass spectrometry (UPLC-Q-TOF MS) is a powerful platform for the untargeted relative quantitation of small molecules over time (Want *et al.*, 2005; Colin A Smith *et al.*, 2006), enabling a high throughput investigation of DOM transformations at the molecular level. While EEMs analysis provided bulk level characterization of the evolution of fluorescent components of DOM, high resolution UPLC-Q-TOF MS was used to track changes in abundance of individual molecular constituents at four time points (days 0, 27, 63, and 98) during the 98 day incubations. A total of 5,040 distinct molecular constituents were detected across all carbon sources and time points. The relative abundance of each molecular constituent was ascertained and pairwise comparisons between time points (time ranges: early= days 0-27; mid = days 27-63, late= days 63-98) were used to calculate variances in abundances

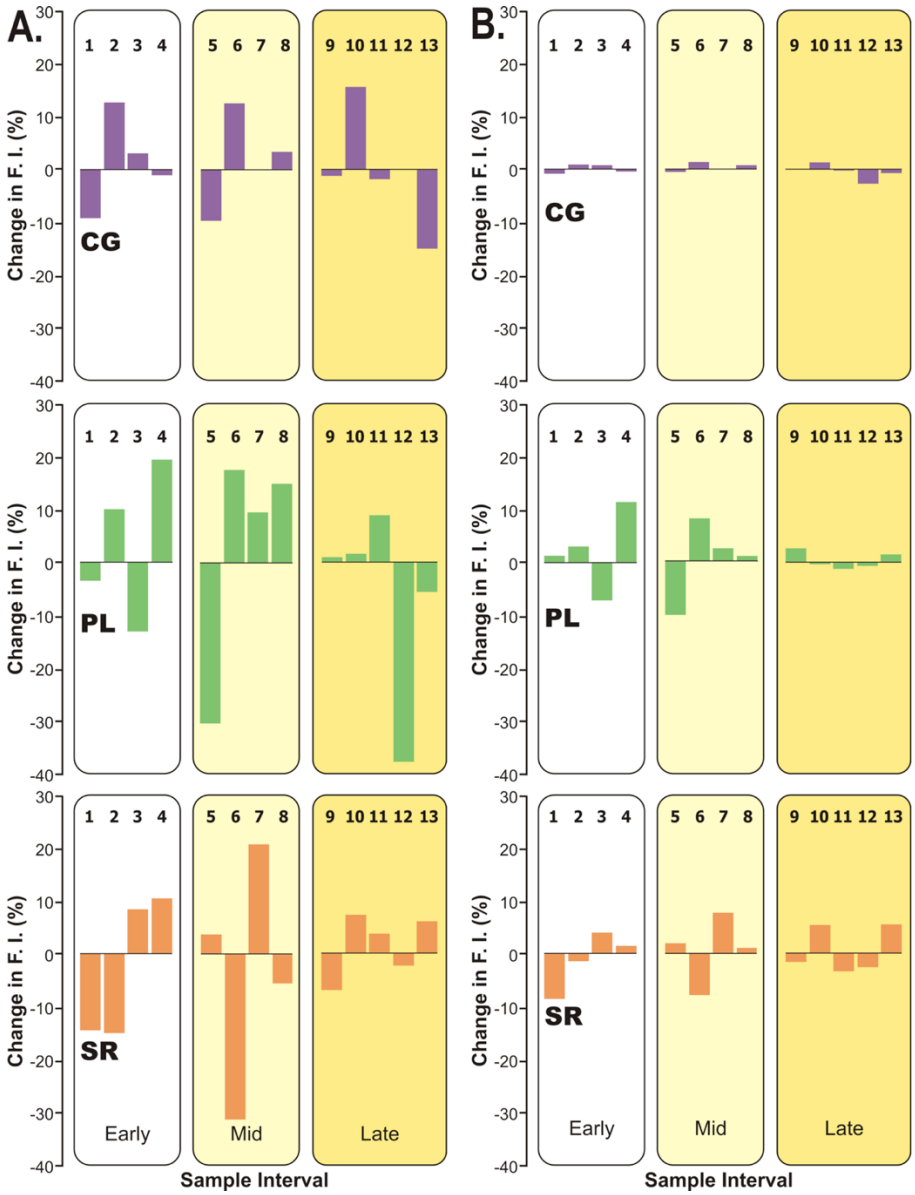

Figure 4.4. Change in fluorescent intensity (F.I.) for Cotton Glacier (CG), Pony Lake (PL), and Suwannee River (SR) calculated from normalized EEMs for (A) percent more-labile fraction of DOM fluorescence and B) percent less-labile fraction of DOM fluorescence, at each sampling point, relative to the total amount of change in labile fluorescence throughout the duration of the experiment (98 days). Sample intervals (SI) are the difference in F. I. between two sampling points. S.I.1=d2-10, S.I.2=d10-18, S.I.3=d18-26, S.I.4=d26-34, S.I.5=d34-41, S.I.6=41-49, S.I.7=49-55, S.I.8=d55-60, S.I.9-d60-72, S.I.10=d72-78, S.I.11=d78-83, S.I.12=d83-90, S.I.12=d90-97. Experimental phases correspond to exometabolome time ranges, and early = d0-27, mid = d28-63, and late = d64-98.

of constituents over time. While significant (adjusted $P< 0.05$) changes in abundance occurred throughout the incubations, the number of transformed constituents was highest in the early time range (Figure 4.3B). The late time range contained the lowest number of transformed molecular constituents for CG and SR, coinciding with the decrease in respiration rates. Conversely, the number of PL transformed constituents in the late time range remained constant relative to the mid time range.

In an attempt to highlight the biologically relevant molecular constituents, a one way ANOVA was carried out for each constituent in each of the carbon sources. Overall, 3057 molecular constituents showing a significant (adjusted $P< 0.01$) abundance change over time were retained. The unique mass/retention time of each constituent was then used to determine similarities between the carbon sources (Figure AD.2A). Over the course of the experiment, 38% of significantly changed constituents were found in all three carbon sources, while 26% were unique to CG. PL (8%) and SR (5%) had fewer uniquely transformed molecular constituents. Two-way ANOVAs (time point, carbon source) of each of the constituents detected in all carbon sources were used to assess how the trends in constituent abundance over time compared between the carbon sources. Of these constituents, 749 demonstrated a significant change in abundance over time that was different depending on the carbon source (adjusted $P<0.01$). Cluster analysis of the molecular constituents based on abundance change demonstrated both the source and time dependence of DOM transformation by CG3 (Figure 4.5). Only the early time range clustered exclusively by time, indicating that transformations during this time frame were more similar across all carbon sources than those during later time periods.

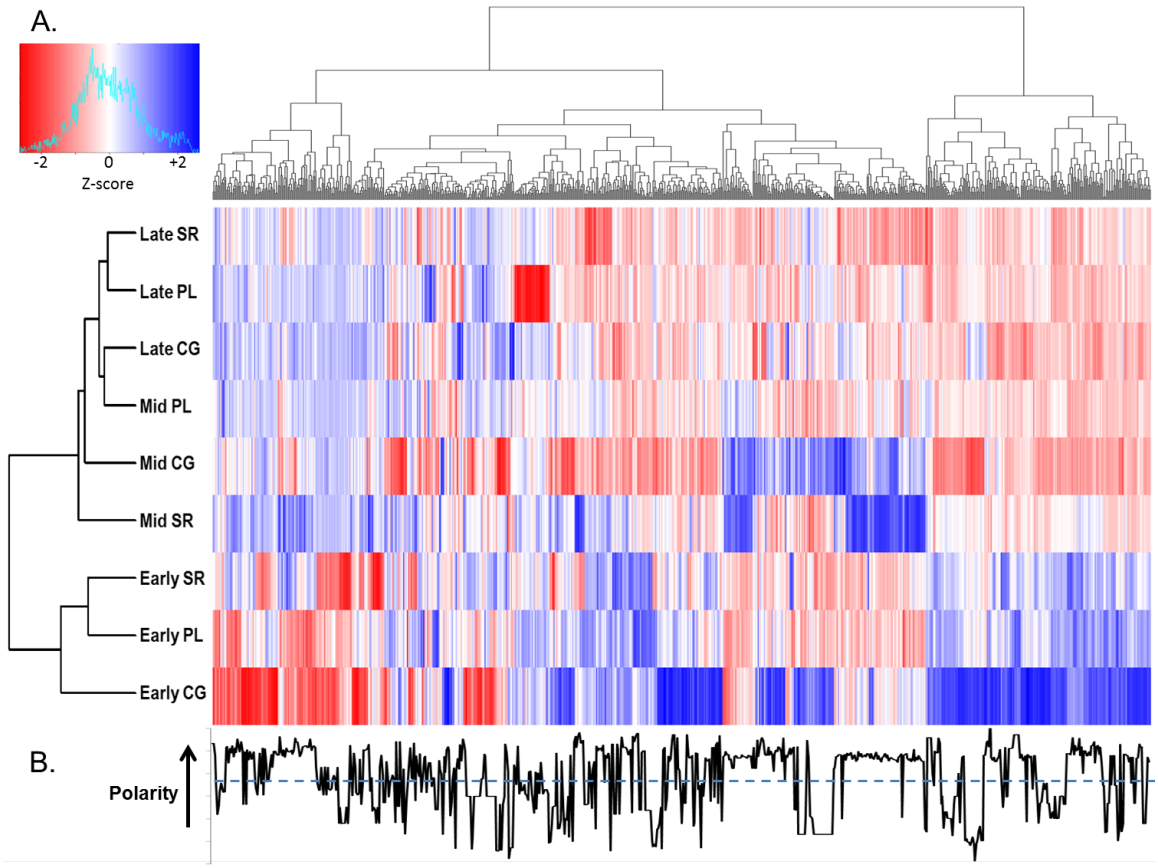

Figure 4.5. Profile of significant (adjusted P<0.01) molecular constituent abundance changes in CG3-DOM incubations detected by UPLC-Q-TOF MS analysis. A) Heatmap of CG3 molecular constituent abundance fold changes across time range (Early: d0-27, Mid: d28-63, Late: d64-98) and carbon source (Cotton Glacier: CG, Pony Lake: PL, Suwannee River: SR). Abundance increases and decreases are shown in blue and red, respectively. Constituents (columns) that cluster together have similar abundance patterns over time with respect to each carbon source. B) Profile of the UPLC retention time based relative polarity of constituents. The dashed line represents the cutoff used to classify more- (below) and less- (above) labile constituents.

The effect of carbon source and time on the mean magnitude of molecular constituent abundance change was found to significantly differ depending on the UPLC-Q-TOF-based lability classification (more- or less- labile) of the constituents (P<0.001). Subsequently, to discern how our chemically-defined lability related to the degree of change over time, the fold change magnitude for more- (i.e., less polar) and less- labile

(i.e., more polar) constituents were compared for each carbon source over time (Figure A4.3). The lability classification showed no significant effect on the degree of CG constituent fold change over time ($P>0.05$), while the degree of constituent fold change for both PL and SR was significantly influenced ($P<0.001$) by the chemical lability classification at least at the mid time range.

Discussion

Across natural environments heterogeneity in DOM composition promotes ecosystem stability by providing diverse compounds, potentially varying in lability, as energy sources to different heterotrophic bacteria (Wetzel, 2003). Ecologically, it still remains to be determined which specific community members, either rare or abundant, have an influential role in DOM processing. It is not known if a single organism is capable of processing compositionally diverse DOM, or if DOM transformations are reliant on a cascade of events between various community members. To begin to understand the complicated network of DOM processing, single organism studies conducted under environmentally relevant conditions are necessary. CG3 was selected based on its global ubiquity and the predicted genomic ability to interact with a variety of naturally occurring, chemically diverse DOM sources. Despite different starting points along the lability continuum, all three DOM sources were capable of supporting biological respiration at the single organism level for the duration of the experiment.

Environmental DOM lability is typically characterized by the extent of microbial interaction over time. Combining what is known about the labile nature of glacially derived DOM with the known increases in bacterial metabolic activity after the addition

of a simple sugar carbon source (Gruber *et al.*, 2006; Hartley *et al.*, 2010; Rousk *et al.*, 2014), we predicted that CG DOM would be the most labile carbon source. Specifically, it was anticipated that faster rates of carbon utilization measured by respiration would occur in the early stages of the experiment relative to lability. We did not observe the anticipated initial spike in overall respiration suggested by the simple sugar studies. However, we measured the change in abundances of exometabolites to detect bacterial interaction with each carbon source. These results showed that for all carbon sources, the number and extent of exometabolite changes were greatest during the early time range, indicating that the initial stage did exhibit the greatest degree of DOM transformation. Interpreting the differences in respiration and exometabolite changes with regard to the carbon sources suggests that lability is contextual, being linked to both the microbial response to their energy source (DOM) and also to the chemical composition of the DOM itself. Our findings show that glacial CG DOM is comprised of the greatest amount of more-labile material as identified by the EEMs, FT-ICR MS, and UPLC-Q-TOF MS lability analyses. However, when combined with extended studies of biological processing CG DOM does not support greater rates of cellular respiration or carbon turnover when compared to other representative end-member DOM sources Although there were a greater number of exometabolites transformed in CG DOM, the hierarchical clustering of the early time range transformations was consistent across carbon sources, demonstrating a core of DOM transformations specific to the early time range. Thus, our findings are consistent with the idea that compositionally glacial DOM is labile. However, as biologically labile carbon in the environment is linked to greater carbon

turnover, we suggest that glacial DOM may not necessarily promote sustained cellular activity and urge caution in extrapolating from relatively short term studies.

Based on the accumulation of recalcitrant carbon in marine environments (Ogawa *et al.*, 2001; Jiao *et al.*, 2010), and recent findings that suggest that bacteria are responsible for the formation of structurally complex and persistent molecules (Lechtenfeld *et al.*, 2015), we initially hypothesized that more-labile material would decrease over time and less-labile material would accumulate. Both EEMs and UPLC-Q-TOF MS measurements over 98 days provide evidence for this dynamic temporal cycling of DOM in all carbon sources. We observed increases in fluorescence in the proteinaceous, more-labile region followed by decreases over the same region, which were indicative of temporally dependent DOM processing of all carbon sources. In contrast to previously reported data for marine systems, there was not an accumulation of less-labile material as measured by both EEMs and UPLC-Q-TOF MS analysis. The largest fluorescent changes over time were associated with the proteinaceous region, demonstrating the preferential usage of the more-labile portion of DOM from all carbon sources. Fewer fluctuations in fluorescent DOM were observed in the humic-like, less-labile components over time, indicating that the less-labile fraction of DOM is still biologically altered, but to a lesser extent. Additionally, lability was a significant factor impacting the extent of UPLC-Q-TOF MS based molecular transformations over time. The less-labile exometabolites in PL and SR showed a higher degree of change than the more-labile components, but only during the mid time range. This pattern supports fluctuation seen in the EEMs data, and suggests a temporal pattern whereby CG3 first

processes more-labile components, then transforms less-labile components if available, creating additional labile component interactions.

Microbes have been shown to interact with DOM in a variety of ways, ranging from ignoring, consuming, producing, and fragmenting via extracellular enzymes (Kujawinski, 2011). These interaction strategies present a diverse suite of potential processing pathways that an individual organism may employ depending on the resources available, providing an explanation for the wide range of molecular and fluorescent DOM changes seen throughout this study. DOM transformations can vary at the community level due to community interactions masking carbon cycling intermediates and products generated by individual organisms. As the importance of metabolic intermediates and the effect on overall DOM processing is poorly understood, it is valuable to study individual organisms to better understand the nature of DOM processing at larger ecosystem scales.

It has been proposed that as carbon from glacial environments enters aquatic ecosystems, heterotrophic microbial metabolism will be stimulated (Singer 2012, Hood 2009). The Cotton Glacier stream is an expansive supraglacial hydrologic feature, and to date represents the largest Antarctic supraglacial stream studied (Foreman *et al.*, 2013). Stream water is comprised of meltwater from the surrounding glacier and is transported across the glacial surface where it eventually flushes into the adjacent Ross Sea making this stream an excellent location to study the potential effect that glacial organic carbon could have on neighboring aquatic ecosystems. To accurately assess potential contributions of glacial DOM to downstream aquatic ecosystems we conducted extended incubations for 98 days with three freshwater DOM sources. As the experiment

progressed, the conserved metabolic response became less prominent and the DOM interactions became more divergent. More-labile DOM sources are believed to be very bioavailable and support greater heterotrophic respiration than less-labile carbon sources, when N and P nutrients are not limited (Cherrier *et al.*, 1996; Farjalla *et al.*, 2009). As such, we expected higher respiration rates for DOM containing a greater percentage of more-labile carbon, however that was not observed, and throughout the experiment PL samples had the highest sustained rate of respiration. We speculate that the heterogeneous character of microbially derived PL DOM makes it a more suitable carbon source for long term sustainability of microbial metabolism than either CG or SR DOM. Therefore, we suggest that the analysis of DOM chemical heterogeneity is necessary when evaluating the potential impact of a carbon source on downstream ecosystems

Release of glacial DOM will have heightened ecological relevance as we face a warming climate and there are increases in glacial loss. It will be imperative to assess the biological implications associated with glacially released DOM. This study is the first to propose that although glacially derived DOM is compositionally labile in nature it is not necessarily suitable as a sustainable carbon source for microbial metabolism. These findings argue for a revaluation of the biological implications of glacially released carbon on nearby ecosystems. To date the majority of the glacial organic carbon research conducted has been in Arctic regions, while these areas are undergoing rapid warming leading to increased carbon loss, it is important to recognize that the Antarctic Ice Sheet is estimated to contain 93% of glacially stored organic carbon (Hood *et al.*, 2015). Based on the sheer amount of carbon in Antarctic ecosystems more information is needed about

the chemical composition and biological response to these sources of glacial organic carbon. This information will enable more accurate predictions about the role of glacial DOM in stimulating microbial metabolism of aquatic environments.

While community studies are still needed to understand bulk level DOM processing, single organism studies of this type ultimately lead to greater insight of the contribution of an individual organism's metabolism to community level DOM processing. The metabolic flexibility of CG3 is key to its ability to survive on a range of carbon substrates. Perhaps organisms in cold temperature environments require extensive flexibility based on the intermittent nature of available energy sources in these extreme environments. Our ability to capture the dynamic nature of DOM processing was made possible by a combination of multi-disciplinary methods. In particular, UPLC-Q-TOF MS is well suited for high throughput studies of DOM processing, and can also be used to measure the internal metabolic response of organisms. Internal metabolite response will allow for the reconstruction of the specific pathways involved in the processing of complex and environmentally relevant DOM sources. The approach presented herein allows for an increase in our predicative capabilities about biological lability and DOM-microbe interactions. When evaluating the impact of carbon release from glaciers, it is important to survey not only the quantity but also the chemical heterogeneity as it is linked to the biological lability of a carbon source. Assessment of DOM heterogeneity will allow for more accurate predictions about the role of DOM sources in the microbial loop, DOM transport, and ultimately CO_2 release to the atmosphere.

Acknowledgements

This work was supported by the National Science Foundation Division of Antarctic Sciences through ANT-0838970, ANT-1141978 and ANT 1141936, by the NSF Division of Graduate Education through DGE-0654336, by the NSF Division of Materials Research through DMR 11-57490, the State of Florida, and a NASA Earth and Science Space Fellowship to HJS. We thank J. Hilmer and the Montana State University Mass Spectrometry, Proteomics, and Metabolomics core facility, supported in part by funding from the Murdock Charitable Trust and NIH 5P20RR02437 of the CoBRE program. We acknowledge and thank the CG and PL field teams, in particular D.M. McKnight and Y-P. Chin. We thank Peg Dirckx for graphics assistance. We thank D.C. Podgorski, B. Ruddy, and the Ion Cyclotron Resonance Facility staff members at the National High Magnetic Field Laboratory in Tallahassee, FL. Any opinions, findings, or conclusions expressed in this material are those of the authors and do not necessarily reflect the views of the National Science Foundation.

References

Battin TJ, Kaplan LA, Findlay S, Hopkinson CS, Marti E, Packman AI, *et al.* (2008). Biophysical controls on organic carbon fluxes in fluvial networks. *Nature Geoscience* **1**: 95–100.

Benjamini Y, Hochberg Y. (1995). Controlling the False Discovery Rate - a Practical and Powerful Approach to Multiple Testing. *Journal of the Royal Statistical Society Series B-Methodological* **57**: 289–300.

Bhatia MP, Das SB, Xu L, Charette MA, Wadham JL, Kujawinski EB. (2013). Organic carbon export from the Greenland ice sheet. *Geochimica et Cosmochimica Acta* **109**: 329–344.

Bianchi TS. (2011). The role of terrestrially derived organic carbon in the coastal ocean: a changing paradigm and the priming effect. *Proc Natl Acad Sci USA* **108**: 19473–19481.

Brown TL, Rice JA. (2000). Effect of experimental parameters on the ESI FT-ICR mass spectrum of fulvic acid. *Anal Chem* **72**: 384–390.

Cherrier J, Bauer JE, Druffel E. (1996). Utilization and turnover of labile dissolved organic matter by bacterial heterotrophs in eastern North Pacific surface waters. *Mar Ecol Prog Ser* **139**: 267–279.

Coble PG. (1996). Characterization of marine and terrestrial DOM in seawater using excitation-emission matrix spectroscopy. **51**: 325–346.

Coble PG, Green SA, Blough NV, Gagosian RB. (1990). Characterization of dissolved organic matter in the Black Sea by fluorescence spectroscopy. *Nature* **348**: 432–435.

Cole JJ, Prairie YT, Caraco NF, McDowell WH, Tranvik LJ, Striegl RG, *et al.* (2007). Plumbing the Global Carbon Cycle: Integrating Inland Waters into the Terrestrial Carbon Budget. *Ecosystems* **10**: 172–185.

Cory RM, Kaplan LA. (2012). Biological lability of streamwater fluorescent dissolved organic matter. *Limnol Oceanogr* **57**: 1347–1360.

Dittmar T, Koch B, Hertkorn N, Kattner G. (2008). A simple and efficient method for the solid-phase extraction of dissolved organic matter (SPE-DOM) from seawater. *Limnology and Oceanography-Methods* **6**: 230–235.

D'Andrilli J, Foreman CM, Marshall AG, McKnight DM. (2013). Characterization of IHSS Pony Lake fulvic acid dissolved organic matter by electrospray ionization Fourier transform ion cyclotron resonance mass spectrometry and fluorescence spectroscopy. *Organic Geochemistry* **65**: 19–28.

Emmett MR, White FM, Hendrickson CL, Shi S, Marshall AG. (1998). Application of micro-electrospray liquid chromatography techniques to FT-ICR MS to enable high-sensitivity biological analysis. *J Am Soc Mass Spectrom* **9**: 333–340.

Farjalla VF, Marinho CC, Faria BM, Amado AM, Esteves F de A, Bozelli RL, *et al.* (2009). Synergy of fresh and accumulated organic matter to bacterial growth. *Microb Ecol* **57**: 657–666.

Findlay S, Sinsabaugh RL. (1999). Unravelling the sources and bioavailability of dissolved organic matter in lotic aquatic ecosystems. *Mar Freshwater Res* **50**: 781–790.

Foreman CM, Cory RM, Morris CE, SanClements MD, Smith HJ, Lisle JT, *et al.* (2013). Microbial growth under humic-free conditions in a supraglacial stream system on the Cotton Glacier, Antarctica. *Environ Res Lett* **8**: 035022.

Gowda H, Ivanisevic J, Johnson CH, Kurczy ME, Benton HP, Rinehart D, *et al.* (2014). Interactive XCMS Online: Simplifying Advanced Metabolomic Data Processing and Subsequent Statistical Analyses. *Anal Chem* **86**: 6931–6939.

Gruber DF, Simjouw J-P, Seitzinger SP, Taghon GL. (2006). Dynamics and characterization of refractory dissolved organic matter produced by a pure bacterial culture in an experimental predator-prey system. *Appl Environ Microbiol* **72**: 4184–4191.

Hansell DA, Carlson CA. (2014). Biogeochemistry of Marine Dissolved Organic Matter. Academic Press.

Hartley, Hopkins, Sommerkorn, Wookey. (2010). The response of organic matter mineralisation to nutrient and substrate additions in sub-arctic soils. *Soil Biology and Biochemistry* **42**: 9–9.

Hood E, Fellman J, Spencer RGM, Hernes PJ, Edwards R, D'Amore D, *et al.* (2009). Glaciers as a source of ancient and labile organic matter to the marine environment. *Nature* **462**: 1044–1047.

Jiao N, Azam F, Sanders S (eds). (2013). Microbial Carbon Pump in the Ocean. American Association for the Advancement of Science: Washington, DC.

Jiao N, Herndl GJ, Hansell DA, Benner R, Kattner G, Wilhelm SW, *et al.* (2010). Microbial production of recalcitrant dissolved organic matter: long-term carbon storage in the global ocean. *Nat Rev Microbiol* **8**: 593–599.

Jørgensen L, Lechtenfeld O, Benner R, Middelboe M, Stedmon CA. (2014). Bacterial production and transformation of dissolved neutral sugars and amino acids in seawater. *Biogeosciences Discuss* **11**: 6151–6184.

Kim S, Kramer RW, Hatcher PG. (2003). Graphical method for analysis of ultrahigh-resolution broadband mass spectra of natural organic matter, the van Krevelen diagram. *Anal Chem* **75**: 5336–5344.

Koch BP, Dittmar T. (2006). From mass to structure: an aromaticity index for high-resolution mass data of natural organic matter. *Rapid Commun Mass Spectrom* **20**: 926–932.

Koch BP, Ludwichowski K-U, Kattner G, Dittmar T, Witt M. (2008). Advanced characterization of marine dissolved organic matter by combining reversed-phase liquid chromatography and FT-ICR-MS. **111**: 233–241.

Kujawinski EB. (2011). The Impact of Microbial Metabolism on Marine Dissolved Organic Matter. *Ann Rev Mar Sci* **3**: 567–599.

Lawson EC, Wadham JL. (2013). Greenland Ice Sheet exports labile organic carbon to the Arctic oceans. *Biogeosciences*. **10:** 19311-19345.

Lechtenfeld OJ, Hertkorn N, Shen Y, Witt M, Benner R. (2015). Marine sequestration of carbon in bacterial metabolites. *Nat Commun* **6**: 6711.

Li W-T, Xu Z-X, Li A-M, Wu W, Zhou Q, Wang J-N. (2013). HPLC/HPSEC-FLD with multi-excitation/emission scan for EEM interpretation and dissolved organic matter analysis. *Water Research* **47**: 1246–1256.

McKnight DM, Boyer EW, Westerhoff PK. (2001). Spectrofluorometric characterization of dissolved organic matter for indication of precursor organic material and aromaticity. *Limnol. Oceanogr*. **46:** 38-48.

Mopper K, Stubbins A, Ritchie JD, Bialk HM, Hatcher PG. (2007). Advanced instrumental approaches for characterization of marine dissolved organic matter: extraction techniques, mass spectrometry, and nuclear magnetic resonance spectroscopy. *Chem Rev* **107**: 419–442.

Mou X, Sun S, Edwards RA, Hodson RE, Moran MA. (2008). Bacterial carbon processing by generalist species in the coastal ocean. *Nature* **451**: 708–711.

Muggeo V. (2008). Segmented: An R Package to Fit Regression Models with Broken-Line Relationships. *R News* **8**: 20–25.

Nelson CE, Carlson CA. (2012). Tracking differential incorporation of dissolved organic carbon types among diverse lineages of Sargasso Sea bacterioplankton. *Environ Microbiol* **14**: 1500–1516.

Nelson CE, Wear EK. (2014). Microbial diversity and the lability of dissolved organic carbon. *Proc Natl Acad Sci USA* **111**: 7166–7167.

Nikrad MP, Cottrell MT, Kirchman DL. (2012). Abundance and single-cell activity of heterotrophic bacterial groups in the western Arctic Ocean in summer and winter. *Appl Environ Microbiol* **78**: 2402–2409.

Ogawa H, Amagai Y, Koike I, Kaiser K, Benner R. (2001). Production of refractory dissolved organic matter by bacteria. *Science* **292**: 917–920.

Patti GJ, Tautenhahn R, Siuzdak G. (2012). Meta-analysis of untargeted metabolomic data from multiple profiling experiments. *Nat Protoc* **7**: 508–516.

Pedler BE, Aluwihare LI, Azam F. (2014). Single bacterial strain capable of significant contribution to carbon cycling in the surface ocean. *Proc Natl Acad Sci USA* **111**: 7202–7207.

Pinheiro J, Bates D, DebRoy S. (2015). nlme: Linear and Nonlinear Mixed Effects Models. *CRANR-projectorg*.

Pinheiro JC, Bates DM. (2000). Mixed-Effects Models in S and S-PLUS. Springer Science & Business Media

Rousk J, Hill PW, Jones DL. (2014). Using the concentration-dependence of respiration arising from glucose addition to estimate in situ concentrations of labile carbon in grassland soil. *Soil Biology and Biochemistry* **77**: 81–88.

Santl-Temkiv T, Finster K, Dittmar T, Hansen BM, Thyrhaug R, Nielsen NW, *et al.* (2013). Hailstones: A Window into the Microbial and Chemical Inventory of a Storm Cloud. *PLoS ONE* **8**. doi:10.1371/journal.pone.0053550.

Smith CA, Want EJ, O'Maille G, Abagyan R, Siuzdak G. (2006). XCMS: processing mass spectrometry data for metabolite profiling using nonlinear peak alignment, matching, and identification. *Anal Chem* **78**: 779–787.

Smith H, Akiyama T, Foreman C, Franklin M, Woyke T, Teshima H, *et al.* (2013). Draft Genome Sequence and Description of Janthinobacterium sp. Strain CG3, a Psychrotolerant Antarctic Supraglacial Stream Bacterium. *Genome Announc* **1**.

Stedmon CA, Bro R. (2008). Characterizing dissolved organic matter fluorescence with parallel factor analysis: a tutorial. *Limnol Oceanogr Methods*. **6:** 572-579.

Stedmon CA, Markager S, Bro R. (2003). Tracing dissolved organic matter in aquatic environments using a new approach to fluorescence spectroscopy. **82**: 239–254.

Stenson AC. (2008). Reversed-phase chromatography fractionation tailored to mass spectral characterization of humic substances. *Environ Sci Technol* **42**: 2060–2065.

Suzuki R, Shimodaira H. (2013). Hierarchical clustering with P-values via multiscale bootstrap resampling. *R Package*.

Tautenhahn R, Patti GJ, Kalisiak E, Miyamoto T, Schmidt M, Lo FY, *et al.* (2011). metaXCMS: Second-Order Analysis of Untargeted Metabolomics Data. *Anal Chem* **83**: 696–700.

Tautenhahn R, Patti GJ, Rinehart D, Siuzdak G. (2012). XCMS Online: A Web-Based Platform to Process Untargeted Metabolomic Data. *Anal Chem* **84**: 5035–5039.

Vahatalo AV, Aarnos H, Mantyniemi S. (2010). Biodegradability continuum and biodegradation kinetics of natural organic matter described by the beta distribution. *Biogeochemistry* **100**: 227–240.

Want EJ, Cravatt BF, Siuzdak G. (2005). The expanding role of mass spectrometry in metabolite profiling and characterization. *Chembiochem* **6**: 1941–1951.

Warnes G, Bolker B, Bonebakker L, Gentleman R, Huber W, Liaw A, *et al.* (2015). gplots: Various R Programming Tools for Plotting Data. *R Package*.

Wetzel R. (2003). Dissolved organic carbon: Detrital energetics, metabolic regulators, and drivers of ecosystem stability of aquatic ecosystems. In: *Aquatic ecosystems: Interactivity of dissolved organic matter*, Findlay, S & Sinsabaugh, RL (eds), Elsevier Science, pp 455–477.

Wu FC, Evans RD, Dillon PJ. (2003). Separation and Characterization of NOM by High-Performance Liquid Chromatography and On-Line Three-Dimensional Excitation Emission Matrix Fluorescence Detection. *Environ Sci Technol* **37**: 3687–3693.

CHAPTER 5

BIOFILMS ON GLACIAL SURFACES: HOTSPOTS FOR BIOLOGICAL ACTIVITY

Adapted from: Heidi Smith, Amber Schmidt, Rachel Foster, Sten Littmann, Marcel Kuypers, and Christine Foreman (In Review: Nature Biofilms and Microbiomes)

Contribution of Authors and Co-Authors

Author: Heidi J Smith

Contributions: Designed the experiment, conducted experiments, analyzed data, wrote the manuscript.

Co-Author: Amber Schmidt

Contributions: Assisted with acquisition of confocal laser scanning microscopy images and thermogravimetric analyses.

Co-Author: Rachel Foster

Contributions: Assisted with nanoSIMS experimental design and data collection, edited manuscript.

Co-Author: Sten Littmann

Contributions: NanoSIMS data collection and edited manuscript.

Co-Author: Marcel Kuypers

Contributions: Provided support for nanoSIMS analysis and edited manuscript

Co-Author: Christine Foreman.

Contributions: Principal investigator of laboratory experiments, data analysis, manuscript preparation and editing

Manuscript Information Page

Heidi Smith, Amber Schmidt, Rachel Foster, Sten Littmann, Marcel Kuypers, and Christine Foreman
Nature Biofilms and Microbiomes
Status of Manuscript:
____ Prepared for submission to a peer-reviewed journal
__X__ Officially submitted to a peer-review journal
____ Accepted by a peer-reviewed journal
____ Published in a peer-reviewed journal

Nature Partner Journals. Submitted February 13, 2016

Abstract

Glaciers are important constituents in the Earth's hydrological and carbon cycles, and current warming will lead to increases in glacial melt and the transport of stored nutrients to adjacent and downstream aquatic ecosystems. Recently, microorganisms inhabiting the surface of glaciers have been linked to a reduction in albedo and increased melt. In this study we show via confocal laser scanning microscopy that microbial communities on glacial surfaces persist in biofilms. Overall, ~35% of the cryoconite sediment surfaces were covered by biofilm. Nanoscale scale secondary ion mass spectrometry (nanoSIMS) measured significant enrichment of ^{13}C and ^{15}N above background in both *Bacteroidetes* and filamentous *Oscillatoria* cells when incubated in the presence of ^{13}C-DIC and $^{15}NH_4$. This transfer of newly synthesized organic compounds was dependent on the distance of heterotrophic *Bacteroidetes* from filamentous *Oscillatoria*. We conclude that the spatial organization within these biofilms promotes efficient transfer and cycling of nutrients. Further, these results support the hypothesis that biofilm formation leads to the accumulation of organic matter on cryoconite minerals with a positive feedback on surface albedo reduction.

Introduction

Dissolved organic matter (DOM) in freshwater Glaciers cover roughly 10% of Earth's land surface. As the Earth warms, losses in glacial mass will lead to an export of freshwater to marine ecosystems and ultimately a rise in sea level. Not only is the sheer volume of freshwater of concern, but also the release of geochemical constituents stored in glacial ice. Glacial ecosystems have been shown to be large reservoirs of organic carbon (OC), derived from deposition or biological processes. It was recently predicted that the Antarctic Ice Sheet (AIS) alone contains six petagrams of OC, which represents 93% of the total OC stored in glaciers globally (Hood *et al.*, 2015). Of particular interest for carbon cycling are glaciological features known as cryoconite, which contain both mineralogical and biological materials. Cryoconite are cylindrical holes that form in the ablation zone of glaciers as aeolian debris melts into the ice surfaces. These features are hotspots of microbial activity, capable of fixing significant fractions of carbon (Anesio *et al.*, 2009). Sophisticated models exist to explain carbon fluxes in cryoconite, but due to a lack of data these have explicitly excluded Antarctic cryoconite.

Although research on the role of biological processes on glacier surfaces is still in its infancy, recent reports have linked biological growth to a reduction in glacial surface albedo through increased surface darkening and enhanced melting (Lutz *et al.*, 2014). Biologically driven aggregation of particles is influenced by the quantity, quality, and decomposition of organic matter (OM), and strong correlations between granule size and OM content have been reported (Cook *et al.*, 2015). Binding together these aggregates are living matrices, called biofilms, which enhance cell-cell and cell-particle interactions,

leading to a positive feedback increasing biomass and potentially reducing albedo on glacial surfaces. While particle-cell interactions in Arctic and higher latitude cryoconite ecosystems are evident (Cook *et al.*, 2015), agglomerates in Antarctic cryoconite have not been observed (Tedesco *et al.*, 2013) and information on cell-particle interactions is non-existent. In a recent review, Cook *et al*. 2015 emphasize the need for understanding the fundamental mechanisms that control cryoconite from different geographical locations, in order to develop general models that are applicable to diverse supraglacial environments. We propose that the biofilm matrix is integral to biological activity in cryoconite through enhanced nutrient storage, cell adhesion, and the promotion of efficient nutrient transfer between community members. As such, development of the biofilm structure supports entrapment of microbes and OM, stimulating the formation of cryoconite granules. This accumulation of microbes and OM will enlarge these aggregates, ultimately contributing to surface darkening and a reduction of glacial albedo (Cook *et al.*, 2015).

Methods

Study Site and Sample Collection and Preparation

Cryoconite sample was collected during the 2011 Austral summer from the surface of the Canada Glacier (77°37’ S, 162°57’ E). The cryoconite hole sampled was 38 cm by 34 cm with a total depth of 25 cm. The water depth of the sampled cryoconite was 12 cm and the depth of sediment was 0.5 cm. Liquid water and sediment were extracted from the glacial surface using ethanol cleaned spatulas and syringes and placed

into sterile Whirl-Pak® bags. Sediments (117.14 g of sediment in total) from the sampled cryoconite were prepared for different analytical methods in two ways, sediment subsamples (2 g) were placed into sterile cryo vials and stored at -80°C. A second subsample (40 g) of cryoconite sediment was added to 500 ml of DI water and placed on an orbital shaker at 1,500 rpm at 10°C for 24 hrs. After shaking, the supernatant containing the dislodged bacterial cells were separated from the sediment and used for subsequent analyses. Cryoconite from the Canada Glacier have been studied over the last several years and there is information available regarding cryoconite distribution, biogeochemical data, community structure, and exposure intervals to atmospheric conditions for cryoconites from this location (Fountain *et al.*, 2004; 2008; Foreman *et al.*, 2007; Bagshaw *et al.*, 2011; 2007; 2013). Therefore, a single sample from the well-studied glacial surface was advantageous for the methodologically intensive nature of this study.

Bacterial Community Composition

Genomic DNA was extracted from 0.25g of cryoconite sediment using a MO BIO PowerSoil™ DNA Isolation Kit, following manufacturers protocols (MO BIO Laboratories Inc., Carlsbad, CA, USA). The extracted DNA was cleaned and concentrated with the Wizard® SV Gel and PCR Clean-Up System (Promega Corporation, Madison, WI, USA) following established manufacturers protocols. SSU rRNA gene sequences were amplified with barcoded universal bacterial primers FD1 (5′-ctcgcgtgtcAGAGTTTGATCCTGGCT- CAG-3′) and 529R (5′-ctcgcgtgtcCGCGGCTGCTGGCAC- 3′) for the V1,V2 and V3 regions. The amplification

protocol began with a hot start (94°C for 4 min), followed by 28 cycles of a 30 second 94°C denaturation, a one minute annealing step at 58°C, and an elongation step at 72°C for one minute. After the completion of the 28 amplification cycles, there was a final elongation at 72°C for 10 minutes. PCR products were excised from a 0.8 % agarose gel and cleaned using an Ultrafree®-DA gel extraction column (Millipore Corporation, Bedford, MA, USA). The gel extract was cleaned and concentrated after the gel extraction using the Wizard® SC Gel and PCR Clean-Up System and the dsDNA PCR product was quantified with a Qubit fluorometer (Invitrogen, Carlsbad, CA, USA). Adaptor sequences were ligated onto the amplicon products and sequencing was performed using a 454 GS Jr. (454 Life Sciences, Branford, CT, USA). Sequences were trimmed to one standard deviation below the mean sequence length, and the data was processed using the Quantitative Insights Into Microbial Ecology (QIIME) toolkit (Caporaso *et al.*, 2010). Briefly, sequences were clustered into OTUs using a 97% identity threshold, and the most abundant sequence from each OTU was selected as a representative sequence for the OTU. Taxonomy was assigned for each representative sequence using the Basic Local Alignment Search Tool (BLAST) against the Silva database. Chimeric sequences were removed with Chimera Slayer (Haas *et al.*, 2011) and chimeric sequences were confirmed using Bellerophon (Huber *et al.*, 2004).

NanoSIMS Sample Preparation

For incubation and bacterial enumeration cryoconite supernatant was incubated with ^{15}N-labeled ammonium chloride (~99% ^{15}N, Cambridge Isotopes Laboratories Inc., Andover, MA, USA, 0.1mM final concentration) and ^{13}C-labeled sodium bicarbonate

(~99% ^{13}C, Cambridge Isotopes Laboratories Inc., Andover, MA, USA, 1mM final concentration) in 1 L bottles in a light incubator to simulate *in situ* light (50.6 photons per m^2) and temperature (4°C) conditions for 72 hours. After incubation samples were fixed with paraformaldehyde (final concentration 2%) for 1.5 hours at room temperature. Subsamples (10 mls) were then filtered onto gold-palladium coated 0.2µm GTTP polycarbonate filters (Millipore) under low vacuum pressure (< 7 psi) and washed three times with 1X phosphate buffered saline (PBS). Filters were dried and stored in cryovials at -20°C until further processing.

Preparation Hybridization and
Microscopic Evaluation

Sections (5 mm diameter) of the gold-paladium coated filters containing cells were excised and hybridized with FISH horseradish peroxidase (HRP)-labeled oligonucleotide probes following the CARD-FISH protocol described by (Pernthaler *et al.*, 2002) and HISH-SIMS protocol described by (Musat *et al.*, 2008). To avoid detachment of cells through sample preparation protocols the 5 mm spheres were initially embedded in 0.1% low melting point agarose. For the analysis of gram–negative *Bacteroidetes* bacteria, cells were permeabilized with a lysozyme (10 mg ml^{-1} in 0.05 M EDTA (pH 8.0) and 0.1M Tris-HCl) treatment at 37°C for one hour. After permeabilization filters were washed three times with ultrapure water (MQ, Millipore) and endogenous peroxidases were bleached with 3% H_2O_2 for 10 minutes at room temperature. Prior to hybridization filters were washed three times for one minute with ultrapure water and submerged in 96% ethanol for one minute and allowed to air dry completely. Filters were subjected to a one hour pre-hybridization step without the probe,

then probes were added (1:150 v/v) and hybridized at 46°C for 6 hours using a previously described protocol(Musat *et al.*, 2008). The oligonucleotide probes and corresponding formamide concentrations used for this study are provided in Table SI4. For FISH with HRP labeled oligonucleotide probes a tyramide signal amplification step was done following the protocol described in (Pernthaler *et al.*, 2002), and fluorine containing tyramides for the HISH-SIMS assays followed the protocol described by (Musat *et al.*, 2008). Hybridized cells were counterstained with 4',6'-diamindino-2-phenylindole (DAPI) at a final concentration of 1 μg mL^{-1} in the dark for 10 minutes. The 5 mm filter sections were covered in mountant (4 parts Citifluor (Citifluor , Ltd., London, United Kingdom), 1 part VectaShield (Vector Laboratoires, Burlingame, CA)) and 10 randomly chosen fields (grid size of 15625 μm^2) corresponding to 1,000-1,200 DAPI stained cells were counted using a Zeiss Axioskop II fluorescence microscope (Zeiss, Berlin, Germany) with a final magnification of 1000x. Counts are reported as mean averages from triplicate cell counts of cells g^{-1} of sediment that have been converted based on phylogenetic classification to percentages of the total number of cells counted. *Bacteroidetes* sp. cells identified with CARD-FISH and *Oscillatoria* sp. cells of interest were identified by morphology and excitation under blue (450-490 nm) and green (510-560 nm) excitation filter sets and imaged. Areas of interest for nanoSIMS were marked using a Laser Micro Dissection (LMD) microscope 6500 (Leica, Wetzlar, Germany). Microscopic pictures were taken and used for orientation purposes during the subsequent nanoSIMS analysis and for post processing using look@nanoSIMS software (see below).

NanoSIMS Analysis

NanoSIMS analysis was performed using a Cameca NanoSIMS 50L instrument (Cameca, Gennevilliers, France) at the Max Planck Institute for Marine Microbiology in Bremen. After re-identifying the area of interest marked by the LMD with the nanoSIMS CCD camera, samples were pre-sputtered with a Cesium (Cs+) primary ion beam with a current of ~300 pA. For the measurements a primary ion beam with a beam current between 1 and 3 pA and a beam size <100 nm was used to raster the analyzed area. The measurements were performed with an image size of 256 x 256 pixels over a chosen raster size of 20 x 20 μm with a dwelling time of 1 or 2 ms per pixel. Mass resolving power in the majority of the measurements was >8000. Negative secondary ion images of $^{12}C^-$, $^{13}C^-$, $^{19}F^-$, $^{12}C^{14}N^-$, $^{12}C^{15}N^-$ and $^{32}S^-$ were recorded simultaneously with the multi-collection system of the instrument. All scans (40-50 planes) were corrected for drift of the beam and sample stage after acquisition and accumulated using "Look@NanoSIMS" software package (Polercky et al. 2012). Region of interest (ROIs) were defined using the $^{19}F^-$ images representing the HISH labeled *Bacteroidetes* sp. cells, and ROIs for the non-labeled filamentous cyanobacterial cells were chosen based on the $^{12}C^{14}N$ image compared to fluorescent images for DAPI stained cells.

The equations used for ^{13}C and ^{15}N assimilation were as previously described in(Foster *et al.*, 2011). The cell diameter for both cyanobacterial cells and *Bacteroidetes* sp. were estimated from nanoSIMS images after cells were circled using the Look@NanoSIMS software analysis package (Polerecky *et al.*, 2012). Cell heights for both cell types were determined using a Nanoscope III extended-multimode atomic force

microscope (Vecco, Santa Barbara, CA). Underestimations of cell diameter are possible due to the fixation step (2% PFA for 1.5 hours). The cell diameter measures were used in equations for bio-volume estimation as described in Sun and Lui (2003)(Sun, 2003) For filamentous cyanobacterial cells, the bio volume was estimated using the equation of a cylinder:

$$V = (\pi/4) \times d^2 \times h) \quad (1)$$

where d is cell diameter and h is cell height. Average height for individual cyanobacterial filaments was equal to 1.57 μm..

For estimating bio volume of individual *Bacteroidetes* sp. cells the equation of a sphere was used

$$(V = (\pi/6) \times d^3) \quad (2)$$

where d is cell diameter. The initial cellular carbon content was estimated based on the relationship between bio volume and carbon content previously described in Verity at al. (1992) (Verity *et al.*, 1992):

$$Log[C] = -0.363 + (0.863 \times (Log(V)) \quad (3)$$

Logarithms (LOG) are base 10 and C content was used to estimate the N content. As none of the analyzed organisms are isolated standard elemental analysis was not possible and therefore we based our estimates of initial C and N content on the Redfield ratio (C:N) of 6.6.

Cell specific C (A_C)and N (A_N) assimilation was calculated following the equations presented in Foster et al. 2013 and are as follows:

$$A_C = ({}^{13}C_{ex} \times C_{inital})/C_{SR} \quad (4)$$

$$A_N = ({}^{15}N_{ex} \times N_{inital})/N_{SR} \quad (5)$$

where ${}^{13}C_{ex}$ and ${}^{15}N_{ex}$ is the atom (AT) % of ${}^{13}C$ and ${}^{15}N$, respectively, corrected for by the mean value of the respective ratios in non-enriched bulk samples (time 0) measured by elemental analysis isotope ratio mass spectrometry (EA-IRMS) analyses. The $C_{initial}$ and $N_{initial}$ variables are the initial C and N content as presented in equation 3, while C_{SR} and N_{SR} are the labeling percentage of ${}^{13}C$ and ${}^{15}N$, respectively, in the experiment. The calculated assimilation values were divided by the incubation time (h) to determine the cell specific C fixation and N fixation rates. It should be noted that there is the potential for a dilution of ${}^{13}C$ and ${}^{15}N$ signals as a result of the HISH-SIMS fixation procedures, and hence the calculated uptake rates (Musat *et al.*, 2014)

It was recently highlighted that microbial cells interact at the microscale (Stocker, 2015), to investigate these microscale interactions and to quantify the C and N transfer from autotrophic *Oscillatoria* sp. to heterotrophic *Bacteroidetes* sp., the enrichment (AT% 13C and AT% 15N) measured in the *Bacteroidetes* cells was divided into two groups and include values from cell residing: close (< 2 μm) or far (> 2 μm) from a *Oscillatoria* sp. cell. Phytoplankton exudates are known to form diffusion limited chemical gradients around the cell surface, (Bell and Mitchell, 1972; Jackson, 1987) the diffusivity of this boundary layer can be estimated using the relationship between cell

size and organic matter leakage calculated according to Jackson (1987) (Jackson, 1987). Where ϕ is the relationship between the cell radius and cell carbon content, as determined by Mullin et al. (1966) (Mullin *et al.*, 1966) for planktonic photoautotrophic organisms:

$$\phi = ba^{2.28} \quad (1)$$

Where b is a constant equal to 2.67 x 10^{-4} mol multiplied by the cells radius a = 1.99 μm$^{2.28}$. Organic matter leakage was subsequently calculated according to Jackson (1987) (Jackson, 1987):

$$C = \left(\frac{L}{4\pi D}\right) r^{-1} + C_{\infty} \quad (2)$$

Where the carbon leakage rate of L = fμϕ. Standard values from Jackson (1987) were used for the following parameters: where f is the organic matter leakage rate from photoautotrophic cells, μ is the specific growth rate, D is the molecular diffusivity of organic matter, r^{-1} is the distance from the cell surface. C_{∞}, the concentration in the bulk which was assumed to be nominally small and therefore set to zero. The concentration of exuded organic matter was then calculated incrementally for distances ranging from very near the cell surface (0.1 μm) to 10 μm away from the cell surface. To preserve these distances and inhibit cell loss or movement through sample preparation and analysis filters were covered with a thin layer of low met agarose (0.1%) after the initial sample filtration. Using the *stats* package in R (Team, 2014) a liner model was used to separately

analyze ^{13}C and ^{15}N AT% enrichment of both the close and far *Bacteroidetes* sp. cells. The model included either ^{13}C AT% or ^{15}N AT% as a response to an interaction effect added for each analyzed section and distance from filament.

Confocal Laser Scanning Microscopy (CLSM) Imaging and Data Processing

For imaging, cryoconite granules were thawed on ice, placed into a sterile petri dish and stained for 20 minutes in the dark. Fully hydrated cryoconite granules were stained with either SYBR Green, a nucleic acid stain (Invitrogen; Life Technologies) 40 X final concentration; or calcofluor white, which has a long history of use for staining of chitin, cellulose and polysaccharides (Fluka; Sigma-Aldrich) final concentration 1 μM. After staining, cryoconite granules were rinsed with 0.2 μm filter sterilized DI water three times to remove any excess stain. Stains were chosen for this study after comparing a variety of different stains to determine which stains would be the most sample appropriate and the least reactive with abiotic material. Sediment samples were imaged with a Leica TCS SP5 II upright confocal microscope using either a 25 X water immersion objective, 0.95 NA, WD 2.5mm; or a 63 X water immersion objective, 0.9 NA, WD 2.2mm. Fluorophore excitation lasers and emission bandwidths are as follows: SYBR Green (ex 497/em 520) 488nm excitation, 500–550nm emission collection; autofluorescence, 561nm excitation, 580–700nm emission collection; calcofluor white (ex355, em433), 405nm excitation, 450–490nm emission collection; and reflection imaging, 488nm excitation. A minimum of 10 randomly selected images were collected to enumerate cellular biomass (SYBR green, autofluoresence, reflection) and biotic

material biomass (calcofluor white and reflection). Z-stacks were collected in either 0.54 μm steps for the 25X objective or 0.64 μm steps for the 63X objective. To ensure that the stains selected for this study were not binding to abiotic material cryoconite granules were combusted at 450°C for 5 hours to remove any biotic material present. Combusted granules were then stained and imaged following the same protocol as previously described. The 3D structure of individual cryoconite granules and associated biotic material was reconstructed from the CLSM images using IMARIS software (version 7.6.4). Surface area (μm^2) for each channel imaged was determined using the surface area calculation function in the IMARIS software. Surface area calculation parameters were optimized to sample and image specific properties. For the autofluorescent and SYBR Green images used to quantify individual cells images were smoothed at a surface area detail level of 0.5 μm^2, thresholding was based on a background subtraction method, and all voxels greater than zero were collected. Biofilm images were processed with the same parameters described above, with the exception that all voxels greater than 10 were collected. Sediment surface area was calculated the same way as for biofilm except that the surface was divided in half based on the inability of light to penetrate the sediment samples and the resulting overestimation of surface area. Calculated surface areas for cells identified with SYBR Green or autofluorescence, and biotic material were all normalized to the surface area of cryoconite granules in the corresponding field of view analyzed.

Fluorescence Spectroscopy

Dissolved organic matter (DOM) extracted from cryoconite sediment was analyzed using excitation emission spectroscopy (EEMs). Scans were collected over an excitation range of 240–450 nm in 10 nm increments and emission was monitored from 300–560 nm in 2 nm increments on a Fluoromax-4 spectrofluorometer (HORIBA Jobin-Yvon). Samples were analyzed for UV absorbance with a Thermo Scientific Genesys 10 scanning UV spectrophotometer from 190-1100 nm on optically dilute samples (absorbance values < 0.3 at 254 nm). EEMs data were post-processed to correct for instrument-specific bias using manufacturer-generated correction files for excitation, emission, and blank subtraction. Specific regions of fluorescence were defined for each carbon source corresponding to previously identified natural organic matter fluorophores (Coble, 1996). Fluorescence intensity values in the proteinaceous regions (B and T fluorophores) were summed and classified as more-labile, while humic-like fluorescence regions (A and C fluorophores) were combined and classified as less-labile and more recalcitrant. The fluorescence for both defined regions was individually summed for the two samples (cryoconite water and sediment extracted DOM).

Sediment Analysis

Powder X-ray diffraction (XRD) was used to determine the mineralogical composition of studied cryoconite sediment. Samples were ground into a homogenous powder with a mortar and pestle to homogenize the sediment mixture. XRD analysis was completed with a Scintag XGen-4000 X-ray Powder Diffraction Spectrometer. X-ray spectra were generated across a 2θ range of 5-70° in 0.02° steps with a scan rate of

2°/minute for an initial survey and across regions of prominent peaks at 24 0.5°/minute for greater detail. X-ray spectra were analyzed using the Scintag Diffraction Management System for NT (DMSNT) computer software package to determine peak positions and relative intensities and subsequently compared to the International Centre for Diffraction Data (ICDD) powder diffraction file catalog for identification of crystalline minerals. Stepwise thermo-gravimetric analysis was conducted to determine bulk organic matter content and composition following methods from (Kristensen, 1990). Briefly, 500mg sub-samples of cryoconite sediment (in triplicate for each combustion temperature) were weighed and placed into crucibles and dried for three days at 38ºC. Individual samples were weighed to obtain sample dry weight. Samples were placed in a muffle furnace at four different combustion temperatures (105ºC, 200ºC, 350ºC, and 520ºC) for four hours. After combustion samples were placed into a desiccator to cool, once cool samples were weighed for the second time. The difference in the dry weight and the weight post combustion for each sample represents the percent organic matter lost at different temperatures of ignition. These percent differences were used to calculate the total organic content and different lability classifications which has been previously described by (Walter E Dean, 1974; Kristensen, 1990; Langford *et al.*, 2010). The following differentiations were used: the loss of water (38-200°C), thermolabile (200-350°C), and stable organic matter (350-520°C) (Cuypers *et al.*, 2002).

Chemical Analyses

Samples run in triplicate for chlorophyll a (chl *a*) extraction and analysis were filtered in the dark through 25 mm pre-combusted GF/F filters wrapped in aluminum foil and kept at -20°C until. Chl *a* was extracted in a 1:1 solution of 90% and dimethyl sulfoxide for 12 hours in the dark at -20°C. Extracted chl *a* was analyzed with a Turner 10-AU flouorometer. Anion samples in triplicate were filtered through 0.4 μm 47 mm nucleopore filters, deionized water was used as a filtration blank, and samples were analyzed on a Dionex ICS-1100 ion chromatography system.

Results and Discussion

A suite of analytical methods was applied to investigate cryoconite particles from the Canada Glacier in the McMurdo Dry Valleys, Antarctica, and to elucidate the role of biofilms on glacial surfaces. A diverse microbial community associated with these particles was determined from 454 pyrosequencing to be dominated by *Cyanobacteria*, *Bacteroidetes*, and *Actinobacteria* (Table 5.1). The photoautotrophic cyanobacteria were further identified by epi-fluorescent microscopy to be *Oscillatoria*. Class specific fluorescent *in situ* hybridization (FISH) probes (Table 5.2) enabled the visualization of *Bacteroidetes* cells within the biofilm localized inside the *Oscillatoria* phycosphere.

Table 5.1. Comparison of the relative abundances of 454 Pyrosequencing sequences for A.) dominant cryoconite sediment organisms at the phylum taxonomic classification level and B.) Cyanobacterial sequences at the genus classification.

A.	**Bacterial Community**	**B.**	**Cyanobacterial Community**
Phylum Level Taxonomic Classification	Relative Abundance (%)	Genus Level Taxonomic Classification	Relative Abundance (%)
Acidobacteria	0.94	*Tolypothrix*	8.61
Actinobacteria	23.69	*Chamaesiphon*	6.55
Alphaproteobacteria	4.13	*Pseudanabaena*	5.84
Bacteroidetes	18.81	*Nostoc*	12.16
Betaproteobacteria	12.26	*Phormidium*	4.56
Chloroflexi	0.04	*Oscillatoria*	61.30
Cyanobacteria	27.37	Unclassified	0.98
Deltaproteobacteria	2.01		
Firmicutes	3.80		
Gammaproteobacteria	3.28		
Gemmatimonadetes	1.93		
Planctomycetes	1.46		
Unclassified	0.29		

Table 5.2. Summary of 16S rRNA targeted oligonucleotide probes, target organisms, competitor sequences, formamide (FA) concentrations, and references used in CARD-FISH. The FA concentrations used were all optimal and recommended by each respective probe publication

Probe and Target Organism	Probe Sequence (5'-3')	Target Position	Target	% FA	Reference
For Bacteria (used in equal amounts)					
EUB338-I	GCT GCC TCC CGT AGG AGT	338-355	16S	35	Amann *et al.* (1990)
EUB338-II	GCA GCC ACC CGT AGG TGT	338-355	16S	35	Damis *et al.* (1999)
EUB338-III	GCT GCC ACC CGT AGG AGT	338-355	16S	35	Damis *et al.* (1999)
Antisense of EUB338					
NON338	ACT CCT ACG GGA GGC AGC	338-355	16S	35	Wallner *et al.* (1993)
Most Flavobacteria, some Bacteroidetes and some Sphingobacteria					
CF319a	TGG TCC GTG TCT CAG TAC	319-336	16S	35	Manz *et al*. (1996)
CF319b	TGG TCC GTA TCT CAG TAC	319-336	16S	35	Manz *et al*. (1996)

Particle-cell interactions were visualized with confocal laser scanning microscopy (CLSM) using auto-fluorescence and nucleic acid specific fluorescent stains while simultaneously imaging the surface structure of individual cryoconite mineral particles (Figure 5.1). Unlike traditionally used techniques such as scanning electron microscopy (SEM), this novel approach allowed for both the visualization and quantification of

hydrated cellular and biofilm biomass. Imaging hydrated biofilms exposes them to a constant fluid shear throughout the image collection process, reaffirming the presence of biofilm structure and the attachment of cells to a surface, rather than artificial attachment as a result of fixation or dehydration processes commonly used in SEM. Importantly, there was no non-specific staining of combusted cryoconite mineral particles for any stain used in this study (Figure 5.1F), confirming that all fluorescently stained material was biotic in nature. Beyond visualization of particle-cell interactions, total cellular biomass represented 14.5±1.26% of the cryoconite sediment surface area, while auto-fluorescent, cellular biomass covered 1.70±0.861%. Calcofluor white, a stain that binds to cellulose and polysaccharides (Chen *et al.*, 2007) was used to identify the presence of extracellular polymeric substances (EPS) in the biofilm. EPS-like material covered over 19.2±1.02% of the total surface area and was imaged as diffuse non-microbial staining, unassociated with cellular-like structures, which is another clear indication of the presence of biofilm. Combined, ~35% of the cryoconite sediment surface was covered by biofilm.

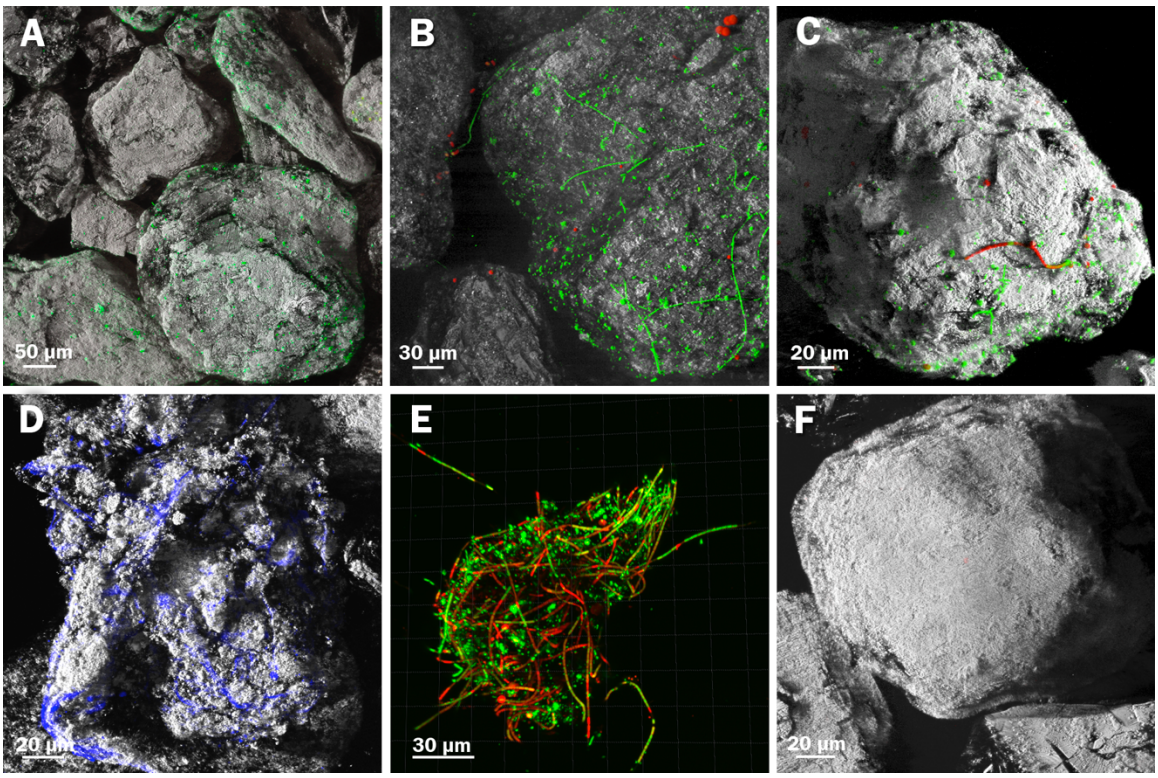

Figure 5.1: Representative confocal laser scanning microscopy images of cryoconite sediment with associated microbial communities and biofilm. A.) Green = SYBR Green stain, grey = reflection of the sediment. B-C.) Red = auto-fluorescence, green = SYBR Green stain, grey = reflection of the sediment. D.) Blue = Calcofluor-white stain, grey = reflection of the sediment. E.) Red = Propidium Iodide (dead cells) Green = Syto9 stain (live cells) F.) Control image of combusted cryoconite sediment following described staining protocol, grey = reflection of the sediment.

To further elucidate the role of biofilm in glacial surface microbial community interactions a nanoscale secondary ion mass spectrometry (Wagner, 2009) (nanoSIMS; Supplementary Information) approach was applied in combination with halogenated *in situ* hybridization (HISH-SIMS) (Musat *et al.*, 2008) using ^{13}C- bicarbonate and ^{15}N-ammonium for labeling experiments. All filamentous *Oscillatoria* cells analyzed (n=37) were significantly enriched in ^{13}C and ^{15}N above background compared to the natural isotope abundance of cryoconite (^{13}C atom %=1.074 and ^{15}N atom %=0.366). Incorporation of ^{13}C-labeled bicarbonate and ^{15}N ammonium ranged between 1.2-3.0

fmol C $cell^{-1}$ h^{-1} and 0.10-0.35 fmol N $cell^{-1}$ h^{-1}, respectively. Simulation of organic matter leakage from a cell with a relatively large leakage rate (0.5 d^{-1}, Jackson, 1987) under standard conditions showed that there was an inversely proportional relationship between the concentration of exuded organic matter and the distance from the filament surface. Within the phycosphere of a filamentous cell, with a 1.99 μm radius, 10% of the cell surface concentration was estimated to extend 1um away of the cell surface, and at 2 μm from the cell surface only 5% of the initial concentration will extend (Figure 5.2). We therefore conclude that >2 μm is a conservative delineation where exuded organic matter concentrations are too diffuse and below the threshold for bacterial chemosensory detection. The incorporation of newly released cyanobacterial ^{13}C-exudates and ^{15}N by heterotrophic *Bacteroidetes* cells decreased with increasing distance to *Oscillatoria* biofilms, with cells close to cyanobacteria being significantly more enriched in ^{13}C and ^{15}N ($p<0.0001$) (Figure 5.3C). These results indicate that biofilm on cryoconite sediments provides a matrix for cell arrangements, increases nutrient and energy transfer between community members, and allows heterotrophs in close proximity to autotrophs to effectively scavenge excreted products; factors critical for survival and proliferation in these extreme environments. Such close cellular interactions are of particular importance in Antarctic cryoconite as they may remain entombed over annual to decadal scales, promoting microbial processes that recycle resources (Bagshaw *et al.*, 2016).

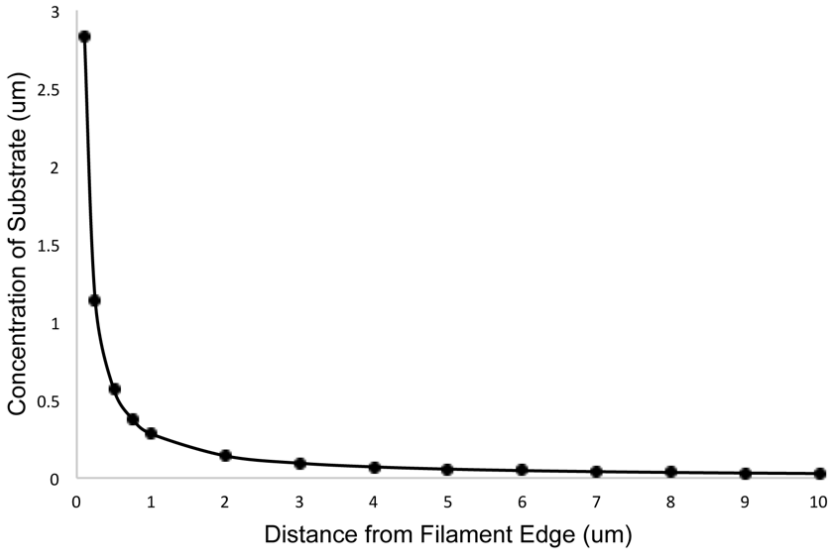

Figure 5.2. Concentration of exuded organic matter in the boundary layer of a cell with a 1.99 μm radius, assuming an exudation rate of 0.5 d^{-1} (Jackson 1987).

Cryoconite particles were composed of primary minerals such as silicate oxides, cordierite, and orthoclase. Calcite was identified as an associated secondary mineral-weathering product (Figure 5.4). Total organic matter accounted for 7.7% of the cryoconite dry weight (Table 5.2), which was higher than previously reported for Canada Glacier (Foreman *et al.*, 2007), but bracketed the lower range for Arctic cryoconite (Cook *et al.*, 2015).

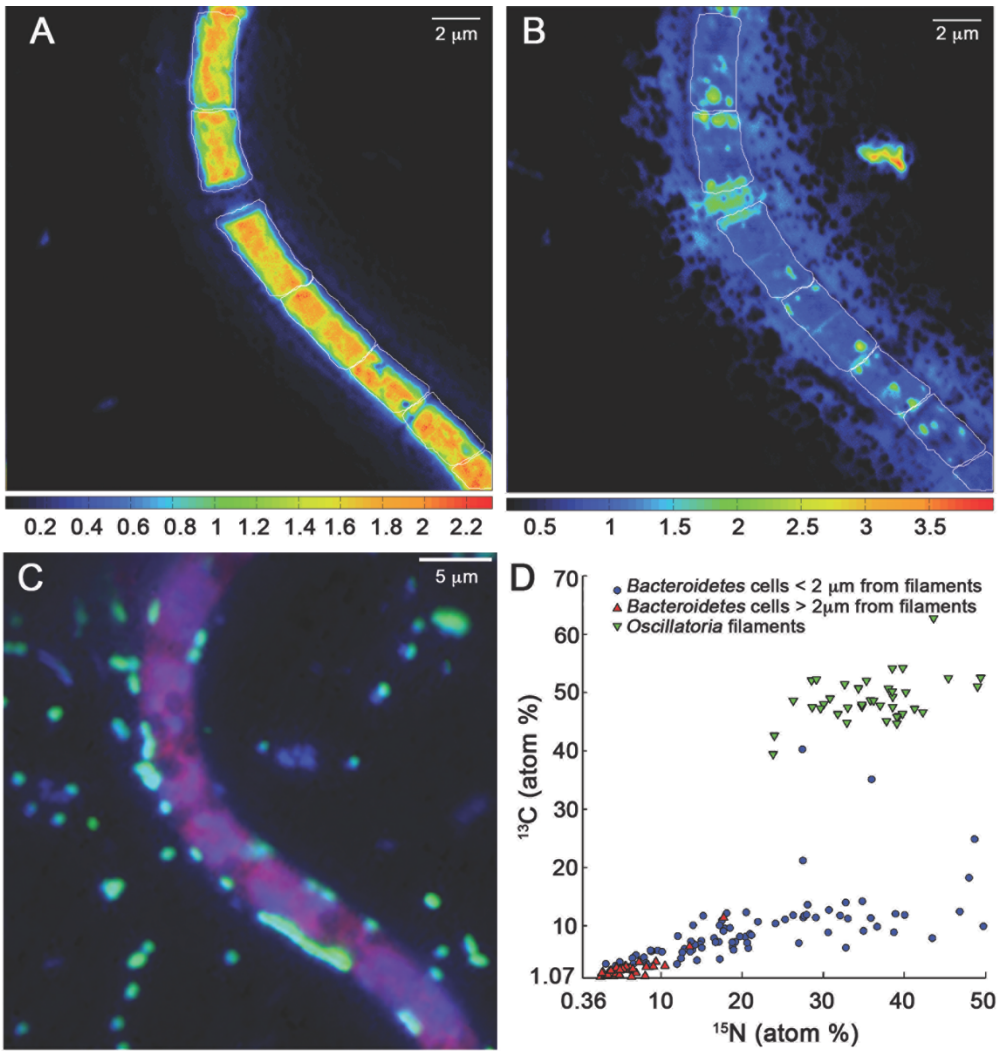

Figure 5.3. Example of nanoSIMS isotope ratio images of an analyzed *Oscillatoria* sp. filament for (A.) the $^{13}C/^{12}C$ ratio (B.) the $^{15}N/^{14}N$ ratio (C.) the epifluorescence overlay used to confirm cell identification of hybridized *Bacteroidetes* cells (green), DAPI stained (blue), and an autofluorescent filament (red). White lines indicate regions of interest (ROIs) section of an analyzed *Oscillatoria* sp. filament. (D.) NanoSIMS analysis of ^{13}C and ^{15}N enrichment measurements atom % (AT%) for *Bacteroidetes* sp. cells based on proximity to filamentous *Oscillatoria,* and *Oscillatoria* cells (▼). Cells < 2 µm from a filamentous cell (●), and cells > 2 µm from a filamentous cell (▲).

Table 5.3. Triplicate thermo-gravimetric analysis of organic matter (as percentage of dry weight) from cryoconite sediments, and characterization of organic matter present (Kristensen, 1990). Total organic matter accounted for 7.7% of the cryoconite dry weight.

Temperature	Sample Average % Dry Weight ± SD	Classification	Description
38-105°C	0.49 ± 0.73	Loss of Water	Crystalline lattice water, and hygroscopic water of salts and organic matter
105-200°C	4.3 ± 2.08		
200-350°C	2.19 ± 1.02	Thermolabile	Dominated by carbohydrates
350-520°C	0.76 ± 0.80	Stable Organic Matter	Oxidation of aromatic groups (lignin, humic substances, kerogens) and char

To further investigate the quality and composition of OC in the cryoconite environment we utilized excitation emission spectroscopy and thermogravimetric analyses. Fluorescent DOM was detected in both the cryoconite water and in the sediment extracted DOM. The fluorescent signature of the sediment extracted DOM has fluorescence in the B and T regions, compared to the water where fluorescence was only present in the T regions. Similarly, between both samples fluorescence was not detected in the humic-like regions, rather the fluorescent DOM present was predominately in the more-labile, microbially derived regions. The sediment extracted DOM was comprised of 89.07% more-labile DOM and 10.92% less labile DOM, and the overlaying water consisted of 93.57% more-labile and 6.42% less labile DOM (Figure 5.5). These compositional characteristics suggest a microbial origin of the OC and resemble the types of compounds derived from microbial exudation processes.

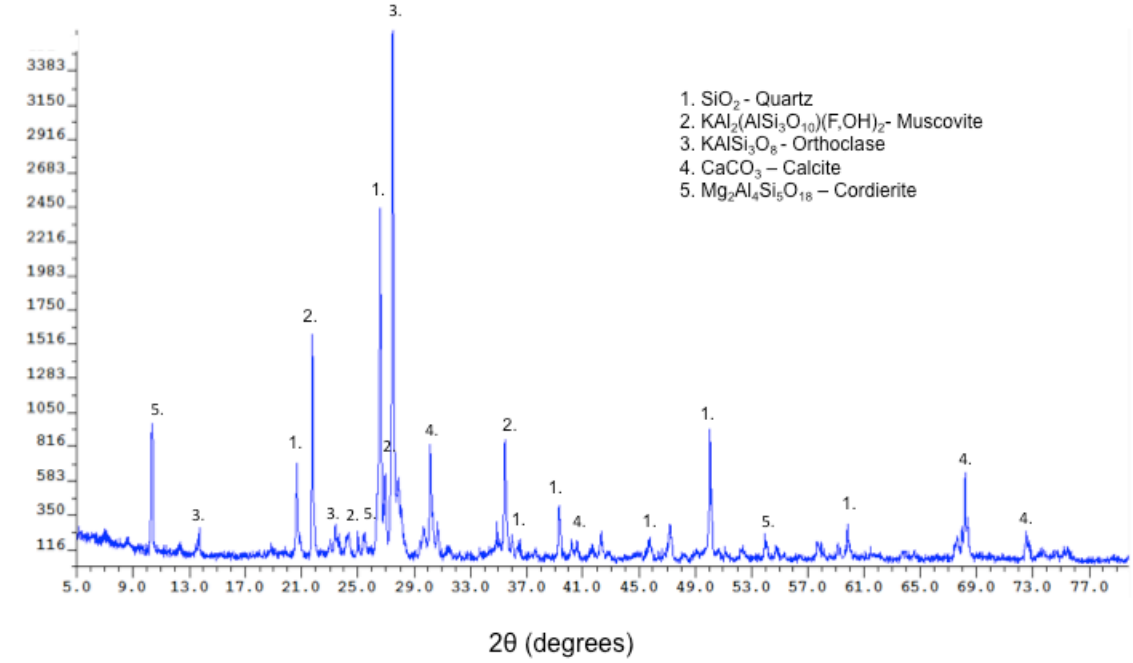

Figure 5.4. Powder XRD spectral profile of cryoconite sediments, used to illustrate the interpretation of present constituents. Cryoconite sediment diffraction patterns suggest a dominance of silicate materials, specifically quartz and corresponding weathering products.

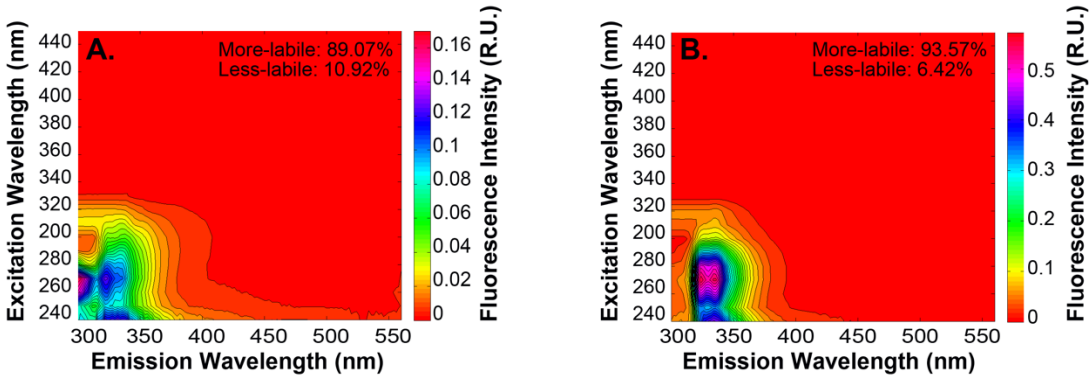

Figure 5.5. 3D excitation emission matrices of cryoconite DOM extracted from sediment (A.) and cryoconite water (B.) and corresponding percentages of more- and less-labile components.

Biofilms have been found in diverse environments and proven to be ecologically advantageous for survival (Hall-Stoodley *et al.*, 2004). Our unprecedented data show evidence of prominent biofilm formation on Antarctic cryoconite mineral particles, where the close arrangement of heterotrophs and autotrophs promotes increases in cellular activity enabling a highly efficient nutrient transfer between community members. It has been estimated that ~4.5% or 365,184m^2 of the Canada Glacier is covered by cryoconite (Foreman *et al.*, 2007). Taken together with results from our study this suggests that ~127,814m^2 of the Canada glacier surface is covered by biotic material. Considering the average number of photosynthetic days (226; Priscu *et al.*, 1999), the amount of cryoconite sediment on the surface of the Canada Glacier (Foreman *et al.*, 2007), and the experimentally determined cell specific rate of carbon fixation, we estimated that *Oscillatoria* cells may fix 1.60 kg C within cryoconite across the Canada Glacier per season. A recent study by Telling et al. 2014 (Telling *et al.*, 2014), which was synchronized with the sample collection of cryoconite from Canada Glacier in this study, estimated a total bulk carbon fixation potential of 9.07 kg C per season for Canada Glacier photosynthetic communities. As such, *Oscillatoria* cells may contribute ~20% of the total seasonal C fixation. Bacterial productivity in glacial environments is strongly influenced by the quality and quantity of fixed OC (Bagshaw *et al.*, 2016) thus, it is important to consider both bulk and species specific primary production.

Antarctic cryoconite have been shown to be "hotspots" of biological activity; herein we show that cryoconite biofilm may play a significant role in promoting this activity. The role and magnitude of different factors such as impurities (e.g., black

carbon, dust), biological activity, and snow grain size on glacial surface albedo has yet to be quantified and incorporated into models. This gap in our fundamental knowledge of these factors limits our ability to predict drivers of albedo change and future melting. As the transport and deposition of black carbon is less in Antarctica (Bauer *et al.*, 2013), microbial process may have more substantial effects on albedo and thus the surface energy balance of glaciers. Tedesco *et al.* 2013 confirmed the primary role of organic material covering Antarctic cryoconite minerals in reducing the reflectance of visible light. Thus, we hypothesize that future increases in temperature and longer melt seasons will stimulate biofilm communities and the accumulation of organic matter on cryoconite particles, heightening a positive feedback on glacial surface darkening. The importance of biofilm formation in cryoconite merits further research to determine their development, the formation of larger aggregates composed of organic and inorganic material, and thus, their potential for reducing surface albedo and increasing melting of glaciers.

Acknowledgements

This work was supported by the National Science Foundation Division of Antarctic Sciences through ANT-0838970 and ANT-1141978, by the NSF Division of Graduate Education through DGE-0654336, and a NASA Earth and Science Space Fellowship to HJS. The Max Plank Society supported the nanoSIMS and EA-IRMS analyses. We thank Betsey Pitts for assistance with microscopy, T. Nylen and J. Telling for collection of the cryoconite. We thank Dr. Phil Stewart for constructive comments on an earlier version of

this manuscript. Daniela Tienken from the Max Planck Institute for Marine Microbiology assisted the nanoSIMS analysis. RAF is funded by the Knut and Alice Wallenberg Foundation. Any opinions, findings, or conclusions expressed in this material are those of the authors and do not necessarily reflect the views of the National Science Foundation.

References

Anesio AM, Hodson AJ, Fritz A. (2009). High microbial activity on glaciers: importance to the global carbon cycle. *Glob Change Biol* **15:** 955–960.

Bagshaw EA, Tranter M, Fountain AG, Welch K, Basagic HJ, Lyons WB. (2013). Do Cryoconite Holes have the Potential to be Significant Sources of C, N, and P to Downstream Depauperate Ecosystems of Taylor Valley, Antarctica? *Arctic, Antarctic, and Alpine Research* **45**: 440–454.

Bagshaw EA, Tranter M, Fountain AG, Welch KA, Basagic H, Lyons WB. (2007). Biogeochemical evolution of cryoconite holes on Canada Glacier, Taylor Valley, Antarctica. *J Geophys Res* **112** G04S35.

Bagshaw EA, Tranter M, Wadham JL. (2011). High-resolution monitoring reveals dissolved oxygen dynamics in an Antarctic cryoconite hole. *Hydrol Process* **25**: 2868–2877.

Bagshaw EA, Tranter M, Wadham JL, Fountain AG, Dubnick A, Fitzsimons S. (2016). Processes controlling carbon cycling in Antarctic glacier surface ecosystems. *Geochem Persp Let* **2**: 44–54.

Bauer SE, Bausch A, Nazarenko L, Tsigaridis K, Xu B, Edwards R, *et al.* (2013). Historical and future black carbon deposition on the three ice caps: Ice core measurements and model simulations from 1850 to 2100. *Journal of Geophysical Research: Atmospheres* **118**: 7948–7961.

Bell W, Mitchell R. (1972). Chemotactic and Growth Responses of Marine Bacteria to Algal Extracellular Products. *Biological Bulletin* **143**: 265.

Caporaso JG, Kuczynski J, Stombaugh J, Bittinger K, Bushman FD, Costello EK, *et al.* (2010). QIIME allows analysis of high-throughput community sequencing data. *Nat Meth* **7**: 335–336.

Chen M-Y, Lee D-J, Tay J-H, Show K-Y. (2007). Staining of extracellular polymeric substances and cells in bioaggregates. *Appl Microbiol Biotechnol* **75**: 467–474.

Coble PG. (1996). Characterization of marine and terrestrial DOM in seawater using excitation-emission matrix spectroscopy. **51**: 325–346.

Cook J, Edwards A, Takeuchi N, Irvine-Fynn T. (2015). Cryoconite The dark biological secret of the cryosphere. *Progress in Physical Geography* 1–46.

Cuypers C, Grotenhuis T, Nierop KGJ, Franco EM, de Jager A, Rulkens W. (2002). Amorphous and condensed organic matter domains: the effect of persulfate oxidation on

the composition of soil/sediment organic matter. *Chemosphere* **48**: 919–931.

Foreman CM, Sattler B, Mikucki JA, Porazinska DL, Priscu JC. (2007). Metabolic activity and diversity of cryoconites in the Taylor Valley, Antarctica. *J Geophys Res* **112**: G04S32.

Foster RA, Kuypers MMM, Vagner T, Paerl RW, Musat N, Zehr JP. (2011). Nitrogen fixation and transfer in open ocean diatom–cyanobacterial symbioses. *ISME J* **5**: 1484–1493.

Fountain AG, Nylen TH, Tranter M, Bagshaw E. (2008). Temporal variations in physical and chemical features of cryoconite holes on Canada Glacier, McMurdo Dry Valleys, Antarctica. *J Geophys Res* **113**: G01S92.

Fountain AG, Tranter M, Nylen TH, Lewis KJ, Mueller DR. (2004). Evolution of cryoconite holes and their contribution to meltwater runoff from glaciers in the McMurdo Dry Valleys, Antarctica. *Journal of Glaciology* **50**: 35–45.

Haas BJ, Gevers D, Earl AM, Feldgarden M, Ward DV, Giannoukos G, *et al.* (2011). Chimeric 16S rRNA sequence formation and detection in Sanger and 454-pyrosequenced PCR amplicons. *Genome Res* **21**: 494–504.

Hall-Stoodley L, Costerton JW, Stoodley P. (2004). Bacterial biofilms: from the natural environment to infectious diseases. *Nat Rev Microbiol* **2**: 95–108.

Hood E, Battin TJ, Fellman J, O'Neel S, Spencer RGM. (2015). Storage and release of organic carbon from glaciers and ice sheets. *Nature Geoscience* **8**: 91–96.

Huber T, Faulkner G, Hugenholtz P. (2004). Bellerophon: a program to detect chimeric sequences in multiple sequence alignments. *Bioinformatics* **20**: 2317–2319.

Jackson GA. (1987). Simulating chemosensory responses of marine microorganisms. *Limnol Oceanogr* **32**: 1253–1266.

Kristensen E. (1990). Characterization of biogenic organic matter by stepwise thermogravimetry. *Biogeochemistry* **9**: 135–159.

Langford H, Hodson A, Banwart S, Bøggild C. (2010). The microstructure and biogeochemistry of Arctic cryoconite granules. *Annals of Glaciology* **51**: 87–94.

Lutz S, Anesio AM, Villar SEJ, Benning LG. (2014). Variations of algal communities cause darkening of a Greenland glacier. *FEMS Microbiol Ecol* **89**: 402–414.

Mullin MM, Sloan PR, Eppley RW. (1966). Relationship Between Carbon Content, Cell Volume, and Area in Phytoplankton. *Limnol Oceanogr* **11**: 307–311.

Musat N, Halm H, Winterholler B, Hoppe P, Peduzzi S, Hillion F, *et al.* (2008). A single-cell view on the ecophysiology of anaerobic phototrophic bacteria. *Proc Natl Acad Sci USA* **105**: 17861–17866.

Musat N, Stryhanyuk H, Bombach P, Adrian L, Audinot J-N, Richnow HH. (2014). The effect of FISH and CARD-FISH on the isotopic composition of ^{13}C- and ^{15}N-labeled Pseudomonas putida cells measured by nanoSIMS. *Systematic and Applied Microbiology*.

Pernthaler A, Pernthaler J, Amann R. (2002). Fluorescence in situ hybridization and catalyzed reporter deposition for the identification of marine bacteria. *Appl Environ Microbiol* **68**: 3094–3101.

Polerecky L, Adam B, Milucka J, Musat N, Vagner T, Kuypers MMM. (2012). Look@NanoSIMS--a tool for the analysis of nanoSIMS data in environmental microbiology. *Environ Microbiol* **14**: 1009–1023.

Priscu JC, Wolf CF, Takacs CD, Fritsen CH, Laybourn-Parry J, Roberts EC, *et al.* (1999). Carbon Transformations in a Perennially Ice-Covered Antarctic Lake. *BioScience* **49**: 997–1008.

Stocker R. (2015). The 100 µm length scale in the microbial ocean. *Aquat Microb Ecol* **76**: 189–194.

Sun J. (2003). Geometric models for calculating cell biovolume and surface area for phytoplankton. *Journal of Plankton Research* **25**: 1331–1346.

R Development Core Team. R: a language and environment for statistical computing. Vienna, Austria: R Foundation for Statistical Computing. (2012).

Tedesco M, Foreman CM, Anton J, Steiner N, Schwartzman T. (2013). Comparative analysis of morphological, mineralogical and spectral properties of cryoconite in Jakobshavn Isbrae, Greenland, and Canada Glacier, Antarctica. *Annals of Glaciology* **54**: 147–157.

Telling J, Anesio AM, Tranter M, Fountain AG, Nylen T, Hawkings J, *et al.* (2014). Spring thaw ionic pulses boost nutrient availability and microbial growth in entombed Antarctic Dry Valley cryoconite holes. *Front Microbiol* **5**: 694–694.

Verity PG, Robertson CY, Tronzo CR, Andrews MG, Nelson JR, Sieracki ME. (1992). Relationships between cell volume and the carbon and nitrogen content of marine photosynthetic nanoplankton. *Limnol Oceanogr* **37**: 1434–1446.

Wagner M. (2009). Single-Cell Ecophysiology of Microbes as Revealed by Raman Microspectroscopy or Secondary Ion Mass Spectrometry Imaging. *Annu. Rev. Micro.* 411–229.

Walter E Dean Jr. (1974). Determination of Carbonate and Organic Matter in Calcareous Sediments and Sedimentary Rocks by Loss on Ignition: Comparison With Other Methods. *SEPM JSR* **Vol. 44**: 242–248.

CHAPTER 6

EPILOGUE

Despite the low OC concentrations in glacial ecosystems, recent studies have highlighted the relevance of glaciers to global carbon fluxes (Hood *et al.*, 2015). The origin of this carbon is from aerosols (Stubbins *et al.*, 2012), legacy carbon stored within the ice (Hood *et al.*, 2009), terrestrial inputs (Bhatia *et al.*, 2010), and microbial synthesis (Singer *et al.*, 2012). The origin of DOM largely affects DOM composition, ecosystem function, and biogeochemical cycling. While studies have mainly focused on the ecosystem implications of carbon from terrestrial or anthropogenic sources (Hood *et al.*, 2009; Stubbins *et al.*, 2012; Singer *et al.*, 2012) it is now recognized that *in situ* primary production plays a crucial role in the glacial carbon budget (Anesio *et al.*, 2009; Cook *et al.*, 2012; Hodson *et al.*, 2007; 2015). As a result, more refined supraglacial carbon flux models have been developed (Hodson *et al.*, 2010; Anesio *et al.*, 2009; Cook *et al.*, 2012). However, while these models have acknowledged the impact on local and adjacent habitats, detailed information on supraglacial carbon cycling (i.e., carbon fixation, exudation, and transformation) and the microbial food web (i.e., direct interactions between photoauto- and heterotrophs) is still lacking. The main objective of this dissertation was to determine how the *in situ* microbial community was linked to DOM quality and successive DOM bioprocessing and vice versa. An in-depth analysis that spanned across physical scales (from 1,000s of km down to nanometer scales) allowed

for a multi-level analysis of environmental processes in supraglacial ecosystems (Figure 6.1).

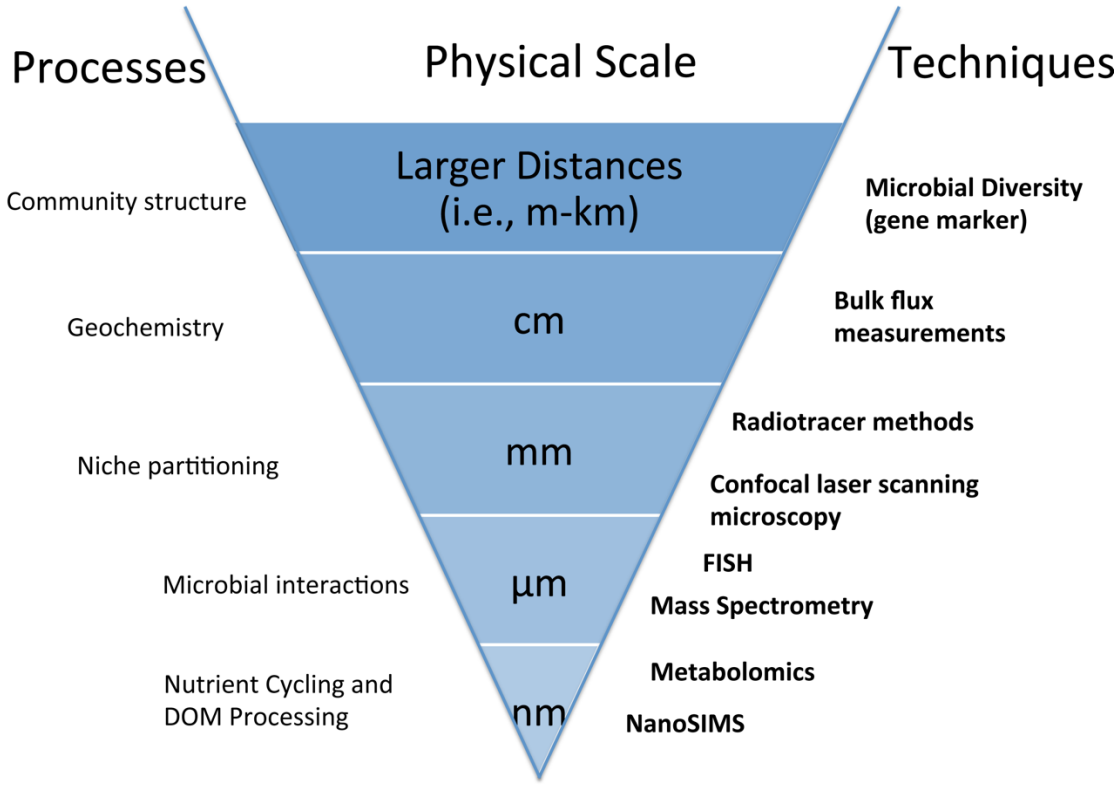

Figure 6.1. A multi-scale approach for environmental analysis, techniques employed in this research appear in bold font (adapted from Herrmann *et al*. 2007).

On the biogeographical scale, supraglacial microbial assemblages varied significantly based on the location (i.e., Cotton Glacier, Canada Glacier, and Greenland) and habitat type (i.e., stream water, stream sediments, ice, snow, and cryoconite) with the exception of a moderate overlap in microbial assemblages found in Cotton Glacier ice and stream water. However, differences between ice and stream water indicate that not all

microbial phylotypes seeded from the ice were able to establish themselves in the stream water community.

To date, the relationship between species composition and ecosystem function is still poorly understood and a topic of debate. Previous work has shown that microbial communities differ across environmental gradients (Ghiglione *et al.*, 2012; Cameron, Hagedorn, *et al.*, 2015; Staley and Gosink, 1999), with only a few studies addressing glacial biodiversity and the physico-chemical factors that shape these communities (Cameron *et al.*, 2012; Cameron *et al.*, 2015; Stibal, *et al.*, 2015; Wilhelm *et al.*, 2013; Hell *et al.*, 2013). While physical parameters were inadequate to explain differences in the microbial assemblages found in the present investigation, dissimilarities were explained by the variation in DOM quality. DOM composition from geographically distinct glacial habitats reflected differences in the quality of protein- and humic-like compounds, properties which could be tightly coupled to changes in bacterial productivity and community composition (Judd *et al.*, 2006).

The dependency of microbial community structure on DOM composition inspired an array of lab based studies designed to better understand supraglacial carbon cycling on a close range scale (cm to nm). Experiments included (i) a multi-step analysis of bulk fluxes resulting from potential photosynthesis, bacterial production, and percent exudation using radiolabeled tracers to determine if PER meets bacterial carbon demands, (ii) calculating rates of exuded carbon uptake in community incubations using a combination of CARD-FISH and nanoSIMS techniques, (iii) investigating the lability of glacial DOM in comparison to other end member DOM sources using single species

cultures, and (iv) the detection of biofilm in an Antarctic supraglacial habitat to determine if cellular organization enhances biogeochemical cycling.

These experiments allowed for the detailed and high resolution reconstruction of close range microbial interactions in the context of carbon cycling in supraglacial environments. In contrast to the traditional view of aeolian and anthropogenically derived OC as the primary contributor to glacial carbon cycling (Hood *et al.*, 2009; Stubbins *et al.*, 2012), microbially fixed and exuded carbon was a major source of DOM in these supraglacial habitats. *In situ* rates of carbon exudation were in excess of the bacterial carbon demand. Exudates were highly bioavailable carbon substrates that were rapidly assimilated by natural microbial members (in particular *Betaproteobacteria* and *Bacteroidetes* lineages).

Interactions between microbial communities and DOM processing are inherently difficult to assess due to both the complex nature of natural microbial communities and DOM. Additionally, it is commonly assumed that DOM degradation is linked to microbial diversity and the fundamental theory of resource allocation between competing species (Hutchinson, 1957). Until recently this notion had not been explicitly tested, and whether a single organism can process diverse sources of DOM is not yet understood. A recent study suggests that single organisms are indeed capable of the removal of the entire labile fraction of DOM (Pedler *et al.*, 2014). To bridge this gap, a single phylotype isolated from the CG stream (*Janthinobacterium* CG3; Smith *et al.*, 2013) was incubated in compositionally diverse sources of DOM. In contrast to the DOM exudates mentioned above, the predicted compositional lability of the bulk DOM from the CG stream did not

correspond to biological lability when compared to other more humic or terrestrially influenced DOM sources from Pony Lake and Suwanee River, respectively. CG DOM was unable to sustain the same magnitude of microbial metabolism throughout the incubation time investigated (98 d). While none of the tested carbon sources were found to be truly bio-labile by definition (supporting increased activity over hours to days), the microbially derived and recalcitrant Pony Lake DOM supported cellular respiration throughout the entire incubation period. Unlike the work of Pedler *et al.* 2014, a significant decrease in DOC, or the complete drawdown of the labile DOM pool was not observed. Rather there were oscillations in the consumption and production of labile DOM throughout the course of the experiment for all carbon sources, which indicates that DOM processing in glacial habitats would be reliant on a more complex functional diversity.

The role of biofilm on mineral surfaces in supraglacial habitats further emphasized cell-DOM interactions on a micro- to nanometer scale. Biofilm covered ~35% of the sediment surface with cellular organization largely enhancing nutrient transfer between photoautotrophs (*Oscillatoria*) and heterotrophs (*Bacteroidetes)*. Cell specific analysis of filamentous *Oscillatoria* revealed high levels of carbon fixation and nitrogen assimilation, while biogeochemical cycling of exuded DOM was most pronounced in the close proximity (<2μm) of filamentous cells .

Typically aquatic habitats are analyzed across tens of hundreds of liters, which translates into large physical scales (Stocker, 2015). Bulk approaches provide valuable information on the overall microbial composition, and biogeochemical fluxes but prove

difficult in capturing environmental heterogeneity. The data presented herein spans large distances from km to cell specific (i.e. nm) dynamics, providing a unique insight into the microbial functioning of glacial ecosystems. From previous studies (Cameron *et al.*, 2012; Cameron, Hagedorn, *et al.*, 2015; Wilhelm *et al.*, 2013; Van Horn *et al.*, 2013; Hodgson *et al.*, 2010; Namsaraev *et al.*, 2010) it is known that bacterial communities are spatially variable, which is comparable to our findings. Surprisingly, we did not identify a core microbial community across all sampled environmental locations (3.1% OTU overlap), supporting the idea of community development in response to localized environmental factors. Differences in microbial community structures identified in earlier investigations could be explained by geographical factors and the environment type, providing no further understanding of geochemical impacts on microbial assemblage composition. The present comprehensive study went beyond the effect of geographical parameters in shaping communities, and identified DOM as an underlying geochemical factor. We also detected environmentally relevant organisms in DOM bio-processing.

Variations in glacial DOM have long been recognized including, ancient vs. young (Stubbins *et al.*, 2012; Hood *et al.*, 2009), or terrestrial vs. black carbon (Bauer *et al.*, 2013; Li *et al.*, 2008), rendering DOM quality more or less bioavailable for microbial uptake. To date the lability of glacial DOM has been determined with two lines of evidence. Bulk bioavailability assays have termed ancient carbon as the labile source of carbon for microbial communities (Hood et al. 2009), and bulk bio-lability has only speculated based on the molecular composition of DOM (Antony *et al.*, 2014; Bhatia *et al.*, 2010; Singer *et al.*, 2012). Time scales used in these incubations (30 d) were outside

the operational definition of labile carbon (hrs to d), and solely focused on a single fraction within the DOM pool. Our findings support not only these speculations but clearly showed that microbially derived DOM is highly bio-labile (hrs) and capable of supporting *in situ* bacterial carbon demands. This finding was also in contrast to other Antarctic environments; specifically that microbially exuded carbon was insufficient to support bacterial production in McMurdo Dry Valley lakes (Takacs et al. 2001). Further support for the reliance of glacial habits on microbially produced DOM was found in the efficient transfer and cycling of nutrients promoted by cellular spatial organization in biofilms. Thus, I propose that glacial food webs are largely dependent on autochthonous carbon resources, with bio-labile microbially produced carbon now adding a fourth compartment to supraglacial carbon cycling. Future studies focusing on glacial surface processes need to include both cell specific and bulk biogeochemical measurements with an emphasis on discerning the role of biofilms in supraglacial habitats.

It is concluded that the heterogeneous character of DOM facilitates sustained microbial metabolism in comparison to other DOM sources. I therefore suggest that it is important to survey not only DOM quality and quantity but also DOM chemical heterogeneity, which appears to be linked to biological lability. Further experimentation with other targeted organisms is necessary to determine whether it is possible for a single organism to utilize labile DOM fractions from diverse source materials, as our studies indicate that DOM processing in glacial habitats is likely reliant on community metabolic diversity. Lastly, mixed community consortia studies that include metabolically diverse

organisms are necessary to address DOM bio-transformations in natural glacial environments.

Taken together, this study suggests that glacial DOM plays an integral role in both shaping microbial assemblage composition and influencing metabolic activity. A localized microbial loop is responsible for the production of labile carbon in excess, which is rapidly assimilated supporting bacterial growth demands. In conclusion I hypothesize that future increases in temperature accompanied by longer melt seasons will stimulate the microbial production of labile DOM in both planktonic and biofilm habitats leading to increases in the transport and accumulation of DOM in glacial environments.

Lastly, I would like to emphasis the need for proper design and analysis of high-throughput sequencing specifically when applied to the field of microbial ecology The application of molecular techniques specifically, next generation sequencing (NGS) technology to environmental DNA has drastically deepened our global understanding of biodiversity (Sogin *et al.*, 2006; Wilhelm *et al.*, 2013). The importance of including controls at several steps during sample collection, DNA extraction, and DNA amplification has recently been highlighted (Nguyen *et al.*, 2015). To ensure that community sequencing data from this study was void of artifacts from contamination or sample preparation several blanks were included throughout the stages of sample collection and sequencing preparation. Quality sequences were retrieved from all sequenced blank samples, OTUs amplified from blank samples were removed from corresponding environmental samples. Future work should include replicate samples, sequence blanks, as well as include a ‘mock community’ as a positive control. These

controls are becoming increasingly important, especially when addressing the biodiversity of rare phylotypes and low biomass samples.

References

Anesio AM, Hodson AJ, Fritz A. (2009). High microbial activity on glaciers: importance to the global carbon cycle. *Glob Change Biol* **15**: 955–960.

Antony R, Grannas AM, Willoughby AS, Sleighter RL, Thamban M, Hatcher PG. (2014). Origin and sources of dissolved organic matter in snow on the East Antarctic ice sheet. *Environ Sci Technol* **48**: 6151–6159.

Bauer SE, Bausch A, Nazarenko L, Tsigaridis K, Xu B, Edwards R, *et al.* (2013). Historical and future black carbon deposition on the three ice caps: Ice core measurements and model simulations from 1850 to 2100. *Journal of Geophysical Research: Atmospheres* **118**: 7948–7961.

Bhatia MP, Das SB, Longnecker K, Charette MA, Kujawinski EB. (2010). Molecular characterization of dissolved organic matter associated with the Greenland ice sheet. *Geochimica et Cosmochimica Acta* **74**: 3768–3784.

Cameron KA, Hagedorn B, Dieser M, Christner BC, Choquette K, Sletten R, *et al.* (2015). Diversity and potential sources of microbiota associated with snow on western portions of the Greenland Ice Sheet. *Environ Microbiol* **17**: 594–609.

Cameron KA, Hodson AJ, Osborn AM. (2012). Structure and diversity of bacterial, eukaryotic and archaeal communities in glacial cryoconite holes from the Arctic and the Antarctic. *FEMS Microbiol Ecol* **82**: 254–267.

Cameron KA, Stibal M, Zarsky JD, Gözdereliler E, Schostag M, Jacobsen CS. (2015). Supraglacial bacterial community structures vary across the Greenland ice sheet. *FEMS Microbiol Ecol*.

Cook JM, Hodson AJ, Anesio AM. (2012). An improved estimate of microbially mediated carbon fluxes from the Greenland ice sheet. *Journal of Glaciology* **58**: 1098–1108.

Ghiglione J-F, Galand PE, Pommier T, Pedrós-Alió C, Maas EW, Bakker K, *et al.* (2012). Pole-to-pole biogeography of surface and deep marine bacterial communities. *Proc Natl Acad Sci USA* **109**: 17633–17638.

Hell K, Edwards A, Zarsky J, Podmirseg SM, Girdwood S, Pachebat JA, *et al.* (2013). The dynamic bacterial communities of a melting High Arctic glacier snowpack. *ISME J* **7**: 1814–1826.

Hodgson DA, Convey P, Verleyen E, Vyverman W, McInnes SJ, Sands CJ, *et al.* (2010). The limnology and biology of the Dufek Massif, Transantarctic Mountains 82° South. *Polar Science* **4**: 197–214.

Hodson A, Anesio AM, Ng F, Watson R, Quirk J, Irvine-Fynn T, *et al.* (2007). A glacier respires: Quantifying the distribution and respiration CO 2flux of cryoconite across an entire Arctic supraglacial ecosystem. *J Geophys Res* **112**: G04S36.

Hodson A, Ben Brock, Pearce D, Laybourn-Parry J, Tranter M. (2015). Cryospheric ecosystems: a synthesis of snowpack and glacial research. *Environ Res Lett* **10**: 110201.

Hodson A, Bøggild C, Hanna E, Huybrechts P, Langford H, Cameron K, *et al.* (2010). The cryoconite ecosystem on the Greenland ice sheet. *Annals of Glaciology* **51**: 123–129.

Hood E, Battin TJ, Fellman J, O'Neel S, Spencer RGM. (2015). Storage and release of organic carbon from glaciers and ice sheets. *Nature Geoscience* **8**: 91–96.

Hood E, Fellman J, Spencer RGM, Hernes PJ, Edwards R, D'Amore D, *et al.* (2009). Glaciers as a source of ancient and labile organic matter to the marine environment. *Nature* **462**: 1044–1047.

Hutchinson GE. (1957). Cold spring harbor symposium on quantitative biology. Concluding remarks.

Judd KE, Crump BC, Kling GW. (2006). Variation in dissolved organic matter controls bacterial production and community composition. *Ecology* **87**: 2068–2079.

Li F, Ginoux P, Ramaswamy V. (2008). Distribution, transport, and deposition of mineral dust in the Southern Ocean and Antarctica: Contribution of major sources. *Journal of Geophysical Research: Atmospheres* **113**.

Namsaraev Z, Mano MJ, Fernandez R, Wilmotte A. (2010). Biogeography of terrestrial cyanobacteria from Antarctic ice-free areas. *Annals of Glacilogy* **51**: 171–177.

Nguyen NH, Smith D, Peay K, Kennedy P. (2015). Parsing ecological signal from noise in next generation amplicon sequencing. *New Phytol* **205**: 1389–1393.

Pedler BE, Aluwihare LI, Azam F. (2014). Single bacterial strain capable of significant contribution to carbon cycling in the surface ocean. *Proc Natl Acad Sci USA* **111**: 7202–7207.

Singer GA, Fasching C, Wilhelm L, Niggemann J, Steier P, Dittmar T, *et al.* (2012). Biogeochemically diverse organic matter in Alpine glaciers and its downstream fate. *Nature Geoscience* **5**: 710–714.

Smith H, Akiyama T, Foreman C, Franklin M, Woyke T, Teshima H, *et al.* (2013). Draft Genome Sequence and Description of Janthinobacterium sp. Strain CG3, a Psychrotolerant Antarctic Supraglacial Stream Bacterium. *Genome Announc* **1**: e00960–13.

Sogin ML, Morrison HG, Huber JA, Mark Welch D, Huse SM, Neal PR, *et al.* (2006). Microbial diversity in the deep sea and the underexplored "rare biosphere". *Proc Natl Acad Sci USA* **103**: 12115–12120.

Staley JT, Gosink JJ. (1999). Poles Apart: Biodiversity and Biogeography of Sea Ice Bacteria - Annual Review of Microbiology, 53(1):189. *Annual Reviews in Microbiology*.

Stocker R. (2015). The 100 µm length scale in the microbial ocean. *Aquat Microb Ecol* **76**: 189–194.

Stubbins A, Hood E, Raymond PA, Aiken GR, Sleighter RL, Hernes PJ, *et al.* (2012). Anthropogenic aerosols as a source of ancient dissolved organic matter in glaciers. *Nature Geoscience* **5**: 198–201.

Van Horn DJ, Van Horn ML, Barrett JE, Gooseff MN, Altrichter AE, Geyer KM, *et al.* (2013). Factors Controlling Soil Microbial Biomass and Bacterial Diversity and Community Composition in a Cold Desert Ecosystem: Role of Geographic Scale. *PLoS ONE* **8**: e66103.

Wilhelm L, Singer GA, Fasching C, Battin TJ, Besemer K. (2013). Microbial biodiversity in glacier-fed streams. *ISME J*.

REFERENCES CITED

Amon RMW, Benner R. (1996). Photochemical and microbial consumption of dissolved organic carbon and dissolved oxygen in the Amazon River system. *Geochimica et Cosmochimica Acta* **60**: 1783–1792.

Anesio AM, Bellas CM. (2011). Are low temperature habitats hot spots of microbial evolution driven by viruses? *Trends Microbiol* **19**: 52–57.

Anesio AM, Granéli W, Aiken GR, Kieber DJ, Mopper K. (2005). Effect of Humic Substance Photodegradation on Bacterial Growth and Respiration in Lake Water. *Appl Environ Microbiol* **71**: 6267–6275.

Anesio AM, Hodson AJ, Fritz A. (2009). High microbial activity on glaciers: importance to the global carbon cycle. *Glob Change Biol* **15**: 955–960.

Anesio AM, Laybourn-Parry J. (2012). Glaciers and ice sheets as a biome. *Trends Ecol Evol (Amst)* **27**: 219–225.

Anesio AM, Sattler B, Foreman C, Telling J. (2010). Carbon fluxes through bacterial communities on glacier surfaces. *Annals of Glacioloy* **51**: 32–40.

Antony R, Grannas AM, Willoughby AS, Sleighter RL, Thamban M, Hatcher PG. (2014). Origin and sources of dissolved organic matter in snow on the East Antarctic ice sheet. *Environ Sci Technol* **48**: 6151–6159.

Bagshaw EA, Tranter M, Fountain AG, Welch K, Basagic HJ, Lyons WB. (2013). Do Cryoconite Holes have the Potential to be Significant Sources of C, N, and P to Downstream Depauperate Ecosystems of Taylor Valley, Antarctica? *Arctic, Antarctic, and Alpine Research* **45**: 440–454.

Bagshaw EA, Tranter M, Fountain AG, Welch KA, Basagic H, Lyons WB. (2007). Biogeochemical evolution of cryoconite holes on Canada Glacier, Taylor Valley, Antarctica. *J Geophys Res* **112**.

Bagshaw EA, Tranter M, Wadham JL. (2011). High-resolution monitoring reveals dissolved oxygen dynamics in an Antarctic cryoconite hole. *Hydrol Process* **25**: 2868–2877.

Bagshaw EA, Tranter M, Wadham JL, Fountain AG, Dubnick A, Fitzsimons S. (2016). Processes controlling carbon cycling in Antarctic glacier surface ecosystems. *Geochem Persp Let* **2**: 44–54.

Barker JD, Dubnick A, Lyons WB, Chin YP. (2013). Changes in Dissolved Organic Matter (DOM) Fluorescence in Proglacial Antarctic Streams. *Arctic, Antarctic, and Alpine Research* **45**: 305–317.

Barker JD, Sharp MJ, Fitzsimons SJ, Turner RJ. (2006). Abundance and Dynamics of

Dissolved Organic Carbon in Glacier Systems. *Arctic, Antarctic, and Alpine Research* **38**: 163–172.

Battin TJ, Kaplan LA, Findlay S, Hopkinson CS, Marti E, Packman AI, *et al.* (2008). Biophysical controls on organic carbon fluxes in fluvial networks. *Nature Geoscience* **1**: 95–100.

Bauer SE, Bausch A, Nazarenko L, Tsigaridis K, Xu B, Edwards R, *et al.* (2013). Historical and future black carbon deposition on the three ice caps: Ice core measurements and model simulations from 1850 to 2100. *Journal of Geophysical Research: Atmospheres* **118**: 7948–7961.

Bell W, Mitchell R. (1972). Chemotactic and Growth Responses of Marine Bacteria to Algal Extracellular Products. *Biological Bulletin* **143**: 265.

Benjamini Y and Hochberg Y. (1995). Controlling the False Discovery Rate - a Practical and Powerful Approach to Multiple Testing. *Journal of the Royal Statistical Society Series B-Methodological* **57**: 289–300.

Benner R, Kaiser K. (2011). Biological and photochemical transformations of amino acids and lignin phenols in riverine dissolved organic matter. *Biogeochemistry* **102**: 209–222.

Bhatia MP, Das SB, Longnecker K, Charette MA, Kujawinski EB. (2010). Molecular characterization of dissolved organic matter associated with the Greenland ice sheet. *Geochimica et Cosmochimica Acta* **74**: 3768–3784.

Bhatia MP, Das SB, Xu L, Charette MA, Wadham JL, Kujawinski EB. (2013). Organic carbon export from the Greenland ice sheet. *Geochimica et Cosmochimica Acta* **109**: 329–344.

Bianchi TS. (2011). The role of terrestrially derived organic carbon in the coastal ocean: a changing paradigm and the priming effect. *Proc Natl Acad Sci USA* **108**: 19473–19481.

Boetius A, Anesio AM, Deming JW, Mikucki JA, Rapp JZ. (2015). Microbial ecology of the cryosphere: sea ice and glacial habitats. *Nat Rev Microbiol*.

Brown TL, Rice JA. (2000). Effect of experimental parameters on the ESI FT-ICR mass spectrum of fulvic acid. *Anal Chem* **72**: 384–390.

Brussaard CPD. (2004). Optimization of procedures for counting viruses by flow cytometry. *Appl Environ Microbiol* **70**: 1506–1513.

Cameron KA, Hagedorn B, Dieser M, Christner BC, Choquette K, Sletten R, *et al.* (2015). Diversity and potential sources of microbiota associated with snow on western portions of the Greenland Ice Sheet. *Environ Microbiol* **17**: 594–609.

Cameron KA, Hodson AJ, Osborn AM. (2012). Structure and diversity of bacterial, eukaryotic and archaeal communities in glacial cryoconite holes from the Arctic and the Antarctic. *FEMS Microbiol Ecol* **82**: 254–267.

Cameron KA, Stibal M, Zarsky JD, Gözdereliler E, Schostag M, Jacobsen CS. (2015). Supraglacial bacterial community structures vary across the Greenland ice sheet. *FEMS Microbiol Ecol*.

Caporaso JG, Kuczynski J, Stombaugh J, Bittinger K, Bushman FD, Costello EK, *et al.* (2010). QIIME allows analysis of high-throughput community sequencing data. *Nat Meth* **7**: 335–336.

Carpenter EJ, Lin S, Capone DG. (2000). Bacterial Activity in South Pole Snow. *Applied and Environmental Microbiology* **66**: 4514–4517.

Cavicchioli R. (2015). Microbial ecology of Antarctic aquatic systems. *Nat Rev Microbiol* **13**: 691–706.

Chao A. (1984). Nonparametric Estimation of the Number of Classes in a Population on JSTOR. *Scandinavian Journal of statistics*.

Chen M-Y, Lee D-J, Tay J-H, Show K-Y. (2007). Staining of extracellular polymeric substances and cells in bioaggregates. *Appl Microbiol Biotechnol* **75**: 467–474.

Cherrier J, Bauer JE, Druffel E. (1996). Utilization and turnover of labile dissolved organic matter by bacterial heterotrophs in eastern North Pacific surface waters. *Mar Ecol Prog Ser* **139**: 267–279.

Chown SL, Clarke A, Fraser CI, Cary SC, Moon KL, McGeoch MA. (2015). The changing form of Antarctic biodiversity. *Nature* **522**: 431–438.

Christian RR, Capone DG. (2002). Overview of issues in aquatic microbial ecology. 2nd ed. Manual of Environmental Microbiology.

Christner BC, Kvitko BH II, Reeve JN. (2003). Molecular identification of Bacteria and Eukarya inhabiting an Antarctic cryoconite hole. *Extremophiles* **7**: 177–183.

Christner BC, Priscu JC, Achberger AM, Barbante C, Carter SP, Christianson K, *et al.* (2014). A microbial ecosystem beneath the West Antarctic ice sheet. *Nature* **512**: 310–313.

Clarke KR, Warwick RM. (2001). Change in Marine Communities: An approach to statistical analysis and interpretation, 2nd edition. *Primer-E Ltd, Plymouth UK*.

Coble PG. (1996). Characterization of marine and terrestrial DOM in seawater using excitation-emission matrix spectroscopy. **51**: 325–346.

Coble PG, Green SA, Blough NV, Gagosian RB. (1990). Characterization of dissolved organic matter in the Black Sea by fluorescence spectroscopy. *Nature* **348**: 432–435.

Cole JJ, Likens GE, Strayer DL. (1982). Photosynthetically produced dissolved organic carbon: An important carbon source for planktonic bacteria. *Limnol Oceanogr* **27**: 1080–1090.

Cole JJ, Prairie YT, Caraco NF, McDowell WH, Tranvik LJ, Striegl RG, *et al.* (2007). Plumbing the Global Carbon Cycle: Integrating Inland Waters into the Terrestrial Carbon Budget. *Ecosystems* **10**: 172–185.

Cook J, Edwards A, Takeuchi N, Irvine-Fynn T. (2015). Cryoconite The dark biological secret of the cryosphere. *Progress in Physical Geography* 1–46.

Cook JM, Hodson AJ, Anesio AM. (2012). An improved estimate of microbially mediated carbon fluxes from the Greenland ice sheet. *Journal of Glaciology* **58**: 1098–1108.

Cory RM, Kaplan LA. (2012). Biological lability of streamwater fluorescent dissolved organic matter. *Limnol Oceanogr* **57**: 1347–1360.

Coveney MF. (1982). Bacterial Uptake of Photosynthetic Carbon from Freshwater Phytoplankton. *Oikos* **38**: 8.

Crump BC, Kling GW, Bahr M, Hobbie JE. (2003). Bacterioplankton community shifts in an arctic lake correlate with seasonal changes in organic matter source. *Appl Environ Microbiol* **69**: 2253–2268.

Cuypers C, Grotenhuis T, Nierop KGJ, Franco EM, de Jager A, Rulkens W. (2002). Amorphous and condensed organic matter domains: the effect of persulfate oxidation on the composition of soil/sediment organic matter. *Chemosphere* **48**: 919–931.

Dittmar T, Koch B, Hertkorn N, Kattner G. (2008). A simple and efficient method for the solid-phase extraction of dissolved organic matter (SPE-DOM) from seawater. *Limnology and Oceanography-Methods* **6**: 230–235.

D'Andrilli J, Foreman CM, Marshall AG, McKnight DM. (2013). Characterization of IHSS Pony Lake fulvic acid dissolved organic matter by electrospray ionization Fourier transform ion cyclotron resonance mass spectrometry and fluorescence spectroscopy. *Organic Geochemistry* **65**: 19–28.

Edgar RC, Haas BJ, Clemente JC, Quince C, Knight R. (2011). UCHIME improves sensitivity and speed of chimera detection. *J Gerontol* **27**: 2194–2200.

Edwards A, Mur LAJ, Girdwood SE, Anesio AM, Stibal M, Rassner SME, *et al.* (2014). Coupled cryoconite ecosystem structure-function relationships are revealed by comparing

bacterial communities in alpine and Arctic glaciers. *FEMS Microbiol Ecol* **89**: 222–237.

Edwards A, Pachebat JA, Swain M, Hegarty M, Hodson AJ, Irvine-Fynn TDL, *et al.* (2013). A metagenomic snapshot of taxonomic and functional diversity in an alpine glacier cryoconite ecosystem. *Environ Res Lett* **8**: 035003.

Emmett MR, White FM, Hendrickson CL, Shi S, Marshall AG. (1998). Application of micro-electrospray liquid chromatography techniques to FT-ICR MS to enable high-sensitivity biological analysis. *J Am Soc Mass Spectrom* **9**: 333–340.

Farjalla VF, Marinho CC, Faria BM, Amado AM, Esteves F de A, Bozelli RL, *et al.* (2009). Synergy of fresh and accumulated organic matter to bacterial growth. *Microb Ecol* **57**: 657–666.

Fasching C, Behounek B, Singer GA, Battin TJ. (2014). Microbial degradation of terrigenous dissolved organic matter and potential consequences for carbon cycling in brown-water streams. *Sci Rep* **4**: 4981.

Fellman JB, Hood E, Spencer RGM. (2010). Fluorescence spectroscopy opens new windows into dissolved organic matter dynamics in freshwater ecosystems: A review. *Limnol Oceanogr* **55**: 2452–2462.

Findlay S, Sinsabaugh RL. (2003). Aquatic Ecosystems. Elsevier Science: San Diego.

Findlay S, Sinsabaugh RL. (1999). Unravelling the sources and bioavailability of dissolved organic matter in lotic aquatic ecosystems. *Mar Freshwater Res* **50**: 781–790.

Foreman CM, Cory RM, Morris CE, SanClements MD, Smith HJ, Lisle JT, *et al.* (2013). Microbial growth under humic-free conditions in a supraglacial stream system on the Cotton Glacier, Antarctica. *Environ Res Lett* **8**: 035022.

Foreman CM, Sattler B, Mikucki JA, Porazinska DL, Priscu JC. (2007). Metabolic activity and diversity of cryoconites in the Taylor Valley, Antarctica. *J Geophys Res* **112**: G04S32.

Foreman CM, Wolf CF, Priscu JC. (2004). Impact of Episodic Warming Events. *Aquat Geochem* **10**: 239–268.

Foster RA, Kuypers MMM, Vagner T, Paerl RW, Musat N, Zehr JP. (2011). Nitrogen fixation and transfer in open ocean diatom–cyanobacterial symbioses. *ISME J* **5**: 1484–1493.

Fountain AG, Nylen TH, Monaghan A, Basagic HJ, Bromwich D. (2010). Snow in the McMurdo Dry Valleys, Antarctica. *International Journal of Climatology* **30**: 633–642.

Fountain AG, Nylen TH, Tranter M, Bagshaw E. (2008). Temporal variations in physical

and chemical features of cryoconite holes on Canada Glacier, McMurdo Dry Valleys, Antarctica. *J Geophys Res* **113**: G01S92.

Fountain AG, Tranter M, Nylen TH, Lewis KJ, Mueller DR. (2004). Evolution of cryoconite holes and their contribution to meltwater runoff from glaciers in the McMurdo Dry Valleys, Antarctica. *Journal of Glaciology* **50**: 35–45.

Ghiglione J-F, Galand PE, Pommier T, Pedrós-Alió C, Maas EW, Bakker K, *et al.* (2012). Pole-to-pole biogeography of surface and deep marine bacterial communities. *Proc Natl Acad Sci USA* **109**: 17633–17638.

Gowda H, Ivanisevic J, Johnson CH, Kurczy ME, Benton HP, Rinehart D, *et al.* (2014). Interactive XCMS Online: Simplifying Advanced Metabolomic Data Processing and Subsequent Statistical Analyses. *Anal Chem* **86**: 6931–6939.

Gruber DF, Simjouw J-P, Seitzinger SP, Taghon GL. (2006). Dynamics and characterization of refractory dissolved organic matter produced by a pure bacterial culture in an experimental predator-prey system. *Appl Environ Microbiol* **72**: 4184–4191.

Guillemette F, del Giorgio PA. (2011). Reconstructing the various facets of dissolved organic carbon bioavailability in freshwater ecosystems. *Limnol Oceanogr* **56**: 734–748.

Gunnigle E, Ramond J-B, Guerrero LD, Makhalanyane TP, Cowan DA, Lund DP. (2015). Draft genomic DNA sequence of the multi-resistant Sphingomonas sp. strain AntH11 isolated from an Antarctic hypolith Lund, DP (ed). *FEMS Microbiology Letters* **362**.

Haas BJ, Gevers D, Earl AM, Feldgarden M, Ward DV, Giannoukos G, *et al.* (2011). Chimeric 16S rRNA sequence formation and detection in Sanger and 454-pyrosequenced PCR amplicons. *Genome Res* **21**: 494–504.

Hall-Stoodley L, Costerton JW, Stoodley P. (2004). Bacterial biofilms: from the natural environment to infectious diseases. *Nat Rev Microbiol* **2**: 95–108.

Hansell DA, Carlson CA. (2014). Biogeochemistry of Marine Dissolved Organic Matter. Academic Press.

Hartley, Hopkins, Sommerkorn, Wookey. (2010). The response of organic matter mineralisation to nutrient and substrate additions in sub-arctic soils. *Soil Biology and Biochemistry* **42**: 9–9.

Hell K, Edwards A, Zarsky J, Podmirseg SM, Girdwood S, Pachebat JA, *et al.* (2013). The dynamic bacterial communities of a melting High Arctic glacier snowpack. *ISME J* **7**: 1814–1826.

Hodgson DA, Convey P, Verleyen E, Vyverman W, McInnes SJ, Sands CJ, *et al.* (2010).

The limnology and biology of the Dufek Massif, Transantarctic Mountains 82° South. *Polar Science* **4**: 197–214.

Hodson A, Anesio AM, Ng F, Watson R, Quirk J, Irvine-Fynn T, Dye A, Clark C, McCloy P, Kohler J, Sattler B. (2007a). A glacier respires: Quantifying the distribution and respiration CO 2flux of cryoconite across an entire Arctic supraglacial ecosystem. *J Geophys Res* **112**: G04S36.

Hodson A, Anesio AM, Ng F, Watson R, Quirk J, Irvine-Fynn T, Dye A, Clark C, McCloy P, Kohler J, Sattler B. (2007b). A glacier respires: Quantifying the distribution and respiration CO 2flux of cryoconite across an entire Arctic supraglacial ecosystem. *J Geophys Res* **112**: G04S36.

Hodson A, Anesio AM, Tranter M, Fountain A, Osborn M, Priscu J, *et al.* (2008). Glacial Ecosystems LACIAL ECOSYSTEMS. *Ecological Monographs* **78**: 41–67.

Hodson A, Ben Brock, Pearce D, Laybourn-Parry J, Tranter M. (2015). Cryospheric ecosystems: a synthesis of snowpack and glacial research. *Environ Res Lett* **10**: 110201.

Hodson A, Bøggild C, Hanna E, Huybrechts P, Langford H, Cameron K, *et al.* (2010). The cryoconite ecosystem on the Greenland ice sheet. *Annals of Glaciology* **51**: 123–129.

Hood E, Battin TJ, Fellman J, O'Neel S, Spencer RGM. (2015). Storage and release of organic carbon from glaciers and ice sheets. *Nature Geoscience* **8**: 91–96.

Hood E, Fellman J, Spencer RGM, Hernes PJ, Edwards R, D'Amore D, *et al.* (2009). Glaciers as a source of ancient and labile organic matter to the marine environment. *Nature* **462**: 1044–1047.

Hooper DU, Chapin FS III, Ewel JJ, Hector A, Inchausti P, Lavorel S, *et al.* (2008). Effects of Biodiversity on Ecosystem Functioning: A Consensus of Current Knowledge .

Huber T, Faulkner G, Hugenholtz P. (2004). Bellerophon: a program to detect chimeric sequences in multiple sequence alignments. *Bioinformatics* **20**: 2317–2319.

Hutchinson GE. (1957). Cold spring harbor symposium on quantitative biology. Concluding remarks.

Irvine-Fynn TDL, Edwards A, Newton S, Langford H, Rassner SM, Telling J, *et al.* (2012). Microbial cell budgets of an Arctic glacier surface quantified using flow cytometry. *Environ Microbiol* **14**: 2998–3012.

Jackson GA. (1987). Simulating chemosensory responses of marine microorganisms. *Limnol Oceanogr* **32**: 1253–1266.

Jiao N, Azam F, Sanders S (eds). (2013). Microbial Carbon Pump in the Ocean.

American Association for the Advancement of Science: Washington, DC.

Jiao N, Herndl GJ, Hansell DA, Benner R, Kattner G, Wilhelm SW, *et al.* (2010). Microbial production of recalcitrant dissolved organic matter: long-term carbon storage in the global ocean. *Nat Rev Microbiol* **8**: 593–599.

Judd KE, Crump BC, Kling GW. (2006). Variation in dissolved organic matter controls bacterial production and community composition. *Ecology* **87**: 2068–2079.

Jørgensen L, Lechtenfeld O, Benner R, Middelboe M, Stedmon CA. (2014). Bacterial production and transformation of dissolved neutral sugars and amino acids in seawater. *Biogeosciences Discuss* **11**: 6151–6184.

Karlstrom L, Gajjar P, Manga M. (2013). Meander formation in supraglacial streams. *Journal of Geophysical Research: Earth Surface* **118**: 1897–1907.

Kawasaki N, Benner R. (2006). Bacterial release of dissolved organic matter during cell growth and decline: Molecular origin and composition. *Limnol Oceanogr* **51**: 2170–2180.

Keskitalo J, Leppäranta M, Arvola L. (2013a). First records of primary producers of epiglacial and supraglacial lakes in western Dronning Maud Land, Antarctica. *Polar Biol* **36**: 1441–1450.

Keskitalo J, Leppäranta M, Arvola L. (2013b). First records of primary producers of epiglacial and supraglacial lakes in western Dronning Maud Land, Antarctica. *Polar Biol* **36**: 1441–1450.

Kim S, Kramer RW, Hatcher PG. (2003). Graphical method for analysis of ultrahigh-resolution broadband mass spectra of natural organic matter, the van Krevelen diagram. *Anal Chem* **75**: 5336–5344.

Kirchman D, K'nees E, Hodson R. (1985). Leucine incorporation and its potential as a measure of protein synthesis by bacteria in natural aquatic systems. *Appl Environ Microbiol* **49**: 599–607.

Kirchman DL, Malmstrom RR, Cottrell MT. (2005). Control of bacterial growth by temperature and organic matter in the Western Arctic. *Deep Sea Research Part II: Topical Studies in Oceanography* **52**: 3386–3395.

Knighton AD. (1981). Channel Form and Flow Characteristics of Supraglacial Streams, Austre Okstindbreen, Norway. *Arctic and Alpine Research* **13**: 295.

Koch BP, Dittmar T. (2006). From mass to structure: an aromaticity index for high-resolution mass data of natural organic matter. *Rapid Commun Mass Spectrom* **20**: 926–932.

Koch BP, Ludwichowski K-U, Kattner G, Dittmar T, Witt M. (2008). Advanced characterization of marine dissolved organic matter by combining reversed-phase liquid chromatography and FT-ICR-MS. **111**: 233–241.

Kohler TJ, Stanish LF, Crisp SW, Koch JC, Liptzin D, Baeseman JL, *et al.* (2015). Life in the Main Channel: Long-Term Hydrologic Control of Microbial Mat Abundance in McMurdo Dry Valley Streams, Antarctica. *Ecosystems* **18**: 310–327.

Kristensen E. (1990). Characterization of biogenic organic matter by stepwise thermogravimetry (STG) - Springer. *Biogeochemistry* **9**: 135–159.

Kuipers Munneke P, Picard G, Broeke den MR, Lenaerts JTM, Meijgaard E. (2012). Insignificant change in Antarctic snowmelt volume since 1979. *Scientific Investigations Report* **39**: n/a–n/a.

Kujawinski EB. (2011). The Impact of Microbial Metabolism on Marine Dissolved Organic Matter. *Ann Rev Mar Sci* **3**: 567–599.

Langford H, Hodson A, Banwart S, Bøggild C. (2010). The microstructure and biogeochemistry of Arctic cryoconite granules. *Annals of Glaciology* **51**: 87–94.

Langille MGI, Zaneveld J, Caporaso JG, McDonald D, Knights D, Reyes JA, *et al.* (2013). Predictive functional profiling of microbial communities using 16S rRNA marker gene sequences. *Nat Biotechnol* **31**: 814–821.

Lanoil B, Skidmore M, Priscu JC, Han S, Foo W, Vogel SW, *et al.* (2009). Bacteria beneath the West Antarctic ice sheet. *Environ Microbiol* **11**: 609–615.

Lawaetz AJ, Stedmon CA. (2009). Fluorescence intensity calibration using the Raman scatter peak of water. *Appl Spectrosc* **63**: 936–940.

Lawson EC, Wadham JL. (2013). Greenland Ice Sheet exports labile organic carbon to the Arctic oceans. *Biogeosciences* **10**: 19311–19345.

Laybourn-Parry J, Tranter M, Hodson A (eds). (2012). The Ecology of Snow and Ice Environments.

Lechtenfeld OJ, Hertkorn N, Shen Y, Witt M, Benner R. (2015). Marine sequestration of carbon in bacterial metabolites. *Nat Commun* **6**: 6711.

Li F, Ginoux P, Ramaswamy V. (2008). Distribution, transport, and deposition of mineral dust in the Southern Ocean and Antarctica: Contribution of major sources. *Journal of Geophysical Research: Atmospheres* **113**.

Li W-T, Xu Z-X, Li A-M, Wu W, Zhou Q, Wang J-N. (2013). HPLC/HPSEC-FLD with multi-excitation/emission scan for EEM interpretation and dissolved organic matter

analysis. *Water Research* **47**: 1246–1256.

Logue JB, Stedmon CA, Kellerman AM, Nielsen NJ, Andersson AF, Laudon H, *et al.* (2015). Experimental insights into the importance of aquatic bacterial community composition to the degradation of dissolved organic matter. *ISME J*.

Lutz S, Anesio AM, Villar SEJ, Benning LG. (2014). Variations of algal communities cause darkening of a Greenland glacier. *FEMS Microbiol Ecol* **89**: 402–414.

Margesin R, Miteva V. (2011). Diversity and ecology of psychrophilic microorganisms. *Research in Microbiology* **162**: 346–361.

Margesin R, Schinner F, Marx JC, Gerday C. (2007). Psychrophiles: From Biodiversity to Biotechnology.

McCarren J, Becker JW, Repeta DJ, Shi Y, Young CR, Malmstrom RR, *et al.* (2010). Microbial community transcriptomes reveal microbes and metabolic pathways associated with dissolved organic matter turnover in the sea. *Proc Natl Acad Sci USA* **107**: 16420–16427.

McIntyre NF. (2011). Cryoconite hole thermodynamics. *Canadian Journal of Earth Sciences* **21**: 152–156.

McKnight DM, Boyer EW, Westerhoff PK. (2001). Spectrofluorometric characterization of dissolved organic matter for indication of precursor organic material and aromaticity. *Limnol and Oceanogr* **46**: 38–48.

McKnight DM, Tate CM. (1997). Canada Stream: A Glacial Meltwater Stream in Taylor Valley, South Victoria Land, Antarctica. *Journal of the North American Benthological Society* **16**: 14.

Mernild SH, Liston GE. (2012). Surface melt extent for the Greenland Ice Sheet, 2011. *Geografisk Tidsskrift-Danish Journal of Geography* **112**: 84–88.

Mikucki JA, Pearson A, Johnston DT, Turchyn AV, Farquhar J, Schrag DP, *et al.* (2009). A contemporary microbially maintained subglacial ferrous "ocean". *Science* **324**: 397–400.

Miller MP, McKnight DM. (2010). Comparison of seasonal changes in fluorescent dissolved organic matter among aquatic lake and stream sites in the Green Lakes Valley. *Journal of Geophysical Research: Biogeosciences (2005–2012)* **115**: G00F12.

Mopper K, Stubbins A, Ritchie JD, Bialk HM, Hatcher PG. (2007). Advanced instrumental approaches for characterization of marine dissolved organic matter: extraction techniques, mass spectrometry, and nuclear magnetic resonance spectroscopy. *Chem Rev* **107**: 419–442.

Mou X, Sun S, Edwards RA, Hodson RE, Moran MA. (2008). Bacterial carbon processing by generalist species in the coastal ocean. *Nature* **451**: 708–711.

Muggeo V. (2008). Segmented: An R Package to Fit Regression Models with Broken-LineRelationships. *R News* **8**: 20–25.

Mullin MM, Sloan PR, Eppley RW. (1966). Relationship Between Carbon Content, Cell Volume, and Area in Phytoplankton. *Limnol Oceanogr* **11**: 307–311.

Musat N, Halm H, Winterholler B, Hoppe P, Peduzzi S, Hillion F, *et al.* (2008). A single-cell view on the ecophysiology of anaerobic phototrophic bacteria. *Proc Natl Acad Sci USA* **105**: 17861–17866.

Musat N, Stryhanyuk H, Bombach P, Adrian L, Audinot J-N, Richnow HH. (2014). The effect of FISH and CARD-FISH on the isotopic composition of ^{13}C- and ^{15}N-labeled Pseudomonas putida cells measured by nanoSIMS. *Systematic and Applied Microbiology* 1–10.

Musilova M, Tranter M, Bennett SA, Wadham J, Anesio AM. (2015). Stable microbial community composition on the Greenland Ice Sheet. *Front Microbiol* **6**: 193.

Namsaraev Z, Mano MJ, Fernandez R, Wilmotte A. (2010). Biogeography of terrestrial cyanobacteria from Antarctic ice-free areas. *Annals of Glaciology* **51**: 171–177.

Nelson CE, Carlson CA. (2012). Tracking differential incorporation of dissolved organic carbon types among diverse lineages of Sargasso Sea bacterioplankton. *Environ Microbiol* **14**: 1500–1516.

Nelson CE, Wear EK. (2014). Microbial diversity and the lability of dissolved organic carbon. *Proc Natl Acad Sci USA* **111**: 7166–7167.

Nemergut DR, Costello EK, Hamady M, Lozupone C, Jiang L, Schmidt SK, *et al.* (2011). Global patterns in the biogeography of bacterial taxa. *Environ Microbiol* **13**: 135–144.

Nguyen NH, Smith D, Peay K, Kennedy P. (2015). Parsing ecological signal from noise in next generation amplicon sequencing. *New Phytol* **205**: 1389–1393.

Nikrad MP, Cottrell MT, Kirchman DL. (2012). Abundance and single-cell activity of heterotrophic bacterial groups in the western Arctic Ocean in summer and winter. *Appl Environ Microbiol* **78**: 2402–2409.

Nordenskjöld NE. (1875). Cryoconite found 1870, July 19th-25th, on the inland ice, east of Auleitsivik Fjord, Disco Bay, Greenland. *Geological Magazine* **2**: 157–162.

Ogawa H, Amagai Y, Koike I, Kaiser K, Benner R. (2001). Production of refractory dissolved organic matter by bacteria. *Science* **292**: 917–920.

Osterholz H, Singer G, Wemheuer B, Daniel R, Simon M, Niggemann J, *et al.* (2016). Deciphering associations between dissolved organic molecules and bacterial communities in a pelagic marine system. *ISME J*.

Paterson, W. S. B. (1996). The Physics of Glaciers 3rd edition. *Hydrological Sciences Journal-Journal des Sciences Hydrologiques*, **41**: 272-272.

Patti GJ, Tautenhahn R, Siuzdak G. (2012). Meta-analysis of untargeted metabolomic data from multiple profiling experiments. *Nat Protoc* **7**: 508–516.

Pautler BG, Dubnick A, Sharp MJ, Simpson AJ. (2013). Comparison of cryoconite organic matter composition from Arctic and Antarctic glaciers at the molecular-level. ... *et Cosmochimica Acta* **104**: 1–18.

Pautler BG, Simpson AJ, Simpson MJ, Tseng L-H, Spraul M, Dubnick A, *et al.* (2011). Detection and structural identification of dissolved organic matter in Antarctic glacial ice at natural abundance by SPR-W5-WATERGATE 1H NMR spectroscopy. *Environ Sci Technol* **45**: 4710–4717.

Pautler BG, Woods GC, Dubnick A, Simpson AJ, Sharp MJ, Fitzsimons SJ, *et al.* (2012). Molecular characterization of dissolved organic matter in glacial ice: coupling natural abundance 1H NMR and fluorescence spectroscopy. *Environ Sci Technol* **46**: 3753–3761.

Peat HJ, Clarke A, Convey P. (2007). Diversity and biogeography of the Antarctic flora. *Journal of Biogeography* **34**: 132–146.

Pedler BE, Aluwihare LI, Azam F. (2014). Single bacterial strain capable of significant contribution to carbon cycling in the surface ocean. *Proc Natl Acad Sci USA* **111**: 7202–7207.

Pernthaler A, Pernthaler J, Amann R. (2002). Fluorescence in situ hybridization and catalyzed reporter deposition for the identification of marine bacteria. *Appl Environ Microbiol* **68**: 3094–3101.

Pernthaler A, Pernthaler J, Amann R, Kowalchuk GA, Bruijn FJ de, Head IM, *et al.* (2004). Sensitive multi-color fluorescence in situ hybridization for the identification of environmental microorganisms. Kluwer Academic Publishers.

Pinheiro J, Bates D, DebRoy S, Sarkar D. (2007). Linear and nonlinear mixed effects models. *R package version*, *3* **57**.

Pinheiro JC. (2000). Mixed-Effects Models in S and S-PLUS, José C. Pinheiro and Douglas M. Bates. *Statistics and Computing Series. Springer-Verlag, New York, NY*.

Polerecky L, Adam B, Milucka J, Musat N, Vagner T, Kuypers MMM. (2012). Look@NanoSIMS--a tool for the analysis of nanoSIMS data in environmental microbiology. *Environ Microbiol* **14**: 1009–1023.

Porazinska DL, Fountain AG, Nylen TH, Tranter M, Virginia RA, Wall DH. (2004). The Biodiversity and Biogeochemistry of Cryoconite Holes from McMurdo Dry Valley Glaciers, Antarctica. *Arctic, Antarctic, and Alpine Research* **36**: 84–91.

Priscu JC, Adams EE, Lyons WB, Voytek MA, Mogk DW, Brown RL, *et al.* (1999). Geomicrobiology of subglacial ice above Lake Vostok, Antarctica. *Science* **286**: 2141–2144.

Priscu JC, Christner BC. (2004). Earth's icy biosphere. *Microbial Diversity and Prospecting*.

Priscu JC, Tulaczyk S, Studinger M, Christner BC, Foreman CM. (2008). Antarctic subglacial water: origin, evolution and ecology. Polar lakes and rivers.

Priscu JC, Wolf CF. (2000). Priscu: Limnological methods for the McMurdo Dry Valleys Long Term Ecological Research Program. (www.mcmlter.org/data/lakes/MCM Limno Methods.pdf).

Priscu JC, Wolf CF, Takacs CD, Fritsen CH, Laybourn-Parry J, Roberts EC, *et al.* (1999). Carbon Transformations in a Perennially Ice-Covered Antarctic Lake. *BioScience* **49**: 997–1008.

Prosser JI. (2010). Replicate or lie. *Environ Microbiol* **12**: 1806–1810.

Reitner B, Herndl GJ, Herzig A. (1997). Role of ultraviolet-B radiation on photochemical and microbial oxygen consumption in a humic-rich shallow lake. *Limnol Oceanogr* **42**: 950–960.

Rennermalm AK, Moustafa SE, Mioduszewski J, Chu VW, Forster RR, Hagedorn B, *et al.* (2013). Understanding Greenland ice sheet hydrology using an integrated multi-scale approach. *Environ Res Lett* **8**: 015017.

Rothlisberger H, Lang H. (1987). Glacial hydrology. Glacio-Fluvial Sediment Transfer: An Alpine Perspective. *John Wiley and Sons*, New York New York 207-284.

Rousk J, Hill PW, Jones DL. (2014). Using the concentration-dependence of respiration arising from glucose addition to estimate in situ concentrations of labile carbon in grassland soil. *Soil Biology and Biochemistry* **77**: 81–88.

Salter SJ, Cox MJ, Turek EM, Calus ST, Cookson WO, Moffatt MF, *et al.* (2014). Reagent and laboratory contamination can critically impact sequence-based microbiome analyses. *BMC Biology* **12**: 87.

M. D. SanClements, H. J. Smith, D. M. McKnight, C. M. Foreman, and M. Tedesco. Characterizing the functioning of a supraglacial ecosystem: The Cotton Glacier Stream. Submitted: Arctic Antarctic and Alpine research

Santl-Temkiv T, Finster K, Dittmar T, Hansen BM, Thyrhaug R, Nielsen NW, *et al.* (2013). Hailstones: A Window into the Microbial and Chemical Inventory of a Storm Cloud. *PLoS ONE* **8**. doi:10.1371/journal.pone.0053550.

Säwström C, Anesio MA, Granéli W, Laybourn-Parry J. (2007). Seasonal viral loop dynamics in two large ultraoligotrophic Antarctic freshwater lakes. *Microb Ecol* **53**: 1–11.

Säwström C, Lisle J, Anesio AM, Priscu JC, Laybourn-Parry J. (2008). Bacteriophage in polar inland waters. *Extremophiles* **12**: 167–175.

Schloss PD, Gevers D, Westcott SL. (2011). Reducing the effects of PCR amplification and sequencing artifacts on 16S rRNA-based studies. *PLoS ONE* **6**: e27310.

Schloss PD, Westcott SL, Ryabin T, Hall JR, Hartmann M, Hollister EB, *et al.* (2009). Introducing mothur: open-source, platform-independent, community-supported software for describing and comparing microbial communities. *Appl Environ Microbiol* **75**: 7537–7541.

Scott D, Hood E, Nassry M. (2010). In-stream uptake and retention of C, N and P in a supraglacial stream. *Annals of Glaciology* **51**: 80–86.

Simon C, Wiezer A, Strittmatter AW, Daniel R. (2009). Phylogenetic diversity and metabolic potential revealed in a glacier ice metagenome. *Appl Environ Microbiol* **75**: 7519–7526.

Simpson EH. (1949). Measurement of diversity. *Nature* **163**: 688–688.

Singer GA, Fasching C, Wilhelm L, Niggemann J, Steier P, Dittmar T, Battin TJ. (2012). Biogeochemically diverse organic matter in Alpine glaciers and its downstream fate. *Nature Geoscience* **5**: 710–714.

Smith CA, Want EJ, O'Maille G, Abagyan R, Siuzdak G. (2006). XCMS: processing mass spectrometry data for metabolite profiling using nonlinear peak alignment, matching, and identification. *Anal Chem* **78**: 779–787.

Smith H, Akiyama T, Foreman C, Franklin M, Woyke T, Teshima H, Davenport K, Daligault H, Erkkila T, Goodwin L, Gu W, Xu Y, Chain P. (2013). Draft Genome Sequence and Description of Janthinobacterium sp. Strain CG3, a Psychrotolerant Antarctic Supraglacial Stream Bacterium. *Genome Announc* **1**: e00960–13.

Smith HJ, Foreman CM, Ramaraj T. (2014). Draft Genome Sequence of a Metabolically

Diverse Antarctic Supraglacial Stream Organism, Polaromonas sp. Strain CG9_12, Determined Using Pacific Biosciences Single-Molecule Real-Time Sequencing Technology. *Genome Announc* **2**.

Smith LC, Chu VW, Yang K, Gleason CJ, Pitcher LH, Rennermalm AK, *et al.* (2015). Efficient meltwater drainage through supraglacial streams and rivers on the southwest Greenland ice sheet. *Proc Natl Acad Sci USA* **112**: 1001–1006.

Smith, H., Foster, R., J. Lisle, M.M. Kuypers, and C.M. Foreman. Microbial formation of labile glacial organic carbon. In Prep: Nature Geosciences Letters.

Sogin ML, Morrison HG, Huber JA, Mark Welch D, Huse SM, Neal PR, *et al.* (2006). Microbial diversity in the deep sea and the underexplored "rare biosphere". *Proc Natl Acad Sci USA* **103**: 12115–12120.

Spencer RGM, Vermilyea A, Fellman J, Raymond P, Stubbins A, Scott D, *et al.* (2014). Seasonal variability of organic matter composition in an Alaskan glacier outflow: insights into glacier carbon sources. *Environ Res Lett* **9**: 055005.

Staley JT, Gosink JJ. (1999). Poles Apart: Biodiversity and Biogeography of Sea Ice Bacteria. *Annual Reviews in Microbiology* **53**: 189–215.

Stedmon CA, Bro R. (2008). Characterizing dissolved organic matter fluorescence with parallel factor analysis: a tutorial. *Limnol Oceanogr Methods* 572–579.

Stedmon CA, Markager S, Bro R. (2003). Tracing dissolved organic matter in aquatic environments using a new approach to fluorescence spectroscopy. **82**: 239–254.

Stenson AC. (2008). Reversed-phase chromatography fractionation tailored to mass spectral characterization of humic substances. *Environ Sci Technol* **42**: 2060–2065.

Stibal M, Lawson EC, Lis GP, Mak KM, Wadham JL, Anesio AM. (2010). Organic matter content and quality in supraglacial debris across the ablation zone of the Greenland ice sheet. *Annals of Glaciology* **51**: 1–8.

Stibal M, Sabacka M, Zarsky J. (2012). Biological processes on glacier and ice sheet surfaces. *Nature Geoscience* **5**: 771–774.

Stibal M, Schostag M, Cameron KA, Hansen LH, Chandler DM, Wadham JL, *et al.* (2015). Different bulk and active bacterial communities in cryoconite from the margin and interior of the Greenland ice sheet. *Environ Microbiol Rep* **7**: 293–300.

Stibal M, Tranter M. (2007). Laboratory investigation of inorganic carbon uptake by cryoconite debris from Werenskioldbreen, Svalbard. *Journal of Geophysical Research: Biogeosciences (2005–2012)* **112**.

Stibal M, Tranter M, Benning LG. (2008). Microbial primary production on an Arctic glacier is insignificant in comparison with allochthonous organic carbon input. *Environmental Microbiology* **10**: 2172–2178.

Stocker R. (2015). The 100 μm length scale in the microbial ocean. *Aquat Microb Ecol* **76**: 189–194.

Stubbins A, Hood E, Raymond PA, Aiken GR, Sleighter RL, Hernes PJ, *et al.* (2012). Anthropogenic aerosols as a source of ancient dissolved organic matter in glaciers. *Nature Geoscience* **5**: 198–201.

Sun J. (2003). Geometric models for calculating cell biovolume and surface area for phytoplankton. *Journal of Plankton Research* **25**: 1331–1346.

Suttle CA. (2007). Marine viruses - major players in the global ecosystem. *Nat Rev Microbiol* **5**: 801–812.

Suzuki R, Shimodaira H. (2013). Hierarchical clustering with P-values via multiscale bootstrap resampling. *R package*.

Šabacká M, Priscu JC, Basagic HJ, Fountain AG. (2012). Aeolian flux of biotic and abiotic material in Taylor Valley, Antarctica. *Geomorphology*.

Takacs CD, Priscu JC, McKnight DM. (2001). Bacterial dissolved organic carbon demand in McMurdo Dry Valley lakes, Antarctica. *Limnol Oceanogr* **46**: 1189–1194.

Takeuchi N, Kohshima S, Seko K. (2001). JSTOR: Arctic, Antarctic, and Alpine Research, Vol. 33, No. 2 (May, 2001), pp. 115-122. *Arctic*.

Tautenhahn R, Patti GJ, Kalisiak E, Miyamoto T, Schmidt M, Lo FY, *et al.* (2011). metaXCMS: Second-Order Analysis of Untargeted Metabolomics Data. *Anal Chem* **83**: 696–700.

Tautenhahn R, Patti GJ, Rinehart D, Siuzdak G. (2012). XCMS Online: A Web-Based Platform to Process Untargeted Metabolomic Data. *Anal Chem* **84**: 5035–5039.

Team, R. C. (2014). R: A language and environment for statistical computing. Vienna, Austria: R Foundation for Statistical Computing; 2013.

Tedesco M, Foreman CM, Anton J, Steiner N, Schwartzman T. (2013). Comparative analysis of morphological, mineralogical and spectral properties of cryoconite in Jakobshavn Isbrae, Greenland, and Canada Glacier, Antarctica. *Annals of Glaciology* **54**: 147–157.

Tedesco M, Willis IC, Hoffman MJ, Banwell AF, Alexander P, Arnold NS. (2013). Ice dynamic response to two modes of surface lake drainage on the Greenland ice sheet. *Environ Res Lett* **8**: 034007.

Teira E, Pazó MJ, Serret P. (2001). Dissolved organic carbon production by microbial

populations in the Atlantic Ocean - Teira - 2001 - Limnology and Oceanography - Wiley Online Library. *Limnology and Oceanogr* **46**: 1370–1377.

Telling J, Anesio AM, Tranter M, Fountain AG, Nylen T, Hawkings J, *et al.* (2014). Spring thaw ionic pulses boost nutrient availability and microbial growth in entombed Antarctic Dry Valley cryoconite holes. *Front Microbiol* **5**: 694–694.

Telling J, Anesio AM, Tranter M, Stibal M, Hawkings J, Irvine-Fynn T, *et al.* (2012). Controls on the autochthonous production and respiration of organic matter in cryoconite holes on high Arctic glaciers. *J Geophys Res* **117**: G01017.

Vahatalo AV, Aarnos H, Mantyniemi S. (2010). Biodegradability continuum and biodegradation kinetics of natural organic matter described by the beta distribution. *Biogeochemistry* **100**: 227–240.

Van den Meersche K, Middelburg JJ. (2004). Carbon-nitrogen coupling and algal-bacterial interactions during an experimental bloom: Modeling a 13C tracer experiment - Van den Meersche - 2004 - Limnology and Oceanography - Wiley Online Library. *Limnology and Oceanogr* **49**: 862–878.

Van Horn DJ, Van Horn ML, Barrett JE, Gooseff MN, Altrichter AE, Geyer KM, *et al.* (2013). Factors Controlling Soil Microbial Biomass and Bacterial Diversity and Community Composition in a Cold Desert Ecosystem: Role of Geographic Scale. *PLoS ONE* **8**: e66103.

Verity PG, Robertson CY, Tronzo CR, Andrews MG, Nelson JR, Sieracki ME. (1992). Relationships between cell volume and the carbon and nitrogen content of marine photosynthetic nanoplankton. *Limnol Oceanogr* **37**: 1434–1446.

Vick TJ, Priscu JC. (2012). Bacterioplankton productivity in lakes of the Taylor Valley, Antarctica, during the polar night transition. *Aquat Microb Ecol* **68**: 77–90.

Wagner M. (2009). Single-Cell Ecophysiology of Microbes as Revealed by Raman Microspectroscopy or Secondary Ion Mass Spectrometry Imaging.

Walter E Dean Jr. (1974). Determination of Carbonate and Organic Matter in Calcareous Sediments and Sedimentary Rocks by Loss on Ignition: Comparison With Other Methods. *SEPM JSR* **Vol. 44**: 242–248.

Wang Q, Garrity GM, Tiedje JM, Cole JR. (2007). Naive Bayesian classifier for rapid assignment of rRNA sequences into the new bacterial taxonomy. *Appl Environ Microbiol* **73**: 5261–5267.

Want EJ, Cravatt BF, Siuzdak G. (2005). The expanding role of mass spectrometry in metabolite profiling and characterization. *Chembiochem* **6**: 1941–1951.

Warnes G, Bolker B, Bonebakker L, Gentleman R, Huber W, Liaw A, *et al.* (2015). gplots: Various R Programming Tools for Plotting Data. *R Package*.

Wetzel R. (2003). Dissolved organic carbon: Detrital energetics, metabolic regulators, and drivers of ecosystem stability of aquatic ecosystems. In: *Aquatic ecosystems: Interactivity of dissolved organic matter*, Findlay, S & Sinsabaugh, RL (eds), Elsevier Science, pp 455–477.

Wetzel R. (2001). Limnology. Third. Elsevier: San Diego.

Wharton RA Jr., Vinyard WC, Parker BC, Simmons GM Jr., Seaburg KG. (1981). Algae in cryoconite holes on Canada Glacier in Southern Victorialand, Antarctica. *Phycologia* **20**: 208–211.

Wigington CH, Sonderegger D, Brussaard CPD, Buchan A, Finke J, Fuhrman J, *et al.* (2016). Re-examination of the relationship between marine virus and microbial cell abundances. *Nature*.

Wilhelm L, Singer GA, Fasching C, Battin TJ, Besemer K. (2013). Microbial biodiversity in glacier-fed streams. *ISME J*. doi:10.1038/ismej.2013.44.

Wilhelm SW, Suttle CA. (1999). Viruses and Nutrient Cycles in the Sea Viruses play critical roles in the structure and function of aquatic food webs. *BioScience* **49**: 781–788.

Wilkins D, Yau S, Williams TJ, Allen MA, Brown MV, DeMaere MZ, *et al.* (2012). Key microbial drivers in Antarctic aquatic environments. *FEMS Microbiol Rev* **37**: 303–335.

Wu FC, Evans RD, Dillon PJ. (2003). Separation and Characterization of NOM by High-Performance Liquid Chromatography and On-Line Three-Dimensional Excitation Emission Matrix Fluorescence Detection. *Environ Sci Technol* **37**: 3687–3693.

Zweifel UL. (1999). Factors Controlling Accumulation of Labile Dissolved Organic Carbon in the Gulf of Riga. *Estuarine, Coastal and Shelf Science* **48**: 357–370.

APPENDICES

APPENDIX A

GENOME SEQUENCE OF JANTHINOBACTERIUM SP. CG23_2, A VIOLACEIN PRODUCING ISOLATE FROM AN ANTARCTIC SUPRAGLACIAL STREAM

Contribution of Authors and Co-Authors

Author: Heidi J Smith

Contributions: Isolation, DNA extraction, data analysis, and manuscript preparation

Co-Author: Christine M. Foreman

Contributions: Principal investigator of laboratory experiments and genome analysis, manuscript preparation and editing

Co-Author: Tatsuya Akiyama

Contributions: Data analysis

Co-Author: Michael J. Franklin

Contributions: Data analysis, manuscript editing

Co-Author: Nicolas P. Devitt

Contributions: Data analysis

Co-Author: Thiruvarangan Ramaraj

Contributions: Sequencing, data analysis, manuscript preparation

Manuscript Information Page

Heidi J. Smith, Christine M. Foreman, Tatsuya Akiyama, Michael J. Franklin Nicolas P. Devitt, Thiruvarangan Ramaraj
Genome Announcements
Status of Manuscript:
____ Prepared for submission to a peer-reviewed journal
____ Officially submitted to a peer-review journal
____ Accepted by a peer-reviewed journal
__X_ Published in a peer-reviewed journal

Volume 4, Number 1, 2016, e01486-15, doi:10.1128/genomeA.01468-15.

Abstract

Here we present the draft genome sequence for the violacein-producing *Janthinobacterium* sp. CG23_2 isolated from an Antarctic supraglacial stream. The genome is ~7.85 Mb, with a G+C content of 63.5%. The genome includes 7,247 candidate protein coding genes, which may provide insight into UV tolerance mechanisms.

Organisms inhabiting Antarctic supraglacial environments are subjected to a variety of environmental stresses. Organisms inhabiting Antarctic supraglacial environments are subjected to a variety of environmental stresses. Ozone depletion over Antarctica has altered the spectral composition of solar radiation (Irgens *et al.*, 1996), and harmful UVC (100-280 nm) radiation is present on ice surfaces (Simon *et al.*, 2009; Michaud *et al.*, 2012; Clocksin *et al.*, 2007; Lanoil *et al.*, 2009; Wang *et al.*, 2014). Inescapable to microorganisms throughout the course of the austral summer, UV radiation damages biological macromolecules, including nucleic acids, lipids, and proteins and may lead to cell death. In order for microorganisms to inhabit environments with high UV radiation, efficient protective mechanisms and DNA and protein repair mechanisms are necessary. One mechanism for the protection from UV induced biological damage is for cells to produce protective pigments (Darcy *et al.*, 2011).

The purple pigment violacein is produced by certain members of the - Proteobacteria, including some *Janthinobacterium* strains. Violacein has been investigated for its antimicrobial (Jeon, 2004; Yagi *et al.*, 2009; Coleman *et al.*, 2002), antioxidant (Wang *et al.*, 2014), and UV protection properties (Mojib *et al.*, 2013). Although the exact mechanism of violacein protection against UV damage is currently

not well understood, evidence suggests that violacein can detoxify free radicals induced by UV radiation (Mojib *et al.*, 2013).

Janthinobacterium sp. are found in a many different environments, including lakes, soils, and glaciers(Kim *et al.*, 2012; Hornung *et al.*, 2013; Shoemaker *et al.*, 2015). We recently reported the genome sequence of a non-pigmented *Janthinobacterium* sp. isolated from a supraglacial stream. Here we present the genome sequence of a violacein producing strain *Janthinobacterium* sp. CG23_2, isolated from the same system in Antarctica. Genomic analyses of these strains will offer insight into UV tolerance mechanisms from environmentally relevant isolates.

Janthinobacterium sp. strain CG23_2 was isolated from the Cotton Glacier in the Antarctic Dry Valleys (77°07S, 161°50E). The organism was isolated on R2A agar medium incubated in the dark at 4° C for 12 days. *Janthinobacterium* sp. strain CG23_2 is a psychrotolerant, aerobic, violacein pigmented, rod shaped, gram negative, catalase positive organism. Genomic DNA was isolated following standard cetryltrim-ethylammonium bromide (CTAB) isolation protocols (http: //www.jgi.doe.gov).

Whole genome DNA sequencing was performed using a Pacific Biosciences (PacBio, Menlo Park, CA) RS II instrument (Korlach *et al.*, 2010). A SMRT cell library was constructed with 10μg input DNA using the PacBio 20-kbps protocol. The library was then loaded onto one single molecule real-time (SMRT) cell and sequenced using P5 polymerase and C3 chemistry with 180-minute movie times. Sequencing yielded a total of 99,287 reads with mean read length of 5.9 kbps, totaling 581,513,481 bps (≈85-fold coverage). *De novo* assembly was constructed using the hierarchical genome assembly

process (HGAP2) protocol from SMRT Analysis v2.0, including consensus polishing with Quiver (Chin *et al.*, 2013; Koren *et al.*, 2013). The final assembly consists of four contigs with a total genome size of ≈7.85 Mbps. Approximately 93% of the genome is contained within two large contigs (4.2 and 3.1 Mbps). Remaining sequences were divided into two smaller contigs ranging from 420 to 153 kbps. A total of 7,247 candidate protein- coding genes were predicted using RAST (Aziz *et al.*, 2008) with a total G+C content of 63.5%. Upon comparison with genomes available within the RAST the closest relative to *Janthinobacterium* sp. CG23_2 was determined to be *Janthinobacterium* sp. Marseille (score 542).

Nucleotide Sequence Accession Numbers

This genome sequence has been deposited in EMBL/GenBank under the accession no. CYSS00000000. The version described in this paper is the first version, CYSS00000000.

References

Aziz RK, Bartels D, Best AA, DeJongh M, Disz T. (2008). The RAST Server: Rapid Annotations using Subsystems Technology. *BMC Genomics* **9:**75.

Chin C-S, Alexander DH, Marks P, Klammer AA, Drake J, Heiner C, *et al.* (2013). Nonhybrid, finished microbial genome assemblies from long-read SMRT sequencing data. *Nat Meth* **10**: 563–569.

Dieser M, Greenwood M, Foreman CM. (2010). Carotenoid pigmentation in Antarctic heterotrophic bacteria as a strategy to withstand environmental stresses. *Arctic, Antarctic, and Alpine Research* **42:** 396-405.

Durán N, Menck CFM. (2001). Chromobacterium violaceum: A Review of Pharmacological and Industiral Perspectives. *Critical Reviews in Microbiology* **27**: 201–222.

Hornung C, Poehlein A, Haack FS, Schmidt M, Dierking K, Pohlen A, *et al.* (2013). The Janthinobacterium sp. HH01 genome encodes a homologue of the V. cholerae CqsA and L. pneumophila LqsA autoinducer synthases. *PLoS ONE* **8**: e55045.

Kim SJ, Shin SC, Hong SG, Lee YM, Lee H, Lee J, *et al.* (2012). Genome sequence of Janthinobacterium sp. strain PAMC 25724, isolated from alpine glacier cryoconite. *J Bacteriol* **194**: 2096.

Konzen M, De Marco D, Cordova CAS, Vieira TO, Antônio RV, Creczynski-Pasa TB. (2006). Antioxidant properties of violacein: Possible relation on its biological function. *Bioorganic & Medicinal Chemistry* **14**: 8307–8313.

Koren S, Harhay GP, Smith TP, Bono JL, Harhay DM, McVey SD, *et al.* (2013). Reducing assembly complexity of microbial genomes with single-molecule sequencing. *Genome Biol* **14**: R101.

Korlach J, Bjornson KP, Chaudhuri BP, Cicero RL, Flusberg BA, Gray JJ, *et al.* (2010). Real-Time DNA Sequencing from Single Polymerase Molecules. *Methods in Enzymology* **472:** 431–455.

Mojib N, Farhoomand A, Andersen DT, Bej AK. (2013). UV and cold tolerance of a pigment-producing Antarctic Janthinobacterium sp. Ant5-2. *Extremophiles* **17**: 367–378.

Nienow JA, McKay CP, Friedmann EI. (1988). The cryptoendolithic microbial environment in the Ross Desert of Antarctica: Light in the photosynthetically active region. *Microb Ecol* **16**: 271–289.

Shoemaker WR, Muscarella ME, Lennon JT. (2015). Genome Sequence of the Soil

Bacterium Janthinobacterium sp. KBS0711. *Genome Announc* **3**: e00689-15.

Staehelin J, Harris NRP, Appenzeller C, Eberhard J. (2001). Ozone trends: A review. *Reviews of Geophysics* **39**: 231–290.

APPENDIX B

DRAFT GENOME SEQUENCE OF A METABOLICALLY DIVERSE ANTARCTIC SUPRAGLACIAL STREAM ORGANISM: POLAROMONAS SP. STRAIN CG9_12 DETERMINED USING PACIFIC BIOSCIENCES SINGLE-MOLECULE REAL TIME (SMRT) SEQUENCING TECHNOLOGY

Contribution of Authors and Co-Authors

Author: Heidi J Smith

Contributions: Isolation, DNA extraction, data analysis, and manuscript preparation

Co-Author: Christine M. Foreman

Contributions: Principal investigator of laboratory experiments and genome analysis, manuscript preparation and editing

Co-Author: Thiruvarangan Ramaraj

Contributions: Sequencing, data analysis, manuscript preparation

Manuscript Information Page

Heidi J. Smith, Christine M. Foreman, Thiruvarangan Ramaraj
Genome Announcements
Status of Manuscript:
____ Prepared for submission to a peer-reviewed journal
____ Officially submitted to a peer-review journal
____ Accepted by a peer-reviewed journal
__X_ Published in a peer-reviewed journal

Volume 2, Number 6, 2014, e01242-14, doi:10.1128/genomeA.01242-14.

Abstract

Polaromonas species are found in a diversity of environments, and are particularly common in icy ecosystems. *Polaromonas sp.* Strain CG9_12 is an aerobic, gram negative, catalase positive, white-pigmented bacterium of the *Proteobacteria* phylum. Here we present the draft genome sequence of *Polaromonas sp.* Strain CG9_12 isolated from an Antarctic supraglacial stream.

Organisms from the genus *Polaromonas* are receiving increased attention due to their environmental ubiquity. The genus *Polaromonas* was originally proposed to describe marine, psychrophilic, Antarctic organisms (Irgens *et al.*, 1996), and *Polaromonas* sequences have been retrieved from a wide variety of icy environments (Simon *et al.*, 2009; Michaud *et al.*, 2012; Clocksin *et al.*, 2007; Lanoil *et al.*, 2009; Wang *et al.*, 2014). It is hypothesized that the widespread distribution of phylotypes could be due to the presence of genetic *hipA* machinery, which produces dormant cells (Darcy *et al.*, 2011). Organisms from the *Polaromonas* genus are also studied for their role in pollutant degradation. Currently, there are only five whole genomes publically available, four isolated from the sediment/groundwater environment (Jeon, 2004; Yagi *et al.*, 2009; Coleman *et al.*, 2002) and one from an Arctic Glacier (Wang *et al.*, 2014).

Recently, *Polaromonas* organisms were shown to be capable of utilizing a variety of energy sources from recalcitrant organic compounds (Jeon *et al.*, 2003) to arsenic (Osborne *et al.*, 2010), dichloroethane (Coleman *et al.*, 2002), and hydrogen (Sizova and Panikov, 2007). As a result of their metabolic diversity they have been described as having an opportunistic metabolism (Darcy *et al.*, 2011). Recent studies suggest that Polaromonads are widespread, but still there is relatively little known about their

metabolic strategies and environmental roles. To gain further insight into dispersal and metabolic strategies additional *Polaromonas* genomic sequences are necessary.

Polaromonas sp. Strain CG9_12 was isolated from a supraglacial stream on the Cotton Glacier, Antarctica (77°07'S, 161°50'E). The organism was isolated on R2A agar medium incubated in the dark at 4°C for twelve days. *Polaromonas sp.* Strain CG9_12 is a psychrotolerant, aerobic, rod shaped, gram negative, catalase positive, white-pigmented organism, which has *hipA* dormancy genes. Genomic DNA was isolated following standard CTAB isolation protocols (www.jgi.doe.gov).

Sequencing was performed on a Pacific Biosciences (PacBio, Menlo Park, CA) RSII instrument (Korlach *et al.*, 2010). A SMRTbell library was constructed with 5μg input DNA using the PacBio low-input 10k base pairs (bp) protocol. The library was then loaded onto two SMRT cells and sequenced using P4 polymerase and C2 chemistry with 180 minute movie times. Sequencing yielded a total of 281,150 reads with mean read length of 3.2kbp, totaling 900,510,276 bp (≈150X coverage). *De novo* assembly was carried out using the Hierarchical Genome Assembly Process (HGAP) protocol from SMRT Analysis v2.0, including consensus polishing with Quiver (Chin *et al.*, 2013; Koren *et al.*, 2013). The final assembly consists of seven contigs with a total genome size of ≈4.9Mbp. Approximately 91% of the genome is contained within one large 4.5Mbp contig. Remaining sequences were divided into six smaller contigs ranging from 19-183kbp. 4,975 candidate protein-coding genes were predicted with a total G + C content of 60.1%. The small-subunit rRNA gene sequences had 99% sequence identity to *Polaromonas glacialis* strain Cr4-12, which was isolated from an alpine glacier

cryoconite (GenBank:NR109013). SMRT DNA modification detection analysis (Murray *et al.*, 2012) detected three 6-methyladenine modified motifs, 5′-G**A**CN_7AATC-3′, 5′-G**A**TTN_7GTC-3′, and 5′-TG**A**GT-3′, exhibiting >99% confidence of their being methylated in the genome. Another motif, 5′-GAC**A**TG-3′, detected in the genome with high (>94%) confidence level was categorized as an unknown modification.

Nucleotide Sequence Accession Numbers

The draft whole-genome sequences have been deposited at DDBJ/EMBL/GenBank under BioProject number PRJEB6335 and whole genome accession numbers: CCJP01000001-CCJP01000007. The version described in this paper is the first version.

References

Chin C-S, Alexander DH, Marks P, Klammer AA, Drake J, Heiner C, *et al.* (2013). Nonhybrid, finished microbial genome assemblies from long-read SMRT sequencing data. *Nat Meth* **10**: 563–569.

Clocksin KM, Jung DO, Madigan MT. (2007). Cold-active chemoorganotrophic bacteria from permanently ice-covered Lake Hoare, McMurdo Dry Valleys, Antarctica. *Appl Environ Microbiol* **73**: 3077–3083.

Coleman NV, Mattes TE, Gossett JM, Spain JC. (2002). Biodegradation of cis-dichloroethene as the sole carbon source by a beta-proteobacterium. *Appl Environ Microbiol* **68**: 2726–2730.

Darcy JL, Lynch RC, King AJ, Robeson MS, Schmidt SK. (2011). Global distribution of Polaromonas phylotypes--evidence for a highly successful dispersal capacity. *PLoS ONE* **6**: e23742.

Irgens RL, Gosink JJ, Staley JT. (1996). Polaromonas vacuolata gen. nov., sp. nov., a psychrophilic, marine, gas vacuolate bacterium from Antarctica. *Int J Syst Bacteriol* **46**: 822–826.

Jeon CO. (2004). Polaromonas naphthalenivorans sp. nov., a naphthalene-degrading bacterium from naphthalene-contaminated sediment. *INTERNATIONAL JOURNAL OF SYSTEMATIC AND EVOLUTIONARY MICROBIOLOGY* **54**: 93–97.

Jeon CO, Park W, Padmanabhan P, DeRito C, Snape JR, Madsen EL. (2003). Discovery of a bacterium, with distinctive dioxygenase, that is responsible for in situ biodegradation in contaminated sediment. *Proc Natl Acad Sci USA* **100**: 13591–13596.

Koren S, Harhay GP, Smith TP, Bono JL, Harhay DM, McVey SD, *et al.* (2013). Reducing assembly complexity of microbial genomes with single-molecule sequencing. *Genome Biol* **14**: R101.

Korlach J, Bjornson KP, Chaudhuri BP, Cicero RL, Flusberg BA, Gray JJ, *et al.* (2010). Real-Time DNA Sequencing from Single Polymerase Molecules. *Methods in Enzymology* **472:** 431–455.

Lanoil B, Skidmore M, Priscu JC, Han S, Foo W, Vogel SW, *et al.* (2009). Bacteria beneath the West Antarctic ice sheet. *Environ Microbiol* **11**: 609–615.

Michaud L, Caruso C, Mangano S, Interdonato F, Bruni V, Giudice Lo A. (2012). Predominance of Flavobacterium, Pseudomonas, and Polaromonas within the prokaryotic community of freshwater shallow lakes in the northern Victoria Land, East Antarctica. *FEMS Microbiol Ecol* **82**: 391–404.

Murray IA, Clark TA, Morgan RD, Boitano M, Anton BP, Luong K, *et al.* (2012). The methylomes of six bacteria. *Nucleic Acids Res* **40**: 11450–11462.

Osborne TH, Jamieson HE, Hudson-Edwards KA, Nordstrom DK, Walker SR, Ward SA, *et al.* (2010). Microbial oxidation of arsenite in a subarctic environment: diversity of arsenite oxidase genes and identification of a psychrotolerant arsenite oxidiser. *BMC Microbiol* **10**: 205.

Simon C, Wiezer A, Strittmatter AW, Daniel R. (2009). Phylogenetic diversity and metabolic potential revealed in a glacier ice metagenome. *Appl Environ Microbiol* **75**: 7519–7526.

Sizova M, Panikov N. (2007). Polaromonas hydrogenivorans sp. nov., a psychrotolerant hydrogen-oxidizing bacterium from Alaskan soil. *International Journal of Systematic and Evolutionary Microbiology* **57**: 616–619.

Wang Z, Chang X, Yang X, Pan L, Dai J. (2014). Draft Genome Sequence of Polaromonas glacialis Strain R3-9, a Psychrotolerant Bacterium Isolated from Arctic Glacial Foreland. *Genome Announc* **2**. doi:10.1128/genomeA.00695-14.

Yagi JM, Sims D, Brettin T, Bruce D, Madsen EL. (2009). The genome of Polaromonas naphthalenivorans strain CJ2, isolated from coal tar-contaminated sediment, reveals physiological and metabolic versatility and evolution through extensive horizontal gene transfer. *Environ Microbiol* **11**: 2253–2270.

APPENDIX C

DRAFT GENOME SEQUENCE AND DESCRIPTION OF JANTHINOBACTERIUM SP. STRAIN CG3, A PSYCHROTOLERANT ANTARCIC SUPRAGLACIAL STREAM BACTERIUM

Contribution of Authors and Co-Authors

Author: Heidi J Smith

Contributions: Isolation, DNA extraction, data analysis, and manuscript preparation

Co-Author: Tatsuya Akiyama

Contributions: Plasmid experimentation and data analysis

Co-Author: Christine M. Foreman

Contributions: Principal investigator of laboratory experiments and genome analysis, manuscript preparation and editing

Co-Author: Michael J. Franklin

Contributions: Data analysis, manuscript editing

Co-Author: Tanja Woyke

Contributions: Sequencing, data analysis, and manuscript editing

Co-Author: Hazuki Teshima

Contributions: Sequencing and data analysis

Co-Author: Karen Davenport

Contributions: Sequencing and data analysis

Co-Author: Hajnalka Daligault

Contributions: Sequencing and data analysis

Co-Author: Tracy Erkkila

Contributions: Sequencing and data analysis

Co-Author: Lynne Goodwin

Contributions: Sequencing and data analysis
Co-Author: Wei Gu

Contribution of Authors and Co-Authors

Contributions: Sequencing and data analysis

Co-Author: Yan Xu

Contributions: Sequencing and data analysis

Co-Author: Patrick Chain

Contributions: Sequencing and data analysis

Manuscript Information Page

Heidi J. Smith, Tatsuya Akiyama, Christine Foreman, Michael Franklin, Tanja Woyke, Hazuki Teshima, Karen Davenport, Hajnalka Daligault, Tracy Erkkila, Lynne Goodwin, Wei Gu, Yan Xu, Patrick Chain
Genome Announcements
Status of Manuscript:
____ Prepared for submission to a peer-reviewed journal
____ Officially submitted to a peer-review journal
____ Accepted by a peer-reviewed journal
__X_ Published in a peer-reviewed journal

Volume 1, Number 6, 2014, e00960-13, doi:10.1128/genomeA.00960-13.

Abstract

Here we present the draft genome of *Janthinobacterium* sp. strain CG3, a psychrotolerant non-violacein producing bacterium that was isolated from the Cotton Glacier supraglacial stream. The genome sequence of this organism will provide insight as to the mechanisms necessary for bacteria to survive in UV stressed icy environments.

Psychrophiles often possess mechanisms to protect themselves from environmental conditions including extremes of UV radiation, temperature, freeze-thawing events, and desiccation, which cause severe damage to non-adapted organisms (Dieser *et al.*, 2010). Reductions in stratospheric ozone have resulted in formation of the Antarctic ozone hole, causing increased levels of ultraviolet B radiation (UV-B) to reach the Earth's surface, specifically effecting Antarctica (Madronich *et al.*, 1998). The highly damaging effects of short-wavelength radiation, UV-B and ultraviolet A radiation (UV-A) to biological systems has been well documented (3). Short-wave radiation induces cellular damage to a variety of macromolecules (e.g. DNA, RNA, proteins and lipids) by indirectly increasing the formation of reactive oxygen species (Lesser *et al.*, 2001). The pigment violacein has been shown to possess strong antioxidant properties, protecting cellular lipid membranes from hydroxyl radicals by mitigating peroxidation (Konzen *et al.*, 2006).

Janthinobacterium sp. strain CG3 was isolated from a supraglacial fluvial system on the Cotton Glacier, Antarctica (77°07S, 161°50E). The bacterial strain was isolated on R2A agar media incubated at 4°C in the dark for 12 days. Isolate *Janthinobacterium* sp. strain CG3 has characteristics of the genus *Janthinobacterium*: strictly aerobic, gram negative, rod shaped cells; but does not show evidence of violacein production.

Additionally, *Janthinobacterium* sp. strain CG3 does not possess genetic evidence of the vioA operon, which is responsible for violacein production (Pantanella *et al.*, 2007). As *Janthinobacterium* sp. strain CG3 lacks the genetic machinery necessary for violacein production, the genome sequence of this psychrotolerant organism will provide insight into strategies that have been evolved by organisms lacking pigments to survive in UV stressed polar environments.

The draft genome of *Janthinobacterium* sp. strain CG3 was generated at the DOE Joint Genome Institute (JGI) using Illumina data (Bennett, 2004). Short-insert paired-end (insert size 190 bp) and long-insert paired-end libraries (insert size 10800 bp) generated 19,156,074 and 21,678,138 reads, respectively. A total of 6,125 Mbp of Illumina data were used to assemble the genome by Allpaths, Velvet, and Parallel Phrap. Initial assemblies generated by Allpaths version 39750 and Velvet version 1.1.05 (Zerbino and Birney, 2008) were computationally shredded into 10 Kbp or 1.5 Kbp overlapping fake reads, respectively. Overlapping fake reads from Allpaths and two Velvet assemblies were combined with the Illumina long-insert paired-end reads to generate final assembly by Parallel Phrap version 4.24. Possible mis-assemblies were corrected with manual editing in Consed (Ewing *et al.*, 1998; Ewing and Green, 1998; Gordon *et al.*, 1998). Sequence gaps were closed by Repeat Resolution Software and sequencing of bridging PCR fragments.

The draft genome of *Janthinobacterium* sp. strain CG3 consists of 71 contigs in 7 scaffolds with an estimated size of 6.4 Mbp. A total of 5,426 candidate protein-coding genes were predicted with a total G + C content of 65.5%. The small-subunit rRNA gene

sequences had 99% sequence identity to a *Janthinobacterium* sp. isolate from an Arctic glacier (GenBank accession number FM955878). Scaffolds 3, 4, and 7 were circularized with sequences of bridging PCR fragments, suggesting the presence of three plasmids in *Janthinobacterium* sp. strain CG3 isolate.

Nucleotide Sequence Accession Numbers

This whole-genome shotgun project has been deposited at DDBJ/EMBL/GenBank under accession number APFF01000000. The version described in this paper is version APFF01000000.

References

Bennett S. (2004). Solexa Ltd. *Pharmacogenomics* **5**: 433–438.

Dieser M, Greenwood M, Foreman CM. (2010). Carotenoid pigmentation in Antarctic heterotrophic bacteria as a strategy to withstand environmental stresses. *Arctic, Antarctic, and Alpine Research* **42:** 396-405.

Ewing B, Green P. (1998). Base-calling of automated sequencer traces using phred. II. Error probabilities. *Genome Res* **8**: 186–194.

Ewing B, Hillier L, Wendl MC, Green P. (1998). Base-Calling of Automated Sequencer Traces Using Phred. I. Accuracy Assessment. *Genome Res* **8**: 175–185.

Gordon D, Abajian C, Green P. (1998). Consed: a graphical tool for sequence finishing. *Genome Res* **8**: 195–202.

Konzen M, De Marco D, Cordova CAS, Vieira TO, Antônio RV, Creczynski-Pasa TB. (2006). Antioxidant properties of violacein: Possible relation on its biological function. *Bioorganic & Medicinal Chemistry* **14**: 8307–8313.

Lesser MP, Farrell JH, Walker CW. (2001). Oxidative stress, DNA damage and p53 expression in the larvae of atlantic cod (Gadus morhua) exposed to ultraviolet (290-400 nm) radiation. *J Exp Biol* **204**: 157–164.

Madronich S, McKenzie RL, Björn LO, Caldwell MM. (1998). Changes in biologically active ultraviolet radiation reaching the Earth's surface. *J Photochem Photobiol B, Biol* **46**: 5–19.

Pantanella F, Berlutti F, Passariello C, Sarli S, Morea C, Schippa S. (2007). Violacein and biofilm production in Janthinobacterium lividum. *J Appl Microbiol* **102**: 992–999.

Zerbino DR, Birney E. (2008). Velvet: algorithms for de novo short read assembly using de Bruijn graphs. *Genome Res* **18**: 821–829.

APPENDIX D

SUPPLEMENTAL INFORMATION TO CHAPTER 4

SI Results

Bacterial Abundances

Bacterial cell abundances in the CG, PL, and SR treatments were enumerated over four time points at day 0 (T1), day 27 (T2), day 63 (T3), and day 98 (T4) (Table S2). For the CG carbon source, bacterial cellular abundances ranged from 2.23-7.32 x 10^5 cells/mL ± 1SD (1.3-6.08 X 10^4 cells/mL). PL cellular abundances ranged from 2.88-8.62 x 10^5 cells/mL ± 1SD (1.18-5.94 X 10^4 cells/mL), and SR cellular abundances ranged from 1.63-5.58 x 10^5 cells/mL ± 1SD (2.48-6.02 X 10^4 cells/mL). A significant difference in bacterial cell abundances existed between time points T1 to T2, and T1 to T4 ($P < 0.037$), no significant difference was found between T1 and T3 ($P > 0.395$). For PL, a significant difference in bacterial cell abundances was found between T1 to T2, T3, and T4 ($P < 0.024$). For SR, a significant difference in bacterial cell abundances existed between T1 to T2 ($P < 0.012$), and no significant difference was determined between T1 to T3 and T4 ($P > 0.191$). While the starting concentrations of the bacterial innocula were similar at 10^5 cells/mL, the cell abundances were significantly different ($P < 0.001$) for each carbon source over time. The same overall trend in cellular abundances was observed across all carbon sources, an initial decrease followed by an increase and ending with a final decrease in cellular abundance.

SI Materials and Methods

Cellular Abundances

Samples for bacterial cell enumeration were preserved with prefiltered (0.2 μm) formalin to a final concentration of 2% v/v. Bacteria were filtered onto polycarbonate membranes (0.2 μm pore size) and stained with SYBR® Gold (final concentration 25X, Invitrogen). A Nikon E800 epifluorescence microscope was used to count at least 30 randomly selected fields, with each field containing a minimum of 20 cells per grid [1], resulting in the enumeration of a minimum of 600 cells. Triplicate filters were prepared and counted for each sample. Significant differences in cellular abundances were tested by conducting an analysis of variance (ANOVA). Statistically significant differences in cellular abundances were determined between individual time points by an unpaired two-tail *t*-test.

SI Figures

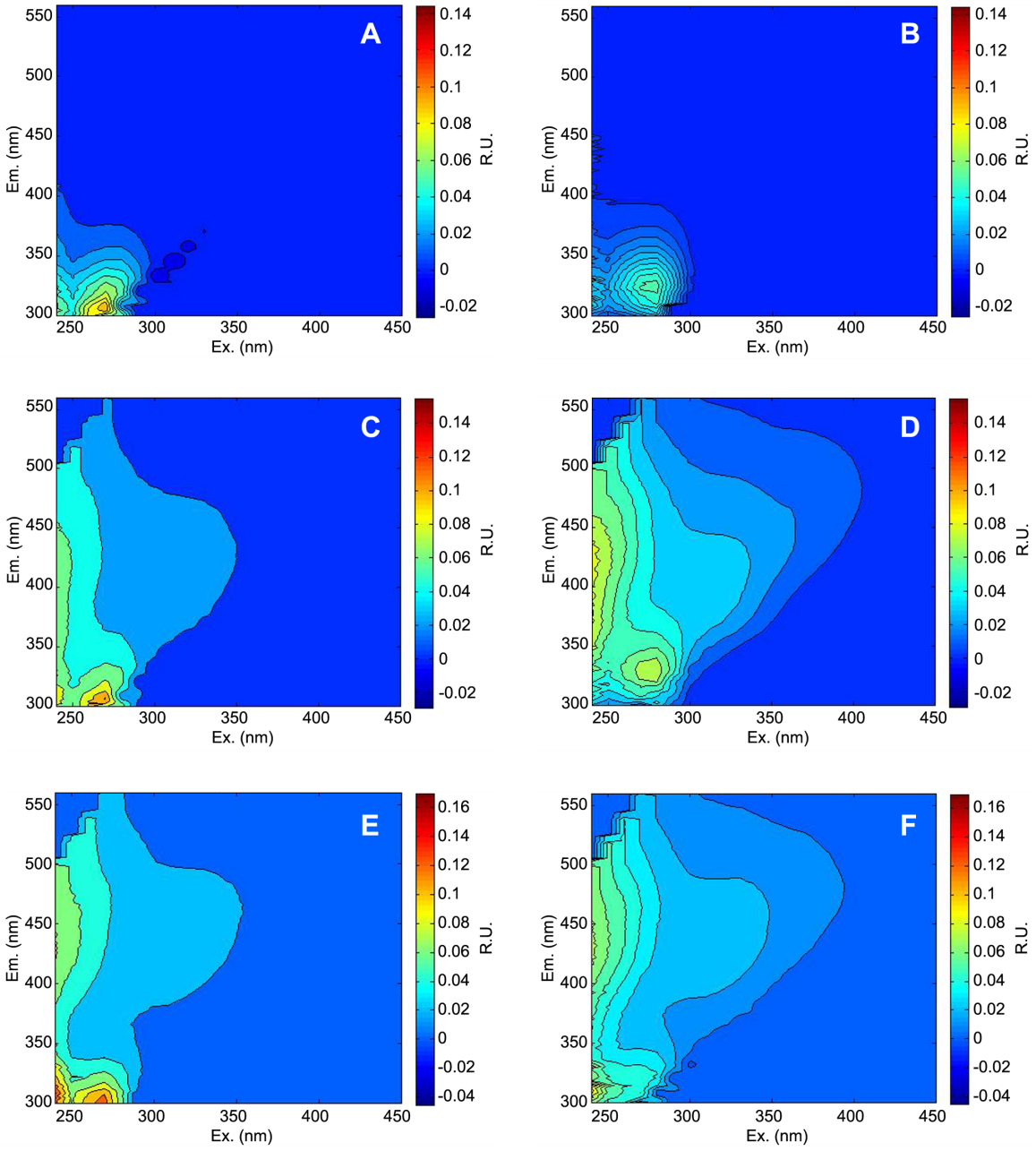

Figure AD.1. EEMs for Cotton Glacier (CG), Pony Lake (PL), and Suwannee River (SR) with normalized fluorescence intensities given in Raman units (R.U.) for the first and last time point where (A) CG d=0, (B) CG d=98, (C) PL d=0, (D) PL d=98, (E) SR d=0, (F) SR d=98.

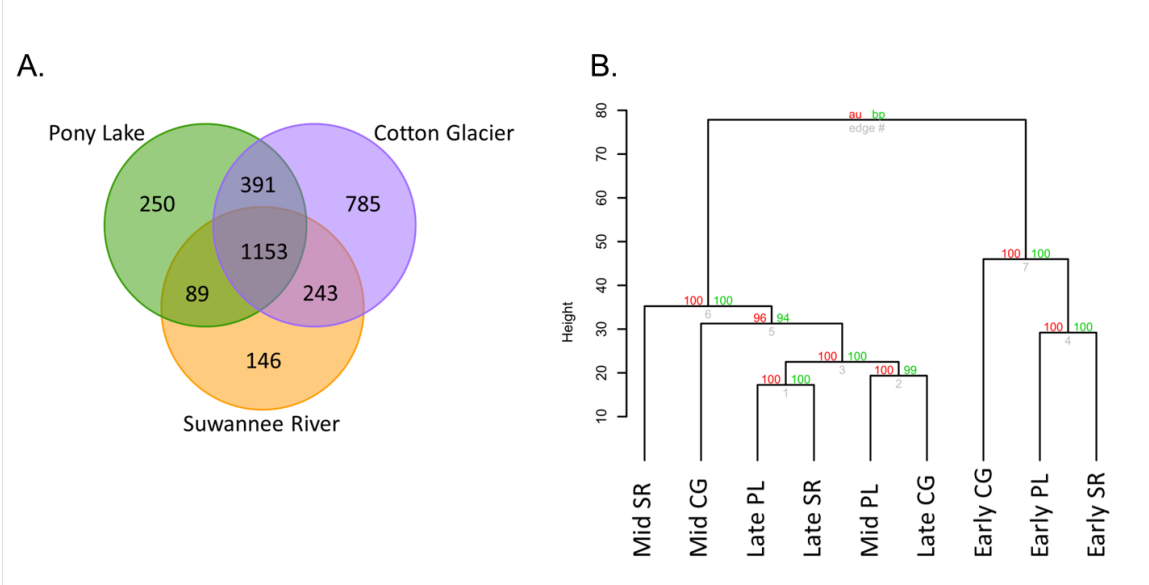

Figure AD.2: Classification of UPLC-Q-TOF MS detected molecular constituents. A) Venn diagram depicting the number of molecular constituents with significant abundance changes (adjusted P<0.01) in the three carbon sources over the course of the study. B) Hierarchical clustering of molecular constituent fold changes (log2 transformed) over the early, mid, and late time ranges for Cotton Glacier (CG), Pony Lake (PL), and Suwannee River (SR). Bootstrapping was based on a resampling size of 10^4, Approximately Unbiased (AU), and Bootstrap Probability (BP) p-value percentages are reported for each cluster in red and green, respectively.

SI Tables

Table AD.1. DOM molecular species percent composition and more- and less-labile nature (richness) for the three carbon sources: Cotton Glacier, Pony Lake, and Suwannee River determined by FT-ICR MS. Pony Lake data adapted from D'Andrilli et al. 2013.

	Cotton Glacier			Pony Lake			Suwannee River		
	Composition (%)	More-Labile (%)	Less-Labile (%)	Composition (%)	More-Labile (%)	Less-Labile (%)	Composition (%)	More-Labile (%)	Less-Labile (%)
CHO	49.8	38.7	61.3	25.9	21.4	78.6	56.6	5.80	94.2
$CHOS_1$	15.9	76.5	23.5	15.3	39.2	60.8	14.8	15.4	84.6
$CHON_1$	17.9	44.5	55.5	19.1	15.8	84.2	18.7	0.280	99.7
$CHON_1S_1$	1.39	96.3	3.70	12.8	26.9	73.1	0.400	0	100
$CHON_2$	14.8	37.3	62.7	16.9	10.3	89.7	8.05	0.480	99.5
$CHON_2S_1$	0.257	100	0	9.98	10.8	89.2	1.44	74.1	22.9
	Overall	46.5	53.5	Overall	20.8	79.2	Overall	6.72	93.3

Table AD.2. Bacterial cell abundances for Cotton Glacier, Pony Lake, and Suwannee River for the four sampling points. Significant differences in cellular abundances relative to T1 for each respective carbon source (ANOVA and unpaired two-tail t test $p < 0.05$) are highlighted in bold.

	Mean Bacterial Abundance (x 10^5 cells ml-1) ± SD x (10^4 cells ml-1)			
Sample	Time Point 1	Time Point 2	Time Point 3	Time Point 4
CG	7.32 ± 6.08	**2.23 ± 8.1**	5.08 ± 1.30	**3.01 ± 4.76**
PL	5.86 ± 1.18	**2.88 ± 6.0**	**8.62 ± 5.22**	**7.84 ± 5.94**
SR	4.88 ± 2.48	**1.63 ± 3.59**	5.58 ± 6.02	4.03 ± 5.42

SI Reference

Lisle JT, Priscu JC. (2004). The occurrence of lysogenic bacteria and microbial aggregates in the lakes of the McMurdo Dry Valleys, Antarctica. *Microb Ecol* **47**: 427–439.